RIKEN R-CCS
Annual Report FY2018
R-CCS Research Activities

Preface

The objectives of the RIKEN Center for Computational Science (R-CCS) are threefold, centered around supercomputing: one is to target high performance computation itself as a scientific objective, or namely, the "Science of Computing"; another is to apply the enormous computational power thus obtained to solve difficult scientific problems, or namely the "Science by Computing"; finally, to collaborate with other scientific disciplines that contribute to advances both sciences, or namely, the "Science for Computing". Our goal is to be recognized as one of the global leadership research centers to advance high-end computational science in this regard.

Computational science employs multitudes of methodologies to essentially recreate various phenomena as computational activities inside machines, thereby allowing to challenge difficult problems encountered by mankind. For example, we could model a phenomenon by a set of physical/mathematical formulas, and the machine-driven solution to the formulas will result in direct 'simulation' of the phenomenon; alternatively, we could analyze the massive data measured on a phenomenon by scientific instruments, and further extrapolate future trends, or so-called 'data science' methodology; furthermore, we could train our 'artificial intelligence' to attain higher-level insights on the data, both simulated and/or analyzed. Here supercomputers will accelerate all such methodologies by many orders of magnitude, allowing synthesis of innovations to tackle the most difficult problems that are of interest to the greater society, and R-CCS intends to be at the forefront of such activities.

Moreover, innovative Information Technologies (IT) researched and developed to advance supercomputing is not only applicable to itself, but rather are the bleeding-edge technologies to advance the entire IT as a whole, from Clouds to the Edge, and thus will contribute to the massive improvement of the economy and our daily lives that are now heavily reliant on IT. We intend to collaborate with other leadership centers of the world to play a central role in advancing IT for the society at large.

R-CCS Organization

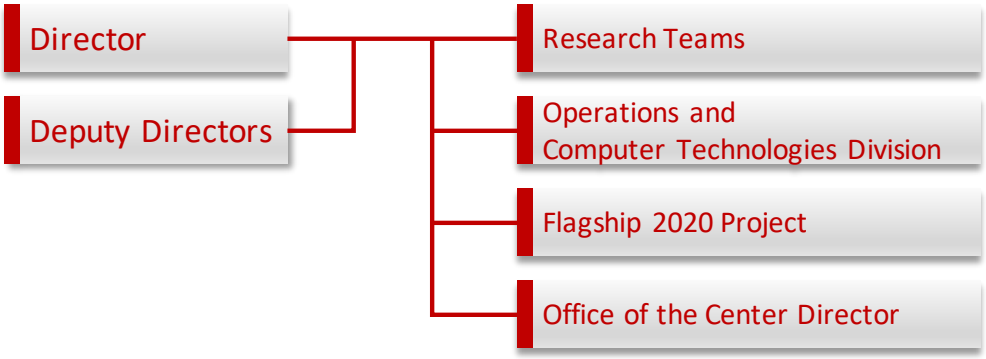

Research Teams

- System Software Research Team
- Programming Environment Research Team
- Processor Research Team
- Large-scale Parallel Numerical Computing Technology Research Team
- HPC Usability Research Team
- Field Theory Research Team
- Discrete Event Simulation Research Team
- Computational Molecular Science Research Team
- Computational Materials Science Research Team
- Computational Biophysics Research Team
- Particle Simulator Research Team
- Computational Climate Science Research Team
- Complex Phenomena Unified Simulation Research Team
- Next Generation High Performance Architecture Research Team
- High Performance Big Data Research Team
- Data Assimilation Research Team
- Computational Disaster Mitigation and Reduction Research Team
- Computational Structural Biology Research Team

Operations and Computer Technologies Division

- Facility Operations and Development Team
- System Operations and Development Team
- Application Tuning Development Team
- HPC Usability Development Team

Flagship 2020 Project

- System Software Development Team
- Architecture Development Team
- Application Development Team
- Co-Design Team

RIKEN R-CCS

Contents

Part I

Research Division

Chapter 1

System Software Research Team

1.1 Members

Yutaka Ishikawa (Team Leader)

Masamichi Takagi (Senior Scientist)

Atsushi Hori (Research Scientist)

Balazs Gerofi (Research Scientist)

Yoshiyuki Morie (Research Scientist)

Masayuki Hatanaka (Research & Development Scientist)

Takahiro Ogura (Research & Development Scientist)

Tatiana Martsinkevich (Postdoctoral Researcher)

The system software research has been conducted in cooperation with the following members of the System Software Development Team in the Flagship 2020 project.

1.2 Research Activities

The system software team focuses on the research and development of an advanced system software stack not only for the "K" computer but also for toward exa-scale computing including Fugaku. We have been mainly focusing on scalable high performance communication and file I/O libraries and/or middlewares. The former research topics, sharing virtual address space and IHK/McKernel light-weight kernel, have been almost taken over by the System Software Development Team, but the research results are shown here.

1.3 Research Results and Achievements

1.3.1 Persistent Collectives

The state-of-the-art interconnects, such as the Tofu2 interconnect of Fujitsu PRIMEHPC FX100, have not only an RDMA offloading capability but also support offloading collective operations. In addition to FIFO-based sequential execution for RDMA requests, such an interconnect supports complex scheduling for RDMA requests, including collective communications, by extending the FIFO-based scheduling to trigger and block the execution of the queued RDMA requests from remote nodes. It allows truly asynchronous progress of collective operations, which require issuing sequence of communication commands, without CPU assist.

The MPI forum, a community for standardizing MPI specification, has been discussing a new feature of collective operations, i.e., persistent collectives. For example, the persistent neighborhood all-to-all collective has the initialization function, MPI_Neighbor_alltoall_init(), that must be executed before initiating the collective operation. An application obtains a request object as a result of this initialization function, and it is used to

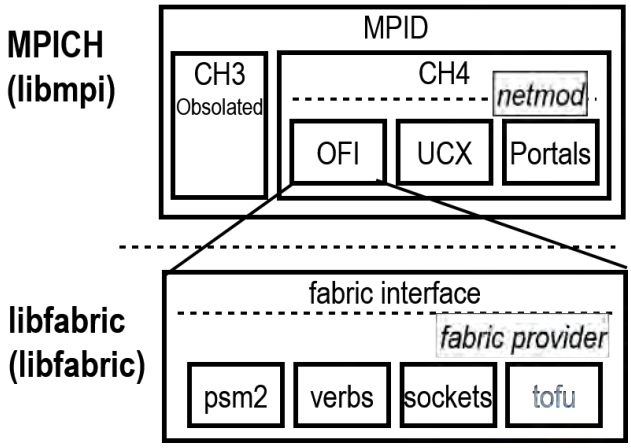

Figure 1.1: MPICH Software Architecture

initiate the collective operation by MPI_Start() function with that object. MPI_Wait() function is used to wait for the completion. MPI_Start() and MPI_Wait() may be repeatedly invoked without re-initialization of the operation. This persistent collective operation was implemented using Tofu2 offloading capability in FY2017 [3]. The offloaded persistent broadcast, requiring more sophisticated algorithm to achieve low latency, was also implemented using Tofu2 offloading capability in FY2017 [6,7].

In order to integrate our past research results into the MPICH MPI implementation, we decided under DoE/MEXT collaboration that the existing Tofu access module is implemented as a "tofu" provider in Open Fabric Interface (OFI), libfabric, to combine with MPICH via OFI. OFI is one of the low-level communication interfaces supported by MPICH 3.3. In the rest of this subsection, an extended feature of OFI is described.

OFI has an API called triggered operations and Deferred Work Queue in which a communication operation is defined with a counter and its threshould. Figure 1.2 shows a definition of the deferred work queue entry. If the *triggering_cntr* in the `fi_deferred_work` structure reaches the *threshold*, the operation specified by *op_type* and *op* is issued. This mechanism is implmented using the Tofu session mode CQ in which triggering counter is realized by the scheduling pointer of a CQ.

```
struct fi_deferred_work { ...
  uint64_t threshold;
  struct fid_cntr * triggering_cntr; ...
  enum fi_tringer_op op_type;
  union { ...
  } op;
};
```

Figure 1.2: Deferred Work (DW) Queue Entry

A persistent non-blocking operation can be realized using the Deferred Work Queue as follows. At the initialization function, such as MPI_Neighbor_alltoall_init(), a series of triggered operations, implementing a collective operation, is created. This command sequences are registered using the fi_control() libfabric interface at the MPI_Start operation. MPI_Wait operation waits for all completions of the commands. The triggered operations are handled by the Tofu network interface, and thus no CPU cycles are involved during the collective operation. However, the command sequences must be registered every execution of the MPI_Start operation. We extended this API so that the registered commands are reused to eliminate re-registation overhead. A prototype implementation was conducted to proof this concept in FY 2018.

1.3.2 Data Transfer Framework

A common type of HPC applications is multi-component workflows in which each component performs a particular task, then passes the result of the computation to the next component for further processing. Components may be either loosely coupled, i.e., by using files to pass data, or they can use coupling software. An example of such applications is a severe weather prediction application called SCALE-LETKF that consists of two independently developed components. In each iteration SCALE performs ensemble simulations, outputs the

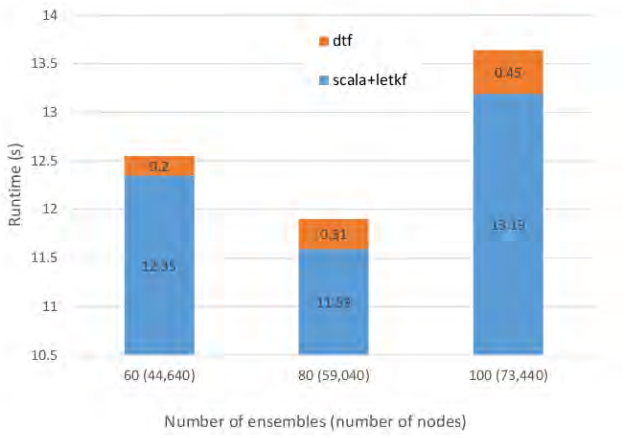

Figure 1.3: Computation time and DTF transfer time per one iteration

results to a set of files, which LETKF reads and assimilates the result with observation data that arrives in real time at fixed intervals. LETKF then outputs the result to files that become the input for SCALE in the next iteration. The program, thus, has a strict timeliness requirement: one iteration, including all the I/O, needs to finish within a fixed time period - before next observation data arrives. This requirement becomes impossible to meet as the amount of I/O grows.

To solve this problem, we proposed the Data Transfer Framework (DTF) that silently bypasses file I/O by sending the data directly over network but does not require rewriting of the original I/O kernels [5]. Current operation of the DTF operates underneath the PnetCDF library - a popular I/O library used by SCALE-LETKF. The DTF intercepts PnetCDF's I/O calls and sends the data to the processes in the other component using MPI library instead of performing file I/O. The DTF does require a slight modification to the user program. In particular, the user is required to add the following API calls to each component in the multi-component workflow:

1. DTF_INIT(config_file, component_name) - initializes the framework, should be called after MPI_Init();
2. DTF_FINALIZE() - finalizes the framework, should be called before MPI_Finalize();
3. DTF_TRANSFER(filename) - the data transfer is performed inside this call, should be called after corresponding PnetCDF read/write calls.

Additionally, to the aforementioned APIs the user needs to provide a DTF configuration file: a simple text file that describes the framework: it gives number and names of components, lists the files that create dependency between the two components and need to be transferred. The DTF is implemented as a library and it comes with a modified version of the PnetCDF library that allows intercepting of the I/O calls. We tested the performance of the DTF with SCALE-LETKF on the K computer. In the test case, the observation data with a resolution of 250 meter was assimilated. The tests were performed on three scales: with 60, 80 and 100 ensembles with 360 processes per ensemble. A total of 2.75 GB of data was moved between processes of one ensemble in one iteration. Figure 1.3 below demonstrates that even for the largest execution the time to transfer the data took less than 0.5 second.

1.3.3 Sharing Virtual Address Space

The two most common parallel execution models for CPUs today are multiprocess and multithread. The multiprocess model allows each process to own a private address space, and the multithreaded model shares all address space by default. We propose a new implementation of the third model, called *Process-in-Process (PiP)*, where multiple processes are mapped into a single virtual address space (VAS). Thus, each process still owns its private storage but can directly access the storage of other processes in the same virtual address space. The idea of address-space sharing is not new. What makes PiP unique, however, is that its design is completely in user space, making it a portable and practical approach for large supercomputing systems.

PiP allows multiple parallel tasks to execute the same or different programs in a shared virtual address space environment while maintaining privatized variable sets. The PiP task does not follow the definition of

conventional process or thread. For instance, PiP tasks share the same virtual address space whereas processes have isolated virtual address space; two PiP tasks can execute arbitrary programs in parallel in the same virtual address space, whereas threads must be derived from the same program. Moreover, in the thread mode, all variables are shared. In PiP, every PiP task has its own privatized variable set like the process model but all variables are also sharable since PiP tasks share the same VAS.

<table>
<tr><th colspan="2"></th><th>Virtual Address Space</th><th colspan="2">Variables</th><th>Data</th><th>Note</th></tr>
<tr><td rowspan="3">Multi-Process</td><td>(default)</td><td rowspan="3">not shared</td><td rowspan="3">privatized</td><td rowspan="2">inaccessible</td><td>inaccessible</td><td></td></tr>
<tr><td>POSIX shmem</td><td>accessible</td><td>only for newly allocated regions</td></tr>
<tr><td>XPMEM</td><td>accessible</td><td>accessible</td><td>Linux Kernel Module</td></tr>
<tr><td rowspan="2">Multi-Thread</td><td>(default)</td><td rowspan="2">shared</td><td colspan="2">shared, accessible</td><td rowspan="2">accessible</td><td></td></tr>
<tr><td>MPC</td><td colspan="2">privatized, accessible</td><td>Compilers needed</td></tr>
<tr><td colspan="2" rowspan="2">SMARTMAP
PVAS</td><td rowspan="2">shared</td><td colspan="2" rowspan="2">privatized, accessible</td><td rowspan="2">accessible</td><td>Kitten OS</td></tr>
<tr><td>patched Linux Kernel</td></tr>
<tr><td colspan="2">Process-in-Process</td><td>shared</td><td colspan="2">privatized, accessible</td><td>accessible</td><td>OS and language system independent</td></tr>
</table>

Table 1.1: Summary of current techniques and PiP

As listed in Table 1.1, two memory-mapping techniques have been widely used for data sharing in the multiprocess model. POSIX shmem includes System-V IPC and UNIX shared mmap. It is a general term to `mmap()` the memory pages owned by another process. This technique allows newly allocated memory segments (i.e., *data*) to be shared. However, a process cannot access statically allocated *variables* of the other processes. Moreover, the setup cost for the memory mapping is high. XPMEM is the other well-known approach. It allows processes to map arbitrarily memory regions (i.e., both *data* and *variables*) owned by other processes. These mappings involve costly system calls to the kernel module, however.

Two OS-based VAS-sharing techniques have been studied in the multiprocess model. SMARTMAP is a built-in function of the Kitten lightweight OS kernel that exploits the PT structure of the x86 architecture. PVAS provides functionality similar to that of SMARTMAP, but it is implemented as a patched Linux kernel. MPC is a thread-based language-processing system designed for hybrid MPI and OpenMP programming. It consists of custom compilers, linker, and runtime libraries; thus the maintenance is costly.

The PiP approach can be categorized into the process-based approach. It avoids the overhead of maintaining thread-safety and existing software stacks can be also used. PiP is implemented at user-level and requires neither the development of a new OS kernel, nor a patch to existing kernels. These properties make PiP highly *practical*.

1.3.3.1 DOE-MEXT Collaboration

SNAP[1] is a proxy application that models the performance of modern discrete ordinates neutral particle transport application. The original implementation uses the hybrid MPI+OpenMP model where the spatial domain is partitioned across MPI ranks and traversed with sweeps along the angular domain. We updated the SNAP code to be PiP-aware. We compared the PiP-aware version (**MPI+PiPs**) with the conventional thread-based approach (**MPI+OMP**), and measured the MPI-only model as a reference.

Figure 1.4 reports the solve time of 10 time steps running on Oakforest-PACS (OFP).. **MPI+PiPs** always outperforms **MPI+OMP**. Especially when scaling to a large number of cores, the communication becomes dominant, and thus PiP delivers more benefit, contributing close to 3.2x performance speedup on 256 cores (4 nodes).

The reduced speedup on 1,024 cores (i.e., 2.2x) indicates that the contention overhead of multithreaded MPI is optimized by the priority locks. Nevertheless, the network utilization issue still exists and relies on the support from PiP. We note that the MPI-only model shows faster solve time than that of the hybrid approaches on a single node (up to 64 cores). The reason is that it assigned every energy domain to a different process whereas the hybrid approaches divided each domain and distributed to four PiP tasks or threads. Thus, the former may

[1] `https://github.com/lanl/SNAP`

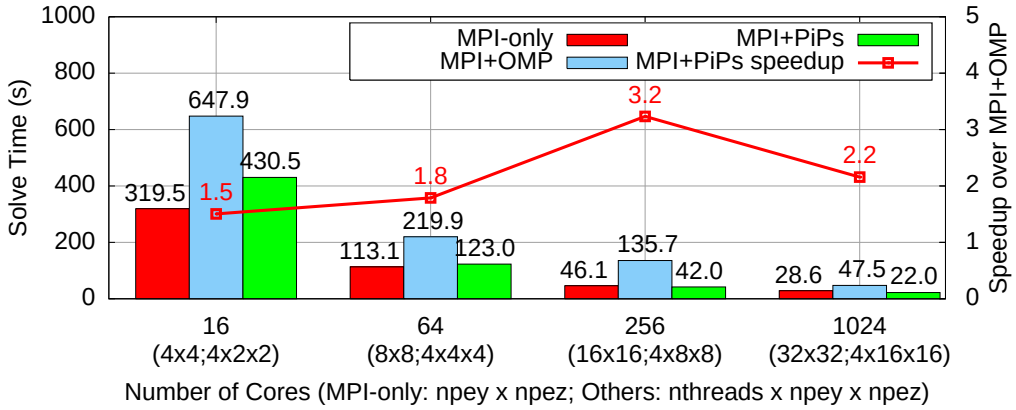

Figure 1.4: Strong scaling of hybrid MPI+OpenMP SNAP on OFP.

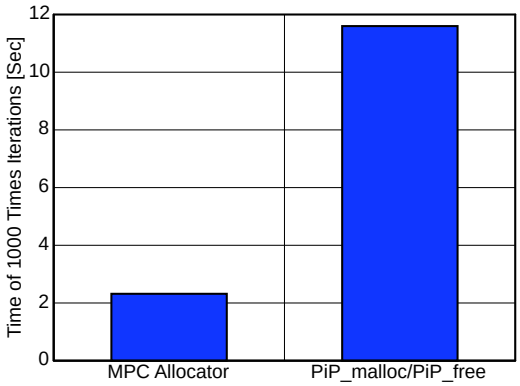

Figure 1.5: Performance comparison between PiP malloc and MPC Allocator

require less intercore data movement. We used only four threads per process in the hybrid approaches because of the limitation of the parallel algorithm in SNAP; however, the performance gap is known to increase when more threads are utilized..

1.3.3.2 CEA-Riken Collaboration

As shown in Table 1.1, CEA is also developing MPC to provide the same address-space sharing technique, but with the different approach from PiP. CEA, however, has been developing MPC for years and has wider experiences with this model.

One big issue of address-space sharing model is that a `malloc()`ed region can be passed to the other task sharing the same address space, but the passed task is unable to `free()` it. This is because each task has a different GLIBC instance and the `malloc` information is not shared among tasks. In PiP, this issue is solved in a very naive way.

If this restriction could be lifted, then users would have more programming flexibility with this execution model. MPC development team already noticed and solved this problem. They have developed another `malloc` library, named *MPC Allocator*. The benefit of having MPC Allocator is not only solving the issue but also the better performance of MPC Allocator than that of GLIBC.

In this collaboration scheme, MPC Allocator was firstly decoupled from the MPC runtime library as a independent library. This was done by CEA, and then Riken checked if MPC Allocator can work on PiP. Eventually we found that MPC Allocator can work on PiP. Figure 1.5 shows the performance difference between the PiP `malloc()`/`free()` and MPC Allocator running on PiP. As shown in this figure, MPC Allocator performs much better than that of PiP's naive implementation (`PiP_malloc` and `PiP_free`).

1.3.4 IHK/McKernel

This Section describes recent research results related to IHK/McKernel. Specifically, results of a custom precise event based sampling (PEBS) device driver for scalable, real-time memory access tracking are presented in Section 1.3.4.1, published in [6].

1.3.4.1 Scalable Memory Access Tracking

The past decade has brought an explosion of new memory technologies. Various high-bandwidth memory types, e.g., 3D stacked DRAM (HBM), GDDR and multi-channel DRAM (MCDRAM) as well as byte addressable non-volatile storage class memories (SCM), e.g., phase-change memory (PCM), resistive RAM (ReRAM) and the recent 3D XPoint, are already in production or expected to become available in the near future.

Management of such heterogeneous memory types is a major challenge for application developers, not only in terms of placing data structures into the most suitable memory but also to adaptively move content as application characteristics changes in time. Operating system and/or runtime level solutions that optimize memory allocations and data movement by transparently mapping application behavior to the underlying hardware are thus highly desired.

One of the basic requirements of a system level solution is the ability to track the application's memory access patterns in real-time with low overhead. Intel's Processor Event-Based Sampling (PEBS) is an extension to hardware performance counters that enables sampling the internal execution state of the CPU (including the most recent virtual address accessed) and periodically storing a snapshot of it into main memory. The overhead of PEBS has been the focus of previous works, however, not in the context of large-scale high-performance computing (HPC).

We have implemented a custom PEBS driver in the IHK/McKernel lightweight multi-kernel operating system and performed systematic evaluation of PEBS' overhead on a number of real HPC applications running at large scale. We demonstration of captured memory access patterns as the function of different PEBS parameters.

Figure 1.6 summarizes our application level findings. The X-axis represents node counts while the Y-axis shows relative overhead compared to the baseline performance. For each bar in the plot, the legend indicates the PEBS reset value and the PEBS buffer size used in the given experiment. The general tendency of overhead for most of the measurements matched our expectations, i.e., the most influential factor in performance overhead is the PEBS reset value, whose impact can be relaxed to some extent by adjusting the PEBS buffer size.

Across all workloads, we observe the largest overhead on GeoFEM (shown in Figure 1.6a) when running with the lowest PEBS reset value of 64 and the smallest PEBS buffer of 8kB, where the overhead peaked at 10.2%. Nevertheless, even for GeoFEM a less aggressive PEBS configuration, e.g., a reset value of 256 with 32kB PEBS buffer size induces only up to 4% overhead.

We concluded that PEBS efficiency matches the basic requirements to be feasible for heterogeneous memory management but further work is necessary to quantify the additional overhead associated with using the recorded data at runtime.

1.3.5 Utility Thread Offloading Interface

The number of cores per node in HPC system has increased to the order of tens to hundreds. This abundance makes it possible to spare some cores for helper threads to increase application performance. A typical example is MPI asynchronous progress thread which performs communication processing in parallel with computation.

Allocating appropriate core is crucial to the technique for two reasons. The first one is that those threads should be put on the dedicated cores for the first place so as not to interfere with computation threads. The second one is that those threads need to communicate computation threads or interconnect and therefore they should be put to cores near the communication target to minimize communication overhead.

However, the implementation is not application transparent because it's done typically by modifying application code or command line. And it is not easy nor portable across systems because no simple, abstracted interface is available.

To respond to this situation, we introduce a application-transparent and portable interface, called Utility Thread Offloading Interface (UTI), and the corresponding library. The library is given abstracted info by runtime (e.g. MPI library) and performs core allocation.

This is on-going work and the followings were done during this fiscal year.

1. Review UTI with CEA. How to incorporate the capability to dynamically change the boundary between helper and computation cores is discussed.

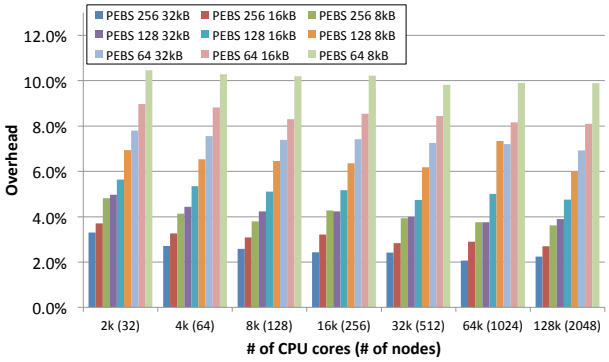

(a) GeoFEM (The University of Tokyo)

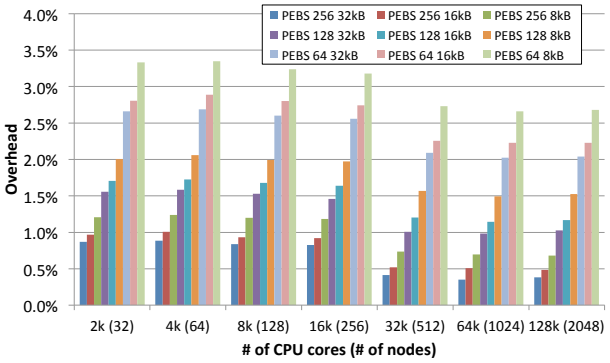

(b) HPCG (CORAL)

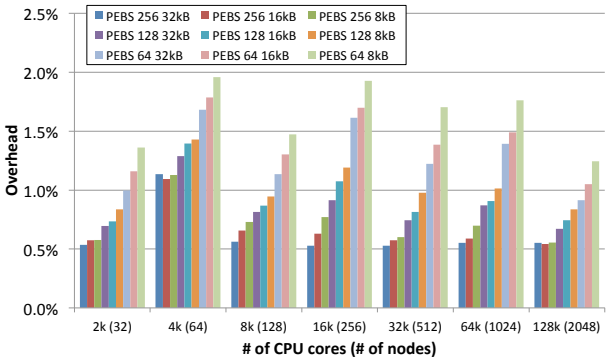

(c) LAMMPS (CORAL)

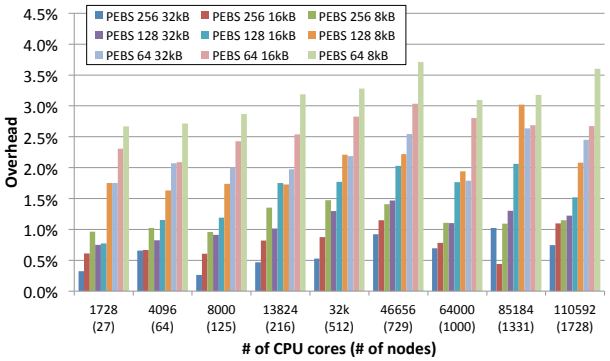

(d) Lulesh (CORAL)

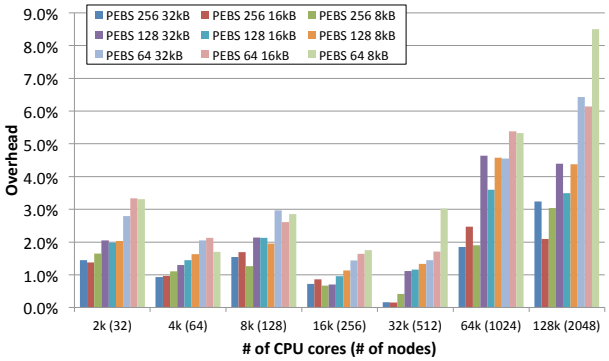

(e) MiniFE (CORAL)

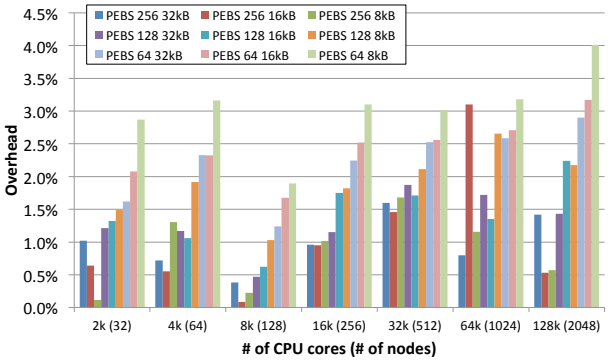

(f) AMG2013 (CORAL)

Figure 1.6: PEBS overhead for GeoFEM, HPCG, LAMMPS, Lulesh, MiniFE and AMG on up to 2,048 Xeon Phi KNL nodes

2. Improve prototype implementation of the library with LLNL. Some issues are reported by the LLNL researcher.

1.4 Schedule and Future Plan

We continue to enhance performance and functionality of our system software stack for Fugaku and other computer architectures, such as Intel Xeon.

1.5 Publications

[1] Hatanaka, M., Takagi, M., Hori, A., and Ishikawa, Y., "Offloaded MPI Persistent Collectives using Persistent Generalized Request Interface," In EuroMPI/USA 2017, Sept. 2017.

[2] Hori, A., Si, M., Gerofi, B., Takagi, M., Dayal, J., Balaji, P., and Ishikawa, Y., "Process-in-process: Techniques for practical address-space sharing," In HPDC '18: The 27th International Symposium on High-Performance Parallel and Distributed Computing, June 2018. (Karsten Schwan Best Paper Award)

[3] Martsinkevich, T., Gerofi, B., Lien, G.-Y., Nishizawa, S., keng Liao, W., Miyoshi, T., Tomita, H., Ishikawa, Y., and Choudhary, A., "DTF: An I/O Arbitration Framework for Multi-component Data Processing Workows," In 2018 International Supercomputing Conference (ISC), June 2018.

[4] Morie, Y., Hatanaka, M., Takagi, M., Hori, A., and Ishikawa, Y., "Prototyping of Offloaded Persistent Broadcast on Tofu2 Interconnect," In SC'17 poster, Nov. 2017.

[5] Morie, Y., Hatanaka, M., Takagi, M., Hori, A., Ishikawa, Y., and Nanri, T., "Evaluation of Prototyping Persistent Collective Communication on FX100," In IPSJ SIG Technical Report, vol. 2018-HPC-163, Feb. 2018. (In Japanese)

[6] Nonell, Aleix Roca and Gerofi, Balazs and Bautista-Gomez, Leonardo and Martinet, Dominique and Querol, Vicenç Beltran and Ishikawa, Yutaka "On the Applicability of PEBS Based Online Memory Access Tracking for Heterogeneous Memory Management at Scale," In Proceedings of the Workshop on Memory Centric High Performance Computing (MCHPC), Nov. 2018

Chapter 2

Programming Environment Research Team

2.1 Members

Mitsuhisa Sato (Team Leader)

Yuetsu Kodama (Senior Research Scientist)

Hitoshi Murai (Research Scientist)

Miwako Tsuji (Research Scientist)

Masahiro Nakao (Research Scientist)

Jinpil Lee (Postdoc Researcher)

Tetsuya Odajima (Postdoc Researcher)

Manabu Yagi (Postdoc Researcher)

Itaru Kitayama (Technical Staff)

Masahiro Yasugi (Senior Visiting Researcher)

Hitoshi Sakagami (Senior Visiting Researcher)

Brian Wylie (Visiting Researcher)

Christian Feld (Visiting Researcher)

Hidetoshi Iwashita (Visiting Researcher)

Hiroko Takahashi (Assistant)

2.2 Overview of Research Activities

In order to exploit full potential computing power of large scale parallel system such as the K computer to carry out advanced computational science, efficient parallel programming is required to coordinate these processors to perform scientific computing. Our team conduct researches and developments on parallel programming models and language to exploit full potentials of large-scale parallelism in the large-scale parallel system and increase productivity of parallel programming.

In 2018FY, in order to archive these objectives above, we carried out the following researches:

(1) We continued working on the development and improvement of XcalableMP (XMP) programming languages. XcalableMP is a directive-based language extension, designed by XcalableMP Specification Working Group (XMP Spec WG) including some members from our team as a community effort in Japan. In this year, we designed directives to optimize parallel stencil computation in XcalableMP. And, as an application for XcalableMP, we investigated the graph algorithm for the the Order/Degree problem. Using this algorithm, we participated in Graph Golf, an international competition of the Order/Degree problem held in Nov. 2018 and won the award.

(2) As an extension of XcalableMP to exascale computing, we are proposing a new programming model, XcalableACC, for emerging accelerator clusters, by integrating XcalableMP and OpenACC. In this year, by additional funding of SPPEXA project which is an international collaboration with French and Germany, we continued working on MUST verification tool to XMP for correctness checking of user applications.

(3) As the post-K computer will be a large-scale multicore-based system, we are investigating programming models for manycore-based parallel systems as XcalableMP 2.0. We focus especially on the integration of dynamic tasking with PGAS programming model. In this year, We continued the design of programming models for task parallelism and PGAS.

(4) Co-design for HPC is a bidirectional approach, where a system would be designed on demand from applications, and applications must be optimized to the system. We are working on the design of tools for co-design, including the SCAMP profiler for the network of large scale systems.

(5) In order to exploit the full performance of large-scale systems, we had been proposed a multi SPMD programming model, which use multiple programming models across different architectural levels and had been developed a software to realize the proposed programming model by adopting a scientific workflow environment and a PGAS language called XcalableMP (XMP). we continued the evaluation using applications. This work has been carried out under the collaboration with MDLS, France.

(6) We expects Field Programmable Gate Array (FPGA) as one of the promising technologies for future acceleration technology. It is difficult for non-domain experts to program FPGAs due to the gap between their applications and hardware-level programming models for FPGAs. In this year, we investigate how to program the FPGA, and propose a C/C++ based programming framework, C2SPD, to describe stream processing on FPGA.

(7) We conducted several collaborations on the performance evaluation with JSC, University of Tsukuba, Kyusyu Institute of Technology and other groups. In this year, we carried out the performance study on NEST brain simulator developed by JSC, using Scalasca.

In addition to the research activities, we conducted promotion activities to disseminate our software. To promote XcalableMP as a means for parallelization of programs, we organized the XcalableMP workshop as follows:

- The 6th XcalableMP workshop (Nov. 1st, 2019, at University of Tsukuba)

2.3 Research Results and Achievements

2.3.1 Directive Extensions for Optimization of Parallel Stencil Computation in XcalableMP

Stencil computation is an important kernel in many applications (e.g. fluid simulation). Temporal blocking (TB) and communication/computation overlapping (OL) are known as techniques to optimize parallel stencil computation. We proposed features for TB and OL of a PGAS language XcalableMP (XMP), that is, the expand and margin clauses of the loop directive, and implemented a function to handle the features in the Omni XMP compiler. Using these features, it is possible to apply TB and OL to a stencil computation as shown in Figure 2.1 and 2.2, where BF stands for the Blocking Factor of temporal blocking.

We applied these features to the HIMENO benchmark and evaluated the performance on the K computer. First, the results of temporal blocking for the case of three-dimensional distribution is shown in Figure 2.3. At maximum 20% speedup is achieved with BF=2 on 512 nodes.

```
! Temporal Blocking
!$xmp shadow a(BF,BF)

do iter = 1, niters , BF
  !$xmp reflect (a)
  do k = BF-1, 0, -1
    !$xmp loop on t(i) expand(k,k)
    do j
      do i
       ....
```

Figure 2.1: Tempral Blocking Code

```
! Comm./Comp. Overlapping
!$xmp shadow a(s,s)

do iter = 1, niters, BF
  !$xmp reflect (a) async(100)
  !$xmp loop on t(i) expand(-s,-s)
  do j
    do i
  !$xmp wait async (100)
  !$xmp loop on t(i) margin(-s,-s)
  do j
    do i
       ....
```

Figure 2.2: Code for Communication/Computation Overlap

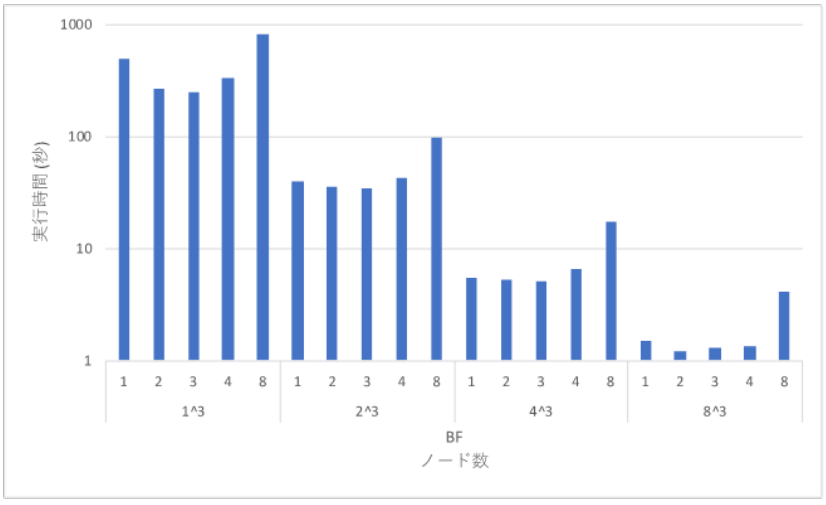

Figure 2.3: Performance of Temporal Blocking (3D distribution)

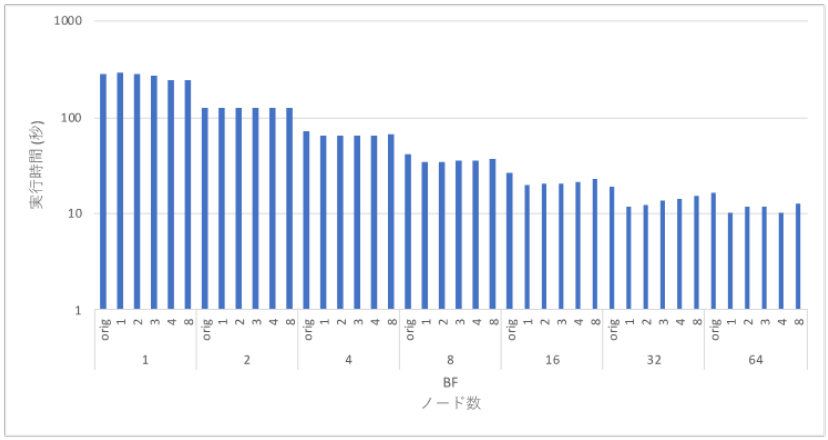

Figure 2.4: Temporal Blocking + Comm./Comp. Overlapping (1D distribution)

Secondly, the results of the combination of temporal blocking and comm./comp. overlapping for the case of one-dimensional distribution is shown in Figure 2.4. At maximum 40% speedup is achieved with BF=4 on 64 nodes.

There are some other cases where TB and/or OL causes performance degradation. It's mainly due to problems of a large overhead of asynchronous stencil communication (reflect directive) and the margin clause in Omni XMP. It is a future work to improve the implementation of them.

2.3.2 SCAMP (SCAlable Mpi Profiler) and auto generation method of pseudo MPI event trace files

In this work, we focus on communication performance prediction for large scale future systems. To estimate the communication performance, trace driven network simulators are widely used because of the ease of use. In order to estimate communication time of a target application, firstly, user should run the application on a real system in parallel to obtain MPI trace files from all MPI processes. Then, the trace files should be input into a network simulator. While the trace driven simulator is straightforward, sometimes it is not appropriate for the simulation of large parallel systems since it is difficult to obtain the number of trace files for the future system if the current system is smaller than the future one.

In order to tackle this scaling-problem in the trace driven simulator, we have been proposed a method called SCAMP (SCAlable Mpi Profiler), which creates a large number of pseudo trace files based on the small number of trace files obtained from a small system and drives the network simulator using the pseudo trace files to estimate the performance of the large systems.

Each of the MPI event trace file contains the arguments and time stamps of all MPI functions called during the real execution. Each of the pseudo MPI event trace files may also contain the arguments and time stamps of corresponding MPI functions, but the values of arguments are replaced with those computed with a new system size, i.e. a different MPI_Comm_size.

We have implemented a pseudo MPI event trace file generator based on the analysis of LLVM's intermediate representations.

Figure 2.5 shows the overview of the pseudo MPI-event trace file generation. the workflow of the automated generation of pseudo MPI-event trace files by LLVM-IR analysis. Firstly, we translate an original C source code into LLVM-IR by using the Clang/LLVM compiler. Then, our MPI-skeleton code generator analyzes LLVM-IR and extracts MPI function calls, their arguments required to estimate the communication performance, and the variables and instructions required to calculate these arguments. The resulted MPI-skeleton code written in LLVM-IR is compiled into an object file by Clang/LLVM compiler. The object file is linked with the dummy MPI library which outputs pseudo MPI-event traces to create an executable. The executable works as a pseudo MPI-event trace file generator. By giving the number of nodes in a target system and an MPI-rank ID, as well as a real MPI-event trace file, the generator creates a corresponding pseudo MPI-event trace file.

Figure 2.6 is the real and estimated execution times on K-computer for a 2-D stencil code. Figure 2.7 is the real and estimated execution times for the FFTE. We have compared the followings:

- real execution time on K computer

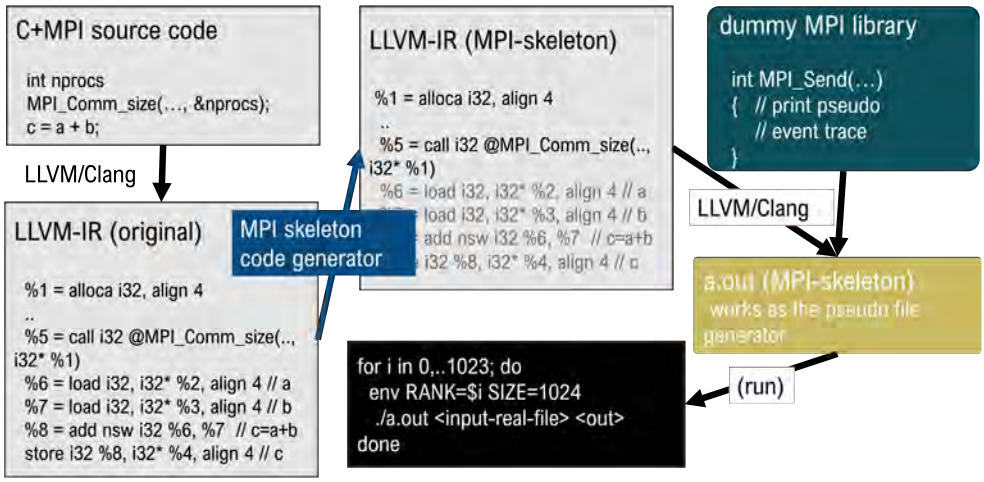

Figure 2.5: Overview of pseudo MPI-event trace file generation

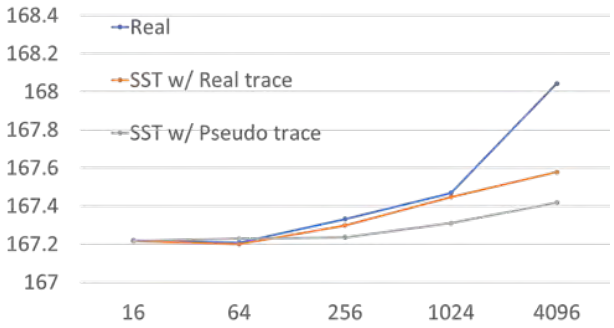

Figure 2.6: Results on K-computer for a 2-D stencil code

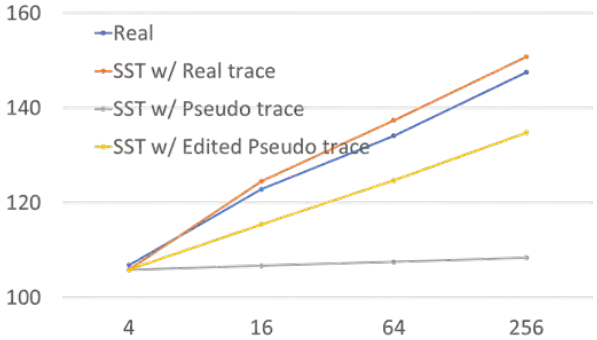

Figure 2.7: Results on K-computer for the FFTE

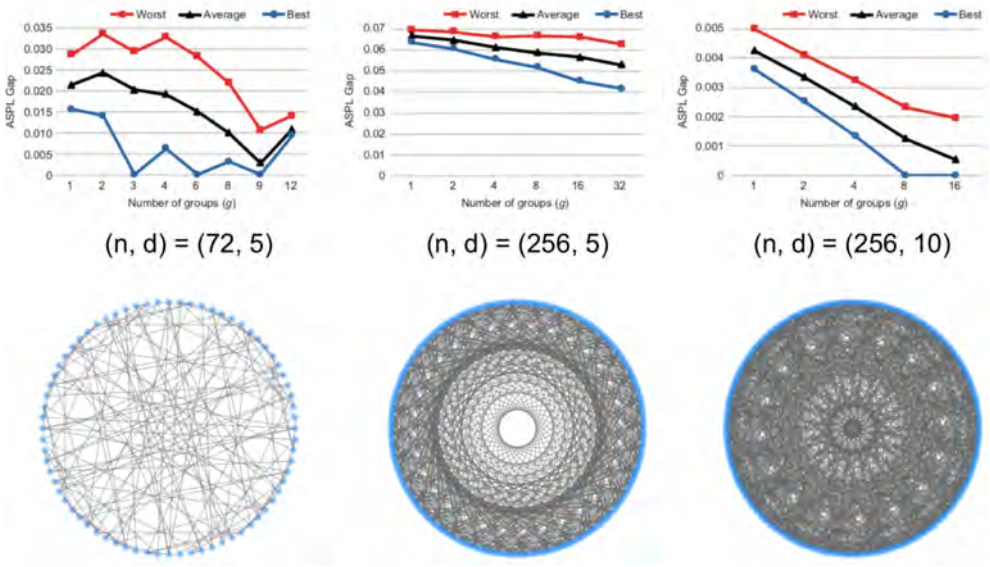

Figure 2.8: Evaluation results of the solution and search performance

- simulated execution time based on real MPI event trace files
- simulated execution time based on pseudo MPI event trace files

While due to the different communication algorithms implemented in the K computer and the network simulator, there are gaps between the simulator w/ real trace and the real system, the simulation with pseudo trace files, which has been proposed in this work, approximates the simulator w/ real traces.

2.3.3 Development optimization algorithm for the Order/Degree problem

We have developed a solver and algorithm for the Order/Degree Problem as one of the real applications of XMP. The Order/Degree problem is the problem of finding the undirected graph with the smallest diameter and ASPL (Average Shortest Path Length) from the set of undirected graphs that satisfy a given number of vertices (Order) and degree (Degree). The problem is an abstraction of the network topology in large-scale systems such as supercomputers and data centers as a graph theory problem, and it is known that it can be used for designing a network with high performance. Our research proposes an optimization algorithm for large-scale Order/Degree problem, and describes its solution search performance and parallelization.

We show the symmetry of the graph can be used to improve both the solution search performance of Simulated Annealing and the calculation time. In addition, hybrid parallelization using OpenMP and MPI is performed to achieve further reduction of calculation time.

The following graphs show parts of the evaluation of the solution search performance. The "number of groups" on the horizontal axis means the number of symmetries. The vertical axis means the difference between the theoretical lower bound of ASPL of the graph and the ASPL of the actually found graph. The best value is 0. The graphs show the results (worst/average/best values) of performing the proposed method 100 times changing the number of groups. The "(n, d)" means (number of vertices, number of degrees). The results show the solution search performance tends to be higher as the value of the number of groups is larger.

To evaluate speed performance for calculation of ASPL, we use the K computer and COMA system (Intel Xeon-E5 2670v2, 10Cores x 2 Sockets) which is located in University of Tsukuba. We use a large problem with (n, d) = (400000, 32).

First, we evaluate the calculation time using the graph symmetry. We measure time required to calculate one ASPL with several the number of groups (g). For comparison purpose, we used COMA system located in University of Tsukuba. Figure 2.9 shows the results of execution with one process and one thread in each calculation environment. The calculation times on the K computer and COMA for g=1 are 6.42×10^4 seconds and 1.96×10^4 seconds, and for g=10000 are 6.54 seconds and 2.02 seconds, respectively. The speed improvement rates are 9.82×10^3 for the K computer and 9.74×10^3 for COMA.

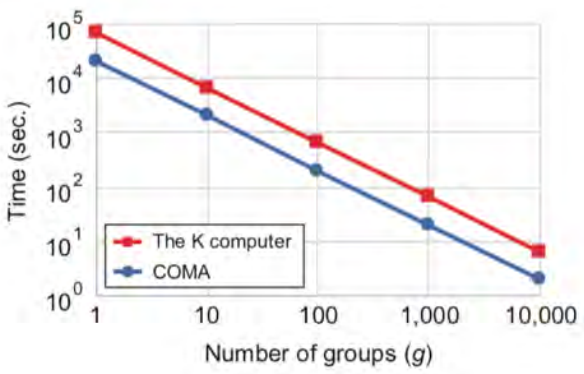

Figure 2.9: Execution time with one process and one thread varying the number of groups

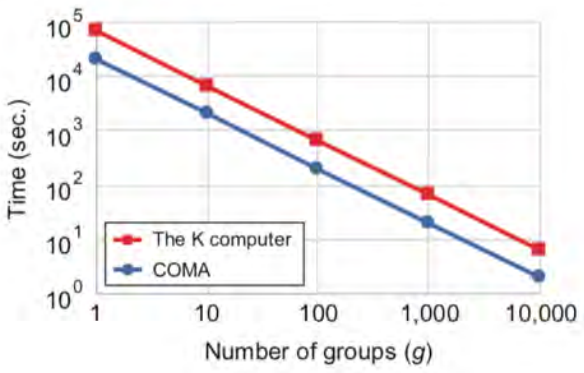

Figure 2.10: Calculation time changing the number of threads by one process (g=10000)

Next, we evaluate the calculation time by hybrid parallelization. In each computing environment, one process is allocated to one CPU. Figure 2.10 and Figure 2.11 show the results for g=10000. Figure 2.10 indicates the calculation times for the maximum number of threads and one process on the K computer and COMA are 1.01 seconds and 0.31 seconds, respectively. The speed improvement rates by thread parallelization are 6.45 for the K computer and 6.42 for COMA.

Finally, Figure 2.11 shows the results of process parallelization with the maximum number of threads. The smallest calculation times on the K computer and COMA are $3.96 \times 10^{(} - 3)$ seconds and $4.42 \times 10^{(} - 3)$ seconds, respectively. The speed improvement rates by process parallelization are 225.81 for the K computer and 71.02 for COMA. From this result, it was found that the K computer had higher parallelization efficiency than COMA.

Using this algorithm, we participated in Graph Golf, an international competition of the Order/Degree

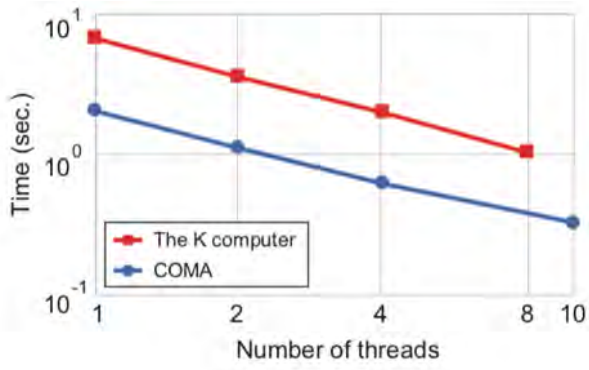

Figure 2.11: Calculation time changing the number of process (g=10000)

SPD Sample Code

```
float in[M][N];
float out[M][N];

#pragma spd region
for (int t = 0; t < TIME_STEP; t++) {
#pragma spd offload
  for (int i = 1; i < M-1; i++) {
    for (int j = 1; j < N-1; j++) {
      out[i][j] = (in[i][j-1] + in[i][j+1]
                +  in[i+1] + in[i-1][j]) * 0.25;
    }
  }
  ...
```

Figure 2.12: Laplace Solver Code with SPD directives

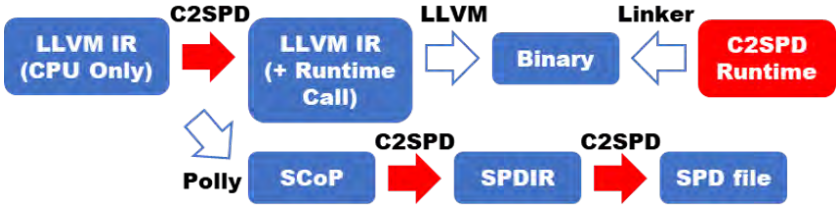

Figure 2.13: Overview of C2SPD Framework

problem held in Nov. 2018. We won the award in the Graph Golf, which indicates that our method is an excellent algorithm.

2.3.4 High productivity Programming and Optimization Framework for Stream Processing on FPGA

Because of the recent slowdown in silicon technology and increasing power consumption of hardware, several dedicated architectures have been proposed in High Performance Computing (HPC) to exploit the limited number of transistors in a chip with low power consumption. Although Field Programmable Gate Array (FPGA) is considered as one of the promising technologies to realize dedicated hardware, it is difficult for non-domain experts to program FPGAs due to the gap between thier applications and hardware-level programming models for FPGAs.

We propose a C/C++ based programming framework, C2SPD, to describe stream processing on FPGA. It uses SPGen, a dataflow High Level Synthesis (HSL) tool, as the FPGA backend. C2SPD can program FPGAs by adding directives to serial code, and the compiler translates it into optimized SPGen code. Figure 2.12 shows the laplace solver code with SPD directives as an example. The range of application is limited in C2SPD due to its domain-specific approach. However it can generate efficient hardware on FPGAs when the programming model matches the target application.

Figure 2.13 shows the overview of the C2SPD framework. It takes C/C++ code as input and translates it into SPGen's DSL code and CPU binary code. The DSL code is translated into Verilog HDL code by the SPGen backend and passed to the vendor's FPGA compiler to generate hardware. The CPU binary code includes C2SPD runtime calls to manipulate FPGA, and transfer data between CPU and FPGA.

2D-stencil computation is written in C2SPD to evaluate the performance of our C2SPD compiler implementation. 2 lines of the C2SPD directives are added into the serial C code to generate FPGA hardware. The Optimized FPGA hardware achieves 175.41 GFLOPS by using 256 stream cores, which is 222 times faster than a single stream core.

2.4 Schedule and Future Plan

We have been developing a production-level XcalableMP compiler, and make it available for the K computer's users as well as the users of conventional clusters. We are now working on the next version, XcalableMP 2.0, for cutting-edge high performance systems with manycore processors by multitasking with integrations of PGAS model and synchronization models for dataflow/multitasking executions. In this new programming model, the execution of the program is decomposed into several tasks executed according the dependency between tasks. This model will enables less overhead of synchronization eliminating expensive global synchronization, overlap between computation and communication in manycore, and light-weight communication by RDMA in PGAS model. we will extend this programming model to combine several kinds of accelerators such as GPU, FPGA and special-purpose processors with large-scale general-purpose manycore systems.

It enables some task to be offloaded into the accelerators such as FPGA as well as each core in modern manycore processor. We consider this configuration as a general global architecture of the future system as some part of system will be specialized for high performance and power efficiency. Our programming model will make it easy to adopt the existing computational science program to the new systems.

Our long-term goal is to establish the programming model for high-performance computing systems in Post-Moore's era. Recently, the slow-down in progress of the semiconductor fabrication technologies is pointed out as a serious problem of the future computer system, and it is said that the "post-Moore" era is coming in near future after Moore's low ends. Since modern high-performance computing systems has improved its performance by advanced semiconductor technologies, it is necessary to reconsider overall structure of computer architecture including hardware and software for the evolution the architecture of system, in order to improve performance in the post-Moore's era.

Our approach is to reconsider system's architecture from programing model's point of view. Since even new systems in post Moore's era should be shared by many computational science users, the system must have a certain degree of generality to make the cost for transition to the new systems lower. As well as providing comprehensive architectural view of the system, the programming models for the systems should bridge the gap between the new architecture and user's view.

2.5 Publications

2.5.1 Articles/Journal

[1] Masahiro Nakao, Hitoshi Murai, Hidetoshi Iwashita, Taisuke Boku, Mitsuhisa Sato: Implementation and evaluation of the HPC challenge benchmark in the XcalableMP PGAS language. IJHPCA 33(1) (2019)
[2] Y. Maruyama and A. Mitsutake "Analysis of Structural Stability of Chignolin", J. Phys. Chem. B 122, 3801-3814 (2018).

2.5.2 Conference Papers

[1] Joachim Protze, Simon Schwitanski, Matthias S. Müller, Hitoshi Murai an Miwako Tsuji, Taisuke Boku, Serge Petiton and Nahid Emad,MYX - MUST Correctness Checking for YML and XMP Programs, ISC,On Line, 2018.06.24-06.28,Messe Frankfurt Frankfurt Germany,ISC-18,2018.
[2] Thomas Dufaud, Miwako Tsuji and Mitsuhisa Sato, Design of Data Management for Multi-SPMD Workflow Programming Model, Fourth International IEEE Workshop on Extreme Scale Programming Models and Middleware, On Line, 2018.11.10-11.16, Kay Bailey Hutchison Convention Center Dallas TX USA,IEEE,2018.
[3] Jérôme Gurhem, Miwako Tsuji, Serge G. Petiton, Mitsuhisa Sato: Distributed and Parallel Programming Paradigms on the K computer and a Cluster. HPC Asia 2019: 9-17
[4] Masahiro Nakao, Hitoshi Murai, Mitsuhisa Sato: Multi-accelerator extension in OpenMP based on PGAS model. HPC Asia 2019: 18-25
[5] Miwako Tsuji, Taisuke Boku, Mitsuhisa Sato: Scalable communication performance prediction using auto-generated pseudo MPI event trace. HPC Asia 2019: 53-62
[6] Masahiro Nakao, Hitoshi Murai, Mitsuhisa Sato: A Method for Order/Degree Problem Based on Graph Symmetry and Simulated Annealing with MPI/OpenMP Parallelization. HPC Asia 2019: 128-137
[7] Ksander Ejjaaouani, Olivier Aumage, Julien Bigot, Michel Mehrenberger, Hitoshi Murai, Masahiro Nakao, Mitsuhisa Sato: InKS, a Programming Model to Decouple Performance from Algorithm in HPC Codes. Euro-Par Workshops 2018: 757-768

[8] Jinpil Lee, Tomohiro Ueno, Mitsuhisa Sato, Kentaro Sano: High-productivity Programming and Optimization Framework for Stream Processing on FPGA. HEART 2018: 5:1-5:6
[9] Hitoshi Murai, Mitsuhisa Sato, Masahiro Nakao, Jinpil Lee: Metaprogramming Framework for Existing HPC Languages Based on the Omni Compiler Infrastructure. CANDAR Workshops 2018 (6th International Workshop on Large-scale HPC Application Modernization): 250-256
[10] Joseph Schuchart, Keisuke Tsugane, José Gracia, Mitsuhisa Sato: The Impact of Taskyield on the Design of Tasks Communicating Through MPI. IWOMP 2018: 3-17
[11] Yutaka Watanabe, Jinpil Lee, Taisuke Boku, Mitsuhisa Sato: Trade-Off of Offloading to FPGA in OpenMP Task-Based Programming. IWOMP 2018: 96-110
[12] Yutaka Maruyama: Correction term for 3D-RISM solvation free energy functional based on reference-modified density functional theory, Joint Conference of EMLG/JMLG Meeting 2018 and 41st Symposium on Solution Chemistry of Japan

2.5.3 Invited Talks

[1] Mitsuhisa Sato, CREST and other Japanese Exascale Initiatives, Second French-Japanese-German Workshop on Programming and Computing for Exascale and Beyond Embassy of Germany in Tokyo, October 30-31, 2018.
[2] Mitsuhisa Sato, XcalableMP: Directive-based language extensions for PGAS programming model, SPP-EXA MXY projects Meeting, Aachen, Germany, March, 2019.
[3] Mitsuhisa Sato, Co-design for Post-K ARM for HPC - Co-design Opportunities, Birds of a Feather ISC 2018.
[4] Mitsuhisa Sato, Update of HPC in Japan, HPC in Aisa, ISC 2018, June 27, 2018
[5] Mitsuhisa Sato, The post-K for general-purpose, energy-efficient and sustained application performance, ATIP's 2nd International Workshop on Exascale and Next-Generation Computing Programs and Workforce Development, at SC 18, 11th Nov 2018
[6] Mitsuhisa Sato, The post-K for general-purpose, energy-efficient and sustained application performance, Arm HPC User Group Session, at SC 18, 12th Nov 2018
[7] Mitsuhisa Sato, Task parallelism and PGAS - Trends and Challenges on Programming Models for Extreme-Scale Computing -, The International HPC Summer School on Challenges in Computational Sciences 2018 in Ostrava, Czech Republic.
[8] Mitsuhisa Sato, XcalableMP PGAS language as a parallel tool, Keynote of the 12th International Parallel Tools Workshop in Stuttgart, Germany, 17th Sep. 2018
[9] Mitsuhisa Sato, Overview of the Post-K processor, CCS International Symposium 2018, Univ. of Tsukuba, 15th Oct 2018.
[10] Mitsuhisa Sato, Omni Compiler project: An infrastructure for source-to-source transformation of directive-based programming language, International Workshop on Legacy HPC Application Migration, at CANDAR'18, Nov. 28, 2018

2.5.4 Software

- Omni XcalableMP compiler ver. 1.3 (registered as an R-CCS-supported software)

2.5.5 Patents

None.

Chapter 3

Processor Research Team

3.1 Members in the fiscal year of 2018

Kentaro Sano (Team Leader)

Tomohiro Ueno (Postdosctoral Researcher)

Takaaki Miyajima (Postdosctoral Researcher)

Jens Christoph Huthmann (Postdosctoral Researcher)

Artur Podobas (Postdosctoral Researcher)

Antoniette Pangilinan Mondigo (Student Trainee)

Shin Abiko (Student Trainee)

Kohei Hijikata (Student Trainee)

Kouki Watanabe (Student Trainee)

3.2 Aim of Team

The aim of the processor research team is to explore and establish data-flow-based parallel computing models and high-performance computer architectures which are promising and necessary as next-generation computing technologies in the forthcoming post-Moore era. We are researching and developing general-purpose processor architectures different from existing multi/many-core processors, hardware and system software for reconfigurable computing, and any specific custom computing machines, as well as system software for data/task-flow-based high-performance computing to efficiently utilize large-scale parallel machines such as the K computer and the post-K computer.

In the next decade, sooner or later, the Moore's law as planar lithography-scaling is going to end and therefore we will be no longer able to rely on two-dimensional scaling of CMOS devices. In this "post-Moore" era, transistor integration, power consumption per transistor, and relative latency of data movement to the transistor's switching speed are not sufficiently improved. Consequently, it is predicted that the conventional approaches cannot increase the performance and performance per power, which have been so far improved mainly by the semiconductor scaling. Accordingly, we will need to more efficiently and effectively utilize available hardware resources to achieve target performance. In particular, the conventional many-core architectures and large-scale computing systems with the paralel computing model based on global synchronization will be confronted with performance issues due to the following reasons:

1) dark silicon problem where most of transistors cannot be utilized due to the upper limit of on-chip power consumption. Since power per transistor does not decrease, we need to inactivate a large portion of transistors even if we have more transistors integrated on a chip,

2) relatively-increasing latency to transistor's switching/processing speed. Due to the increasing latency, we can no longer shorten cycle time to update memory elements with some computation, cycle time to control computation based on some decision, and the synchronization time among a large number of physically-distributed nodes,

3) inefficient data-movement among on-chip cores via a memory subsystem or through a global network in a system, and

4) a large overhead in global synchronization for large-scale parallel computation which is affected by relatively-increasing delay of data transfer through a system-wide network.

That is, the existing approaches are not designed to scale the performance under these severe conditions. For example, the von-Neumann architecture is based on two cycles of "memory-element update" and "control" which cannot be accelerated any more, and therefore parallel processing is introduced as pipelining, super-scalar, and many cores as well as latency-hiding techniques of memory hierarchy with cache memories, speculative execution with branch prediction, and simultaneous multi-threading. These additional mechanisms make semiconductor resource utilization much worse for target processing and computing. In addition, the global barrier in parallel computation degrades overall performance as more nodes are utilized.

On the other hand, we have good hope that bandwidth can be improved in a package and in a system with technologies of new memory devices, silicon interposer, 3D stacking, and photonics. We can also expect a larger number of transistors in a system with more chips, even if each chip cannot scale. Then, the challenge for computer architects like us is how to efficiently utilize hardware resource available under the above limitations for performance improvement. For this challenge, we believe that custom and spatially-mapped computing based on a data-flow model without explicit global-synchronization is a key to solution.

The custom computing allows us to efficiently utilize hardware resources for target computation while architectural overhead for reconfiguration, which can be seen in FPGA device, is also suitable for the dark silicon problem. The spatially-mapped computing and the data-flow allow us to avoid or mitigate cycles in processing. By spreading a sequence of operations onto space on hardware with a data flow, we can avoid instruction execution cycles with memory-element update and control so that we can increase a computing throughput with fine-grain parallelism increased naturally. The data-flow or task-flow approach also allows us to avoid the global synchronization in large-scale parallel computing. If we automatically schedule and control task execution based on task-flow with task dependency, we can efficiently execute tasks without global synchronization when they become ready to be executed. Thus, we think that the localized feature of control, synchronization, and data-movement of the data/task-flow is necessary essentially for future computer architectures in the post-Moore era, and therefore we are researching them

In addition to these researches on future computer architectures, we will also contribute to improve performance of applications on the K or post-K computer by introducing the concept of the system-wide data/task-flow computing and reconfigurable computing. We are also researching applications which should be required to evaluate future computer architectures. Some of these researches are being conducted in collaboration with other research teams in R-CCS, universities in Japan (Tohoku university, University of Tsukuba, and Nagasaki university), and a research institute (Argonne national laboratory, US).

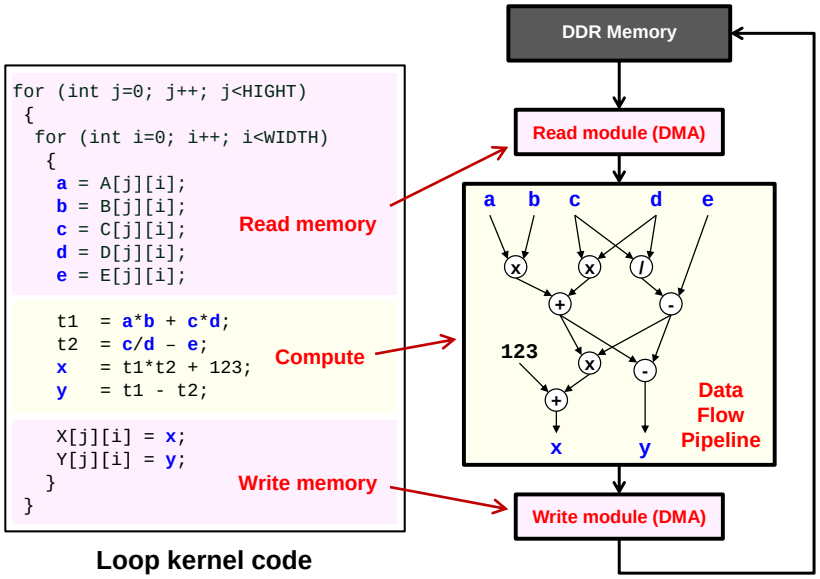

Figure 3.1: Data-flow stream computing of a nested-loop kernel on separated hardware components.

3.3 Research activities

3.3.1 Data-flow stream computing with FPGAs

We are researching a mechanism for data-flow stream computing with FPGAs. So far, we have defined a data-flow computing model for hardware implementation of a nested loop kernel. As shown in Fig.3.1, we separate memory read and write from computation and then map them to different hardware modules, respectively. In order to generate the data-flow pipeline module based on the data-flow computing model, we have also developed software of stream processor generator (SPGen) shown in Fig.3.2 which generates Verilog-HDL codes synthesizable for FPGA. SPGen takes an input of codes in our defined format, SPD (stream processing description).

In SPD, we can write two types of hardware structures hierarchically: 1) a data-flow graph (DFG) to define a processing element (PE) by writing formula with a static single assignment (SSA) form, and 2) an overall connection of existing PEs to define a new PE by writing module calls, as shown in Fig.3.2. Each node in a DFG and each PE follow the locally-synchronized firing rule of the data-flow computing model, where an operation or computation of the node or the PE can start only when all the input data arrive and become available. The hardware modules synthesized by SPGen contains control logic to support the the locally-synchronized firing rule as well as the flow-control mechanism with back pressures going upstream through the circuits.

By applying the data-flow stream computing model to several benchmark applications including Tsunami simulation, fluid dynamics simulation based on the lattice Boltzmann method, and N-body simulation, we have demonstrated the model and implementation. With Intel Arria10 FPGA, we achieved 442 GFlops for tsunami simulation in single precision at 36.3 W for power consumption of PCI-Express board while AMD Radeon R9 280X GPU achieves only 219 GFlops at 185 W, resulting in more than 10 times better performance per power than the GPU.

3.3.2 FPGA-based custom computing system

In order to achieve data-flow stream computing with FPGAs, we have researched and developed the FPGA-based custom computing system shown in Fig.3.3, where the data-flow compiler, SPGen, is utilized to generate an application core to be embedded into FPGA shell. On FPGA device in the prototype of a tightly-coupled FPGA cluster, we have implemented FPGA shell as system-on-chip (SoC) and Linux driver and API software to control the shell. The FPGA shell contains the controllers of extermal DDR3/4 memories, the PCI-Express interface, the network subsystems which are still under development, the user logic region, and a system interconnect for them.

Using the system, we have implemented and demonstrated FPGA-based custom computing for several applications described in Section 3.3.1. Once the data-flow based hardware is generated by SPGen with codes

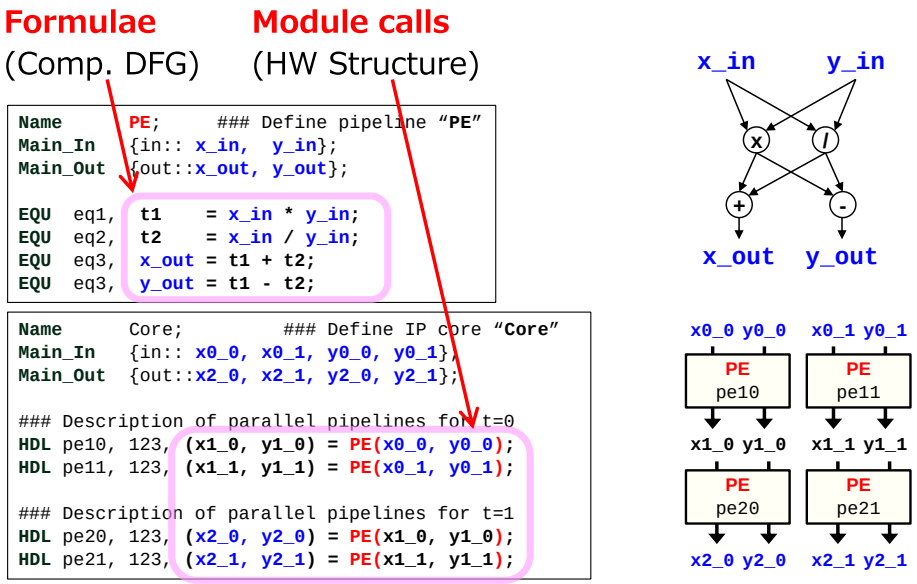

Figure 3.2: Stream processing description (SPD) format for SPGen (stream processor generator.

written in SPD, we program it to the FPGA and then execute software with the host CPU. The software opens the FPGA, uploads the data into FPGA's external memories, and starts computation with the data-flow based hardware on FPGA by writing some values into its control registers. These procedures can be programmed by using our defined APIs. The system was implemented with Intel Arria10 FPGA while we were also transplanting it to a new FPGA, Intel Stratix10 FPGA.

3.3.3 Inter-FPGA network for tightly-coupled FPGA cluster

The demonstration described in Section 3.3.1 was made with only a single FPGA. To further scale the performance with multiple FPGAs available in a system, we were researching and developing inter-FPGA network subsystem for a tightly-coupled FPGA cluster, as dedicated network to connect FPGAs. So far, we have developed a high-speed serial link (HSSL) to directly connect FPGAs with a flow control for back pressure. By using HSSL, we have developed a 1D ring network to scale the performance of stream comping with multiple FPGAs. We have demonstrated and evaluated scalability of the 1D ring approach of Fig.3.4a with our own performance model and experiments using Intel Arria10 FPGAs.

For more general-purpose communication among FPGAs, we were also designing and developing an on-chip router for 2D torus network with packet switching as shown in Fig.3.4b. We have implemented an initial version of the router and were verifying it. We were also considering and designing a virtual circuit switching network which implemented on the top of Ethernet-based network subsystem using high-speed Ethernet switches of 40Gb/s or 100Gb/s throughput. We considered a mechanism required for virtual circuit-switching and flow control of virtual links which are implemented as an upper protocol layer than the layer of Ethernet frames.

3.3.4 Feasibility study on extension of an existing supercomputer

As extended work of the FPGA-based custom computing system described in Section 3.3.2, we started feasible study on extending a supercomputer with custom computing machines with a tightly-coupled FPGA cluster, where some kernels suitable for custom hardware are offloaded from the supercomputer. We built the experimental prototype machine shown in Fig.3.5, which is composed of the ARM-based host servers, x86-based FPGA-gateway servers, and FPGAs connected to each other directly by the dedicated inter-FPGA network, which is described in Section 3.3.3.

We also developed a software to bridge the ARM servers and the x86 FPGA-gateway servers so that application software running on ARM servers can transparently access and utilize FPGAs installed on the x86 servers as if the FPGAs were installed on the ARM servers. We will develop system hardware and software for the tightly-coupled FPGAs, and evaluate performance of applications and kernels offloaded to them. We will also consider cooperative operation of the FPGA cluster with such an existing supercomputer like Fugaku.

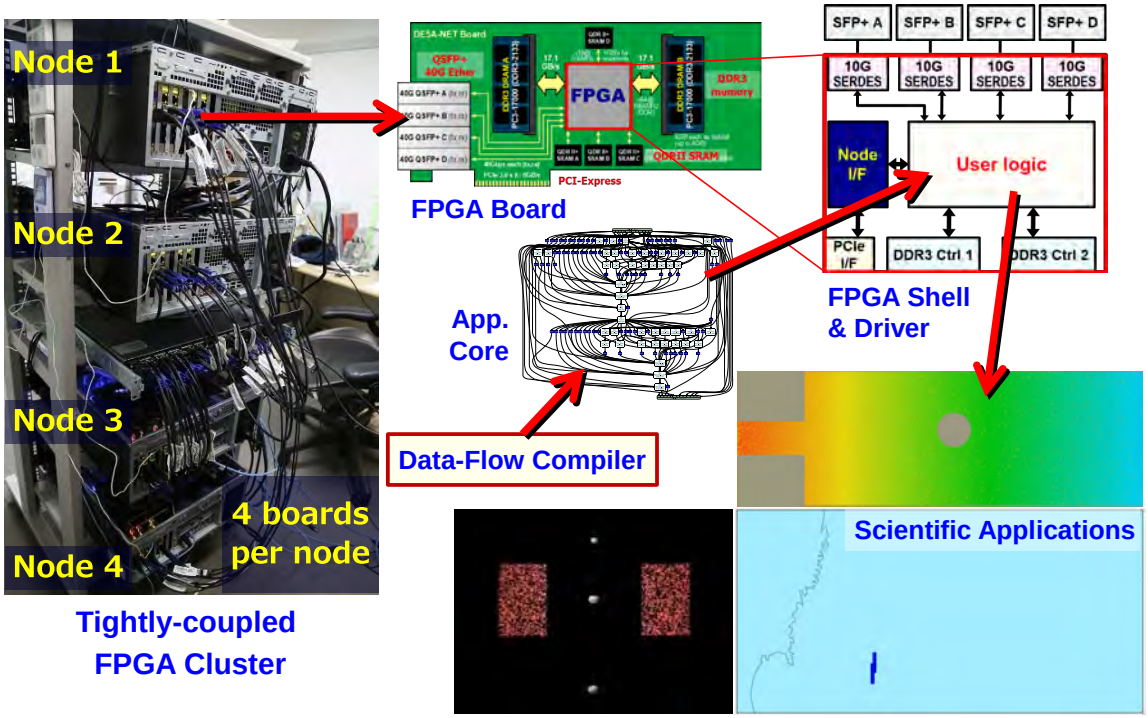

Figure 3.3: Overview of FPGA-based custom computing system.

3.4 Future Plan

In addition to the present researches, we are planning to conduct researches on the following topics as a result of the research activities.

3.4.1 Task-flow management for large-scale parallel computers

For such a hybrid system like the experimental prototype machine of Fig.3.5, we need to efficiently manage task execution with host CPUs and FPGAs. For this purpose, we will research and develop a system software with a task-flow-based mechanism to schedule and control tasks which are executed on hosts servers or offloaded to FPGAs. With this mechanism, programmers do not have to explicitly program schedules of task execution on hosts and FPGAs, but can achieve efficient execution of tasks with less overhead due to the scheduing automatically made by the software.

3.4.2 Future processor architectures based on coarse-grain reconfigurable array (CGRA)

Although FPGA is a feasible device to achieve data-flow-based custom computing for now, it is not always the best device for reconfigurable computing or custom computing in future. There should exist more appropriate architectures than FPGA for a domain of target applications and kernels. We will explore such future processor architectures focusing on coarse-grain reconfigurable arrays (CGRAs), where programmable functional units are connected in an array so that data-flow graphs can be mapped efficiently on them. We also need to research and develop a simulator and a compiler for CGRA processors. We will evaluate performance, efficiency as a unit utilization ratio, requirement of external memory-bandwidth, area and power consumption for CMOS implementation, and so on. We are also researching processor architectures for neuromorphic computing.

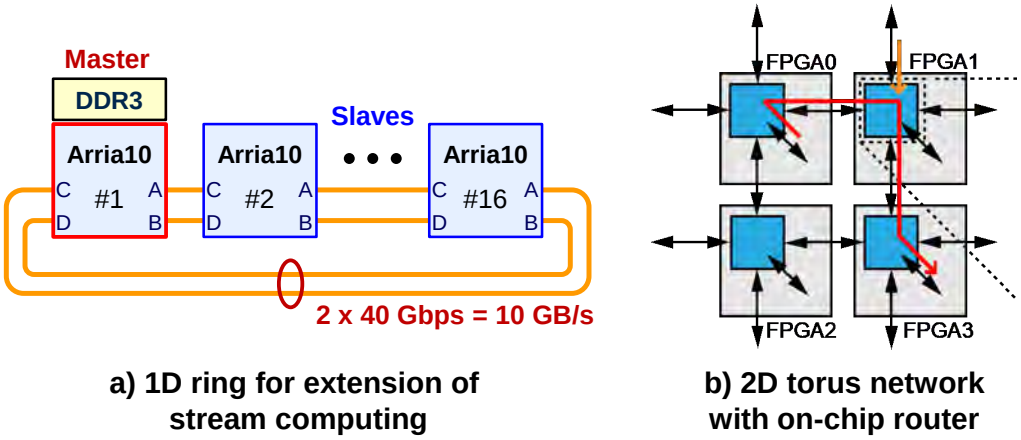

Figure 3.4: Inter-FPGA network examples.

3.5 Research Outputs

3.5.1 Publications with peer review

[1] Jens Huthmann, Shin Abiko, Artur Podobas, Kentaro Sano and Hiroyuki Takizawa, "Scaling performance for N-Body Stream Computation with a ring of FPGAs," Proceedings of the International Symposium on Highly-Efficient Accelerators and Reconfigurable Technologies (HEART), (to appear), 2019.

[2] Takaaki Miyajima, Tomoya Hirao, Naoya Miyamoto, Jeongdo Son, and Kentaro Sano, "An implementation and evaluation of local and remote direct memory transfer on FPGA cluster," Proceedings of the International Symposium on Highly-Efficient Accelerators and Reconfigurable Technologies (HEART), (to appear), 2019.

[3] Antoniette Mondigo, Tomohiro Ueno, Kentaro Sano, and Hiroyuki Takizawa, "Scalability Analysis of Deeply Pipelined Tsunami Simulation with Multiple FPGAs," IEICE Transactions on Information and Systems (Special Section on Reconfigurable Systems), Vol.E102-D,No.5, May. 2019.

[4] Jinpil Lee, Tomohiro Ueno, Mitsuhisa Sato, and Kentaro Sano, "High-productivity Programming and Optimization Framework for Stream Processing on FPGA," Proceedings of the International Symposium on Highly-Efficient Accelerators and Reconfigurable Technologies (HEART), (to appear), 2018.

[5] Tomohiro Ueno*, Kentaro Sano, and Takashi Furusawa, "Performance Analysis of Hardware-Based Numerical Data Compression on Various Data Formats," Proceedings of the Data Compression Conference (DCC), pp.345-354, DOI:10.1109/DCC.2018.00043, March, 2018.

[6] Antoniette Mondigo, Kentaro Sano, and Hiroyuki Takizawa, "Enhancing Memory Bandwidth in a Single Stream Computation with Multiple FPGAs," Proceedings of International Conference on Field-Programmable Technology (FPT'18), (3 pages), Dec 12, 2018.

[7] Takaaki Miyajima, Tomohiro Ueno, and Kentaro Sano, "Stream Computing of Lattice-Boltzmann Method on Intel Programmable Accelerator Card," Fourth International Workshop on Heterogeneous High-performance Reconfigurable Computing (H2RC'18), (1 page), Nov 11, 2018.

3.5.2 Invited talks (keynote, plenary talk, invited talk, panelist position talk)

[8] 佐野 健太郎, "FPGAを用いた高性能計算の可能性とデータフロープログラミング," 東北大学NPC(New Paradigm Computing)研究会, 東北大学電気・情報系3号館　2F セミナールーム, March 4, 2019.

[9] Kentaro Sano, "Reconfigurable Computing for HPC: Will It Make It this Time?," SC18 Panel: Reconfigurable Computing for HPC Will It Make It this Time, Dallas Convention Center, November 14, 2018.

[10] Kentaro Sano, "Benchmarking Scientific Reconfigurable/FPGA Computing," SC18 BOF: Benchmarking

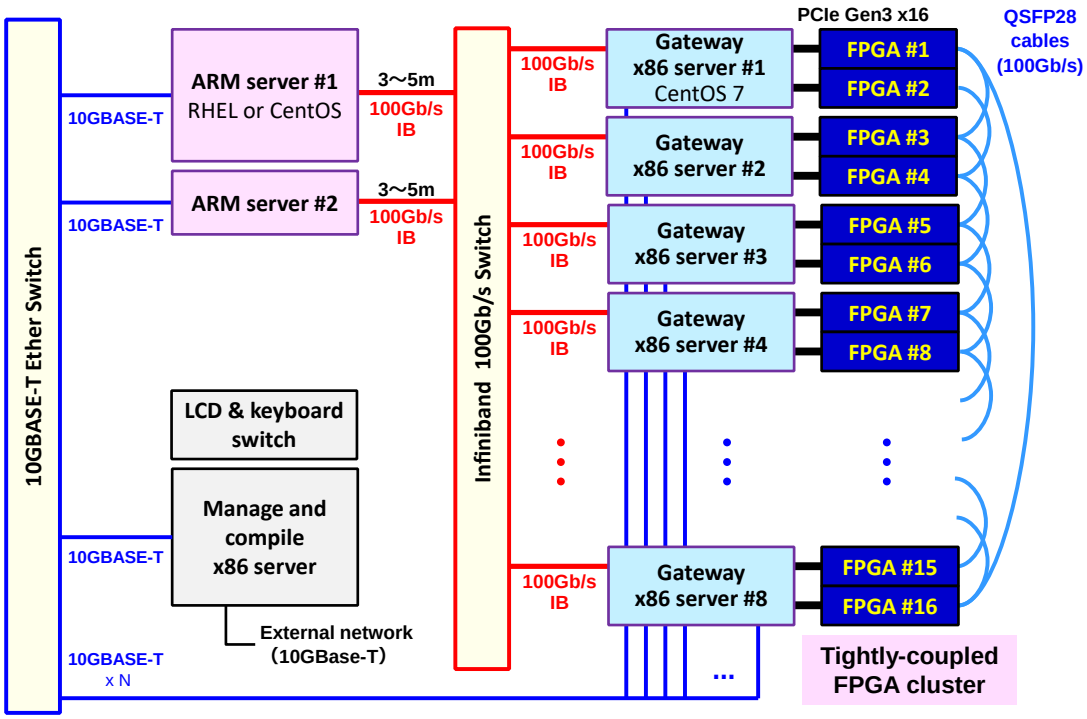

Figure 3.5: Experimental prototype machine for extension of an existing supercomputer.

Scientific Reconfigurable FPGA Computing, Dallas Convention Center, November 14, 2018.

[11] Kentaro Sano, "FPGA-based Data-Flow Computing for High-Performance Numerical Simulation," 13th International Meeting on High Performance Computing for Computational Science (VECPAR), Sao Pedro, SP, Brazil, September 18, 2018.

[12] Kentaro Sano, "FPGA-based Data-Flow Computing for Tsunami Simulation," Open Lecture at Argonne National Laboratory, August 23, 2018.

[13] Kentaro Sano, "FPGA-based Data-Flow Computing for Tsunami Simulation," 8th JLESC (Joint Laboratory on Extreme Scale Computing) Workshop, Barcelona Supercomputing Centre (UPC Campus Nord premises), Barcelona, Spain, April 19, 2018.

3.5.3 Papers with no review

[14] 渡部 裕, 李 珍泌, 佐野 健太郎, 朴 泰祐, 佐藤 三久, "FPGAへのオフロード最適 化のためのSPGenとOpenCLの統合の検討," 第168回ハイパフォーマンスコンピューティング研究発 表会 情報処理学会研究報告, Vol.2019-HPC-168, No.11, pp.1-10, Mar, 2019.

[15] 宮島 敬明, イェンス ハットマン, 佐野 健太郎, "Lattice-Boltzmann Method の IntelProgrammable Accelerator Card への実装と評価," 電子情報通信学会リコンフィギャラブ ルシステム研究会 信学技法, Vol.118, No.432, pp.125-130, Jan 30-31, 2019.

[16] 木田 智大, 川俣 裕一, 柴田 裕一郎, 佐野 健太郎, "データフロー型計算アプリ ケーション用DMACの高位合成による自動設計," 電子情報通信学会リコンフィギャラブルシステム 研究会 信学技法, Vol.118, No.432, pp.95-99, Jan 30-31, 2019.

[17] 川俣 裕一, 木田 智大, 柴田 裕一郎, 佐野 健太郎, "FPGA上での部分再構成を使 用したストリーム向けクロスバの実装と検証," 電子情報通信学会リコンフィギャラブルシステム 研究会 信学技法, Vol.118, No.432, pp.113-118, Jan 30-31, 2019.

[18] 李 珍泌, 上野 知洋, 佐藤 三久, 佐野 健太郎, "ストリーム計算ハードウェアコ ンパイラSPGenのためのPolyhedral Model を用いたループスケジュール最適化," 第167回ハイパ フォーマンスコンピューティング

研究発表会 情報処理学会研究報告, Vol.2018-HPC-167, No.12, pp.1-6, Dec,2018.

[19] 高木 雄介, 渡邊 実, 佐野 健太郎, “ロボット制御アルゴリズムのFPGAへの実装,” 電子情報通信学会リコンフィギャラブルシステム研究会 信学技法, Vol. 118, No. 340, RECONF2018-44,pp.55-60, Nov 28, 2018.

[20] 上野知洋, 土方康平, 佐野健太郎, “大規模FPGA クラスタのためのRDMA 通信機構,” 電子情報通信学会リコンフィギャラブルシステム研究会 信学技法, Vol.118, No.215, pp.49-54, Sep, 2018.

Chapter 4

Large-scale Parallel Numerical Computing Technology Research Team

4.1 Members

Toshiyuki Imamura (Team Leader)

Yiyu Tan (Research Scientist)

Shuhei Kudo (Postdoctoral Researcher)

Tetsuya Sakurai (Senior Visiting Researcher, University of Tsukuba)

Daisuke Takahashi (Senior Visiting Researcher, University of Tsukuba)

Franz Franchetti (Senior Visiting Researcher, Carnegie Mellon University)

Takeshi Fukaya (Visiting Researcher, Hokkaido University)

Daichi Mukunoki (Visiting Researcher, Tokyo Women Christian University)

Yusuke Hirota (Visiting Researcher, Tokyo Denki University)

Sarah Huber (Visiting Researcher, Bergische Universtät Wuppertal)

Martin Galgon (Visiting Researcher, Bergische Universtät Wuppertal)

Andreas Marek (Visiting Researcher, Max-Plank Computing & Data Facility)

Doru Adrian Thom Popovich (Student Trainee, Carnegie Mellon University)

Masaaki Aoki (Student Trainee, Kobe University)

Masatoshi Takayanagi (Student Trainee, Yamanashi University)

Mike Tsai Yaohung (Intern, University of Tennessee Knoxville)

Patric Daniel Howard (Intern, Notre Dame University)

Ryo Yoda (Intern, Kougakuin University)

Aya Motohashi (Assistant)

4.2 Research Activities

The Large-scale Parallel Numerical Computing Technology Research Team conducts research and development of large-scale, highly parallel and high-performance numerical software for the national flagship systems, K computer and supercompter Fugaku. In general, simulation programs require various numerical techniques to solve systems of linear equations, to solve eigenvalue problems, to compute and solve non-linear equations, and

to do fast Fourier transforms. Naturally, our primary mission is to develop and deploy highly-parallelized and scalable numerical software and a user-friendly integration framework on the K computer, namely KMATHLIB. It comprises above-mentioned software components (numerical software) in order to run a specific simulation code which come from scientific and engineering domain problems. Also, the K- and Fugaku- related issues are also our challenging works such as

- communication reducing and avoidance,
- cooperation with advanced devices,
- fault detection (soft-error), and
- precision-aware computing (higher-or-reduced/variable-or-mixed accuracy).

Since 2016 we have added three research themes; i) investigation of unexplored numerical fields like a tensor decomposition, ii) acceleration on some emerging devices such as an FPGA (Field Programmable Gate-Array), and iii) numerical reproducibility.

We are going to complete our mission through a tighter collaboration among trilateral communities from computational science (simulation), computer science (hardware and software), and numerical mathematics. Our final goal is to establish fundamental techniques to develop numerical software libraries for next-generation supercomputer systems based on active cooperation within R-CCS.

4.2.1 Kevd: a highly-optimized symmetric EVD solver targeted to manycore CPUs

Kevd was developed as an optimized implementation of the eigenvalue decomposition (EVD) solver for the K-computer and extended to the supercomputer Fugaku. In particular, the tridiagonalization part of Kevd, which is known as the bottleneck part of the EVD algorithm, was vectorized on the ARM-SVE format and other SIMD formats such as Intel AVX, AVX2, and AVX-512, Fujitsu SPARC HPC-ACE, and HPC-ACE2.

In general, the bottleneck of the tridiagonalization comes from its internal constructions on which a sequence of level-2 BLASs operations and all-reduce type communications are mainly utilized. The latest Kevd incorporates with the AoSoA(Array of Structures of Arrays) data-layout and the fixed-width specialized kernels. We exploited a kernel generator and refined the algorithm to obtain sustainable performance portability in the future systems (Figure 4.1). The results were presented at IPSJ SIGHPC165 [21], and HPC Asia 2019 with winning the **best paper award** [1].

4.2.2 A level-3-like micro-kernel construction for the Jacobi rotation

Through the collaboration with Prof. Yusaku Yamamoto from the University of Electro-Communications, the team has investigated the Jacobi methods for eigen- and singular value computation, and developed techniques to improve the performance of them. In FY2018, we developed a method to construct level-3 like kernels to achieve better performance without changing the convergence and the accuracy of the Jacobi methods.

The bottleneck part of the Jacobi methods is the Givens rotation which performs slowly like the level-1 BLAS kernels. We made use of a blocking technique called "full-blocking," which converts the rotations into xGEMM for better performance; however, the method affect the convergence and the error behavior of the Jacobi methods. To overcome the problem, we restructured the nested loops of the Given rotations to extract a micro-kernel structure using a similar technique in the level-3 BLASs. The resulted micro-kernels have high operational density and data-reusability like xGEMM; thus, it can improve the performance of the Jacobi method without the drawbacks of the "full-blocking." We achieved nearly 80% of the peak performance. The work was presented in IPSJ SIGHPC168 [22].

4.2.3 Implementation of a full set of Batched BLAS API

Batched BLAS is one of the new approaches for a task-based BLAS invocation, and it is defined as a new interface that allows users to execute multiple independent BLAS operations as a single subroutine call. Some of the high-demanded batched BLAS routines have been selected and developed for general CPUs, a many-core accelerated processor and GPUs, such as `cblas_batched_xgemm`, and they accelerated deep-learning domain codes. However, the existing implementation was limited to a few specific kernels. A full set of the BLAS routines (including level-1/2/3 routines) has not been provided.

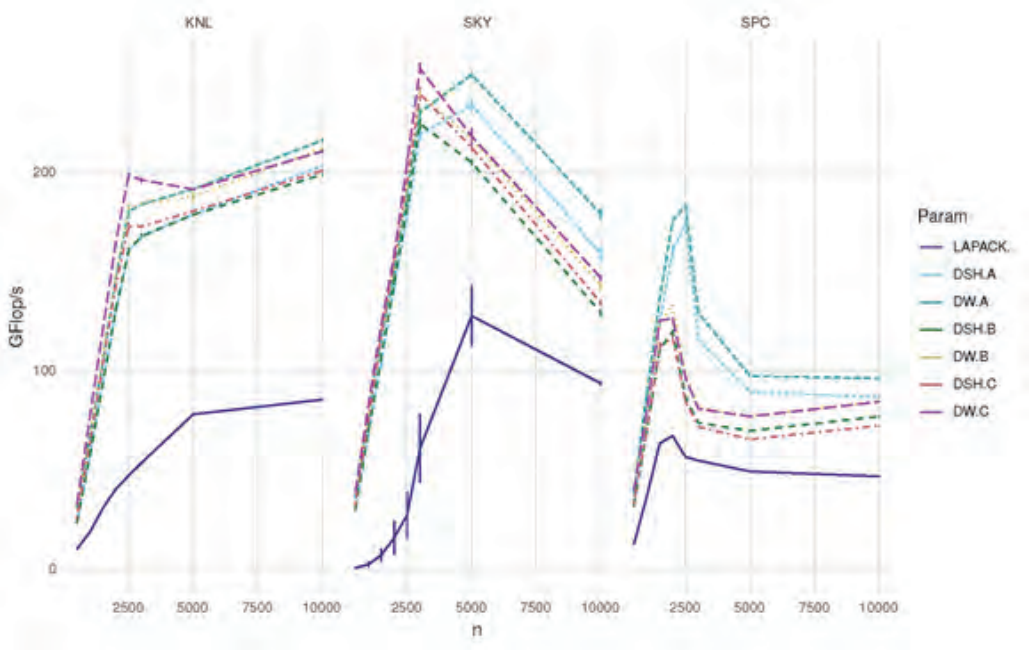

Figure 4.1: The performance of the latest Kevd and LAPACK

We have developed the first implementation of the level 1-2-3 full-set variable Batched (vbatched) BLAS interface compatible with the Intel MKL and MAGMABLAS. To develop the Batched BLAS, we introduced an efficient automatic code generation mechanism. The generated APIs include not only the invocation of underlying serial BLAS kernels but the parallel task scheduling based on a cost description by the user. Our preliminary evaluation on an Intel Xeon Phi 7210 processor demonstrated that the auto-generated batched BLAS routines achieved a competitive performance with the standard BLAS in the conference poster at ISC18 [8]. Our results suggest that such an automatic generation would be an effective method to develop batched BLAS routines for supercomputer Fugaku.

4.2.4 Performance evaluation and tuning of an FPGA-based matrix multiplier

Matrix multiplication is one of the fundamental building blocks of numerical linear algebra. It requires computer systems have huge computing capability and consumes much more power as problem size is increased. In this research, an OpenCL-based matrix multiplier with data parallelism is presented. When data are single-precision floating-points, compared with the software simulations based on the Intel MKL and OpenBLAS libraries carried out on a PC with 32 GB DDR RAM and an Intel i7-6800K processor running at 3.4 GHz, although the proposed matrix multiplier implemented by using the FPGA board DE5-NET achieves much worse performance in computation throughput, it gains 1.17 to 8.47 times, and 1.54 to 11.27 times in energy efficiency (Fig.4.2), respectively, even if the fabrication technology of the FPGA is 28 nm while it is 14 nm in the Intel i7-6800K processor. Furthermore, the performance tuning results show that the matrix multiplier obtains the best performance in the case of the block size being 64x64 and the kernel vectorization being 4. The related results were presented at the conference PTPDA'18 [3] and ATAT'19 [24].

4.2.5 Performance evaluation of a toolkit for sparse tensor decomposition

Tensor decomposition has received much attention because of its ability of identifying latent relations and predicting missing elements in high-dimensional data through operations on low rank forms of tensors. However, the sparseness and high dimensionality of real-world datasets make the tensor decomposition slow, inefficient, and unscalable. In this research, the performance of a sparse tensor decomposition toolkit called SPLATT is implemented and evaluated on the K computer, a cluster based on the Intel Xeon Gold processors, and the Oakforest-PACS supercomputer. The results show that the SPLATT has the best scalability in the K computer among three systems, and the cluster outperforms the other two supercomputers in computation because of its

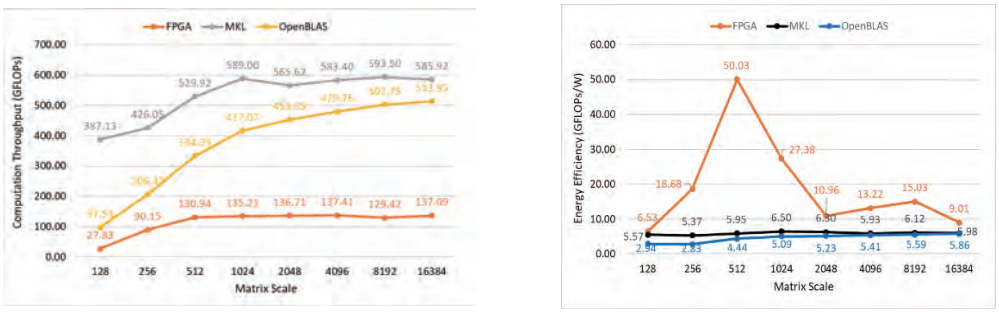

(a) Computation throughput

(b) Energy efficiency

Figure 4.2: Performance of the FPGA-based matrix multiplier

cores running at much higher clock frequency and large memory in each node, and the average computation performance of each core is the worst in the Oakforest-PACS because of its smallest memory size, and slowest clock frequency among three computer systems. In each iteration, the that the operation of multiplying a metricized tensor by a Khatri-Rao product (MTTKRP) consumes most of the time in each iteration and affects the performance significantly. The results were presented on the conference ACM HPDC [7].

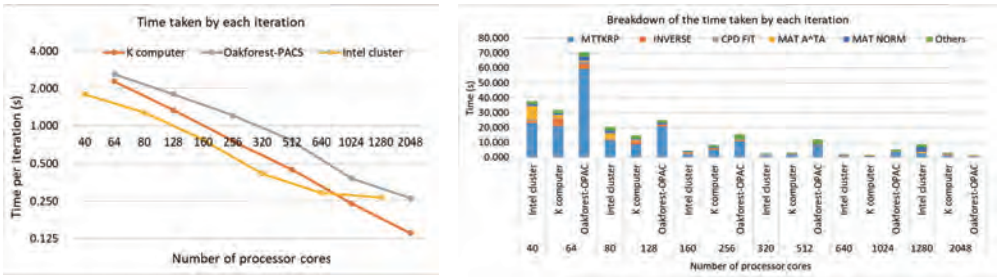

Figure 4.3: Performance tested by the dataset NELL-1

4.2.6 Other activities

In FY2018-2019, the following studies were also conducted, and we published papers:

- Performance optimization of HOTRG by finding Pareto optimum (PDSEC18 [6], MEPA at SWoPP18 [17], and JSIAM18 [18]),
- Communication-avoiding PCG algorithm on a real-3DCFD code (ScaLA18 [2]),
- Performance modeling and evaluation of 2.5D PDGEMM (ICCS18 [4], and [16]),
- Preliminary work of Auto-Tuning on our eigenvalue solver (JSIAM18 [19], and SIAM CSE19 [14]),
- Performance evaluation and algorithm improvement of eigensolvers (iWAPT18 [5], JLESC [9], PMAA18 [10], JIFT [11], and [11, 12, 13, 15, 20, 25]), and
- An embedded processor based on the object model (M&M(63)).

4.3 Schedule and Future Plan

The most significant task in next FY2019 and FY2020 is to complete the numerical software on the supercomputer Fugaku. For a general perspective and milestone on a short-term research, we would like to focus on following two topics and accelerate our research activities as well.

- **Communication avoiding algorithm:**

  We continue to investigate the communication avoiding algorithms and methods in any view of numerical linear algebra. The technologies will be applied on the algorithms of the existing CA-XX linear solvers, both dense and sparse eigenvalue solvers, the multi-dimensional FFT routines, and so on.

- **Precision-and-power aware computing:**

  We have studied high/mixed/reduced-precision numerical software. Recently, reduced-precision computing enforced by deep-learning becomes a significant driving force not only on industry/consumer's market but the HPC community. What is more, other critical issue came from power-saving was pointed out in the annular report last year. We will corporate with the stochastic and approximate approach and arbitrary precision arithmetics with the help of a reconfigurable device to reduce floating point operations and the total volume of the required hardware as well as energy consumption.

4.4 Publications

4.4.1 Articles

[1] Shuhei Kudo, and Toshiyuki Imamura: "Cache-efficient implementation and batching of tridiagonalization on manycore CPUs," Proc. HPC Asia 2019 (Jan. 14—15, 2019, Guangzhou, China), 2019.
[2] Yasuhiro Idomura, Takuya Ina, Susumu Yamashita, Naoyuki Onodera, Susumu Yamada, and Toshiyuki Imamura: "Communication Avoiding Multigrid Preconditioned Conjugate Gradient Method for Extreme Scale Multiphase CFD Simulations," Proc. IEEE CPS — ScalA18: 9th Workshop on Latest Advances in Scalable Algorithms for Large-Scale Systems
[3] Yiyu Tan, and Toshiyuki Imamura: "Performance Evaluation and Tuning of an OpenCL based Matrix Multiplier," Proc. The 24th International Conference on Parallel and Distributed Processing Techniques and Applications, Las Vegas, USA, July, 2018, pp. 107-113.
[4] Daichi Mukunoki and Toshiyuki Imamura: "Performance Analysis of 2D-compatible 2.5D-PDGEMM on Knights Landing Cluster," Proc. International Conference on Computational Science (ICCS 2018), Lecture Notes in Computer Science, Vol. 10862, pp. 853-858, Jun. 2018.
[5] Takeshi Fukaya, Toshiyuki Imamura, and Yusaku Yamamoto: "A case study on modeling the performance of dense matrix computation: Tridiagonalization in the EigenExa eigensolver on the K computer," Proc. The Thirteenth International Workshop on Automatic Performance Tuning (iWAPT2018), held in conjunction with IPDPS2018, pp. 1113-1122, Vancouver, Canada, May 25, 2018.
[6] Haruka Yamada, Akira Imakura, Toshiyuki Imamura, and Tetsuya Sakurai: "Optimization of Reordering Procedures in HOTRG for Distributed Parallel Computing." Proc. PDSEC2018, IPDPS Workshops 2018: 957-966
[7] Tan Yiyu: "A Hardware-oriented Object Model for Java in an Embedded Processor", Microprocessors and Microsystems, Vol. 63, 2018, pp. 85-97.

4.4.2 Oral talks and Poster presentations

[7] Yiyu Tan, and Toshiyuki Imamura: "Performance Evaluation of a Toolkit for Sparse Tensor Decomposition," The 27th International Symposium on High-performance Parallel and Distributed Computing (HPDC), Tempe, Arizona, USA, June, 2018.
[8] Yusuke Hirota, Daichi Mukunoki, and Toshiyuki Imamura: "Automatic Generation of Full-Set Batched BLAS," Research Poster, International Supercomputing Conference (ISC'18), 26 Jun 2018, Messe Frankfurt, Frankfurt, Germany
[9] Toshiyuki Imamura, Inge Gutheil: "Project Report, HPC libraries for solving dense symmetric eigenvalue problems – Performance benchmark of standard eigensolver on KNL systems," 8th JLESC meeting, April 18, 2018, Barcelona Supercomputing Center, Barcelona, Spain
[10] Toshiyuki Imamura: "Communication-Avoiding approaches of dense Eigenvalue / SVD problems," Efficient dense eigensolvers - Methods and applications I/II, 10th International Workshop on Parallel Matrix Algorithms and Applications (PMAA18), June 27-29, 2018, ETH Zurich, Zurich, Switzerland
[11] Toshiyuki Imamura: "Development of exascale matrix solvers based on communication avoiding algorithms," US-Japan JIFT Exascale Computing Workshop, July 30 - 31, Princeton Plasma Physics Laboratory, Princeton University, Princeton, NJ, USA

[12] Toshiyuki Imamura: "Development of a Dense Eigenvalue solver for Exa-scale Systems," International Workshop on Massively Parallel Programming for Quantum Chemistry and Physics 2019, Jan. 15–17, 2019, R-CCS, Kobe, Japan
[13] Toshiyuki Imamura, Yusuke Hirota, Daichi Mukunoki, Shuhei Kudo, Akiyoshi Kuroda, Naoki Sueyasu: "Development of Scientific Numerical Libraries on post-K computer," The 1st R-CCS International Symposium, Feb. 18-19, 2019, Kobe International Convention Center, Kobe, Japan (poster)
[14] Toshiyuki Imamura: "High Performance Eigensolver Exploiting an Online Tuning Mechanism," MS399: State-of-the-Art Auto-tuning: New Approaches and Algorithmic Innovations Towards Exascale Computing - Part II of II, 2019 SIAM Conference on Computational Science and Engineering (CSE19), Feb. 25–March 1, 2019, Spokane, USA.
[15] Toshiyuki Imamura: "Development of Scientific Numerical Libraries on post-K computer," Computing Sciences Seminars, LBNL, March 4, 2019, Berkeley, USA
[16]椋木 大地、今村 俊幸： 「2.5次元アルゴリズムを用いた高性能PDGEMMの開発」, スーパーコンピューティングニュース, 東京大学情報基盤センター、Vol.20, No.4, 2018.07, pp. 31-36.
[17]山田 悠加，今倉 暁，今村 俊幸，櫻井 鉄也: 「n次元モデル向けHOTRGの分散並列計算における配列の並び替えの最適化」, 日本応用数理学会「行列・固有値問題の解法とその応用」研究部会 第25回研究会, 2018年7月30日 (月) – 8月1日 (水), 熊本市国際交流会
[18]山田 悠加, 今倉 暁, 今村 俊幸, 櫻井 鉄也: 「計算手順と配列の並び替え手順の最適化によるn次元HOTRGの計算時間の削減」, 日本応用数理学会2018年度年会, 平成30年9月3日～5日 名古屋大学東山キャンパス(ポスター)
[19]今村 俊幸: 「EigenExaへのオンライン自動チューニング活用の試みについて」, 日本応用数理学会2018年度年会, 平成30年9月3日～5日 名古屋大学東山キャンパス
[20]工藤 周平: 「小・中規模固有値計算の高性能実装」, 研究会「データ駆動科学と高速計算科学」, 2018年7月17日, 東京大学駒場キャンパス
[21]工藤 周平, 今村 俊幸: 「三重対角化におけるメニーコア環境に適した同期手法」, 第165回HPC研究発表会 (SWoPP2018), 2018年8月1日, 熊本市国際交流会館
[22]工藤 周平, 今村 俊幸: 「高い演算密度をもつヤコビ回転カーネルの構成手法」, 第168回HPC研究会, 2019年3月5～7日, 石川県 山代温泉

4.4.3 Invited Talks

[24] Yiyu Tan, and Toshiyuki Imamura: "Design and Implementation of an OpenCL based Matrix Multiplier," 2019 Conference on Advanced Topics and Auto Tuning in High-Performance Scientific Computing (ATAT), Feb. 15-16,2019, College of Science National Sun Yat-sen University, Kaohsiung, Taiwan `https://sites.google.com/site/atathpsc/`
[25] Toshiyuki Imamura: "Development of a Dense Eigenvalue Solver for Exa-Scale Systems," MolSSI Workshop on Solving or Circumventing Eigenvalue Problems in Electronic Structure Theory, August 15-17, 2018, The Graduate Richmond, Richmond, VA, USA `https://wordpress.elsi-interchange.org/index.php/elsi-workshop-2018/`

4.4.4 Software

[26] EigenExa, `http://www.r-ccs.riken.jp/labs/lpnctrt/en/projects/eigenexa/`.
[27] KMATH_EIGEN_GEV, `http://www.r-ccs.riken.jp/labs/lpnctrt/en/projects/kmath-eigen-gev/`.
[28] KMATH_RANDOM, `http://www.r-ccs.riken.jp/labs/lpnctrt/en/projects/kmath-random/`.
[29] KMATHLIB_API, `http://www.r-ccs.riken.jp/labs/lpnctrt/en/projects/kmathlib-api`.
[30] KMATH_FFT3D, `http://www.r-ccs.riken.jp/labs/lpnctrt/en/projects/kmath-fft3d/`.
[31] ASPEN.K2, `http://www.r-ccs.riken.jp/labs/lpnctrt/en/projects/aspen-k2/`.
[32] MUBLAS-GEMV, `http://www.r-ccs.riken.jp/labs/lpnctrt/en/projects/mublas/`.
[33] SLFP, `http://www.r-ccs.riken.jp/labs/lpnctrt/members/mukunoki/slfp-0.0.1.tgz`.

Chapter 5

HPC Usability Research Team

5.1 Members

Hiroya Matsuba (Team Leader)

Motohiko Matsuda (Research Scientist)

Masatoshi Kawai (Postdosctoral Researcher)

5.2 Research Activities

The mission of the HPC Usability Team is to develop a software platform that contributes to increasing the number of uses of K computer. This team focuses on Cyber-physical systems as potential new use cases of supercomputers, expecting that simulation of infrastructure facilities will provide valuable information for its operation. For example, if a simulator of a cooling facility is available, the operator can search for an energy-efficient combination of parameters such as a temperature of cooling water, power of pumps, and positions of valves. Simulation is especially valuable because it enables operators to test parameters that are impossible to apply to the real facilities because of safety reasons.

The main obstacles in utilizing simulation technologies in cyber-physical systems are the difficulties in developing simulation programs. Although there are many simulator products, many of them focus on a specific technical aspects such as fluid dynamics or structural analysis, whereas simulation of industrial facilities requires a combination of various simulation techniques, such as a 1-D circuit, discrete event, or agent simulations as well as fluid or structural simulations. No one commercial software covers such a wide range of simulation techniques. The HPC Usability Research Team aims to develop a new programming framework that enables rapid development of simulation programs or programs that connect existing simulators, especially those for parallel computers. We assume engineers of companies who provide, for example, consulting service for factory management, use this programming framework.

We also aim to contribute to improving operational efficiencies of the K computer by actually adopting the techniques of the cyber-physical systems. By developing a simulator of the cooling and electric facilities of the supercomputer K or Fugaku, we expect we can improve operational efficiencies by, for example, reducing safety margins while ensuring the safety of the operation by using the simulator.

5.2.1 Development of the Pyne Parallel Programming Framework

We are developing a Pyne framework, which is a programming framework that enables ones to develop parallel programs as if they were sequential programs. The main objective of this framework is to improve the productivity of parallel programs, including simulation programs or programs for connecting existing simulators with another simulator or machine learning frameworks.

5.2.1.1 Basic Concepts of Pyne

Pyne enables higher productivity of parallel programs by enabling programmers to write parallel programs as if they were sequential ones. Because parallelizing arbitrary sequential programs efficiently is almost impossible,

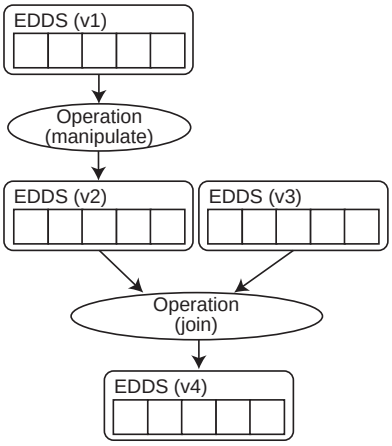

Figure 5.1: Example of Pyne's abstraction of a parallel program

```
 1  def main:
 2    v1 = edds.createVector(init=readStream)
 3    v2 = v1.manipulate(neighSize=1, func=avgFunc)
 4    v3 = edds.createVector(init=init3)
 5    v4 = edds.join(operands=(v2, v3),
 6                   neighSize=(0,0), func=addFunc,
 7                   dist=[1000])
 8    v5 = v4.out(func=writeStream)
 9    edds.final(v5)
10
11  def avgFunc(neigh):
12    return (neigh[0] + neigh[1] + neigh[2]) / 3.0
13
14  def addFunc(neigh):
15    return neigh[0][0] + neigh[1][0]
```

Figure 5.2: Example source code of a Pyne program

Pyne introduces an appropriate restriction on the type of supported application while maintaining as much flexibility as possible. To be specific, Pyne applications are required to be a series of operations on the data structures called the implementation independent data structure (IIDS). Figure 5.1 shows an example of the structure of a simple Pyne program. In this program, after the creation of an IIDS called v1, which is a vector (creation is also an operation but omitted from the figure), manipulate operation is applied to this IIDS. This operation generates the resulting IIDS v2. What is done in this manipulate operation is specified by the programmer as a sequential procedure. Then, after the creation of another IIDS called v3, this program performs the join operation. Finally, the resulting IIDS, which is v4, is generated by this operation.

Figure 5.2 shows the source code to express this program (unimportant details are omitted). The above-described operations are written at Lines 2 to 7, which is the main part of the program. The functions avgFunc and addFunc are to specify the concrete calculation that should be done during the manipulate and join operations, respectively. The important point is the fact that this program can be run with a huge size of vectors. In such a case, vectors are automatically distributed across multiple nodes. How to distribute the vector is determined by Pyne, not by programmers. Therefore, programmers do not have to care about the parallel implementation of the vector, which is why the data structure of Pyne is named implementation independent data structure.

5.2.1.2 Interface Design

Pyne provides an automatic parallelization functionality of programs. The key to realizing this automatic parallelization resides in the interface of each operation. For example, Line 3 of Figure 5.2 indicates that a new IIDS v2 is created by manipulating IIDS v1, where each element of the new IIDS is calculated by the function

```
ROWRES = 360
COLRES = 120
....
def createCoefficientMatrix(p, neigh):
    (25 lines)
def calcTantVelocity(p, neigh):
    (18 lines)
def calcPoissonSourceTerm(p, neigh):
    (9 lines)
def calcVelocity(p, neigh):
    (10 lines)

# Body part
g = iids.createGrid((ROWRES, COLRES),
      edds.makeValue(defaultGridValues),
      name="g")
gInit = g.setNodeValue(
(0, 0), (ROWRES, 1),
       {'south': True})
       .setNodeValue((1, 0),
         (ROWRES-2, COLRES), putNodeIndex)
A, constV = iids.createMatrixFromGrid(
gInit, iids.makeType(0.0),
         lambda p: not p["nid"] is None,
         createCoefficientMatrix,
         neighSize=1)
itr = iids.createScalar(0, name="itr")
```

```
def timeStepLoop(gridInLoop, counter):
    vT = gridInLoop.setNodeValue(
(0, 0), (ROWRES, COLRES),
            calcTantVelocity, neighSize=1)
    gD = vT.setNodeValue((0, 0),
(ROWRES, COLRES),
                  calcPoissonSourceTerm,
neighSize=1)
    D = iids.createVector(gD,
iids.makeType(0.0),
           lambda p: not p["nid"] is None,
           lambda p, neigh: p["d"])
    rhs = iids.createVector((D, constV),
iids.makeType(0.0),
           lambda a, b: a - b, name="rhs")
    solPhiV = iids.solve(A, rhs)
    phi = gD.mapNodeValueFromVector(
solPhiV,
           lambda p: not p["nid"] is None,
           lambda v: True, 'phi')
    newV = phi.setNodeValue((0, 0),
(ROWRES, COLRES), calcVelocity,
neighSize=1)
    newItr = counter.add(1)
    return (newV, newItr)
loopOut = edds.loop(timeStepLoop, gInit,
itr, lambda v: v[1] < 10)
iids.end(loopOut)
```

Figure 5.3: Example program with Pyne (fluid simulation)

avgFunc. Here, another parameter neighSize=1 plays an important role for parallelization. This parameter indicates that when calculating the ith value of v2, the avgFunc uses only the i-1th to the i+1th elements of v1. By this parameter, Pyne knows even if the vector is divided into multiple nodes, only the values that are adjacent to the borders must be exchanged across the border of the processes. In other words, the existence of localities, which is essential for developing scalable parallel programs, is ensured by this parameter. As shown in line 6, neighSize=0 means complete locality where no communication is required for that operation.

Conversely, if the neighSize is so large that it is comparable to the vector size, this means the operation requires almost all the parts of the vectors, or the access pattern is unpredictable. Parallelizing such a program is essentially difficult. Pyne does work with such operations, but it generates warnings and would perform poorly.

5.2.1.3 Productivity Evaluation

Figure 5.3 shows the outline of the Pyne program that implements a 2-D fluid dynamics simulation, which is based on the fractional-step method. At the left side of the figure, an initial state is defined on a lattice grid. The right side of the figure shows the main part of the simulation program, where the temporal velocity field is calculated, and then, the pressure field is calculated by solving a Poisson equation. This program uses three types of IIDS, which are grids, vectors, and matrices. Most operations are performed on the grid, which directly expresses the simulated field. A matrix is used to create and solve the Poisson equation.

This example shows two benefits of using the Pyne framework. One is that Pyne enables programmers to focus on the essential aspects of the application. Because Pyne hides all the parallelization related codes from the programmers, the overall structure of the application is clearly described. Another one is the simplicity of programming. Programmers must write only the essential part of the application. Other parts, such as allocation of the data structure or parallel implementation of the data and procedure, are handled by Pyne. The complete program with Pyne consists of 163 lines of Python code, while the equivalent MPI program has more than 1200 lines of C language source code.

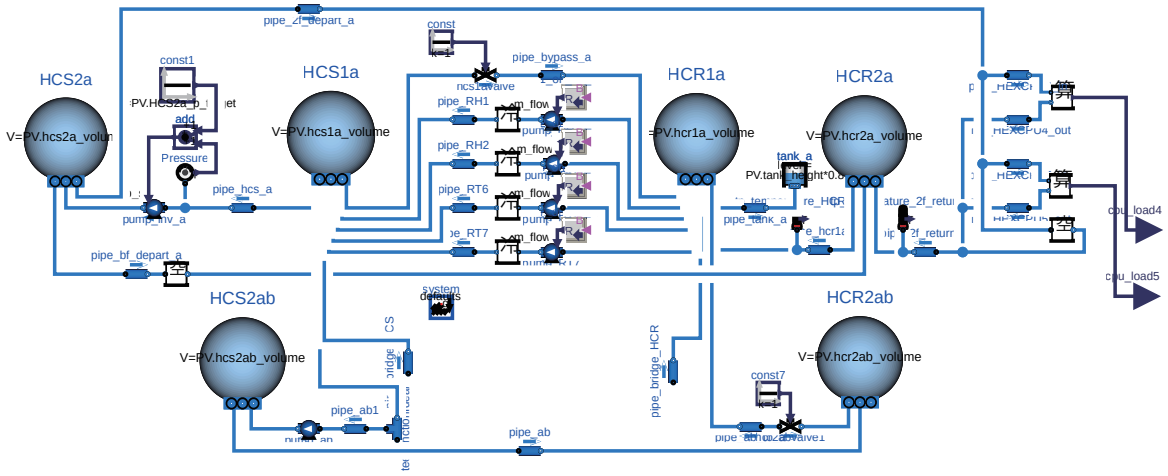

Figure 5.4: Modelica model of the K cooling facility (simplified)

5.2.2 3.2 Development of a Digital Twin of K Cooling Facility

HPC Usability Research Team is collaborating with Operations and Computer Technologies Division on creating a real cyber-physical system. Our target is the cooling facility of the K computer. By reproducing the behavior of the cooling facility of K computer with a simulator, we can do trial and error in searching for efficient operation parameters, such as the temperature of cooling water. The cyber-physical system that uses a simulation of the system of interest to virtually try unknown or potentially dangerous operation is often called a digital twin. This project is to utilize the digital twin for actual contribution to the efficient operation of supercomputers. We also collaborate with AIST (National Institute of Advanced Industrial Science and Technology), who operates ABCI, to utilize the experiences of both parties for the efficient operation of both supercompuers.

5.2.2.1 Creation of the Simulation Model of the K Cooling Facility

The first step in creating the digital twin of a real-world facility is to develop a simulation model of the facility. We use a modeling language called Modelica to develop a simulation of the cooling system of the K computer. Modelica is a modeling language with which we write simulation models with differential algebraic equations (DAE). Currently, only the portion that can be expressed with DAE is modeled. Our final goal is to create a more comprehensive simulator that includes cooling towers, which require 3-D fluid simulation, or behavior of software such as job schedulers. Because such a comprehensive simulator consists of multiple simulation models, Pyne will be used to develop some of them or to connect the models. Figure 5.4 shows the simulation model of the cooling facility of the K computer, which we made with an external contractor. Only the essential part of the half of the facility is shown in the figure. Although Modelica is a programming language with which we write DAEs of the system of interest, it also allows us to create a whole system model with GUI. By connecting GUI components, each of which has associated DAE to express the behavior of the component, simultaneous equations are automatically created by the Modelica compiler. Therefore, creating a simulation model is a procedure to develop a schematic diagram as shown in the figure.

5.2.2.2 Preliminary evaluation

Figure 5.5 shows the temperature of cooling water. This temperature is measured at the point where the cooling water exits from a heat exchanger after cooling another circulation of cooling water, which is directly facing the CPUs. The blue line indicated the measured temperature at the real facility while the orange one indicates the simulated one. As shown in the figure, the simulation successfully reproduces the change of the temperature. However, this is only a preliminary evaluation because the time frame shown in the figure is identical with the one when we obtain data that are used for calibrating the simulation parameter. Therefore, we must pick up data from another time frame and evaluate the accuracy of the simulation model by comparing the calculated and simulated data.

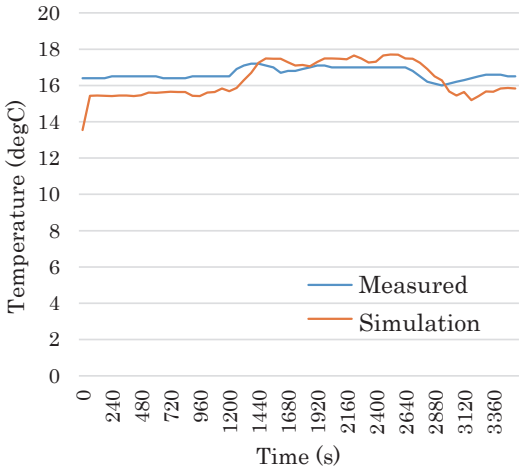

Figure 5.5: Comparison of simulated and measured values

5.3 Schedule and Future Plan

The final goal of Pyne development is to make a practically useful tool for industry users. To this end, we will do the following activities in the coming years.

5.3.0.1 Evaluation of the performance and applicability

As described in the previous section, Pyne's basic abstraction is to express an application as a sequence of operations to data. Because Pyne's program is written as if it were a sequential program, all the processes perform the same operations to different parts of data. This abstraction allows automatic parallelization of programs, but on the other hand, limits the type of parallel programs that can be written with Pyne. We will evaluate what kind of parallel programs can be written with Pyne. We will also evaluate how Pyne's abstraction affects the execution performance.

5.3.0.2 Implementation of algorithms and libraries

Besides vectors, matrices, and grids that are already implemented in the prototype of Pyne, we will implement various data structures and parallel operations so that various parallel programs can be written with Pyne. Also, we will provide self-contained simulators implemented with Pyne. They are for users who want to use existing simulators but requires a little customization for their purposes.

5.3.0.3 Obtaining feedback from potential users

It is essential to have feedback from potential users to develop practical software. We are currently conducting collaborative research with Hitachi, Ltd., who believes Digital Twin is a promising technology to reduce the operating costs of industrial facilities. We will continue this collaboration to have information about customer's needs. Based on the information from the industry, we will adjust Pyne's architecture and coverage to meet the requirements from potential users.

5.3.0.4 Application to real use cases

As described in the previous section, we are developing the Digital Twin of the cooling facility of K computer using only the modeling language Modelica, not Pyne. We will find other practical use cases in which Pyne plays a more important role. We already have some candidates of such use cases through collaborative research with Hitachi, Ltd. We will select one of them and continue the development of Pyne so that we can develop the Digital Twin of the target system with Pyne.

5.3.0.5 Making Pyne production ready

Adequate functionality, high-quality implementation, and helpful documents and examples are essential for practical software. We will make Pyne production ready by our effort and the collaboration with external contractors.

5.3.0.6 Application to the operation of Fugaku

Fugaku will introduce new difficulties of operation because of the increase of power consumption compared with that of the K computer. We will use the simulator of the cooling facility to minimize the waste of energy, to ensure the safety of new operation policy, or to evaluate the effect of the installation of new software or hardware. We already have three potential use cases of the digital twin of the facility. To work on these use cases, we will extend the simulator by integrating the simulator of the cooling facility, which we described in the previous section, with other simulators that are for, for example, power facility or software behavior.

5.3.0.7 Application to industrial data centers

We will aim to apply the digital twin technique to industrial data centers for their cost-effective operation. Although software and hardware technologies of the industrial data center are similar to those for supercomputers, their usage and social role are different. We expect we will have to focus more on the business and social aspects of data center operation, such as pricing or incentive designs of their services. Currently, we do not have industrial collaborators about this project. We start by finding them.

5.4 Publications

5.4.1 Papers (refereed)

[1] H. Matsuba, M. Matsuda and M. Kawai: "Pyne: A programming framework for parallel simulation development". Workshop on Parallel Programming Models and Systems Software for High-End Computing (P2S2) 2019 (to appear).
[2] M. Matsuda, H. Matsuba, J. Nonaka, K. Yamamoto, H. Shibata and T. Tsukamoto: "Modeling the Existing Cooling System to Learn its Behavior for Post-K Supercomputer at RIKEN R-CCS". Energy Efficient HPC State of the Practice Workshop (EE HPC SOP) 2019 (to appear).
[3] K. Hayashi, N. Sakamoto, J. Nonaka, M. Matsuda, and F. Shoji: "An In-Situ Visualization Approach for the K computer using Mesa 3D and KVS". WOIV 2018 (ISC Workshop on In Situ Visualization http://woiv.org/).

5.4.2 Posters (refereed)

[4] J. Nonaka, K. Ono, N. Sakamoto, K. Hayashi, M. Matsuda, F. Shoji, K. Oku, M. Fujita, K. Hatta: "A Large Data Visualization Framework for SPARC64 fx HPC Systems - Case Study: K Computer Operational Environment -", 2018 IEEE 8th Symposium on Large Data Analysis and Visualization (LDAV).
[5] M. Kawai, A. Ida and G. Wellein, "ppOpen-SOL: Robust ILU Preconditioner for Exascale", HPC in Asia, ISC2018, Germany, 2018

5.4.3 Presentations

[6] N. Nomura, K. Nakajima, M. Kawai, A. Fujii, "The Analysis of SA-AMG Method by Applying Hybrid MPI/OpenMP Parallelization on Cluster Supercomputer System", 15th Copper Mountain Conference On Iterative Methods, US, 2019
[7] N. Nomura, K. Nakajima, M. Kawai, A. Fujii, "The Evaluation of The SA-AMG Method By Applying Hybrid Parallelizaionon Cluster Computing System", ASE Seminar, Tokyo, 2019

5.4.4 Patents

[8] M. Mase, T. Sakurai, and H. Matsuba, "Simulation execution method and computer system", Joint application by Riken and Hitachi, Ltd., May, 2018

Chapter 6

Field Theory Research Team

6.1 Members

Yasumichi Aoki (Team Leader)

Yoshifumi Nakamura (Research Scientist)

Eigo Shintani (Research Scientist)

Natsuki Tsukamoto (Intern)

6.2 Overview of Research Activities

Field theory research team performs researches related with the numerical computation of quantum field theory (QFT) in elementary particle and nuclear physics. The quantum field theory is the framework of quantum theory combined with Einstein's special relativity to describe the physical properties of elementary particles. The standard model (SM) of particle physics, which is scripted with QFT, represents the state-of-the-art understanding of the most basic physical low of the elements of matters in this world. This almost perfect low of nature is still incomplete in several reasoning: it does not explain the origin of dark matter; it does not explain the spectrum of elementary particles; it is not natural that highest energy scale in SM is seventeenth order of magnitude lower the Plank scale; etc. These motivate searches of new physics in various theoretical and experimental directions. Among these precision tests of SM and seeking answers of these questions in extensions of SM require precise information of the quantum chromo dynamics (QCD) which governs the strong interaction in SM. The involved QCD dynamics cannot be solved by hand. Computational approach with lattice QCD, discretized version of the QCD on the continuous space-time, is powerful and most effective. After the first lattice QCD simulation about 40 years ago, its technique has become sophisticated and matured to date by tremendous efforts. Realistic simulations with various parameters tuned as in the nature are becoming possible by use of supercomputer like K using a conventional version of the lattice QCD formulation. The required precision to many interesting quantities for the test of the standard model, however, has not been reached yet. In this situation, the breakthrough could be obtained by using methods which are ideal but computationally demanding. We believe using the next generation supercomputers like post-K with related developments makes this happen. To maximize the power of the next generation supercomputers, multifaceted improvements are needed. First, algorithmic development for simulation technique and analysis of the large data set will be more than useful. Second, given the idea in algorithms, efficiency in the future HPC environment need to be maximized. The team conducts researches in such directions.

6.3 Research Results and Achievements

6.3.1 Proton decay matrix elements at the physical quark mass

Proton decay is a smoking gun evidence of new physics beyond the standard model of particle physics. It naturally takes place in grand unified theories (GUTs) which unifies the known forces in the nature except gravity. Ongoing experiments such as SuperKamiokande as well as the ones in preparation: HyperKamiokande

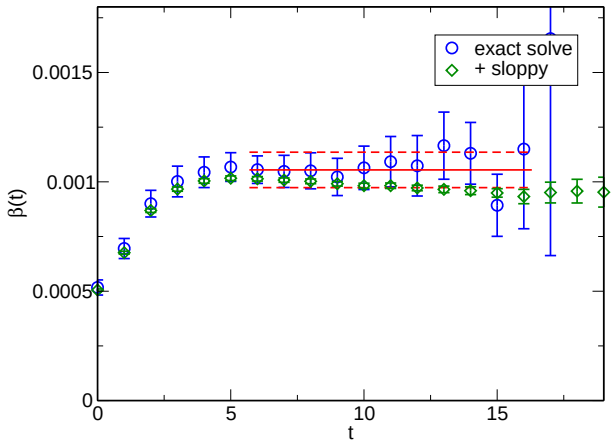

Figure 6.1: Ratio of two point functions for proton decay low energy constant (LEC) β, where results from one exact solve before applying AMA (blue circle) and those after AMA (green square) are compared. Here AMA uses 256 additional sloppy solves, each of which costs 1/5 time for the solver. Even counting the quark contraction and other operations to compose this ratio, more than factor two reduction in computational cost has been achieved. The LEC is extracted from the asymptotic plateau as function of time separation t where the ground state (proton) is disentangled from the excited states.

in Japan and DUNE in USA are aiming to detect the proton decay in deep underground as one of the core missions. Even without the signal of the decay, the lower bound of the proton lifetime will be prolonged with continuous operation of the experiments. That could impose severe constraint on the GUT models (ultimately leading to the way to finding the unique single theory of everything), provided that the proton decay matrix elements are determined in good precision. The underlying theory for the matrix elements is the quantum chromo dynamics, QCD, which describes the strong interaction among quarks, building blocks of proton. For the quantitative treatment for matrix elements, numerical computation using lattice QCD defined on the discrete space-time is only way in our hands.

For long the numerical simulation of lattice QCD with physical value of light quark masses has not been possible due to its demanding computational cost. As such, extrapolations from simulations with unphysically heavy quark masses were performed. Use of K and other equivalent high performance computers and continuous improvement of the algorithms made it possible to now simulate QCD on top of the physical quark mass point. To cope with smaller quark mass, a larger volume needs to be used to control the finite volume error. Ever growing volume provides new room of improvement of the algorithm. All mode averaging (AMA), which one of our team member developed, is a promising new direction for accelerating the simulation for larger volumes. For most of the quantities calculated from QCD, the quark matrix inversion is the most computationally demanding part of the algorithm. The AMA framework guides the way to mix the exact low mode eigenvectors and many sloppy conjugate gradient solver with relaxed convergence criteria to minimize the computational cost for given precision using the covariance property of the matrix. This test is done using the Wilson fermion environment, with an outlook of using it to future chiral fermion simulations.

Using K at R-CCS and Hokusai BigWaterFall at Information System Division of RIKEN we have been testing the effectiveness of AMA technique using the gauge field configurations generated by PACS collaboration using a Wilson fermion formulation. Effectiveness of AMA is tested for the determination of the low energy constants (LECs) of proton decay matrix elements. The LECs are calculated from certain ratios of two-point correlation functions of proton interpolating operator and the proton decay operators. The ratio as a function of the Euclidean time separation of the two operators is shown in Fig. 1. By fitting asymptotic plateau one can obtain the LEC, in this case. Through this study we are confident that obtaining LECs to good precision is possible. We are extending this computation to the form factor of the matrix element, which has more direct relation to the proton lifetime. All the results will eventually be “renormalized”. This final step requires non-perturbative renormalization which also utilizes the lattice QCD computational framework and is underway.

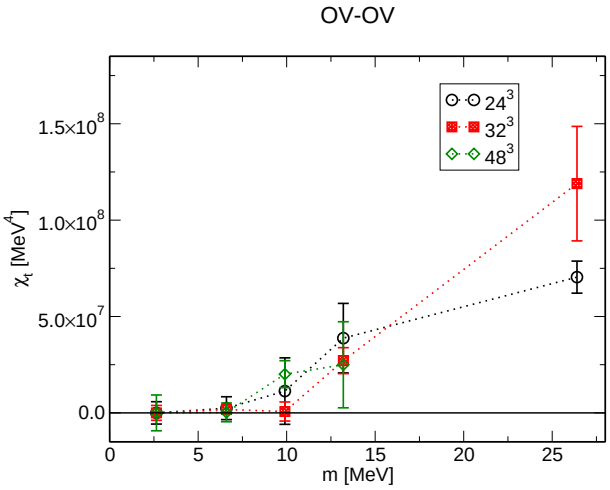

Figure 6.2: Preliminary result of the topological susceptibility as a function of ud-quark mass m for QCD with two dynamical quarks at system temperature about T=220 MeV from JLQCD collaboration with a support of the priority issue 9 to be tackled by o Post-K computer. Use of a chiral fermion makes it possible to unambiguous definition of the topological charge, thus, of its susceptibility as well. Existence of the phase transition around m=10 MeV is implied, which is under further serious test.

6.3.2 Phase transition in QCD at finite temperature

99% of the mass of the visible universe (and our body as well) is made of the energy dynamically generated by QCD interaction. The underlying mechanism of mass generation is the chiral symmetry breaking (Nambu-Goldstone mechanism): the chiral symmetry is spontaneously broken in the present universe. One can think of what happens if we unwind the history of the universe and with the temperature high enough, then the chiral symmetry should recover. If there has been a phase transition or just a crossover is a prime question whose answer would have had great influence on the history of the universe and the fate of the matters inside that. Furthermore, understanding the nature of the transition is necessary to judge the fate of one of the promising dark matter scenarios.

There is a long history of the research of QCD at finite temperature theoretically and experimentally. For theory side, as the strong coupling QCD is the target, numerical computation with lattice QCD is most useful in this case, too. Because the target physics question is an involved interplay of the symmetry and its spontaneous breaking, we need the formulation which respects the symmetry in the first place. The lattice formulation which preserves exact "chiral symmetry", thus being called as chiral fermions, is in our hands. However, it requires tremendous computational effort compared to the conventional lattice formulations, such as Wilson or staggered fermions, which respects only a part of the full chiral symmetry or does not at all. In post-K computer, we aim to conduct computations using chiral fermions and by that we can get rid of the compromises which we were not able to.

A preparation is underway by JLQCD collaboration with a support of the priority issue 9 to be tackled by o Post-K computer with the up- and down-quarks as fermionic dynamical degree of freedom. While the third, strange quark needs to be included for more realistic setting, the two-quark simulation would capture at least a part of same important physics because the strange quark is much heavier than up and down quarks. Also, full understanding of the two-quark simulation provides the boundary information of the phase diagram of full three-quark system. Fig. 2 shows a preliminary result of the topological susceptibility as a function of ud-quark mass m at temperature about $T = 220$ MeV, which is 20-30% higher than the critical temperature expected for the chiral transition at mass-less limit. A sudden growth observed for $m > 10$ MeV may suggest a first-order transition, which is under serious scrutiny. This quantity is related to the axial $U(1)$ anomaly. The axial $U(1)$ symmetry is intact in QCD at classical level, but, broken by quantum anomaly. There is a long history of debate as to whether this symmetry is effectively recovers above phase transition temperature. Chiral symmetric treatment of lattice QCD would provide the final answer to this question.

6.4 Schedule and Future Plan

The chiral fermion simulations of lattice QCD for near future use 2+1 flavor (including the strange quark) physical point for heavy flavor physics targeting B mesons and the other precision tests of the standard model (SM). The same setting will also be used to explore the phase diagram of QCD at finite temperature which could end up simulating lighter quarks than physical. The post-K implementation of the existing algorithms are immediate aim. Extended simulations to larger volume and lighter quarks from the current ones benefit from speedup with algorithmic development and tuning.

6.4.1 Algorithm and code development for the chiral fermion simulation in QCD for next generation supercomputers

The chiral fermion simulations of two-flavor QCD uses Grid, the code set developed mainly by Edinburgh University. We are working on extending this to 2+1 flavor case. Through the co-design works for the Post-K supercomputer involving members of our team, we foresee obstacles of simple extension of the Grid code set. The co-design software team is developing their version of Wilson fermion solvers, which can be used as main building block to simulate chiral fermions, too. A possible international collaboration with developers of Grid, which became one of the international standards, on the optimization for post-K supercomputer, could benefit both sides and potential international users. The large volume and light quark simulations are computationally challenging. The AMA technique, being developed and tested, will be useful. Independent of this technique, implementing and accelerating Multi-Grid algorithm would be a promising direction. In the lattice simulations, parameters not directly related with the physical setting, like the AMA and multi-grid specific ones or like tunable parameters in the hybrid Monte-Carlo potentially provide large rooms of improvement. There, optimizations assisted with deep learning could bring a significant speed up. This direction could serve as a starting point of collaborations with other teams in R-CCS.

6.4.2 QCD phase diagram with chiral fermion simulations

As a test bed of new code development and new algorithms the degenerate three flavor simulation of QCD using chiral fermions can be used. The simulation is simpler than physical, non-degenerate, 2+1 flavor simulation, thus good for tests with situation close to the final target. But, it is also interesting on its own physical perspective. The phase diagram with respect to the change of the degenerate quark mass is one of the important boundary of 2+1 flavor QCD phase diagram. Recent results reported using conventional fermions suffer from huge discretization error. Use of the chiral fermions, thus being able to simulate with correct counting of the light degree of freedom, is expected to solve this problem. The knowledge acquired through these studies provide a base of the simulation of more challenging 2+1 flavor.

6.4.3 Collaboration with priority issue 9 to be tackled by Post-K computer

We plan to have close collaboration with the priority issue 9 to be tackled by Post-K computer. The main partners in the issue is the sub-issue-A which performs researches related with elementary particles and fields. Through this collaboration, we aim to maximize the scientific output of the issues for intensity frontier subjects including flavor physics, as well as for the QCD phase by cutting edge developments. The development on the chiral fermions there can also be applied for Wilson fermions, which are used in the sub-issue-B for nuclear interactions which eventually are led to the understanding of the nucleosynthesis.

6.5 Publications

6.5.1 Articles/Journal

[1] Eigo Shintani, Ken-Ichi Ishikawa, Yoshinobu Kuramashi, Shoichi Sasaki, Takeshi Yamazaki, "Nucleon form factors and root-mean-square radii on a $(10.8\ \mathrm{fm})^4$ lattice at the physical point", Phys. Rev. D99 (2019) 014510.
[2] K.-I. Ishikawa, N. Ishizuka, Y. Kuramashi, Y. Nakamura, Y. Namekawa, Y. Taniguchi, N. Ukita, T. Yamazaki, and T. Yoshié, "Finite size effect on pseudoscalar meson sector in 2 + 1 flavor QCD at the physical point", Phys. Rev. D99 (2019) 014504.

6.5.2 Invited Talks

[4] Yasumichi Aoki, "QCD phase transition", International Workshop on Massively Parallel Programming for Quantum Chemistry and Physics, Kobe Japan, Jan.15, 2019.
[5] Yasumichi Aoki, "Novel features of a familiar theory — QCD near phase boundary analyzed through large scale numerical simulations", Computational Science Forum, Tokyo Japan, Feb.22, 2019.
[6] Yasumichi Aoki, "Novel features of a familiar theory — QCD near phase boundary analyzed through large scale numerical simulations", RCNP seminar, Ibaraki, Osaka, Japan, Feb.25, 2019.
[7] Yasumichi Aoki, "Lattice QCD: topics in finite temperature and proton decay", RBRC SRC meeting, Upton, NY, USA, March 11, 2019.

6.5.3 Oral Talks

[8] Yasumichi Aoki, "Finite temperature phase transition of QCD and topology", workshop of post-K priority issue #9, Tsukuba, Japan, Oct.3, 2018.
[9] Eigo Shintani, "Lattice calculation of nucleon form factor at physical point", 8th International Conference on Quarks and Nuclear Physics (QNP2018), Tsukuba, Japan, Nov.14, 2018.
[10] Yasumichi Aoki, "QCD phase transition – current status and perspective", 2018 symposium on particles, nucleus and the universe – from K to post-K, Tokyo, Japan, Jan. 9, 2019
[11] Yasumichi Aoki, "Novel features of a familiar theory — QCD near phase boundary analyzed through large scale numerical simulations", R-CCS Cafe, Kobe, Japan, March 1, 2019.

Chapter 7

Discrete-Event Simulation Research Team

7.1 Members

Nobuyasu Ito (Team Leader)

Yohsuke Murase(Research Scientist)

Naoki Yoshioka (Research Scientist)

Daigo Umemoto (Postdosctoral Researcher)

Tomio Kamada (Guest Researcher)

Takeshi Uchitane (Guest Researcher)

7.2 Research Activities

Discrete-event simulations cover much wider fields than discretized simulations of continuous models. They comprise various kinds of models, for example, particles, agents, automata, games and so on, and their applications are from material and biomedical sciences to ecological and environmental problems. Social designs and controls have becoming the more interesting target since so-called the "big data sciences" became popular. In addition, continuous simulations are also becoming building block of discrete-event simulations. The discrete-event simulation research team(DESRT) aims to cultivate such applications of supercomputers. There are mainly two directions of activities. One is to develop application softwares. We have been developping job management applications OACIS and CARAVAN The other to study and develop models for complex phenomena, mainly in social ones.

7.2.1 Job management applications, OACIS and CARAVAN

A characteristic feature of discrete-event models is their large and complex parameter spaces, and they often show qualitatively different various behaviors with different parameters. Supercomputers help to overcome such difficulty: their performance with extreme parallelism allows us to simulate huge number of parameter sets.

There are two kinds of computer jobs: one pursues computing capability and the other capacity. Discrete-event simulations are in the capacity computing, and many simulations are necessary to be prepared and executed efficiently. Table 1.1 shows a classification of computer jobs in terms of their capacity. But manual operation and orchestration of thousands and more jobs are hard, and application tools for the purpose are usually used. The OACIS and CARAVAN are applications developed and released in our team. OACIS since 2012 can manage most jobs interactively through web browser up to millions. CARAVAN since 2017 handles more jobs assuming that input and output size of each job be small. In this year 2018, major updated for the OAICS[33] and minor one for the CARAVAN[34] were done, together with user-support activities and tutorials. Now the applications of them are growing, for example a Robocup system[9].

	capability computing	⟵	⟶	capacity computing
class	A	B	C	D
manual execution	easy	tedious	troublesome	desperate
number of simulations	$\sim 10^1$	$\sim 10^4$	$\sim 10^7$	$\sim 10^{10}$ and more
(node · second) per simulation	$\sim 10^{10}$ and more	$\sim 10^7$	$\sim 10^3$	$\sim 10^0$
output per simulation	$\sim$ TB and more	$\sim$ GB	$\sim$ MB	$\sim$ KB

Table 7.1: A classification of jobs in terms of necessary number of simulations. The OACIS is designed for jobs for class A, B and C, and the CARAVAN for C and D.

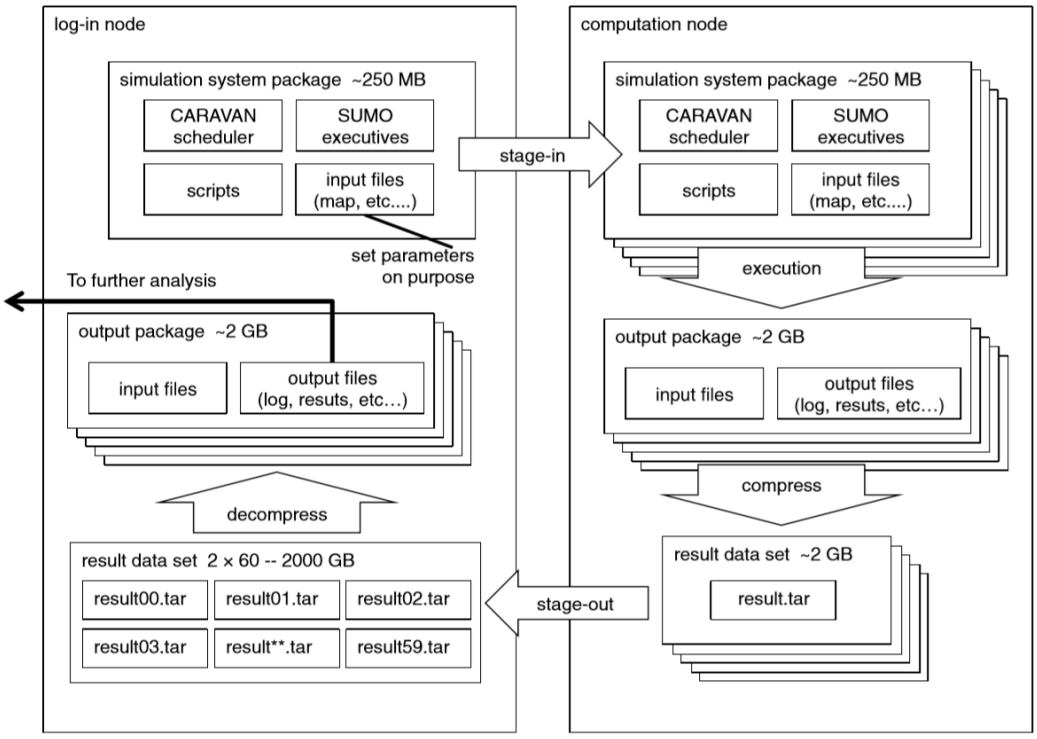

Figure 7.1: Schematic picture of the implementation of exhaustive traffic simulation using the CARAVAN on the K computer is shown.

7.2.2 Social modeling and simulations

7.2.2.1 Traffic model: power-law distribution

The DESRT has been developing a car-traffic simulator of the Kobe city. It is used to see how computer simulations contribute to analyze, predict and optimize modern traffic issues like efficiency, congestion and pollution. After reproducing and analyzing current Kobe traffic in the previous year, simulations of artificial traffic is now challenged. For one traffic situation of the Kobe city, thousands of parameter samples were needed to be simulated to achieve statistically significant analysis. So we developed a simulator executing various artificial situations simultaneously using K computer[3]. It is prepared by combining the CARAVAN and the simulator for each parameter. The implementation and execution are shown in Fig. 7.1. Typically it took thirteen elapse hours for simulations of thousand parameter samples(see also Fig. 7.2).

Using this simulator, various simulations are systematically studied. One discovery is about distribution of traffic on road segments in urban traffic[4]. Simulation results from our Kobe simulator universally show a power-law distribution with decay exponent about 1. Similar power-law distribution was confirmed also on randomly generated road networks, but not on regular network with lattice structure. The latter shows a flat distribution(Fig. 7.3). This finding of universality classes in urban traffic flow may suggest that a randomly developed city and a regularly designed city have different traffic characteristics.

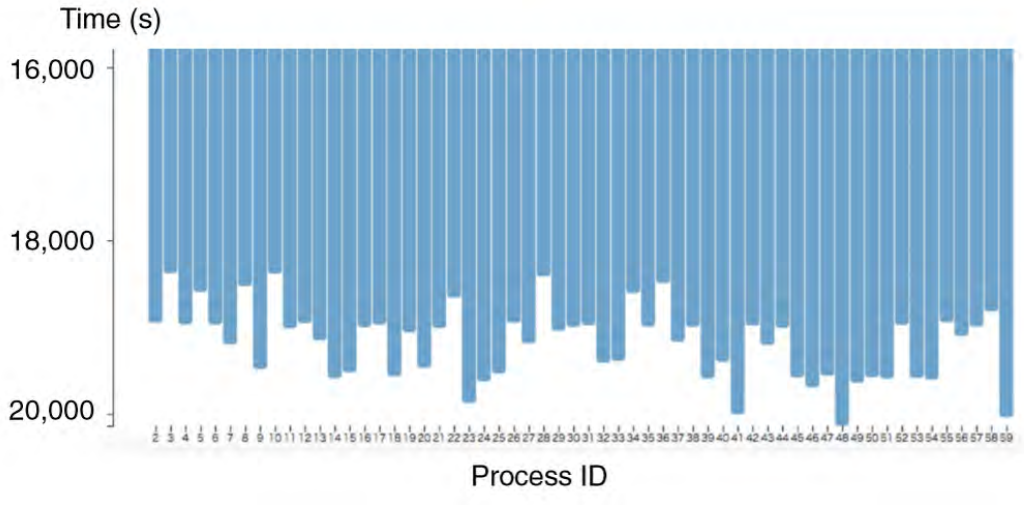

Figure 7.2: A plot of process-load distribution for a set of execution of traffic simulations is shown.

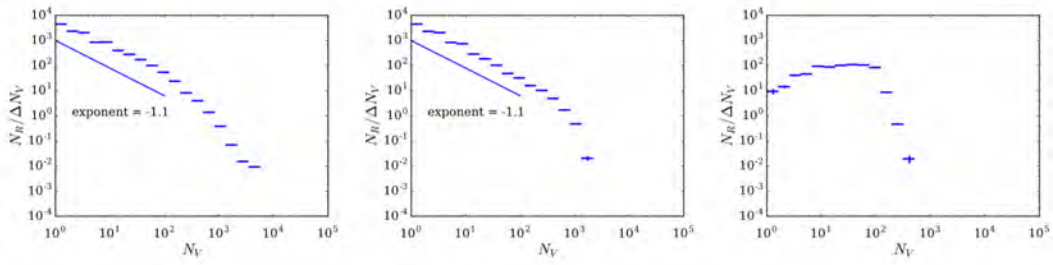

Figure 7.3: Traffic distribution results from the Kobe city network(left), random(middle) and regular lattice(right) are shown. The horizontal axes marked with N_v show total number of car passes through a road segment, that is, traffic of the segment. The vertical axes marked with $N_R/\Delta N_V$ show distribution density of number of road segments having N_V traffic.

$B_{t-3}B_{t-2}B_{t-1}C_{t-3}C_{t-2}C_{t-1}$	$A_{t-3}A_{t-2}A_{t-1}$							
	ccc	*ccd*	*cdc*	*cdd*	*dcc*	*dcd*	*ddc*	*ddd*
cccccc	*c*	*c*	*d*	*c*	*c*	*c*	*d*	*c*
ccccd/ccdccc	*d*	*c*	*c*	*c*	*d*	*c*	*c*	*c*
ccccdc/cdcccc	*c*	*d*	*c*	*d*	*c*	*d*	*c*	*d*
ccccdd/cddccc	*d*	*d*	*d*	*d*	*d*	*d*	*d*	*d*
cccdcc/dccccc	*c*	*c*	*d*	*c*	*c*	*c*	*d*	*c*
cccdcd/dcdccc	*d*	*c*	*c*	*c*	*d*	*c*	*c*	*c*
cccddc/ddcccc	*c*	*d*	*c*	*d*	*c*	*d*	*c*	*d*
cccddd/dddccc	*d*	*d*	*d*	*d*	*d*	*d*	*d*	*d*
ccdccd	*d*	*c*	*c*	*c*	*d*	*c*	*c*	*d*
ccdcdc/cdcccd	*c*	*c*	*c*	*c*	*d*	*c*	*d*	*c*
ccdcdd/cddccd	*d*	*d*	*d*	*d*	*d*	*d*	*d*	*d*
ccddcc/dccccd	*d*	*c*	*c*	*c*	*d*	*c*	*c*	*c*
ccddcd/dcdccd	*d*	*c*	*c*	*d*	*d*	*c*	*c*	*d*
ccdddc/ddcccd	*d*	*c*	*d*	*c*	*d*	*c*	*d*	*c*
ccdddd/dddccd	*d*	*d*	*d*	*d*	*d*	*d*	*d*	*d*
cdccdc	*c*	*d*	*c*	*d*	*c*	*c*	*c*	*d*
cdccdd/cddcdc	*d*	*d*	*c*	*d*	*d*	*d*	*c*	*d*
cdcdcc/dcccdc	*c*	*d*	*c*	*c*	*c*	*d*	*c*	*d*
cdcdcd/dcdcdc	*d*	*c*	*d*	*c*	*d*	*c*	*d*	*c*
cdcddc/ddccdc	*c*	*d*	*c*	*d*	*c*	*d*	*c*	*d*
cdcddd/dddcdc	*d*	*d*	*c*	*d*	*d*	*d*	*c*	*d*
cddcdd	*d*	*d*	*c*	*d*	*d*	*d*	*c*	*d*
cdddcc/dcccdd	*d*	*d*	*d*	*d*	*d*	*d*	*d*	*d*
cdddcd/dcdcdd	*d*	*d*	*d*	*d*	*d*	*d*	*d*	*d*
cddddc/ddccdd	*d*	*d*	*c*	*c*	*d*	*d*	*c*	*d*
cddddd/dddcdd	*d*	*d*	*c*	*d*	*d*	*d*	*c*	*d*
dccdcc	*c*	*c*	*d*	*c*	*c*	*c*	*d*	*c*
dccdcd/dcddcc	*d*	*c*	*c*	*c*	*d*	*c*	*c*	*c*
dccddc/ddcdcc	*c*	*d*	*c*	*d*	*c*	*d*	*c*	*d*
dccddd/ddddcc	*d*	*d*	*d*	*d*	*d*	*d*	*d*	*d*
dcddcd	*d*	*c*	*c*	*d*	*d*	*c*	*c*	*d*
dcdddc/ddcdcd	*d*	*c*	*d*	*c*	*d*	*c*	*d*	*c*
dcdddd/ddddcd	*d*	*d*	*d*	*d*	*d*	*d*	*d*	*d*
ddcddc	*c*	*d*	*c*	*d*	*c*	*d*	*c*	*d*
ddcddd/dddddc	*d*	*d*	*c*	*d*	*d*	*d*	*c*	*d*
dddddd	*d*	*d*	*c*	*d*	*d*	*d*	*c*	*d*

Table 7.2: One of the discovered strategy towards collaboration is listed. Player A decide next collaborative(c) or defective(d) action depending on former three actions of A and other two players, B and C.

7.2.2.2 Collaboration strategy: a game theoretic approach

Global collaboration is no doubt the best way to overcome numerous serious obstacles and to settle our social and personal disputes. So it is a big challenge how to make collaboration without critical free-riders. One approach to this challenge is to use game theoretic models, and design games so that collaborative situations will be Nash equilibrium. Such equilibrium was formulated with a prisoner's dilemma game in case of two players. It had not not been known for more players, but Yohsuke Murase, a member of DESRT, discovered ones for three players playing the tragedy of commons game with three-term memory and the results are published in this year 2018[6]. After prescreening of promising strategies among 5×10^{86}, about trillion(10^{12}) candidates were examined using the K computer. And 256 strategies were identified to make collaborating state the Nash equilibrium . One of them is listed in Tab. 7.2 and it is shown in Fig. 7.4. It looks complicated. We do not have any simple understanding and insight of these results. but this discovery will be a big leap towards global collaboration.

7.2.3 Other activities

In the year of 2017, following studies were published from this team:

[1] Model development of human relationship[5]

[2] Model development of disease propagation[8]

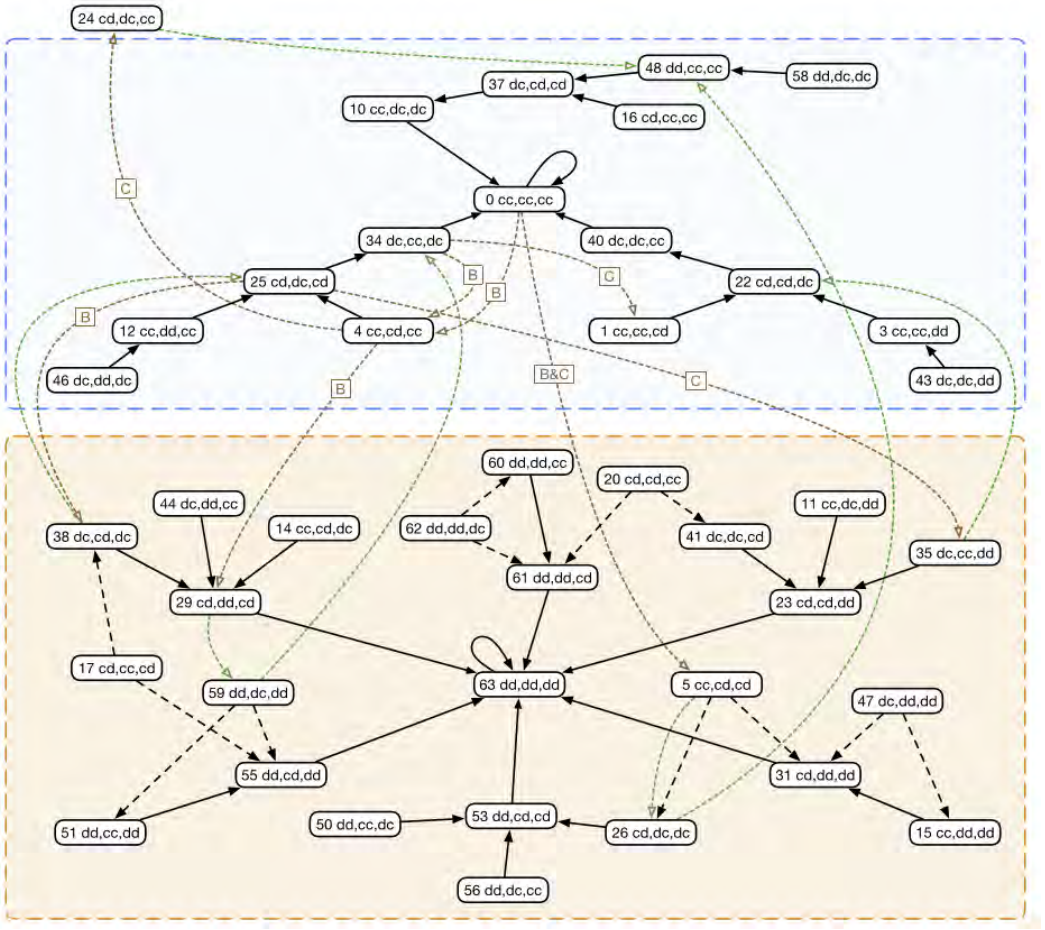

Figure 7.4: Transition paths towards collaboration are shown.

[3] Simulation of quantum computer[10]

7.3 Schedule and Future Plan

From the research activities of DESRT so far, following problems are becoming clear:

[1] Simulation models, typically social ones, comprise with large input parameters and output numbers, and their behaviors are strongly nonlinear with various regimes.

[2] Social "big data" are often not big enough to picture details. It is clearly observed from our multivariate analysis of the traffic data. Thousands of samples are necessary to get minor traffic factors, but such repetitions are not expected in the real traffic. Weather, economics, calendar, accidents and other factors varies every day.

[3] Development of multiscale social and economic models and simulations.

7.4 Publications

7.4.1 Articles

[1] Itsuki Noda, Yohsuke Murase, Nobuyasu Ito, Kiyoshi Izumi, Hiromitsu Hattori, Tomio Kamada, Hideyuki Mizuta "Project CASSIA -Framework for Exhaustive and Large-Scale Social Simulation-" in "Advanced Software Technologies for Post-Peta Scale Computing" (Springer, Singapore, 2019) p.271-299.
[2] Naoki Yoshioka, Kenji Terada, Takashi Shimada and Nobuyasu Ito, "Macroscopic fundamental diagram in simple street networks," Journal of Computational Social Science **2** (2019) p.85-95.
[3] Daigo Umemoto and Nobuyasu Ito, "Large-scale parallel execution of urban-scale traffic simulation and its performance on K computer," Journal of Computational Social Science, **2** (2019) p.97–101.
[4] Daigo Umemoto and Nobuyasu Ito, "Power-law distribution in an urban traffic flow simulation," Journal of Computational Social Science, **1** (2018) p.493-500.
[5] Hang-Hyun Jo, Yohsuke Murase, János T´or´ok, János Kertész and Kimmo Kaski, "Stylized Facts in Social Networks: Community-Based Static Modeling," Physica **A 500** (2018) p.23-39.
[6] Y. Murase and S.K. Baek, "Seven rules to avoid the tragedy of the commons," Journal of Theoretical Biology **449** (2018) p.94-102.
[7] Y. Murase and P.A. Rikvold, "Conservation of population size is required for self-organized criticality in evolution models," New J. Phys. **20** (2018) 083023.
[8] Shih-Chieh Wang and Nobuyasu Ito, "On principal eigenpair of temporal joined adjacency matrix for spreading phenomenon," Journal of Computational Social Science, **2** (2019) p.67-76.
[9] Shunki Takami, Kazuo Takayanagi, Shivashish Jaishy, Nobuhiro Ito, Kazunori Iwata, Yohsuke Murase, and Takeshi Uchitane, "Proposed environment to support development and experiment in RoboCupRescue Simulation," RoboCup 2017: Robot World Cup XXI (2018, ISBN 978-3-030-00308-1) p.71-83.
[10] Hans De Raedt, Fengping Jin, Dennis Wilsch, Madita Nocon, Naoki Yoshioka, Nobuyasu Ito, Shengjun Yuan and Kristel Michielsen, "Massively parallel quantum computer simulator, eleven years later," Computer Physics Communications **237** (2019) 47-61.

7.4.2 Invited Talks

[11] Nobuyasu Ito, "Social simulation and supercomputer," Network Science Workshop in Kobe (2018 Oct. 28th, Kobe Univ., Kobe)
[12] Nobuyasu Ito, "A next generation supercomputer, Post K, and its application to social problems," Statphys-Taiwan-2018(June 25th 2018, Academia Sinica, Taipei, Taiwan).
[13] Nobuyasu Ito, "'Social simulation with supercomputers," Complex network seminar at Shanghai Univ.(29 June 2018, Shanghai, China).
[14] Nobuyasu Ito, "Car traffic simulation of Kobe city," The 8th Japan-Hungary bilateral workshop (2019 January 11, Naha, Okinawa)
[15] Nobuyasu Ito, "Traffic distribution and network structure," The 6th International Workshop on Physics of Social Complexity(PoSCo) (Sobaeksan, Korea, 2018 May 31th - June 1st).

[16] Y. Murase, “Seven rules to avoid the tragedy of the commons,” The 6th International Workshop on Physics of Social Complexity (PoSCo, May 31-June 02 2018, Pohang, Korea).
[17] Y. Murase, “Modeling social networks: a computational approach,” Complex network seminar at Shanghai Univ.(29 June 2018, Shanghai, China).
[18] Nobuyasu Ito, “Optimization of data-transfer cost for quantum-circuit simulations,” The 9th Hungary-Japan bilateral workshop on statistical physics of breakdown phenomena(Oct. 4th 2018, Debrecen, Hungary).
[19] Naoki Yoshioka, Ferenc Kun, and Nobuyasu Ito, “Jump distance distributions of epicenters in thermally induced cracking of fiber bundles,” The 9th Hungary-Japan bilateral workshop on statistical physics of breakdown phenomena(Oct. 4th 2018, Debrecen, Hungary).
[20] Naoki Yoshioka, Ferenc Kun, and Nobuyasu Ito, “Epicenter jump and burst size in thermally induced cracking of fiber bundles,” The 6th International Workshop on Physics of Social Complexity(PoSCo) (Sobaeksan, Korea, 2018 May 31th - June 1st).

7.4.3 Oral Talks

[21] Nobuyasu Ito, “Social Simulations with Supercomputers,” Supercomputing Asia 2019 (2019 March 12, Suntec Convention Centre, Singapore)
[22] Nobuyasu Ito, ”Social simulation and supercomputer” Department of Transportation System Planning and Telematics, Technische Universitaet Berlin, 2018 November 27th.
[23] Daigo Umemoto and Nobuyasu Ito, “Power-law distributuion found in city-scale traffic flow simulation,” 32nd Workshop ”Recent Developments in Computer Simulation Studies in Condensed Matter Physics” (2019 February 19th, The University of Georgia, Athens, U. S. A.).
[24] Naoki Yoshioka, Kenji Terada, Takashi Shimada and Nobuyasu Ito, “Macroscopic fundamental diagram in simple street networks, Social Simulations and Supercomputers,” (2018 October 29, Tokyo, Japan).
[25] Nobuyasu Ito, ”Traffic-flow simuation,” Department of Automation, China Petrolium University, 2018 July 2nd.
[26] Y. Murase, ”What does big data tell? Sampling the social network by communication channel,” Network Science workshop in Kobe(2018 Oct. 25th, Kobe, Japan).
[27] Y. Murase, ”Successful strategies in the tragedy of the commons,” Games on Networks: from Theory to Experiments(2018 June 12th, Paris, France).
[28] 村瀬洋介 「繰り返し公共財ゲームにおける負けないことが保証された直接互恵戦略」、日本物理学会秋季大会 （同志社大学、京田辺、京都、2018年9月9日—12日）
[29] Nobuyasu Ito, ”Simulation of quantum computer,” 32nd Workshop ”Recent Developments in Computer Simulation Studies in Condensed Matter Physics” (2019 February 20th, The University of Georgia, Athens, U. S. A.).
[30] Nobuyasu Ito, ”Simualtion of Quantum Computer,” 19th International Workshop on Computational Physics(CompPhys19, 2018 November 30th, Leipzig, Germany)
[31] Naoki Yoshioka, Ferenc Kun, and Nobuyasu Ito, “Jump distance of epicenters in thermally induced cracking, Fukui Workshop on Fracture Dynamics and Structure of Cracks,” (2018 March 20th-24th, Fukui, Japan).
[32] 吉岡直樹、Ferenc Kun、伊藤伸泰、「熱活性破壊における微小亀裂発生点の統計分布」、日本物理学会秋季大会（同志社大学、京田辺、京都、2018年9月9日—12日）
[32] Naoki Yoshioka, Ferenc Kun, and Nobuyasu Ito, “Jump statistics of epicenters in thermally induced cracking of fiber bundles,” The 9th International Conference on Multiscale Materials Modeling (MMM2018, 2018 October 29th-November 2th, Osaka, Japan).

7.4.4 Software

[33] OACIS v3.0.0-3.2.1 リリース https://github.com/crest-cassia/oacis
[34] CARAVAN(beta) v0.0.1-0.0.2 リリース https://github.com/crest-cassia/caravan

Chapter 8

Computational Molecular Science Research Team

8.1 Members

Takahito Nakajima (Team Leader)

Noriyuki Minezawa (Research Scientist)

Takehiro Yonehara (Research Scientist)

Keisuke Sawada (Postdosctoral Researcher)

William Dawson (Postdosctoral Researcher)

Wataru Uemura (Postdosctoral Researcher)

Nobuki Inoue (Postdosctoral Researcher)

Takahide Matsuoka (Postdosctoral Researcher)

Subrata Tewary (Postdosctoral Researcher)

Kizashi Yamaguchi (Visiting Researcher)

Takashi Kawakami (Visiting Researcher)

Marek Janusz Wójcik (Visiting Researcher)

8.2 Overview of Research Activities

8.2.1 Development of original molecular theory

An atomic- and molecular-level understanding of drug actions and the mechanisms of a variety of chemical reactions will provide insight for developing new drugs and materials. Although a number of diverse experimental methods have been developed, it still remains difficult to investigate the state of complex molecules and to follow chemical reactions in detail. Therefore, a theoretical molecular science that can predict the properties and functions of matter at the atomic and molecular levels by means of molecular theoretical calculations is keenly awaited as a replacement for experiment. Theoretical molecular science has recently made great strides due to progress in molecular theory and computer development. However, it is still unsatisfactory for practical applications. Consequently, our main goal is to realize an updated theoretical molecular science by developing a molecular theory and calculation methods to handle large complex molecules with high precision under a variety of conditions. To achieve our aim, we have so far developed several methods of calculation. Examples include a way for resolving a significant problem facing conventional methods of calculation, in which the calculation volume increases dramatically when dealing with larger molecules; a way for improving the precision of calculations in molecular simulations; and a way for high-precision calculation of the properties of molecules containing heavy atoms such as metal atoms.

8.2.2 Quantum chemistry software NTChem

Quantum chemistry software comprises immensely useful tools in material and biological science research. Widely diverse programs have been developed in Western countries as Japan has lagged. In fact, only a few programs have been developed in Japan. The mission of our research team is to provide K computer users with a high-performance software for quantum molecular simulation. In the early stage of the K computer project, no quantum chemistry software was available for general purpose and massively parallel computation on the K computer because not every program was designed for use on it. Therefore, we have chosen to develop a new comprehensive ab initio quantum chemistry software locally: NTChem. NTChem is completely new software that implements not only standard quantum chemistry approaches, but also original and improved theoretical methods that we have developed in our research work. The main features of the current version, NTChem2013, are the following:

1). Electronic structure calculation of the ground state of atoms and molecules based on Hartree-Fock (HF) and density functional theory (DFT) methods.

2). Linear-scaling or low-scaling DFT: Gaussian and finite-element Coulomb (GFC) resolution-of-the-identity (RI) DFT, pseudospectral DFT/HF, and dual-level DFT.

3). Low-scaling SCF calculation using diagonalization-free approaches: purification density matrix, pseudo-diagonalization, and quadratic convergence SCF.

4). Excited-state DFT calculation: time-dependent DFT (TDDFT) and transition potential (DFT-TP).

5). Accurate electron correlation methods for ground and excited states: Møller-Plesset perturbation theory, coupled-cluster (CC) theory, and quantum Monte Carlo (QMC) method.

6). Massively parallel computing on the K computer and Intel-based architectures: HF, DFT, resolution-of-the-identity second-order Møller-Plesset (RI-MP2) method, and QMC method.

7). Two-component relativistic electronic structure calculation with spin-orbit (SO) interactions: Douglas-Kroll (DK) (DK1, DK2, and DK3), regular approximation (RA) (zeroth-order RA (ZORA) and infinite-order RA (IORA)), and Relativistic scheme for Eliminating Small Components (RESC).

8). Model calculations for large molecular systems: quantum mechanics/molecular mechanics (QM/MM) and Our own N-layered Integrated molecular Orbital and molecular Mechanics (ONIOM).

9). Calculation of solvation effects: COnductor-like Screening MOdel (COSMO) (interfaced with the HONDO program), averaged solvent electrostatic potential/molecular dynamics (ASEP/MD), and QM/MM-MD.

10). Efficient calculation for chemical reaction pathway.

11). Ab initio molecular dynamics calculation.

12). Calculation of magnetic properties: nuclear magnetic resonance (NMR) chemical shifts, magnetizabilities, and electron paramagnetic resonance (EPR) g tensors.

13). Population analysis: Mulliken and natural bond orbital (NBO) analysis (interfaced with NBO 6.0).

14). Orbital interaction analysis: maximally interacting orbital (MIO) and paired interacting orbital (PIO) methods.

8.3 Research Results and Achievements

8.3.1 Massively parallel linear scaling quantum chemistry

[Introduction] The goal of this project is to develop new techniques and software that enable the routine application of quantum chemistry calculations to systems with thousands of atoms. This requires the development of new algorithms and data structures which remove memory bottlenecks and reduce algorithmic scaling. In addition, the heterogeneous nature of large systems will require new methodologies for extracting insight into the origin of important properties.
[Contents A] Building on our previous year's work, we continued to develop a new version of NTChem for performing calculations on large systems. We addressed the construction of the Fock matrix, which was a major bottleneck in the code. We introduced sparse, distributed data structures into this part of the code, which removed the hard limit of system sizes that existed in NTChem due to memory constraints. We further introduced reduced scaling algorithms into the code that can be efficiently parallelized, leading to a dramatic decrease in time to solution for large systems. The capabilities of the code were further expanded to include relativistic effects, making it a promising code for the study of large molecular systems including heavy elements.
[Contents B] As part of the RIKEN-CEA collaboration, we further worked on improving large scale calculations by developing a method for automatically breaking large systems into fragments. This complexity reduction approach generates a simplified description of large systems, allowing users to focus their effort on a subset of the system. In addition, this approach allows for a quantitative description of interactions between fragments, which can be used for graph theory based system analysis or the design of QM/MM partitioning schemes. The partitioning approach is based on the actual properties of the electron density, leading to physically meaningful fragmentations of exotic systems while requiring no a priori knowledge. This fragmentation method was implemented into the new PyBigDFT package, which provides a python based, high level interface for the BigDFT code.
[Results] In the below Fig. (a), we show the performance of the new Fock matrix building routine in NTChem. The new approach enables calculations on systems with thousands of atoms, and calculation costs can be efficiently driven down by employing large numbers of cores. In Fig. (b), we demonstrate the automatic system partitioning technique in application to a laccase enzyme. This enzyme is particularly difficult to partition with standard techniques because of its inclusion of copper atoms. The automatic technique, however, is able to treat all kinds of system moieties, and gives a high level description of the active site.

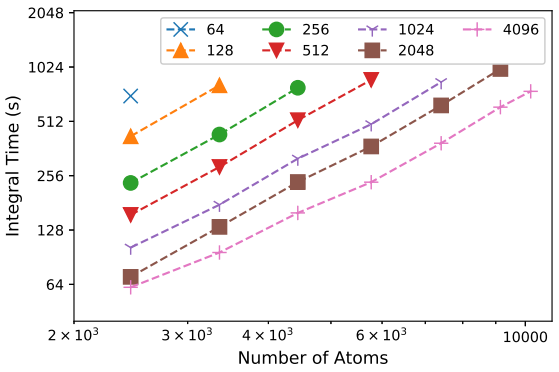

(a) Performance of Fock matrix build (Coulomb and Exchange analytic integrals) for water clusters (6-31G basis set) of various sizes/node counts.

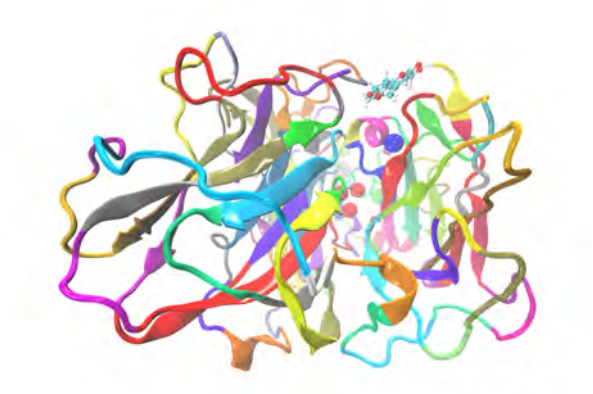

(b) Automatic system partitioning. The partitioned enzyme is colored by fragment in the ribbon representation, and a docked ligand is colored by atomic element and drawn as balls and sticks.

8.3.2 Massive parallelization of the numerical integration in the two-component relativistic linear response time-dependent density functional method

In recent years, high-performance photoresponsive materials have been developed based on spin-orbit interaction, and various applications such as dye-sensitized solar cells and organic electro-luminescence are expected. Various spin phenomena are also attracting attention as a basis of magnetic materials and spintronics materials.

Therefore, there is interest in theoretical methods capable of calculating excitation energy with high accuracy, which can take account of electron correlation and relativistic effects, in particular, spin-orbit interaction.

Relativistic time-dependent density functional theory is a method that can consider electron correlation and spin-orbit interaction with relatively low computational cost, and has recently been applied to calculation of excitation energy of molecules including heavy atoms. In the relativistic linear response time-dependent density functional theory including the damping factor, the excitation spectrum can be obtained directly from the complex polarizability, so it is considered to be applicable to large-scale molecular systems. The implementation has been done in the quantum chemistry package NTChem. The program of this relativistic linear response time-dependent density functional theory is implemented in parallel, and process parallelization is feasible. However, sufficient performance has not been obtained due to the DFT part. Also, since thread parallelization is not sufficiently considered, sufficient performance cannot be obtained when hybrid parallelization is performed. In this year, massive parallelization was performed on the numerical integration part of DFT (density functional theory) calculation in the two-component relativistic linear response time-dependent density functional method.

In the current program, a loop related to a grid in each atom is divided by I/O nodes to store the grid. However, when there is a sufficient number of nodes, the calculation load is not distributed to nodes greater than or equal to the number of atoms, resulting in that the performance of the DFT calculation unit is not improved more than a certain amount at the time of process parallel. Therefore, we changed the parallel structure of the grid / batch loop. As a result, the process scalability was improved, and the DFT calculation process could be accelerated by 5.97 times (1024 processes) at the time of the change.

Next, we implemented thread parallelization for calculating the high cost trial electron density and the trial spin electron density in numerical integration. As a result, thread scalability has been improved, and DFT calculation processing can be sped up by 2.92 times when executed with 8 threads (1024 processes).

In summary, due to the change in parallel structure accompanying I/O and thread parallelization of the high cost part, DFT calculation processing could be speeded up 28.51 times (1024 processes).

8.3.3 Relativistic molecular orbital theory

In this year, in order to enhance the relativistic molecular orbital calculation in NTChem, we have developed new theories and test programs for them based on the following four themes. The progress and achievements of each theme are mentioned.

[**Douglas-Kroll (DK) and IOTC transformation of Dirac-Fock operator**] The conventionally known two-component method determines transformaion from four component operator to two component one only from the one-electron Hamiltonian, ignoring electron repulsion. That is, error from the four-component method is included. We derived exact equation applying the DK and IOTC methods to the Fock matrix. These methods do not include the aforementioned error. The results of numerical calculation are also good. We are currently preparing a paper.

[**Realistic nuclear charge density model**] In electronic state calculations, nuclei are just potentials, and are treated as point charges, uniformly charged spheres, or Gaussian distributions. However, real nuclei have various distributions, and it is considered that innner shells of heavy and superheavy elements affected by this charge distribution. We derived a new nuclear model that can express general charge distribution and is suitable for analytical calculations. The paper will be written as soon as numerical verification is completed (Figure 8.1).

[**Approximation formulas for two-electron integral included small component basis**] For high-accuracy and high-speed calculation of relativistic molecular orbital method, two-electron integration including small components becomes a problem. In order to their high angular momentum gives high computational cost. We derived a new formula that can approximate these integrals with high accuracy. Using these formulas makes it possible to calculate four-component method and high-precision two-component method at almost the same speed as non-relativistic calculation. In this year, we were formulating a formula and performing numerical verification.

[**QED based four-fermion interaction potential for relativistic molecular orbital theory**] Relativistic molecular orbital method is based on relativistic quantum mechanics, but relativistic quantum mechanics is extended to quantum electrodynamics (QED) which is field quantum theory due to problems of negative energy solution etc. There is a historical background that has been done. Therefore, it is desirable to extend the molecular orbital method to one based on QED in order to refine the theory. However, it is difficult to introduce QED formulated by covariant perturbation theory as it is into molecular orbital method. Therefore, we derived the effective potential between the electrons whose photons were internal. Numerical verification is under perspective.

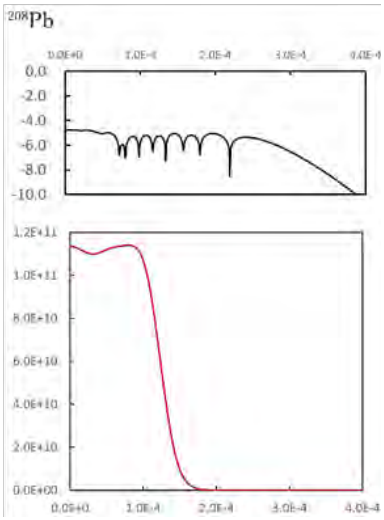

Figure 8.1: Application example to experimental value of nucleon density of lead. The upper is the potential fitting error (log) and the lower is the density fitting.

8.3.4 Antisymmetrized geminal powers with larger chemical basis sets [5]

In previous research, we tested the wave function format of a linear combination of several antisymmetrized geminal power states. A numerical problem in the geminal matrices was noted, which made the total energies of electronic systems with large numbers of electrons unstable. The underlying cause was found to be the large cancellation term in the geminal power series. We have obtained a new format to resolve this problem for the case of total energies and partly for the first-order derivatives within the antisymmetrized geminal power states. By using this new formalism, we have calculated the ground state energies for several electronic systems, including the usage of a larger chemical basis set. The results are, in some cases, very close to the exact result, especially for one-dimensional Hubbard systems. Our result for a water molecule with the Double Zeta basis set is better than the CISD energy and approaches the CCSD energy.

8.3.5 UNO DMRG CAS CI calculations of binuclear manganese complex $Mn(IV)_2O_2(NHCHCO_2)_4$: Scope and applicability of Heisenberg model [6]

Both direct exchange and super-exchange interactions cooperate to realize inter-spin magnetic interaction in binuclear manganese complex $Mn(IV)_2O_2(NHCHCO_2)_4$ with a di-μ-oxo path. We revisited this spin system using DMRG CAS methods and CAS selection procedures. Our results indicate that our previous "dynamically extended spin polarization" (DE-SP) procedure for organic polyradicals and so forth does not work well. Thus, we have examined another selection procedure, the "dynamically extended super-exchange" (DE-SE) procedure. DMRG CASCI [18,18] by UB3LYP(HS)-UNO(DE-SE) can realize antiferromagnetic J values similar to experimental ones (-87 cm^{-1}). In addition, all J values between all spin states (HS[septet], IS[quintet], IS[triplet], LS[singlet]) were also shown to be correct under sufficiently large M values.

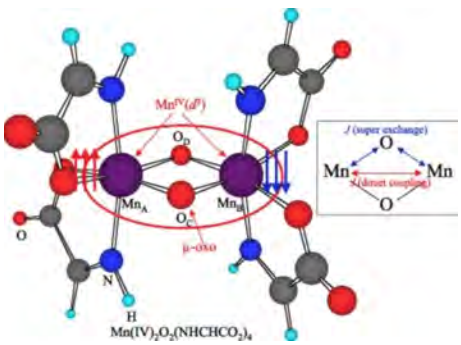

8.3.6 A study on quantum dynamics of excited electrons in molecular aggregates

Our research project is to explore and reveal quantum dynamics of excited electrons in complex networks consisting of chemical bond as well as molecular interaction in functional molecular aggregates. The mechanism of conversion from light energy to chemical functionalities realized in photosynthesis system and organic solar cell using visible region in wave length of light consist of multiple microscopic processes. In this context, one of important topics in physical chemistry is to understand a dynamical propensity of excited electrons depending on molecular as well as external conditions. For this purpose, it is useful to characterize time dependent behaviors of excited electrons, excitons and charge carriers under influence of diffusion, nonadiabatic deactivation, and charge separation, associated with state mixing and transition by light-matter, nonadiabatic and spin-orbit couplings. To obtain an intuitive picture of these quantum mechanical phenomena is important to explore a possible resource of ubiquitous energy and develop a novel nano-science from a view point of quantum dynamics. This research belongs to one of post-K projects intended to explore and develop a scenario of efficient light energy conversion and storage.

In the fiscal year 2018, we investigated effects of molecular fluctuation on electron dynamics. For this purpose, group-diabatic-Fock(GDF) electron dynamics scheme [23] was extended to include an effect of structure fluctuation of molecular aggregates. Nonadiabaticity for electrons by molecular motion was partly included through nuclear derivative couplings of atomic orbitals. NTChem was used for ab initio electronic structure calculation. Molecular dynamics as a noise for electronic Hamiltonian were treated using ab initio dynamics calculation on ground state potential energy surface. Through applications to typical donor-acceptor systems having different characters in initial states and density of states, we observed promotion and depression of charge migration depending on initial electronic states, which indicates a microscopic complexity in charge migration associated with excited electron dynamics [36, 38]. The details on one typical application are given in the caption of Fig. 8.2. Readers can find the full imformation including a calculation level in the abstract of the author's presentation in the MolSci2018 conference [36, 38].

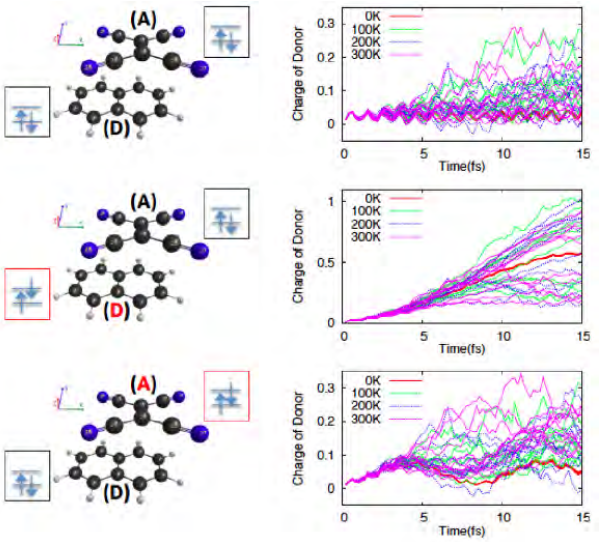

Figure 8.2: Effect of molecular structure fluctuation on charge migration dynamics in naphthalene(NPTL) and tetra-cyano-ethylene(TCNE) dimer. NPTL and TCNE play as electron donnor(D) and acceptor(A), respectively. In the right column, time dependent charges of (D) side are shown corresponding to the hypothetical initial local excitations in group diabatic representation depicted in the left column. The referential relative structure of dimer is the same as the previous work. Values inside the panels in the right column denote microcanonical temperatures in Kelvin evaluated from initial kinetic energies, of which corresponding velocities are randomly produced. The results are shown for 10 trajectories for each cases with different initial excitations of group diabatic local HOMO and LUMO for two monomer. In the top and bottom panels, structure fluctuation promotes charge migration among (D)-(A). On the other hand, in case of group diabatic local HOMO-LUMO excitation of (D) shown in the panel at mid position, molecular fluctuation results in promotion and depression of charge migration for approximately half number trajectories. This indicates that the effect by structure dynamics on charge migration is sensitive to the instantaneous electronic state.

8.3.7 Photochemistry of aqueous coumarin: Quantum mechanics/molecular mechanics trajectory surface hopping simulation approach

We performed the research supported by MEXT as "Priority Issue on Post-K Computer" (Development of new fundamental technologies for high-efficiency energy creation, conversion/storage and use). The aim of the project is (1) to decipher the working mechanisms of organic photovoltaics (OPVs) and (2) to establish the relationship between the microscopic molecular structure and the power conversion efficiency (PCE) by using *ab initio* methods. The formation of the interfacial charge-separated state is an essential factor accounting for high PCE. Thus, it is necessary to simulate the exciton (hole–electron pair) dynamics leading to the charge separation and to extract the critical factors controlling the process. The OPV consists of the donor polymer and the acceptor, and both the mixing ratio and the morphology strongly affect the exciton dynamics. Thus, one must take accounts of the donor–donor interchain and the donor–acceptor intermolecular interactions.

In FY2018, we realized the quantum mechanics/molecular mechanics (QM/MM) nonadiabatic molecular dynamics (NAMD) simulation. For that purpose, we interfaced the molecular mechanics force field taken from the TINKER suite program with our program developed in the past, i.e., the hybrid of Tully's fewest switch surface hopping molecular dynamics (FSSH-MD) and the linear-response time-dependent density functional theory (LR-TDDFT). The approach allows the excited-state NAMD in the complex molecular environment.

We applied the program to the photochemistry of unsubstituted coumarin in an aqueous solution. In the previous study [7], we observed that unsubstituted coumarin in the gas phase has nonradiative decay paths to the ground state via direct ($\pi\pi^* \rightarrow S_0$) or indirect ($\pi\pi^* \rightarrow n\pi^* \rightarrow S_0$) way. Figure 8.3(top) shows a representative trajectory. The molecule relaxes to the S_1 state rapidly ($\leq$ 100 fs), which is consistent with Kasha's rule. During the stay on the S_1 state, the energy gap between the S_0 and S_1 states decreases. At the final time (500 fs), the simulation terminates due to the small energy gap. Figure 8.3(bottom) shows the bond length between the carbonyl carbon and ether oxygen begins to increase at 200 fs. As observed in the gas-phase simulation [7], this bond corresponds to the reaction coordinate of the S_0/S_1 crossing.

In the future, we will apply the current approach to donor-acceptor complexes mimicking OPVs.

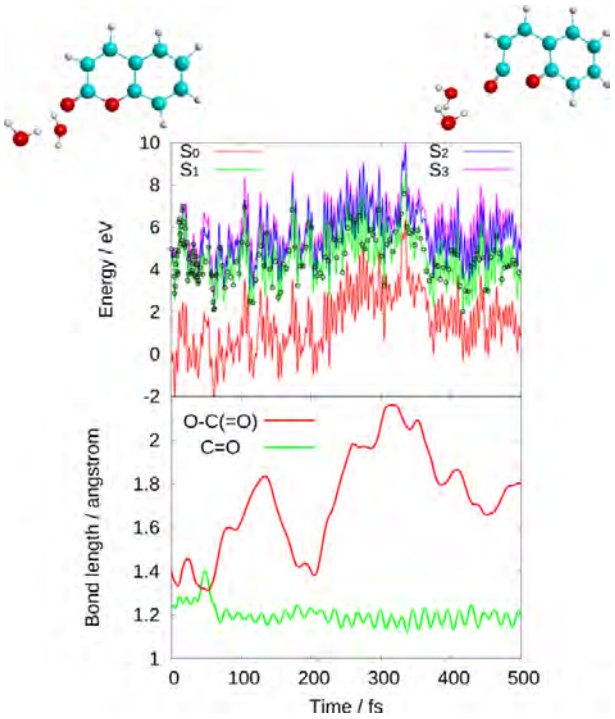

Figure 8.3: (Top) Typical trajectory of coumarin leading to S_0/S_1 crossing. (Bottom) Bond length between carbonyl carbon and ether oxygen and that between carbonyl carbon and oxygen.

8.3.8 A path integral molecular dynamics study on intermolecular hydrogen bond of acetic acid-arsenic acid anion and acetic acid-phosphoric acid anion clusters [8]

We apply ab initio path integral molecular dynamics simulation employing ωB97XD as the quantum chemical calculation method to acetic acid-arsenic acid anion and acetic acid-phosphoric acid anion clusters to investigate the difference of the hydrogen bond structure and its fluctuation such as proton transfer. We found that the nuclear quantum effect enhanced the fluctuation of the hydrogen bond structure and proton transfer, which shows treatment of the nuclear quantum effect was essential to investigate these systems. The hydrogen bond in acetic acid-arsenic acid anion cluster showed characters related to low-barrier hydrogen bonds, while acetic acid-phosphoric acid anion cluster did not. We found non-negligible distinction between these two systems, which could not be found in conventional calculations. We suggest that the difference in amount of atomic charge of the atoms consisting the hydrogen bond is the origin of the difference between acetic acid-arsenic acid and acetic acid-phosphoric acid anion cluster.

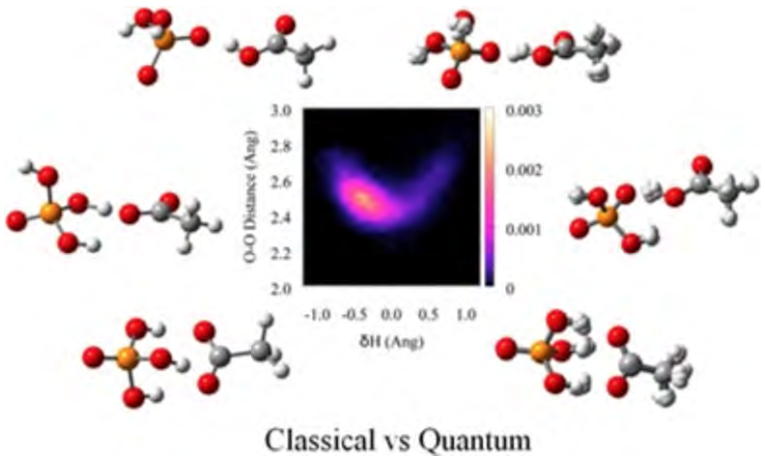

8.3.9 Towards accurate infrared spectral density of weak H-bonds in absence of relaxation mechanisms [9]

Following the previous theoretical developments to completely reproduce the IR spectra of weak hydrogen bond complexes within the framework of the linear response theory (LRT), the quantum theory of the high stretching mode spectral density (SD) of weak H-bonds is reconsidered. Within the LRT theory, the SD is the one sided Fourier transform of the autocorrelation function (ACF) of the high stretching mode dipole moment operator. In order to provide more accurate theoretical bandshapes, we have explored the equivalence between the SDs given in previous studies with respect to a new quantum one, and revealed that in place of the basic equations used in the precedent works for which the SD $I_{Old}(\omega) = 2\mathrm{Re}\int_0^\infty G_{Old}(t)\mathrm{e}^{-i\omega t}dt$ where the ACF $G_{Old}(t) = \langle\mu(0)\mu(t)^+\rangle = tr\{\rho\{\mu(0)\}\{\mu(t)\}^+\}$, one can use a new expression for the SD, given by $I_{New}(t) = 2\omega\mathrm{Re}\int_0^\infty G_{New}(t)\mathrm{e}^{-i\omega t}dt$ where $G_{New}(t) = \langle\mu(0)\mu(t)^+\rangle = \frac{1}{\beta}tr\{\rho_B\int_0^\beta\{\mu(0)\}\{\mu(t+i\lambda\hbar)\}^+d\lambda\}$. Here ρ_B is the Boltzmann density operator, $\mu(0)$ the dipole moment operator at initial time and $\mu(t)$ the dipole moment operator at time t in the Heisenberg picture, $\hbar$ is the Planck constant, β is the inverse of the Boltzmann factor k_BT where T is the absolute temperature and k_B the Boltzmann constant. Using this formalism, we demonstrated that the new quantum approach gives the same final SD as used by previous models, and reduces to the Franck-Condon progression appearing in the Maréchal and Witkowski's pioneering approach when the relaxation mechanisms are ignored. Results of this approach shed light on the equivalence between the quantum and classical IR SD approaches for weak H-bonds in absence of medium surroundings effect, which has been a subject of debate for decades.

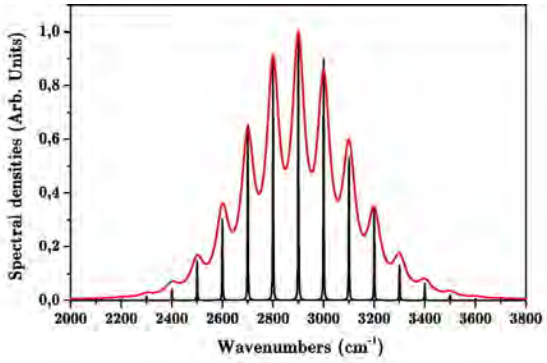

	$I(\omega)=\mathrm{Re}\int_{-\infty}^{+\infty} G^{\circ}(t)\, e^{-i\omega t}dt$	$ACF: G^{\circ}(t)$
Old models	$2\,\mathrm{Re}\int_0^{\infty}\langle\mu(0)\mu(t)^{+}\rangle\, \mathrm{e}^{-i\omega t}dt$	$G^{\circ}(t)_{Old}=tr\left\{\rho\{\mu(0)\}\{\mu(t)\}^{+}\right\}$
New model	$2\omega\,\mathrm{Re}\int_0^{\infty}\langle\mu(0)\mu(t)^{+}\rangle\, \mathrm{e}^{-i\omega t}dt$	$G^{\circ}(t)_{New}=\frac{1}{\beta}tr\left\{\rho\int_0^{\beta}\{\mu(0)\}\{\mu(t+i\lambda\hbar)\}^{+}d\lambda\right\}$
Incorporation of direct relaxation: $G(t)=G^{\circ}(t)\exp(-\gamma^{\circ}t)$		

8.3.10 Excitation energies expressed as orbital energies of KS-DFT with LC functionals

Density functional theory (DFT) is as a powerful computational tool for the chemical systems. Conceptually, it is appealing because, with the one-electron Kohn-Sham (KS) DFT, all properties are in principle obtainable directly from an observable that is the electron density. However, the major obstacle to the application of KS DFT is that the form of the exact functional is yet unknown. As a result, there have been continuous developments of approximate DFT methods. These methods represent a useful way for tackling many chemical problems with adequate accuracy. Though the approximate DFT methods often underestimate barrier heights, yield repulsive van der Waals interactions, underestimate excitations [obtained with time-dependent DFT (TD-DFT)] for Rydberg states, core-excitations and charge transfer states. The reason being that a solution of the exact Kohn-Sham (KS) equation satisfies Koopmans' theorem; therefore, in principle, one-electron excitation energy expressed using KS solutions. Approximate KS-DFT, however, does not satisfy Koopmans' theorem. In comparison, long-range corrected (LC) functionals satisfies the Koopmans' theorem well. As a result, we can obtain accurate one-electron excitation energies as the difference between LC-DFT occupied orbital energies of a neutral molecule and corresponding unoccupied orbital energies of its cation. Two such expressions, with one employing the orbital energies for the neutral and cationic systems, while the other utilizes orbital energies of just the cation. Because the electron affinity of a molecule is the ionization energy of its anion, the two expressions would coincide and give the same excitation energies with the exact functional. When approximate functionals used, however, we would expect the two representations to give different excitation energies. By contrast, in this study, when the present scheme used in conjunction with LC-type functionals, we obtain promising results for valence, inner-valence and core-excitations.

8.3.11 High-throughput screening of perovskite oxynitride and oxide materials for visible-light photocatalysis [10]

We performed a high-throughput screening of 29,160 perovskite oxynitrides and oxides in order to discover novel photocatalysts for water splitting by visible light. Efficient high-throughput simulations with density functional theory were performed on the K computer, which is a massively parallel multi-core supercomputer in Japan. By applying the screening procedure to the entire set of compounds in the database, 42 potential perovskite-photocatalyst candidates for visible-light water splitting were discovered, including 34 newly proposed perovskites. Of the 42 potential candidates, six perovskites, viz., $NaWO_2N$, KWO_2N, $MgWON_2$, $CaVO_2N$, $CaAl_{1/3}W_{2/3}O_2N$, and $CaV_{2/3}Fe_{1/3}O_3$, are desirable in terms of cost.

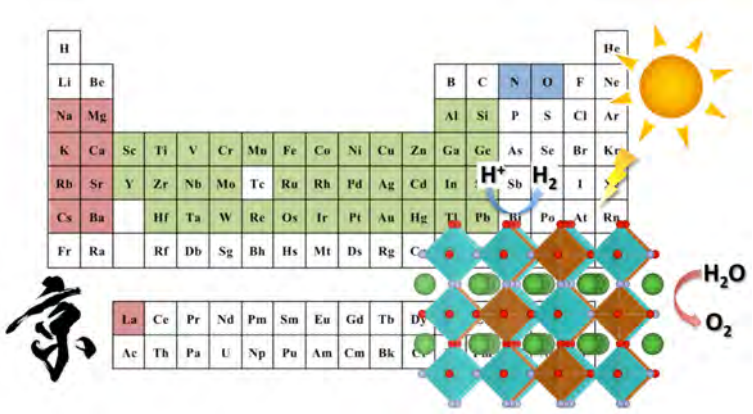

8.3.12 Material design of hole-transporting materials for perovskite solar cells

Spiro-OMeTAD is a hole-transporting material (HTM) known for its high power conversion efficiency (PCE) for perovskite solar cells. For perovskite with compound $Cs_{0.10}FA_{0.90}Pb(I_{0.83}Br_{0.17})_3$, the PCE is 21.1%. The predicted cost of spiro-OMeTAD is approximately \$274/g. Much cheaper material has been found with comparably high PCE (X60: \$120/g, Py-C: \$192/g, etc). Cost effective material with high PCE are yet to be investigated.

Efficient search of optimum hole-transport material can be achieved by applying machine learning techniques. We employed deep neural network (DNN) to predict power conversion efficiency of HTMs by utilizing molecular descriptors as input feature. We also employed Gaussian process regression to evaluate the acquisition function for Bayesian optimization and implement uncertainty and reliability to prediction model. Discrete particle swarm optimization has been applied to tackle optimization problem in the vast chemical space.

We created a machine learning model to predict PCE of perovskite solar cell out of the molecules generated from structural combinations of known HTMs. Total of 400 experimental PCE data have been collected for training the model. We employed 170 hole-transporting molecules, 54 compounds of active layer along with valence band maxima and conduction band minima of those compounds, 6 electron-transporting molecules, dopants, active area, and PCE as input data. The molecular descriptors of the HTMs have been calculated with Mordred. Among the entries collected, PCEs were selected as target variable and the rest as features of the DNN prediction model. We selected 3,4-ethylenedioxythiophene as the main structure with selected moieties of 170 HTMs, functioning as substituents to the main structure. As a virtual experiment, the PCE of the candidate HTM has been predicted from the DNN model. The Gaussian regression model has been improved by repeating the prediction and the virtual experiment, and the best candidate HTM has been chosen by the improved model (Figure 8.4).

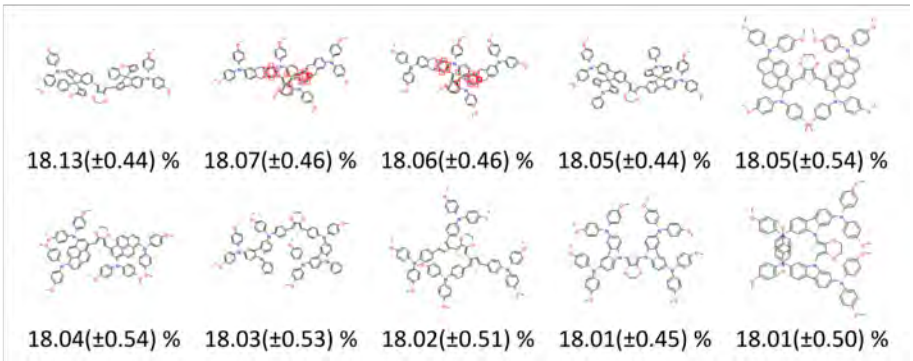

Figure 8.4: Candidate HTMs found by Bayesian optimization.

8.3.13 Theoretical study on mesoscopic-size impurity effects in the charge separation process of organic photocells [11]

A bulk-heterojunction structure is often employed to develop high-performance organic photocells, in which the donor and acceptor regions are complexly intertwined. In such situations, mesoscopic-scale islands and peninsulas that compose the donor materials may be formed in the acceptor region. Alternatively, the donor region may extend deeply into the acceptor region. This yields mesoscopic-size impurities that can create obstacles in the charge separation (exciton dissociation) process of organic photocells and prevents the dissociation of excitons (electron-hole pairs). We previously reported on the effect of the cooperative behavior between the hot charge transfer (CT) state and the dimensional (entropy) effect on the charge separation process. In this paper, we discuss the mesoscopic-scale impurity effect on the charge separation process in PCBM acceptor models by considering the hot CT state and dimensional effects. In addition, we discuss atomic-scale effects such as molecular distortions and conformation changes using molecular dynamics (MD) simulations.

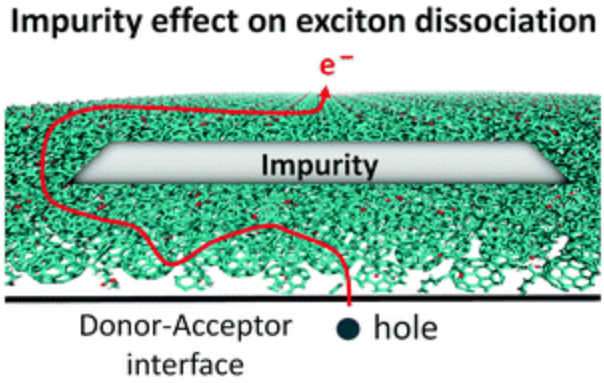

8.3.14 Spectroscopic study of uracil, 1-methyluracil and 1-methyl-4-thiouracil: Hydrogen bond interactions in crystals and ab-initio molecular dynamics [12]

Hydrogen bond networks in uracil, 1-methyluracil and 1-methyl-4-thiouracil were studied by ab initio molecular dynamics as well as analysis of the orbital interactions. The power spectra calculated by ab initio molecular dynamics for atoms involved in hydrogen bonds were analyzed. We calculated spectra by using anharmonic approximation based on the autocorrelation function of the atom positions obtained from the Born-Oppenheimer simulations. Our results show the differences between hydrogen bond networks in uracil and its methylated derivatives. The studied methylated derivatives, 1-methyluracil as well as 1-methyl-4-thiouracil, form dimeric structures in the crystal phase, while uracil does not form that kind of structures. The presence of sulfur atom instead oxygen atom reflects weakness of the hydrogen bonds that build dimers.

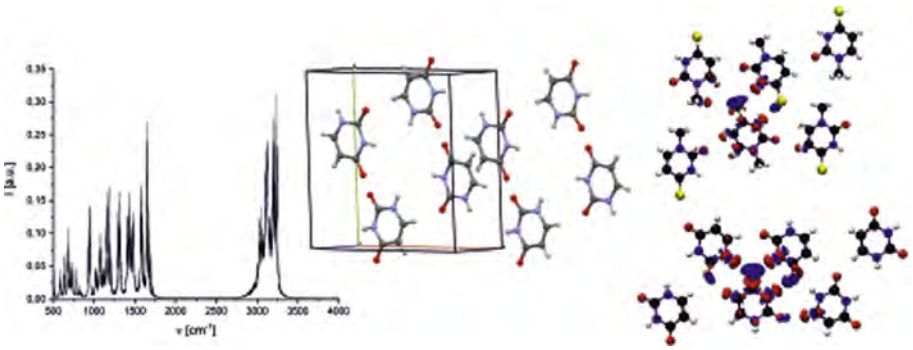

8.3.15 Study of hydrogen bond dynamics in Nylon 6 crystals using IR spectroscopy and molecular dynamics focusing on the differences between α and γ crystal forms [13]

Proton dynamics of hydrogen bonds (HBs) in the α and γ form of Nylon 6 were investigated by Born-Oppenheimer molecular dynamics (BOMD). Our results show differences in the dynamic effects of interchain HB interactions between the α form and the γ form of Nylon 6. Analysis of the time course of the geometrical parameters of HBs along the BOMD simulations has shown that HBs are dynamically favored in the γ form of Nylon. The quantization of the N–H stretching mode enables a detailed discussion of the strengths of HB interactions. Solving the Schrödinger equation for the snapshots of one-dimensional proton potentials, extracted from the ab initio MD, enables the consideration of anharmonicity, thermodynamics, and approximate quantum effects on proton movement. A larger red shift of the N–H stretching band was observed in the γ form compared with the α form. Our study shows that HBs are more stabilized in the γ form than in the α form, which is mainly due to the higher number of HBs. The distribution of HBs along the trajectory clearly reveals the preference of the γ form. The quantization of the N–H motion enables the discussion of the differences in the IR spectra between the two forms.

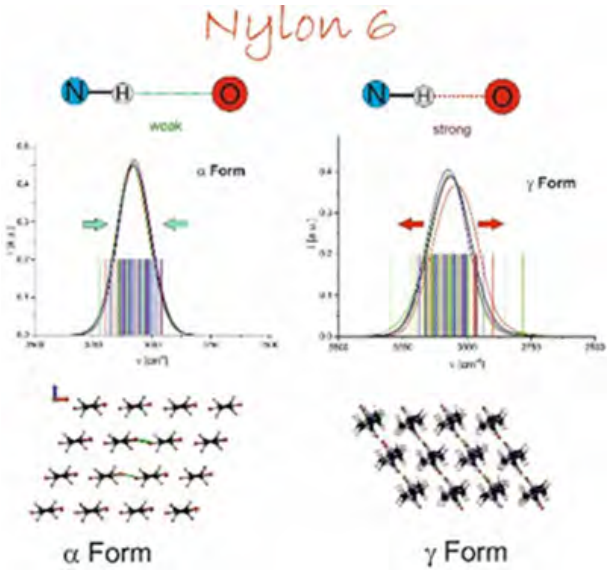

8.3.16 Proton dynamics in crystalline tropolone studied by Born-Oppenheimer molecular simulations [14]

Proton dynamics in a tropolone crystal was studied by 2D quantization of nuclear motions using Born-Oppenheimer molecular dynamics. This study presents the characteristics of the conjugated system of OH stretching vibrations in the tropolone crystal. The MD simulations elucidate the presence of a pseudo-cyclic dimer structure in the crystal phase. The results obtained herein were compared with the IR spectroscopic data for the tropolone crystal. The skeleton and butterfly motions of the seven carbon rings strongly influence the strength of the hydrogen bonds in the cyclic dimers and are extensively discussed in this paper.

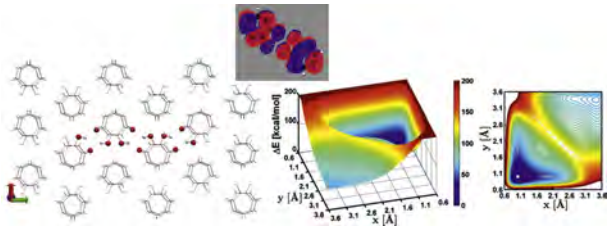

8.3.17 A simple model for relative energies of all fullerenes reveals the interplay between intrinsic resonance and structural deformation effects in medium-sized fullerenes [15]

Fullerenes are sheets of sp^2 carbon atoms wrapped around to form spheres. With this simple consideration, we have in the present study devised and (with over 3600 DFT data points) successfully validated a simple model, termed R+D, for estimating the relative energies of fullerenes. This model contains a resonance component to account for the intrinsic differences between the π-energies of different fullerenes, and a deformation component for treating the distortions from planarity. Notably, we find that both terms (and they alone) are required to obtain good relative energies, which lends support to the formulation of the R+D model. An interesting finding is that for some medium-sized IPR fullerenes, their isomers show similar variations in the two components. We deduce that these fullerenes may represent a good opportunity for tuning molecular properties for practical applications. We hope that the promising results of the present study will encourage further investigations into fullerenes from a fundamental perspective.

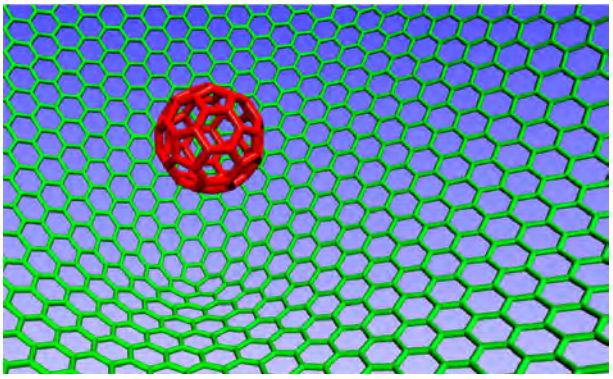

8.3.18 Nonadiabatic one-electron transfer mechanism for the O-O bond formation in the oxygen-evolving complex of photosystem II [16]

The reaction mechanism of the O_2 formation in the S_4 state of the oxygen-evolving complex of photosystem II was clarified at the quantum mechanics/molecular mechanics (QM/MM) level. After the Yz (Y161) oxidation and the following proton transfer in the S_3 state, five reaction steps are required to produce the molecular dioxygen. The highest barrier step is the first proton transfer reaction (0→1). The following reactions involving electron transfers were precisely analyzed in terms of their energies, structures and spin densities. We found that the one-electron transfer from the Mn_4Ca cluster to Y161 triggers the O-O sigma bond formation.

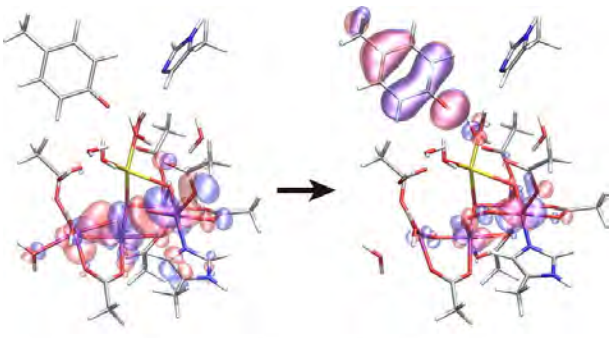

8.3.19 Concerted mechanism of water insertion and O_2 release during the S_4 to S_0 transition of the oxygen-evolving complex in photosystem II [17]

The O_2 release of the oxygen-evolving complex of the photosystem II (PSII) is one of the essential processes responsible for the highly efficient O_2 production. Despite its importance, the detailed molecular mechanism is still unsolved. In the present study, we show that the O_2 release is directly coupled with water insertion into the Mn cluster based on the quantum mechanics/molecular mechanics (QM/MM) calculations. In this mechanism, the O_2 molecule first dissociates from the Mn sites in order, that is, the O atom coordinating to the Mn3 (O5a) first dissociates, then the other O atom coordinating to the Mn1 (O5d) dissociates in the next step in the late S_4 state (1→2). Next, the O_2 migrates to a space surrounded by the Val185 and His332 side chains as one water molecule coordinating to the Ca^{2+} ion (W3) comes into the O_2 bonded site (2→3). Finally, a pre-S_0 state (4) is formed after a proton transfer from the inserted water to the other proton acceptor site (W2) (3→4). The highest activation barrier during these reactions was found at the O_2 release step (2→3) that only requires $E^{\ddagger}$ = 12.7 kcal mol^{-1} ($G^{\ddagger}$ = 10.4 kcal mol^{-1}). A series of the reactions (2→3) look like a chain crash of billiard balls because the W3 is inserted into the catalytic center from the water-abundant side (Ca^{2+} ion side), and then the O_2 moiety is pushed out to the opposite side (Val185 side). The hydrophobic residue of Val185 covers the active O5 site and forms an O_2-specific permeation tunnel. The present sequential reactions clearly demonstrate the efficient removal of the toxic O_2 from the catalytic center and implications of the essential roles of Val185, Ca^{2+} ions and water molecules, which are all present in the active site of PSII as the indispensable constituents.

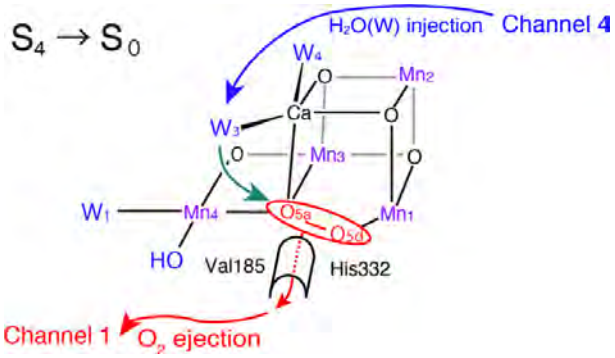

8.3.20 Relative stability between the manganese hydroxide- and oxo-models for water oxidation by CCSD, DMRG CASCI, CASSCF, CASPT2 and CAS-DFT methods; Importance of static and dynamical electron correlation effects for OEC of PSII [18]

Relative stability between manganese hydroxide $(H_2O)_2(OH)_4Mn(IV)OH$ (1) and manganese oxo $(H_2O)_3(OH)_3Mn(IV)O$ (2) species were investigated by coupled cluster (CC) SD and SD(T), DMRG CASCI, CASSCF, CASPT2 and CASDFT methods. The DMRG CASCI and DMRG CASSCF based on thirteen active orbitals and thirteen active electrons {13, 13} CAS space indicted the greater stability of 2 than 1. On the other hand, the relative stability between 1 and 2 was reversed by UCC SD, DLPNO-UCC SD, CASPT2 and CAS-DFT, indicating an important role of dynamical electron correlation corrections. Implications of present results are discussed to elucidate scope and applicability of hybrid DFT (HDFT) methods for 1 and 2.

8.4 Schedule and Future Plan

In the next fiscal year, we will continue to develop new algorithms and improve the parallel efficiency of the NTChem suit of program. We will work to develop a new version of NTChem which can perform quantum chemistry calculations on systems with over thousands of atoms. The NTPoly library will be utilized to develop a memory parallelization scheme, removing a significant cause of system size limitations from NTChem. We will replace the basic solver routines with linear scaling methods based on density matrix minimization and purification. We will also work to implement TDDFT with the same memory parallelization scheme. Moreover, we will continue to develop the SO-TDDFT, related methods for excited-state dynamics, and high-accuracy quantum chemical methods.

8.5 Publications

8.5.1 Articles/Journal

[1] 中嶋隆人, "「京」によるペロブスカイト太陽電池の新材料候補探索", マテリアルズ・インフォマティクスによる材料開発と活用集, 技術情報協会 第7章第5節 (2019).
[2] 中嶋隆人, "『京』で見つけたペロブスカイト太陽電池新素材候補", パリティ, 2018年07月号.
[3] 庄司光男, 磯部寛, 重田育照, 中嶋隆人, 山口兆, "光合成における酸素発生の反応機構", 生物物理, 58, 127–133 (2018). 10.2142/biophys.58.127
[4] M. Kamiya, T. Nakajima, "Relativistic time-dependent density-functional theory for molecular properties", in Frontiers of Quantum Chemistry, edited by M. Wojcik, H. Nakatsuji, B. Kirtman, Y. Ozaki (Springer), 223–247 (2018). 10.1007/978-981-10-5651-2_10
[5] W. Uemura and T. Nakajima, "Antisymmetrized geminal powers with larger chemical basis sets", Phys. Rev. A **99**, 012519 (2019).
[6] T. Kawakami, K. Miyagawa, S. Sharma, T. Saito, M. Shoji, S. Yamada, S. Yamanaka, M. Okumura, T. Nakajima, and K. Yamaguchi, "UNO DMRG CAS CI calculations of binuclear manganese complex $Mn(IV)_2O_2(NHCHCO_2)_4$: Scope and applicability of Heisenberg model", J. Comput. Chem. **40**, 333–341 (2019).
[7] T. Yonehara, N. Minezawa, and T. Nakajima, "Excited state dynamics in NTChem," *Molecular Spectroscopy: A Quantum Chemical Approach*, 1st ed. edited by Y. Ozaki, M. J. Wójcik, and J. Popp (Wiley-VSH, Weinheim, 2019), Chap. 2.
[8] Y. Kawashima, K. Sawada, T. Nakajima, and M. Tachikawa, "A path integral molecular dynamics study on intermolecular hydrogen bond of acetic acid-arsenic acid anion and acetic acid-phosphoric acid anion clusters", J. Comput. Chem. **40**, 172–180 (2019).
[9] N. Rekik, S. Salman, U. Farooq, T. Nakajima, M. J. Wojcik, and P. Blaise, "Towards accurate infrared spectral density of weak H-bonds in absence of relaxation mechanisms", Spectrochim. Acta, Part A **207**, 197–208 (2019).
[10] K. Sawada and T. Nakajima, "High-throughput screening of perovskite oxynitride and oxide materials for visible-light photocatalysis", APL Mater. **6**, 101103 (2018).
[11] T. Shimazaki, M. Tashiro, and T. Nakajima, "Theoretical study on mesoscopic-size impurity effects in the charge separation process of organic photocells", Phys. Chem. Chem. Phys. **20**, 14846–14854 (2018).
[12] M. Z. Brela, M. Boczar, L. M. Malec, M. J. Wojcik, and T. Nakajima, "Spectroscopic study of uracil, 1-methyluracil and 1-methyl-4-thiouracil: Hydrogen bond interactions in crystals and ab-initio molecular dynamics", Spectrochim. Acta, Part A **197**, 194–201 (2018).
[13] M. Z. Brela, M. J. Wojcik, M. Boczar, E. Onishi, H. Sato, T. Nakajima, and Y. Ozaki, "Study of hydrogen bond dynamics in Nylon 6 crystals using IR spectroscopy and molecular dynamics focusing on the differences between α and γ crystal forms", Int. J. Quantum Chem. **118**, e25595 (2018).
[14] M. Z. Brela, M. J. Wojcik, M. Boczar, L. J. Witek, T. Yonehara, T. Nakajima, and Y. Ozaki, "Proton dynamics in crystalline tropolone studied by Born-Oppenheimer molecular simulations", Chem. Phys. Lett. **707**, 54–60 (2018).
[15] B. Chan, Y. Kawashima, W. Dawson, M. Katouda, T. Nakajima, and K. Hirao, "A simple model for relative energies of all fullerenes reveals the interplay between intrinsic resonance and structural deformation effects in medium-sized fullerenes", J. Chem. Theory Comput. **15**, 1255–1264 (2019).
[16] M. Shoji, H. Isobe, Y. Shigeta, T. Nakajima, and K. Yamaguchi, "Nonadiabatic one-electron transfer mechanism for the O-O bond formation in the oxygen-evolving complex of photosystem II", Chem. Phys. Lett. **698**, 138–146 (2018).

[17] M. Shoji, H. Isobe, Y. Shigeta, T. Nakajima, and K. Yamaguchi, "Concerted mechanism of water insertion and O_2 release during the S_4 to S_0 transition of the oxygen-evolving complex in photosystem II", J. Phys. Chem. B **122**, 6491–6502 (2018).
[18] T. Kawakami, K. Miyagawa, H. Isobe, M. Shoji, S. Yamanaka, M. Katouda, T. Nakajima, K. Nakatani, M. Okumura, and K. Yamaguchi, "Relative stability between the manganese hydroxide- and oxo-models for water oxidation by CCSD, DMRG CASCI, CASSCF, CASPT2 and CASDFT methods; Importance of static and dynamical electron correlation effects for OEC of PSII", Chem. Phys. Lett. **705**, 85–91 (2018).
[19] T. Yonehara and T. Nakajima, "Electron dynamics method using a locally projected group diabatic Fock matrix for molecules and aggregates", arXiv:1808.08362.

8.5.2 Posters

[20] W. Dawson and T. Nakajima, "Towards Large-Scale Quantum Chemistry Calculations in NTChem." International Workshop on Massively Parallel Programming for Quantum Chemistry and Physics (Kobe, 2019).
[21] N. Inoue and T. Nakajima, "Douglas—Kroll and IOTC transformation of Dirac—Fock operator", International Workshop on Massively Parallel Programming for Quantum Chemistry and Physics 2019 (Kobe, 2019).
[22] 植村渉, 「AGP状態を用いたより大きな基底関数系による分子系の記述」 重点課題５ 第５回公開シンポジウム (札幌, 2018).
[23] T. Yonehara and T. Nakajima, "Development of quantum dynamics method for investigating photo excited electrons in molecular aggregates accompanied with wave packet bifurcation", International Workshop on Massively Parallel Programming for Quantum Chemistry and Physics 2019 (Kobe, 2019).
[24] 米原丈博, 中嶋隆人 「分子集合系における光励起電子動力学の解明に向けた理論計算手法の開発」, 文部科学省 ポスト「京」重点課題５「エネルギーの高効率な創出、変換・貯蔵、利用の新規基盤技術の開発」第2回実験・産業との連携シンポジウム / 第5回公開シンポジウム (札幌, 2018).
[25] N. Minezawa, "Large-scale nonadiabatic molecular dynamics simulation toward understanding the microscopic processes of photovoltaic solar cells," International Workshop on Massively Parallel Programming for Quantum Chemistry and Physics 2019 (Kobe, 2019).
[26] 嶺澤 範行、中嶋 隆人「太陽電池設計に向けた非断熱分子動力学シミュレーションの実装」第12回分子科学討論会（福岡, 2018）
[27] 嶺澤 範行「太陽電池設計に向けた非断熱分子動力学シミュレーションの実装」ポスト「京」重点課題5第5回公開シンポジウム（札幌, 2018）
[28] T. Matsuoka and T. Nakajima, "Materials Informatics of Hole-Transporting Materials for Perovskite Solar Cells", International Workshop on Massively Parallel Programming for Quantum Chemistry and Physics 2019 (Kobe, 2019).

8.5.3 Invited Talks

[29] 中嶋隆人, "京を利用した第一原理計算による材料設計手法", 技術情報協会 第一原理計算による材料設計, 解析手法と活用事例, 五反田, 2018年10月25日.
[30] T. Nakajima, "Quantum Chemistry on the K Computer", ISC High Performance 2018, Frankfurt, 27 Jun. 2018.
[31] 中嶋隆人, ""京"で新機能材料を探索する", 早稲田大学先進理工学部応用化学科主催セミナー, 西早稲田, 2018年5月18日.
[32] W. Dawson, "Computing Matrix Functions on the K Computer." HPCIC Computational Science Forum (Tokyo and Kobe, 2019).
[33] W. Uemura, "Antisymmetrized Geminal Powers with Larger Chemical Basis Sets," Mainz-Kobe joint workshop on "Solving the Full Configuration Interaction Problem" (Kobe, 2018).

8.5.4 Oral Talks

[34] W. Dawson and T Nakajima, "Analysis Tools for Linear Scaling Quantum Chemistry Calculations." The 12th Annual Meeting of the Japan Society for Molecular Science (Fukuoka, 2018).
[35] W. Dawson, "Computing Matrix Functions on the K Computer." R-CCS Cafe (Kobe, 2018).
[36] 米原丈博, 中嶋隆人 「分子集合系の揺らぎが電子動力学に与える影響」, 第12回分子科学討論会 (福岡, 2018).
[37] 米原丈博, 中嶋隆人 "Development of quantum dynamics methods for investigating a light energy conversion: Non-adiabatic quantum dynamics and excited electron dynamics in photochemical process", 文部科学省

ポスト「京」重点課題５「エネルギーの高効率な創出、変換・貯蔵、利用の新規基盤技術の開発」第1回若手勉強会 (熱海, 2018).
[38] 米原丈博, 中嶋隆人 「分子集合系における光励起電子動力学の解明に向けた量子動力学法の開発」, 第21回理論化学討論会 (岡崎, 2018).
[39] 嶺澤 範行「太陽電池設計に向けた非断熱分子動力学シミュレーション」研究会「化学反応のポテンシャル曲面とダイナミックス」（神戸, 2019）

Chapter 9

Computational Materials Science Research Team

9.1 Members

- Seiji Yunoki (Team Leader)
- Yuichi Otsuka (Research Scientist)
- Shigetoshi Sota (Research Scientist)
- Hiroshi Ueda (Research Scientist)
- Mohammad Khazaei (Research Scientist)
- Akiko Masaki-Kato (Research Scientist)
- Ahamad Ranjbar (Postdoctoral Researcher)
- Sandro Sorella (Senior Visiting Scientist)
- Takami Toyama (Senior Visiting Scientist)
- Susumu Yamada (Visiting Scientist)
- Kazuhiro Seki (Visiting Scientist)
- Michele Casula (Visiting Scientist)
- Tatsuya Shishidou (Visiting Scientist)
- Masako Hirata (Assistant)
- Keiko Matsuoka (Assistant)

9.2 Overview of Research Activities

Strongly correlated materials show great promise for next-generation electronic applications. In order to accelerate the development of functional strongly correlated materials, a reliable theory with good predictability is required. However, the strong interactions that take place in this class of materials do not allow us to apply the traditional band theory based on the density functional theory, which played a major role in the advance of today's electronic technology based on semiconductors.

Consequently, we are developing large-scale numerical simulations for strongly correlated quantum systems, including strongly correlated materials, where the many-body interactions are essential to induce novel phenomena and properties. We are interested particularly in the quantum Monte Carlo method, the density matrix renormalization group method, and the tensor network method to simulate not only the ground state but also the dynamics (thermodynamics, excitation dynamics, and real time dynamics). We have established a platform for advanced research of strongly correlated quantum systems by developing state-of-the-art simulations.

9.3 Research Results and Achievements

9.3.1 Large-scale QMC simulations for interacting fermions

We develop a quantum Monte Carlo (QMC) method, which is one of the most reliable and efficient techniques for Hubbard-type lattice models of interacting electrons. Typical target systems are of the order of 10,000 electrons unless the notorious minus sign problem occurs. One of the main focuses in our QMC project is to clarify quantum criticality of quantum phase transitions in strongly correlated electrons with high accuracy, which would be impossible without the power of K computer.

We have implemented a highly efficient QMC code based on the auxiliary field scheme for lattice fermion systems at zero temperature. Since numerical calculations involved in this formulation are mostly linear algebraic procedure such as matrix-matrix product and numerical orthogonalization, we can take advantage of the highly optimized numerical library on K computer to calculate physical observables with a high degree of accuracy on unprecedentedly large systems.

In this fiscal year, we have revisited the Hubbard model on the honeycomb lattice with a special focus on the fate of the quasiparticle weight. Specifically, we propose a new method to evaluate the quasiparticle weight from the long-distance equal-time single-particle Green's function. If this quantity remains finite in the thermodynamic limit, the low-energy single-particle excitations of the correlated semimetallic phase are described by a Fermi-liquid-type single-particle Green's function. Based on the unprecedentedly large-scale numerical simulations on finite-size clusters containing more than ten thousands sites, we confirm that the quasiparticle weight remains finite in the semimetallic phase below a critical interaction strength. This is also supported by the long-distance algebraic behavior ($\sim r^{-2}$, where r is distance) of the equal-time single-particle Green's function that is expected for the Fermi liquid. Our result thus provides a strong numerical evidence of Fermi liquid theory in two dimensional correlated metals.

We consider the equal-time single-particle Green's function,

$$D_{AB,\sigma}(\vec{r}) \quad = \quad \frac{1}{N_{\rm cell}} \sum_{\vec{r}'} \left\langle \hat{c}^{\dagger}_{B,\vec{r}'+\vec{r},\sigma} \hat{c}_{A,\vec{r}',\sigma} \right\rangle , \tag{9.1}$$

where $\vec{r}$ denotes a relative spatial position of two unit cells at $\vec{r}'$ and $\vec{r}'+\vec{r}$, and $N_{\rm cell}$ is a number of the unit cells in the finite size cluster with a linear dimenstion L. If we assume that the single-particle Green's function near the Fermi level has a Fermi-liquid-type pole, which is quite reasonable when the system is (semi-)metallic, it is easily shown that the quasiparticle weight Z at the Fermi level in the thermodynamic limit is simply evaluated via the ratio of the equal-time single-particle Green's functions in the long-distance limit, i.e.,

$$Z = \lim_{|\vec{r}|\to\infty} \frac{D_{AB,\sigma}(\vec{r})}{D^{(0)}_{AB,\sigma}(\vec{r})}, \tag{9.2}$$

where the superscript "(0)" denotes the quantity in the noninteracting limit.

By using our highly developed QMC code, we numerically examined the long-distance behavior of $D_{AB,\sigma}(\vec{r})$. Since the simulations are always performed on finite-size clusters, we calculate $D_{AB,\sigma}(\vec{r})$ and thereby-obtained Z as a function of the cluster size L,

$$Z(L) = \frac{D_{AB,\sigma}(\vec{r}_{\rm max})}{D^{(0)}_{AB,\sigma}(\vec{r}_{\rm max})}, \tag{9.3}$$

where $r_{\rm max} = |\vec{r}_{\rm max}|$ is the maximum distance available. Figure 9.1 shows $Z(L)$ as a function of $1/L$ and lines are second-order polynomial fits of the form $\sum_{n=0}^{2} c_n L^{-n}$ to the data with $\{c_n\}$ being fitting parameters determined by the least-squares method. The extrapolated values of $c_0 = Z$ and their error bars in the thermodynamic limit are also shown at $1/L = 0$ for the semimetallic phase where the Fermi-liquid-like asymptotic behavior is observed in $D_{AB,\sigma}(r)$. We find that these extrapolated values are consistent within two standard deviations, with our previous result, indicated by stars in Fig. 9.1 and estimated from the jump of the momentum distribution function. Our new calculations is however much more accurate because the error bars are much smaller and performed for much larger cluster, thus providing a clear numerical evidence, supporting the Fermi liquid theory in the correlated semimetallic phase. Considering the Hubbard model as the minimal model for graphene, our results also imply a realization of Fermi liquid in graphene, which has been often only assumed without any unbiased evidence so far.

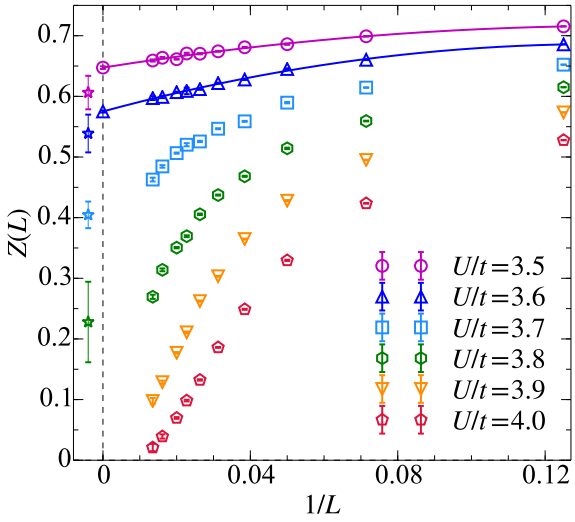

Figure 9.1: The quasiparticle weight $Z(L)$ given in Eq. (9.3) as a function of $1/L$. Lines are polynomial fits to the data for $U/t = 3.5$ and 3.6. The extrapolated values in the thermodynamic limit are also shown at $1/L = 0$. The quasiparticle weight estimated previously from the jump of the momentum distribution function are also shown by stars next to the present results.

9.3.2 First-principles QMC simulations for strongly correlated materials

In graphene, an insulating state does not naturally occur. Strain engineering has long been considered as a promising way to open the symmetry-protected zero gap of semimetallic (SEM) graphene. For example, an insulating state could be achieved by simple isotropic expansive strain. Theoretically, in an idealized rigid-honeycomb Hubbard model, quantum Monte Carlo (QMC) calculations had suggested that the band-width narrowing and thus increasing the effective electron-electron repulsion could push the correlated π electrons towards an undistorted honeycomb antiferromagnetic insulator. Alternatively, isotropically stressed graphene could also distort to form Peierls or Kekulé-like dimerized states.

However, previous studies leave the electronic and structural phase diagram of isotropically strained graphene in a state of uncertainty on two separate accounts. First, the strong band-width narrowing and thus increasing the importance of strong electron correlations, improperly treated by density functional theory (DFT) calculations, calls for a novel QMC approch capable of describing real strained and deformable graphene, a goad never attained so far. Second, the phase diagram under stress must be obtained by comparing enthalpy, therefore including the stress-strain term, rather than just total energy, as was universally done so far.

We thereby performed first-principles QMC simulations, as schematically shown in Fig. 9.2, developed by Sandro Sorella and co-workers on the K computer to study the phase diagram of isotropically expanded graphene. In this method, we first assume and optimize a variational wave function constructed by an antisymmetrized geminal wave function (AGP) and a Jastrow factor for the density correlations. After obtaining the optimal variational wave function, our ab-initio QMC method allows us to obtain more accurate results by performing the lattice-regularized diffusion Monte Carlo (DMC) method with the variational wave function as a guiding function.

The equilibrium state under the tensile stress σ, minimizes the enthalpy $H = \min_S[E(S) - \sigma S]$, rather than energy $E(S)$, where $\sigma = \partial_S E(S)$ with S the mean area. In order to obtain the tensile stress σ efficiently, we have introduced the adjoint algorithmic differentiation method (AAD) in our code.

Figure 9.3 (a) shows the enthalpy H of the strained graphene as a function of the tensile stress σ from both DMC and DFT calculations. The ground-state phase diagram obtained by minimum enthalpy finds the SEM state for $\sigma < \sigma_1 = 25.1$ N/m and a Kekulé dimerized (DIM) state for $\sigma_1 < \sigma < \sigma_u = 30.4$ N/m, above which mechanical failure ensues, as summarized in Fig. 9.3 (b). In DFT, the antiferromagnetic insulating (AFI) state exhibits the lowest enthalpy, which is never stable in the more accurate QMC calculations. This implies that the effect of the electron correlations plays an important rule for the stability of the DIM phase. We have also pointed out that this DIM phase can be regarded as a topological phase.

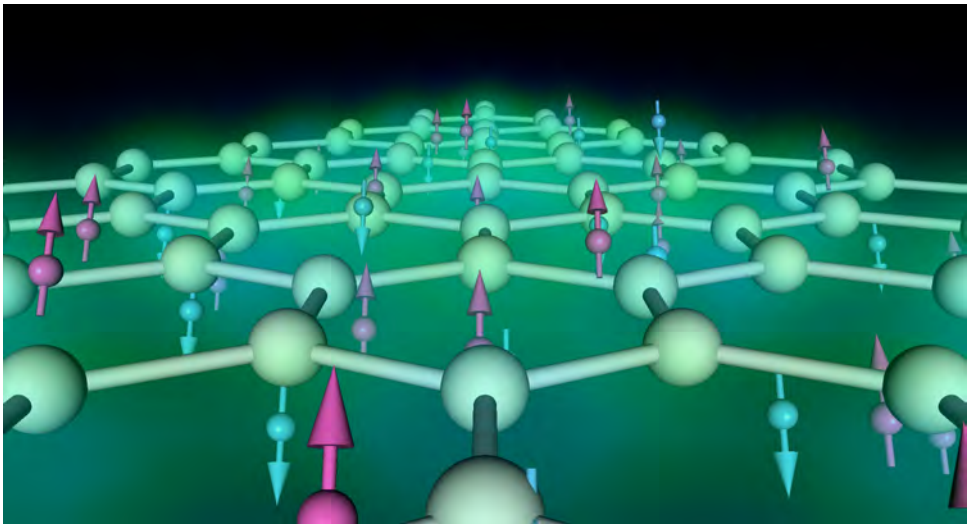

Figure 9.2: Schematic figure of a first-principle QMC simulation. In this method, we assume a variational wave function $\Psi(\mathbf{R})$ where $\mathbf{R} = \{\mathbf{r}_1, \mathbf{r}_2, \cdots, \mathbf{r}_N\}$ represents the set of the electron positions, i.e., electron configuration. We then generate a sample of the electron configurations $\mathbf{R}$ based on the Markov chain Monte Carlo method obeying the probability defined by the wave function squared, $|\Psi(\mathbf{R})|^2$.

9.3.3 Massively parallel density matrix renormalization group (DMRG) algorithms for quantum many-body systems

The density matrix renormalization group (DMRG) method is recognized as one of the most efficient numerical method to investigate one-dimensional (1D) strongly correlated systems. Although the number of bases required to describe such systems exponentially increases with the system size, the DMRG enables us for accurate numerical calculations on those systems by an arbitrary number of bases that are optimized for target states. The application of the DMRG method is severely limited mostly to 1D systems because of the exponential increase of degrees of freedom in higher spatial dimensions. However, owning to high performance computers that are availably recently, it has become realistic to apply the DMRG method even to two-dimensional (2D) systems. We have been developing massively parallel DMRG algorithms to investigate strongly correlated quantum systems in two dimensions. We have already successfully developed our massively parallel DMRG code, employing many efficient parallelization techniques. We have achieved the extremely high peak performance ratio of 73.6% when 82,488 nodes are used on K computer, which is about 7.8 PFLOPS.

We are currently developing four types of massively parallel DMRG software, "2D-DMRG", "DDMRG", "paraDMRG", and "QUARTZ". The 2D-DMRG is developed for ground state calculations on 2D strongly correlated systems. Employing real-space parallelizing optimization of basis sets, we can perform calculations on large systems by increasing the number of MPI processes. The DDMRG is developed for quantum dynamics of strongly correlated systems. Using the kernel polynomial method, we can investigate quantum dynamics of not only 1D systems but also higher dimensional systems. The paraDMRG is developed for full-CI calculations in ab initio simulations. Developing a new DMRG algorithm based on translation matrices, the paraDMRG can be applied to more than 100 orbitals. The QUARTZ is developed to simulate quantum computers. Employing our newly developed time-dependent DMRG method for higher dimensional systems, we can perform simulations of quantum annealing and various quantum circuits. These DMRG programs have been opened in public for users of K computer. We have also held training school of our DMRG softwares.

9.3.4 Tensor network method for many-body systems

We have developed an infinite-size density matrix renormalization group (iDMRG) method, which is one of primitive tensor network method, for SU(4) spin models that can be realized in a low-energy state in one-dimensional systems of two-orbital SU(4) fermionic cold atoms. Our numerical study with the iDMRG method found three types of nontrivial symmetry protected topological (SPT) phase protected by $Z_4 \times Z_4$ symmetry and one trivial phase. A physical back ground of phase transitions between the non-trivial SPT phases is understood

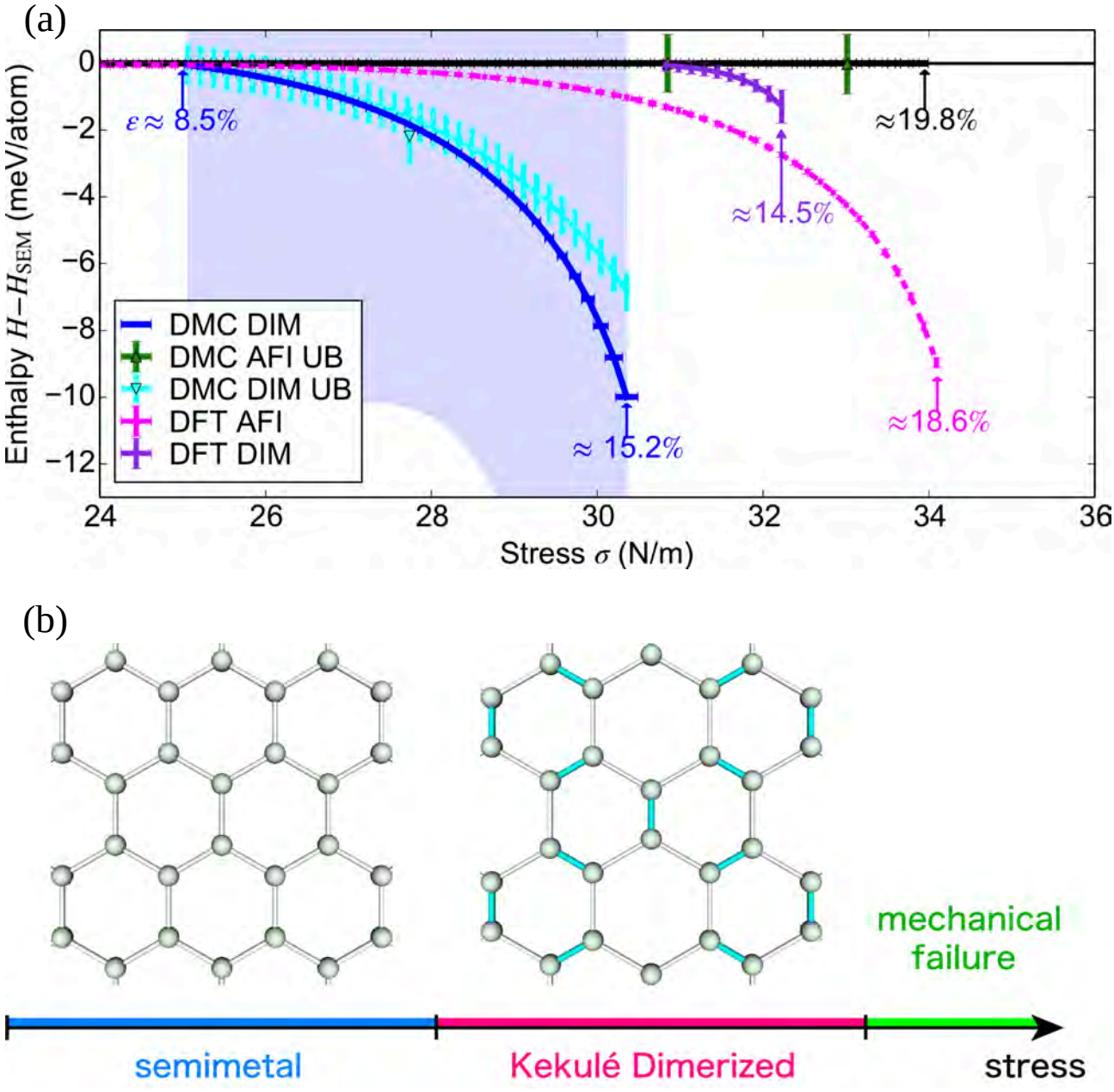

Figure 9.3: (a) Enthalpy H of strained graphene relative to that of the semimetal (SEM) phase, H_{SEM}, with increasing tensile stress σ obtained by the diffusion Monte Carlo method (DMC) and the standard density functional theory (DFT). The blue shaded region indicates the error bars on the enthalpies for Kekulé dimerized (DIM) and antiferromagnetic insulating (AFI) phases by the diffusion Monte Carlo (DMC) simulation. Upper bounds for the DIM and AFI enthalpies also shown (DIM UB and AFI UB) greatly reduce the error bars. The corresponding strain ε at selected points and phases (indicated by arrows) are also shown. (b) Schematic phase diagram obtained from our calculations. With increasing the stress σ, A transition form the SEM phase to the DIM phase occurs at $\sigma \sim 25.1$ N/m. The DIM phase is stable up to $\sigma \sim 30.4$ N/m. Cyan bonds in (b) represent shorter bonds in the Kekulé-type distortion pattern.

by the antisymmetrization effect in neighboring spins (that we quantify with Casimir operators). Furthermore, we demonstrated by using the matrix product state how the Z_4 SPT state with six edge states appears in the SU(4) spin model.

We have also developed a parallel algorithm for the iDMRG that is applicable to one-dimensional (1D) quantum systems with ℓ-site periods, where ℓ is an even number. Combining Hida's iDMRG algorithm applied to random 1D spin systems and a variant of McCulloch's wavefunction prediction, we can apply $\ell/2$ times the computational power to accelerate the investigation of multi-leg frustrated quantum systems in the thermodynamic limit, which is a challenging simulation. We performed benchmark calculations for a spin-1/2 Heisenberg model on a Kagome cylinder using the parallel iDMRG and obtained proper bulk physical quantities. Moreover, the variant of the wavefunction prediction increased the speedup of Lanczos methods in our iDMRG by approximately three times.

Finally, we have improved a massively paralleled corner transfer matrix renormalization group (CTMRG) method, which is also a kind of tensor network method for two-dimensional tensor network, by introducing the EigenExa developed by Dr. Imamura in R-CCS and accelerated the calculation of the CTMRG to clarify the critical behavior of the two dimensional dodecahedron model having twenty local degrees of freedom. Preliminary calculations using the parallel CTMRG shows that the dodecahedron model has a single continuous phase transition by decreasing the temperature, that is qualitatively consistent with the previously reported results obtained by a Monte Carlo method. However, we found meaningful discrepancy with respect to the critical temperature.

9.4 Schedule and Future Plan

9.4.1 Large-scale QMC simulations for interacting fermions

It has been recognized that Dirac fermions offer ideal platforms to study the nature of quantum phase transitions in terms of the celebrated Grosse-Neveu theory. In the course of the recent research activities, we plan to investigate the quantum criticality of the superconducting-to-antiferromagnetic phase transition based on the Hubbard model with the Dirac dispersion by large-scale quantum Monte Carlo simulations. As another example of the phase transition belonging to the chiral-SU(2) universality class, we aim to clarify the Mott transition in the Hubbard model with the d-wave superconducting order parameter which is introduced to build the Dirac dispersion in the non-interacting limit. This phase transition is the same as one we have studied in the Hubbard model on the honeycomb lattice in terms of the symmetry but different in the number of fermion flavors. We thus expect different values of the critical exponents, which would be very informative.

9.4.2 First-principles QMC simulations for strongly correlated materials

We have successfully performed the first-principles QMC simulations for the isotropically strained graphene. Our result is not only quantitatively but also qualitatively different from the result by the traditional calculation based on the density functional theory, suggesting the importance of this method. Therefore, we will continue to develop this method. In the current implementation, we have used the antisymmetrized geminal power (AGP) wave function for the one-body part of the wave function. The AGP wave function corresponds to the BCS wave function with the singlet pairing in the lattice model. Namely, the AGP wave function still limits the representation of the one-body part of the wave function. For the next year, we plan to introduce the pfaffian wave function which yields the most general form of the one-body part of the wave function. It is expected that the pfaffian wave function can efficiently take into account the spin fluctuations of correlated materials.

9.4.3 Massively parallel density matrix renormalization group (DMRG) algorithms for quantum many-body systems

Our massively parallel DMRG codes can calculate both static and dynamical quantities for 2D strongly correlated quantum systems. Our future plan for post-K computer is to extend our massively parallel DMRG method to finite temperature calculations. For 1D systems, several types of the finite temperature DMRG method have been already developed using the transfer matrix or imaginably time evolution. However, it is difficult to employ these finite temperature DMRG algorithms for 2D systems. Recently, we proposed and developed a new finite temperature DMRG method by using the kernel polynomial expansion for the Boltzmann distribution function. Although our finite temperature DMRG method can be applied to 2D systems, it requires

huge computational resources. By using post-K computer, we should be able to perform the finite temperature DMRG calculations for 2D systems. Thus, we will develop the massively parallel finite temperature DMRG method for post-K computer. One of the applications would be to estimate a critical temperature of high-T_c cuprate superconductors.

9.4.4 Tensor network method for many-body systems

Implementation of the numerical code for calculating correlation length and local physical properties in our parallel CTMRG method is an important issue to clarify the non-trivial criticality in the dodecahedron model. In addition, we will investigate the entanglement scaling for Berezinskii-Kosterlitz-Thouless (BKT) transitions in 2D classical systems, because a BKT phase transition is immediately emerged by introducing XY-like anisotropy into 2D polyhedron models.

We also plan to investigate a search algorithm for optimal tensor-network decomposition in non-uniform quantum states from the view point of minimizing a mutual information of entanglement entropy. This is important to accelerate a numerical method based on the tensor network algorithm.

9.5 Publications

9.5.1 Articles/Journal

[1] T. Kaneko, Y. Ohta, and S. Yunoki, "Exciton-phonon cooperative mechanism of the triple-q charge-density-wave and antiferroelectric electron polarization in $TiSe_2$", Physical Review B **97**, 155131/1–23 (2018).

[2] F. Zheng, Q. Zhang, Q. Meng, B. Wang, F. Song, S. Yunoki, and G. Wang, "First-principles study of native defects in bulk Sm_2CuO_4 and its (001) surface structure", Journal Applied Physics **123**, 161504/1–8 (2018).

[3] T. Tohyama, M. Mori, and S. Sota, "Dynamical DMRG study of spin and charge excitations in the four-leg t-t'-J ladder", Physical Review B **97**, 235137/1–7 (2018).

[4] F. Lange, S. Ejima, T. Shirakawa, S. Yunoki, and H. Fehske, "Spin transport through a spin-1/2 XXZ chain contacted to fermionic leads", Physical Review B **97**, 245124/1–9 (2018).

[5] M. Khazaei, V. Wang, C. Sevik, A. Ranjbar, M Arai, and S. Yunoki, "Electronic structures of iMAX phases and their two-dimensional derivatives: A family of piezoelectric materials", Physical Review Materials **2**, 074002/1–11 (2018).

[6] Y. Otsuka, K. Seki, S. Sorella, and S. Yunoki, "Quantum criticality in the metal-superconductor transition of interacting Dirac fermions on a triangular lattice", Physical Review B **98**, 035126/1–8 (2018).

[7] S. Sorella, K. Seki, O. O. Brovko, T. Shirakawa, S. Miyakoshi, S. Yunoki, and E. Tosatti, "Correlation-driven dimerization and topological gap opening in isotropically strained graphene", Physical Review Letters **121**, 066402/1–6 (2018).

[8] H. Ueda, T. Morimoto, and T. Momoi, "Symmetry protected topological phases in two-orbital SU(4) fermionic atoms", Phys. Rev. B **98**, 045128/1–11 (2018).

[9] M. Kishimoto, K. Morita, Y. Matsubayashi, S. Sota, S. Yunoki, and T. Tohyama, "Ground state phase diagram of the Kitaev-Heisenberg model on a honeycomb-triangular lattice", Physical Review B **98**, 054411/1–10 (2018).

[10] K. Seki, T. Shirakawa, and S. Yunoki, "Variational cluster approach to thermodynamic properties of interacting fermions at finite temperatures: A case study of the two-dimensional single-band Hubbard model at half filling", Physical Review B **98**, 205114/1–37 (2018).

[11] H. Ueda, "Infinite-size density matrix renormalization group with parallel Hida's algorithm", J. Phys. Soc. Jpn. **87**, 74005/1–8 (2018).

[12] T. Sato, T. Shirakawa, and S. Yunoki, "Spin-orbit entangled excitonic insulator with quadrupole order", Physical Review B **99**, 075117/1–7 (2019).

[13] S. Kitou, S. Kobayashi, T. Kaneko, N. Katayama, S. Yunoki, T. Nakamura, and H. Sawa, "Honeycomb lattice type charge density wave associated with interlayer Cu ions ordering in $1T$-Cu_xTiSe_2", Physical Review B **99**, 081111(R)/1–6 (2019).

[14] T. Kaneko, T. Shirakawa, S. Sorella,, and S. Yunoki, "Photoinduced eta pairing in the Hubbard model", Physical Review Letters **122**, 077002/1–6 (2019).

[15] K. Seki, Y. Otsuka, S. Yunoki, and S. Sorella, "Fermi-liquid ground state of interacting Dirac fermions in two dimensions", Physical Review B **99**, 125145/1–10 (2019).

9.5.2 Invited Talks

[1] S. Yunoki, "Theory of relativistic Mott insulator and superconductivity in transition metal oxides with a strong spin-orbit coupling", 2018 KPS Spring Meeting, April 25–27 (2018), Daejeon (Korea).
[2] S. Yunoki, "Spin dynamics in two-dimensional S=1/2 antiferromagnet — fate of single magnon excitations —", Workshop Quantum Many body States 2018, April 27–28 (2018), KAIST, Daejeon (Korea).
[3] S. Yunoki, "Quantum Monte Carlo study of interacting Dirac fermions in 2D", International Workshop on New Paradigms in Quantum Matter, June 25–July 6 (2018), IOP, Beijing (China).
[4] Y. Otsuka, "Quantum Monte Carlo study of interacting Dirac fermions", Electron correlation, Quantum biology and Quantum information, July 5–6 (2018), Beijing (China).
[5] S. Yunoki, "Block Lanczos density-matrix renormalization group method for Anderson impurity models: Application to pseudogap Kondo problems", Electron Correlation, Quantum Biology, and Quantum Information, July 5–6 (2018), Kavli ITS, Beijing (China).
[6] S. Yunoki, "Photoinduced superconductivity by η -pairs in the Hubbard model", Computational Approaches to Magnetic Systems 2018, August 27–28 (2018), APCTP, Pohang (Korea).
[7] S. Yunoki, "Emergence of massless Dirac dispersion in graphene on Ni(111) surface", 2nd International Conference on Advanced Functional Materials Science and Engineering (2nd ICAFMA), September 15–17 (2018), Yancheng (China).

9.5.3 Oral Talks

[1] S. Sota, T. Shirakawa, S. Yunoki, and T. Tohyama, "Dynamical DMRG study of inelastic neutron scattering on triangular lattice quantum spin system $Ba_3CoSb_2O_9$", The 3rd CDMSI workshop, July 19-20 (2018), Tokyo (Japan).
[2] S. Sota, K. Shinjo, T. Tohyama, and S. Yunoki, "Ground-state phase diagram of one-dimensional extended Hubbard model by machine learning", Autumn Meeting of Physics Society of Japan, September 9-12 (2018), Kyotanabe (Japan).
[3] S. Sota, K. Shinjo, S. Yunoki, and T. Tohyama, "Improvement of time-dependent DMRG for higher dimensional strongly correlated quantum systems and its applications", Autumn Meeting of Physics Society of Japan, September 9-12 (2018), Kyotanabe (Japan).
[4] K. Morita, M. Fujihala, S. Mitsuda, A. MatsuoA, K. KindoA, S. Sota, and T. Tohyama, "Analysis of magnetic properties of a square kagome lattice antiferromagnet $Cu_6AlBiO_4(SO_4)_5{\cdot}KCl$", Autumn Meeting of Physics Society of Japan, September 9-12 (2018), Kyotanabe (Japan).
[5] S. Sota, T. Tohyama, and S. Yunoki, "Development of massively parallel density matrix renormalization group method algorithm for two-dimensional strongly correlated systems and its applications", The 1st R-CCS International Symposium, Febrary 18-19 (2019), Kobe (Japan).
[6] S. Sota, S. Yunoki, and T. Tohyama, "Quantum spin liquid state and its spin excitation dynamics on triangular lattice antiferromagnetic Heisenberg model", the 74th annual meeting of Physics Society of Japan, March 14-17 (2019), Fukuoka (Japan).
[7] K. Shinjo, S. Sota, S. Yunoki, and T. Tohyama, "Characterization of photoexcited states in the half-filled one-dimensional extended Hubbard model assisted by machine learning", the 74th annual meeting of of Physics Society of Japan, March 14-17 (2019), Fukuoka (Japan).

9.5.4 Posters

[1] K. Sasaki, T. Sugimoto, S. Sota, T. Tohyama, "Magnetic excitation in magnetization plateau of frustrated spin ladder II", Autumn Meeting of Physics Society of Japan, September 9-12 (2018), Kyotanabe (Japan).
[2] Y. Otsuka, K. Seki, S. Yunoki, and S. Sorella, "Semimetal-superconductor phase transition of interacting Dirac fermions on a triangular lattice with π-flux", Tensor Network States: Algorithms and Applications (TNSAA) 2018-2019, December 3–6 (2018), Kobe (Japan).
[3] S. Sota, T. Shirakawa, T. Tohyama, and S. Yunoki, "Dynamical DMRG study of excitation dynamics of triangular lattice antiferromagnetic Heisenberg models", TNSAA 2018-2019, December 3-6 (2018), Kobe (Japan).
[4] S. Sota, K. Shinjo, S. Yunoki, and T. Tohyama, "Development of time-dependent DMRG method for higher-dimensional strongly correlated systems and its applications", The 4th CDMSI symposium, December 17-18, (2018), Kashiwa (Japan).

9.5.5 Press release and research highlight

[1] "New insulating state found in stretched graphene", RIKEN Research Highlight, November 9 (2018). (http://www.riken.jp/en/research/rikenresearch/highlights/20181109_FY20180033/)
[2] "Light pulses provide a new route to enhance superconductivity", Press Release, March 4 (2019). (http://www.riken.jp/en/pr/pres

9.5.6 Software

[1] S. Sota, K. Morita, H. Matsueda, S. Yunoki, T. Tohyama, "DDMRG (Dynamical DMRG) Ver. 2.0", R-CCS Software.

Chapter 10

Computational Biophysics Research Team

10.1 Members

Yuji Sugita (Team Leader (Concurrent))*

Osamu Miyashita (Senior Research Scientist)

Jaewoon Jung (Research Scientist (Concurrent))**

Chigusa Kobayashi (Research Scientist)

Yasuhiro Matsunaga (Research Scientist)

Koichi Tamura (Special Postdoctoral Fellow)

Ai Shinobu (Postdoctoral Fellow)

Hiromi Kano (Assistant)

Takaharu Mori (Research Scientist (Concurrent))***

Kiyoshi Yagi (Research Scientist (Concurrent))****

Ai Nittsu (Special Postdoctoral Fellow (Concurrent))*****

Suyong Re (Research Scientist (Concurrent))******

Hiraku Oshima (Research Scientist (Concurrent))*******

Kento Kasahara (Research Scientist (Concurrent))*******

Mitsunori Ikeguchi (Visiting Scientist)********

Michael Feig (Visiting Scientist)*********

Takao Yoda (Visiting Scientist)**********

Naoyuki Miyashita (Visiting Scientist)***********

* Chief Scientist in RIKEN CPR; TEam leader in RIKEN BDR
** Senior Technical Scientist in RIKEN CPR
*** Research Scientist in RIKEN CPR
**** Senior Research Scientist in RIKEN CPR
***** Special Postdoctoral Fellow in RIKEN CPR
****** Senior Research Scientist in RIKEN BDR
******* Research Scientist in RIKEN BDR

******** The main affiliation is Yokohama City University
********* The main affiliation is Michigan State University
********** The main affiliation is Nagahama Bio Institute.
*********** The main affiliation is Kindai University.

10.2 Research Activities

Our team has developed highly parallelized MD software using the hybrid (MPI+OpenMP) parallelization technique, which is suitable to massively parallel supercomputers, like K or post-K computers. Since 2015, we have released our MD software, GENESIS (Generalized-ensemble simulation system), as freeware under the GPLv2 license and have continued the development for improving performance and reliability in MD simulations. One of the key features for GENESIS is that the efficient parallelization allows us to simulate very large biological systems using supercomputers. GENESIS also includes various enhanced conformational sampling methods for investigating slow conformational dynamics of biomolecules. By developing new functions in GENESIS, we would like to achieve more reliable predictions of biomolecular structure, molecular interaction, and biological function, and contribute to basic life science as well as drug discovery and medical science.

In this fiscal year, we updated GENESIS with better performance and with advanced algorithms, which is released as GENESIS 1.3. For more accurate MD simulations under the isothermal-isobaric (NPT) conditions, we developed a more accurate temperature evaluation. Data-driven MD simulations approaches are also developed.

10.2.1 Release of GENESIS 1.3

In the last fiscal year, we released GENESIS 1.3 including new functions and advanced algorithms. The main features of GENESIS 1.3 are (1) generalized replica exchange with solute tempering (gREST), (2) improvement of nonbonded interaction with GPU, (3) options of pressure_virial/pressure_textunderscore rmsd, which includes virial terms from position/rmsd restraints in pressure evaluations, (4) fixing setup of AMBER force field when constraint is not set, and (5) fixing principal component (PC) restraints for computational performance.

10.2.2 Development of new integration algorithm in MD simulations

In MD simulations, not only the performance but also the reproducible computation result is essential. Recently, we found that accurate evaluation of temperature is important for controlling temperature as well as pressure in the isothermal-isobaric conditions (the NPT ensemble). Based on the Tolman's equipartition theorem, all the particle motions should share a single temperature. However, conventional temperature estimation from kinetic energy does not include Hessian terms properly. As a result, the equipartition theorem is not accurately satisfied in MD simulations with a large time step.

By combining two kinetic energies, which are evaluated at full- and half-time steps in the velocity Verlet integrator, we could estimate instantaneous temperature up to the third order of the time step. The new definition of temperature, which we call "Optimal temperature", is tested for a one-dimensional harmonic oscillator, a pure water system, a Bovine pancreatic trypsin inhibitor (BPTI) in water, and a hydrated DPPC lipid bilayer. In all cases, the optimal temperature estimator fulfills the equipartition theorem better than the existing methods. The MD simulation using Optimal temperature could reproduce physical properties, such as Area per lipid (APL) distribution in the hydrated DPPC lipid bilayer, even for longer time steps (4 fs or 5 fs) (Figure 10.1). In contrast, APLs in the MD simulations with the conventional temperature are deviated for longer time steps, suggesting the higher reliability of the MD simulation with Optimal temperature.

10.2.3 Conformational changes of Ca^{2+}-ATPase

Sarco(endo)plasmic reticulum Ca^{2+}-ATPase is a representative protein of P-type ATPases, which transports Ca^{2+} across membrane against 10^4 times concentration gradient by utilizing ATP hydrolysis. It is, however, difficult to investigate the conformational changes due to its slow time-scale. We introduced a rare event sampling method, string method, into MD simulation package, GENESIS and applied the method to the reaction step dissociating ADP and Ca^{2+}. We show that large scale motion of the cytoplasmic domains causes rearrangements of transmembrane helices, and the rearrangements result in large opening of the lumen gate. We further investigate structures of Ca^{2+}-binding site and the lumen gate. We performed MD simulations for

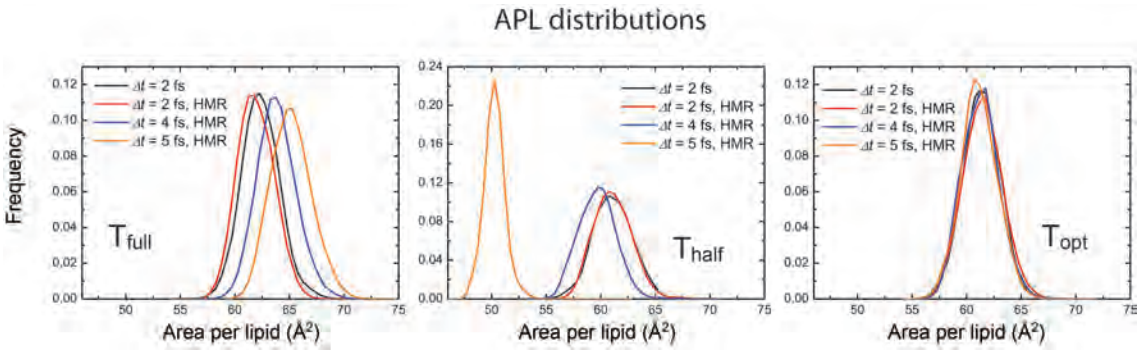

Figure 10.1: Area per lipid (APL) distributions obtained by the MD simulations using the conventional (left and middle) or the optimal temperature (right) . Using the optimal temperature, MD simulations with a longer time step can generate the same APL for the simulation with a shorter time step

the protein with different protonation states in Ca^{2+}-binding site. From the simulation, the lumen gate has a wider open structure when one acidic residue (E908) is protonated, while it is not widely opened when three acidic residues (E309, E771, E908) are protonated. The results suggest that the conformation change of the lumen gate is triggered by the proton transfer to Ca^{2+}-binding site after dissociation of Ca^{2+} (Figure 10.2).

10.2.4 Free energy analysis for the conformational changes of a heme importer

Heme importer BhuUV-T is a member of the type-II ATP-binding cassette (ABC) transporters which transport heme across the biomembrane of a Gram-negative bacterium. Recently, crystal structures of BhuUV-T in the nucleotide-free inward-facing (IF) form have been solved. Based on the structures and biochemical experiments, a molecular mechanism for the heme transport cycle was proposed. According to the proposal, the transport cycle would initiate from the IF form. Binding of two ATPs to the nucleotide-binding domains of the IF state is thought to be essential to induce conformational changes toward the occluded (Occ) intermediate (10.3(a)). However, no structural information on the Occ state is available. In this study, a computational modeling approach is adopted to predict the Occ intermediate with bound nucleotides. The predicted model is further validated by the free energy analysis based on the string method. The computational results support the proposed transport cycle of BhuUV-T (10.3(b,c)).

10.2.5 Simulating large-amplitude transitions in proteins with a coarse-grained Gō model

Biochemical reactions are often coupled with large-amplitude structural transitions. A very common case is a protein transitioning from an open to closed state upon substrate binding. For these types of motions, coarse-grained (CG) models will be the method of choice, since they reduce the computational time by several orders of magnitude, allowing access to millisecond timescales which are unreachable by conventional all-atom MD simulations. In this work, we designed a scheme to effectively simulate such transitions and implemented it in GENESIS.

As a starting model we use the structure-based off-lattice Gō model. In this model, the representation of the protein is reduced to its Cα atoms, which are connected via virtual bonds with potentials acting between its bonds, angles and dihedrals. The heart of the model lies in the stabilization of the native structure of the protein, achieved by applying an attractive potential between the native contacts. In order to describe transitions between two stable minima, we adjust the original off-lattice Gō model, which assumes a single basin. We employ a mixing scheme which combines two potentials, one for each state, and apply varying weights depending on the coordinates of the system at each step of the simulation. Being a structure-based model, the off-lattice Gō model is very sensitive to the choice of initial parameters. Here, we use the Multistate Bennett Acceptance Ratio (MBAR) method for an efficient determination of the parameters. Using the method, we can predict the free energy of an unsampled data in any desired condition, by weighing sampled data obtained from simulations at various other conditions.

We applied the scheme to several well-studied systems and show that our mixing model was successful in describing structural transition for proteins undergoing large-amplitude transitions between distant states.

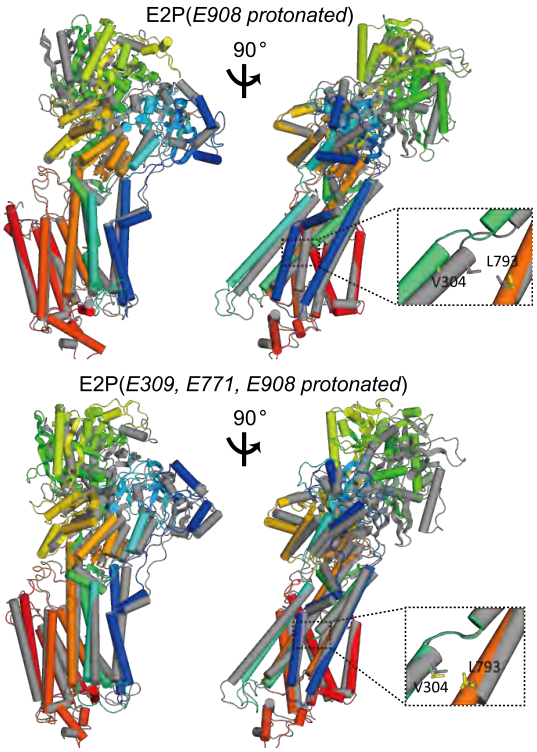

Figure 10.2: Structure of Ca^{2+}-ATPase with different protonation states. Upper: E908 is protonated. Lower: E309, E771, and E908 are protonated

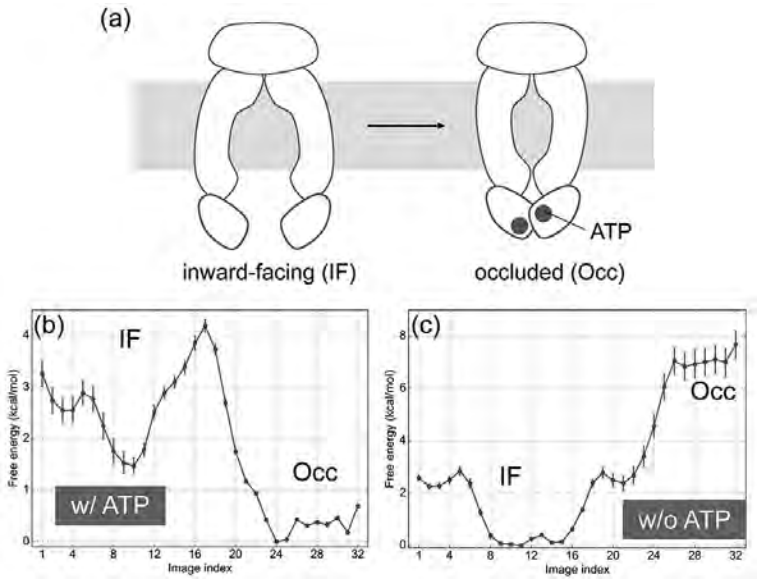

Figure 10.3: Free energy analysis of BhuUV-T. (a) Schematic picture for the proposed IF-to-Occ conformational change of BhuUV-T. (b,c) The predicted free energy along the IF-to-OCC conformational pathway. The result is shown for the system (b) with bound ATP and (c) without ATP

10.3 Publications

10.3.1 Articles

[1] Jaewoon Jung, Chigusa Kobayashi, and Yuji Sugita, "Optimal temperature evaluation in molecular dynamics simulations with a large time step", Journal of Chemical Theory and Computation, vol. 15, 84 – 94 (2019)
[2] Takaharu Mori, Marta Kulik, Osamu Miyashita, Jaewoon Jung, Florence Tama, and Yuji Sugita, "Acceleration of cryo-EM flexible fitting for large biiomolecular systems by efficient space partitioning", Structure, vol. 27, 161 – 174 (2019)
[3] Kiyoshi Yagi, Kenta Yamada, Chigusa Kobayashi, and Yuji Sugita, "Anharmonic vibrational analysis of biomolecules and solvated molecules using hybrid QM/MM coputations", Journal of Chemical Theory and Computation, vol. 15, 1924 – 1938 (2019)

10.3.2 Invited Talks

[4] Yuji Sugita "Optimization and Parallelization of GENESIS on GPU platforms" International Workshop on GPU accelerated Molecular Dynamics Simulations, HKUST, Hong Kong, December 12, 2018
[5] Yuji Sugita and Yasuhiro Matsunaga "Data-driven molecular simulations for integrative dynamic structural biology" The 2nd workshop on Advances in Theory and Computation of Complex Systems - Biological Systems, Nanjing University, Nanjing, China, December 3, 2018
[6] Yuji Sugita, "Molecular Simulations for Understanding Protein Functions in Cellular Environments", The 41st Annual Meeting of the Molecular Biology Society of Japan, Pacifico Yokohama, Yokohama, November 30, 2018
[7] Yuji Sugita, "Mechanisms for Protein-Ligand Binding in Solution and In Cellular Environments", The 18th KIAS Conference on "Protein Structure and Function", KIAS, Seoul, Korea, November 15, 2018
[8] Chigusa Iwahashi, "Development of simulation methods for conformational changes in membrane transport proteins", The 5th project report meeting of the HPCI system including K computer, Tokyo, November 2, 2018
[9] Yuji Sugita, "Protein-Drug Interaction in Dilute Solution and In Cellular Environments", XIVth ICISE Workshop on Computational Biophysics at the Molecular and Meso Scales, Quy Nhon, Vietnam, October 30, 2018
[10] Yasuhiro Matsunaga, "Energetics and conformational pathways of functional rotation in the multidrug transporter AcrB" The 56th Annual Meeting of The Biophysical Society of Japan, Okayama University, September 15 – 17, 2018
[11] Yuji Sugita, "Development of the flexible-fitting MD simulation method for cryo-EM images of large macromolecular structures and dynamics", the 256th ACS National Meeting in Boston on "SESSION: COMP Meets CRYO: New Frontiers in Flexible Fitting, Image Processing & Refinement of Cryo-EM Data", Westin Boston Waterfront, Boston, MA, USA, August 19, 2018.
[12] Yuji Sugita, "Conformational changes between E1P to E2P states of SERCA by MD simulations based on string method and free-energy calculations", the 256th ACS National Meeting in Boston on "Membrane Protein Simulations & Free Energy Approaches", Westin Boston Waterfront, Boston, MA, USA, August 19, 2018
[13] Yuji Sugita and Yasuhiro Matsunaga, "A Machine Learning Approach for Linking Simulations with Single-Molecule Experiments", TSRC Workshop on "Coarse-Grained Modeling of Structure and Dynamics of Biomacromolecules V", Telluride, Colorado, USA, July 25, 2018
[14] Yuji Sugita, "Protein-Ligand Binding in Dilute Solution and Cellular Environments", TSRC Workshop on "Protein and Peptide Interactions in Cellular Environments", Telluride, Colorado, USA, July 19, 2018
[15] Yuji Sugita, "Molecular simulations of protein dynamics in crowded environments", WS on "Protein Aggregation and anti-aggregation" n the 18th Annual Meeting of the Protein Science Society of Japan, Toki Messe, Niigata, June 28, 2018

10.3.3 Oral and Poster presentations

[16] Chigusa Kobayashi, Yasuhiro Matsunaga, Jaewoon Jung, and Yuji Sugita, "Conformational fluctuations and changes of SR-Ca^{2+}-ATPase on the E1/E2 transitionp", The 63rd Annual Meeting of the Biophysical Society, Baltimore, Maryland, March 2 – 6, 2019 (Poster)
[17] Jaewoon Jung, Chigusa Kobayashi, and Yuji Sugita, "Optimal temperature and pressure evaluation in molecular dynamics simulation with a large time step", The 63rd Annual Meeting of the Biophysical Society, Baltimore, Maryland, March 2 – 6, 2019 (Poster)

[18] Jaewoon Jung, Chigusa Kobayashi, and Yuji Sugita, "Optimal temperature evaluation in MD with a large time step", The 32th Molecular Simulation, AIST, Tsukuga, November 28 – 30, 2018 (Oral)
[19] Jaewoon Jung, Chigusa Kobayashi, and Yuji Sugita, "Accurate temperature evaluation in molecular dynamics for long time simulations of biological systems with large time step", The 56th Annual Meeting of The Biophysical Society of Japan, Okayama University, September 15 – 17, 2018 (Oral)
[20] Chigusa Kobayashi, Yasuhiro Matsunaga, Jaewoon Jung, and Yuji Sugita, "Molecular dynamics simulations for dissociation of ligands in SR-Ca^{2+}-ATPase", The 56th Annual Meeting of The Biophysical Society of Japan, Okayama University, September 15 – 17, 2018 (Oral)

10.3.4 Software

[21] A molecular dynamics and modeling software GENESIS, https://www.r-ccs.riken.jp/labs/cbrt. Current release version is GENESIS 1.3.

Chapter 11

Particle Simulator Research Team

11.1 Members

Junichiro Makino (Team Leader)

Keigo Nitadori (Research Scientist)

Yutaka Maruyama (Research Scientist)

Masaki Iwasawa (Research Scientist)

Daisuke Namekata (Postdoctoral Researcher)

Miyuki Tsubouchi (Technical Staff)

11.2 Overview of Research Activities

We are developing particle-based simulation software that can be used to solve problems of vastly different scales.

Simulation schemes for hydrodynamics and structural analysis can be divided into grid-based and particle-based methods. In grid-based methods, the computational region is mapped to regular or irregular grids. Continuous distributions of physical values are represented by discrete values at grid points, and the governing partial differential equation is approximated to a set of finite difference equations.

In the case of the particle-based methods, physical values are assigned to particles, while the partial differential equation is approximated by the interactions between particles.

Both methods are widely used, and they have their advantages and disadvantages. The computational cost of grid-based schemes is generally lower than that of particle-based methods with similar number of freedoms. Thus, if an near-uniform grid structure is appropriate for the problem to be solved, grid-based methods perform better.

The advantage of the particle-based methods comes from the fact that they use "Lagrangian" schemes, in which the particles move following the motion of the fluid in the case of the CFD calculation. In the case of grid-based methods, we generally use "Eulerian" schemes, in which the grid points do not move.

There are three points in which the Lagrangian schemes are better than Eulerian schemes. One is that the Lagrangian schemes are, to some extent, adaptive to the requirement of the accuracy, since when a low-density region is compressed to become high density, Second one is that the timestep criteria are quite different. In the case of the Lagrangian schemes, the timestep is determined basically by local sound velocity, while in the Eulerian scheme by global velocity. Thus, if a relatively cold fluid is moving very fast, the timestep for the Eulerian schemes can be many orders of magnitude shorter than that for Lagrangian schemes. Finally, in the case of fast-moving low-temperature fluid, the required accuracy would be very high for Eulerian scheme, since the error comes from the high velocity, while that error would be transferred to internal energy of the fluid element which is much smaller than that of the kinetic motion.

Of course, there are disadvantages of Lagrangian schemes. The primary one is the difficulty of construction of such schemes in two or higher dimensions. In the case of one-dimensional calculation, it is easy to move grid points following the motion of the fluid, but in two or higher dimensions, the grid structure would severely

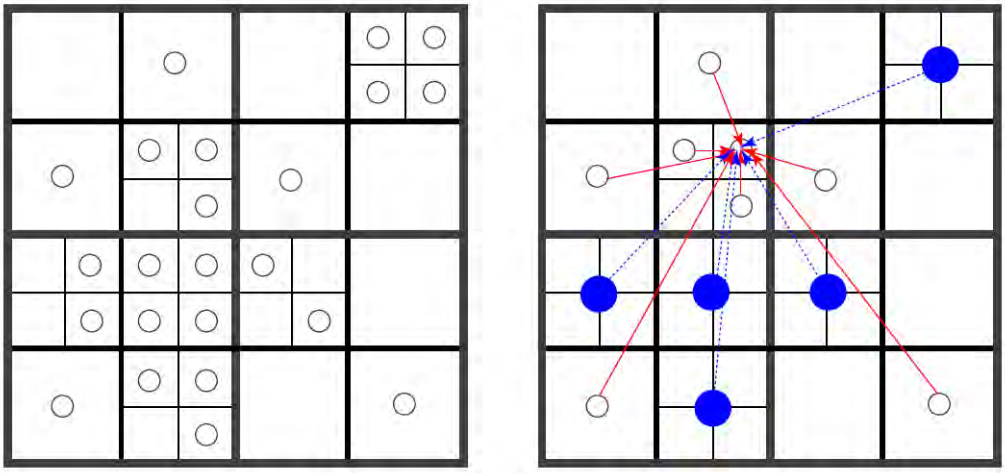

Figure 11.1: Basic idea of tree algorithm

deform if we let the grid points follow the flow. Thus, we have to reconstruct the grid structure every so often. This requirement causes the program to become complex. Moreover, reconstruction of the grid structure (so called remeshing) means we lose numerical accuracy.

Particle-based methods "solve" this difficulty by not requiring any mesh. In particle-based methods, particles interact with its neighboring particles, not through some connection through grid, but through distance-dependent kernel functions. Thus, there is no need of remeshing. As a result, particle-based schemes are simple to implement, and can give reasonable results even when the deformation is very large. Another important advantage is that it is relatively easy to achieve high efficiency with large-scale particle-based simulation.

In the case of grid-based schemes, in order achieve some adaptivity to the solution, we have to use either irregular grid or regular grid with adaptive mesh refinment. In both cases, adaptivity breaks the regularity of the mesh structure, resulting in non-contiguous access to the main memory. In the case of the particle-based schemes, it does require some irregular memory access, but it is relatively straightforward to make good use of spacial locality, and thereby achieving high efficiency. Similarly, very high parallel performance can be achieved.

However, it has its own problems. In the case of the SPH method, it has been known that the standard scheme cannot handle the contact discontinuity well. It also require rather strong artificial viscosity, which results in very low effective Reynolds number.

Thus, in many fields of computational sciences, many groups are working on implementation of high-performance particle-based simulation codes for their specific problem.

One serious problem here is that, high-performance, highly-parallel simulation codes for particle-based simulations are becoming more and more complex, in order to make full use of modern supercomputers. We need to distribute particles to many computing nodes in an appropriate way, so that the communication between nodes is minimized and at the same time near-optimal load balance is achieved. Within each nodes, we need to write an efficient code to find neighbor particles, rearrange data structure so that we can make good use of the locality, make good use of multiple cores and SIMD units within each core.

Even for the case of very simple particle-particle interaction such as the Lenard-Jones potential or Coulomb potential, the calculation code tends to be very large, and since the large fraction of the code is written to achieve a high efficiency on a specific architecture, it becomes very hard to port a code which is highly optimized to one architecture to another architecture.

Our goal is to develop a "universal" software that can be applied to a variety of problems whose scales are vastly different. In designing such universal software, it is important to ensure that it runs efficiently on highly parallel computers such as the K computer. Achieving a good load balance for particle-based simulations is a difficult task, since using a regular spatial decomposition method causes severe load imbalance, though this works well for grid-based software. Consequently, we have developed an adaptive decomposition method that is designed to work in a way that the calculation time on each node is almost the same, resulting in the near-optimal load balance.

The strategy to develop such a universal software is as follows.

We first construct an highly parallel and very efficient implementation of the TreePM algorithm for gravita-

tional N-body problem. This is actually not a completely new implementation, but the GreeM code developed by researchers of the Strategic Program for Innovative Research (SPIRE) Field 5 "The origin of matter and the universe. In collaboration with the Field 5 researchers, we improve the efficiency of the code and study the issues of the data structure, domain decomposition, load balance strategy etc.

In the second stage, we will develop a prototype of the parallel particle simulation platform. We will design the platform so that it can be used for multiple physical systems. In practice, we consider the following three applications as the initial targets.

[1] Gravitational N-body simulation

[2] Smoothed Particle Hydrodynamics

[3] Molecular Dynamics

In the meantime, we will also investigate the way to improve the performance and accuracy of the current particle-based algorithms for hydrodynamics.

11.3 Research Results and Achievements

11.3.1 High-performance gravitational N-body solver.

We use the TreePM algorithm as the basic method for the evaluation of gravitational interaction between particles. TreePM is a combination of the tree method and the P^3M (particle-particle particle-mesh) scheme. Figure 1 shows the basic idea of the tree algorithm. The space is divided into a hierarchical octree structure (quadtree in the figure). Division is stopped when a cell contains one or no particle. When we calculate the force on a particle, we evaluate the force from a group of particles, with size larger for more distant particles. In this way, we can reduce the calculation cost from O(N2) to O(N log N).

The tree algorithm is widely used, but when the periodic boundary condition is applied, we can actually use a more efficient efficient scheme, since we can calculate the long-range, periodic term using FFT. The P^3M scheme has been used for such problem, but it has the serious problem that when the density contrast becomes high, the calculation cost increases very quickly. The TreePM scheme solves this difficulty by using the tree algorithm to evaluate the forces from nearby particles. Even when there are very large number of neighbor particles, the calculation cost does not increase much, since the calculation cost of the neighbor force is proportional to the logarithm of the number of neighbors.

In order to map the problem to the distributed-memory parallel computer such as the K computer, we adopted the approach to divide the space into domains and assign particles in one domain to one calculation node. We used the orthogonal recursive multisection method developed by the team leader some years ago. It is the generalization of the orthogonal recursive bisection (ORB), which has been widely used in many parallel implementations of the tree algorithm.

With ORB, we recursively divide space into two halves, each with the same number of particles. An obvious disadvantage of the ORB approach is that it can utilize the computing nodes of integral powers of two. Thus, in the worst case we can use only half of the available nodes.

The difference between the multisection method and the ORB is that with the multisection method we allow the divisions to arbitrary number of domains, instead of bisection. This would allow too many possible divisions. In our current implementation, we limit the number of levels to three, and make the numbers of divisions at all levels as close as possible. Thus, our domain decomposition is topologically a simple three-dimension grid. This fact makes the multisection method well suited to the machines with the 3D torus network like the K computer.

We have developed a "reference code" for gravitational N-body simulation on the K computer. This code is fairly well optimized for the K computer, and shows quite good scalability for even for relatively small-size problems. The asymptotic speed per timestep for large number of nodes is around 7ms. This speed is comparable to that of highly optimized molecular dynamics codes on K, even though our code is designed to handle highly inhomogenous systems.

We used this code as the reference implementation for more generalized particle simulation platform which will be described in the next subsection.

11.3.2 Particle Simulation Platform.

In FY 2014, We have completed and released Version 1.0 of the particle simulation platform, which we call FDPS (Framework for Developing Particle Simulator). In FY 2015, we have applied a number of improvements to FDPS.

The basic idea of FDPS is that the application developer (or the user) specified the way the particles interact with each other, and the rest is taken care by FDPS. Here, "the rest" includes domain decomposition and re-distribution of particles, evaluation of interactions between particles, including those in different domains (different MPI processes, for example).

In practice, there are many additional details the user should give. Consider a relatively simple case of particles interacting with softened 1/r potential. There are a number of small but important points one has to decide on. For example, what algorithm should be used for the interaction calculation? Even if we limit the possibilities to reasonably adaptive schemes for open boundary problems, we have the choice between Barnes-Hut tree and FMM. For both algorithms, there are many different ways to parallelize them on distributed-memory parallel computers. Also, there are infinitely many variations for the time integration schemes.

The base layer of FDPS offers the domain decomposition based on the recursive multisection algorithm, with arbitrary weighting function for the load balancing. It also offers the parallel implementation of interaction calculation between particles.

The domain decomposition part takes the array of particles on each node as the main argument. It then generates an appropriate domain for each node, redistribute particles according to their locations, and returns.

The interaction calculation part takes the array of particles, the domain decomposition structure, and the specification of the interaction between particles as main arguments. The actual implementation of this part need to take into account a number of details. For example, the interaction can be of long-range nature, such as gravity, Coulomb force, and interaction between computational elements in the boundary element method (BEM). In this case, the user should also provide the way to construct approximations such as the multipole expansion and the way to estimate error. The interaction might be of short-range nature, with either particle-dependent or independent cutoff length. In these cases, the interaction calculation part should be reasonably efficient in finding neighbor particles.

We have successfully implemented all of these functionalities in FDPS version 1.0. (https://github.com/FDPS/FDPS). Using FDPS, a gravitational N-body simulation code can be written in 120 lines, and that code is actually fully scalable even to full-node runs on K computer. For SPH calculations, we have also achieved similar scaling.

FDPS is implemented as a class template library in C++ language. It receives the class definition of particles and a function (or multiple functions in the case of complex interactions) to evaluate the interaction between particles. When a user program is compiled with the FDPS library, the class template is instantiated with the user-specified definition of the particle class. Thus, even though the FDPS library functions are generic ones not specialized to a particular definition of particles, it behaves as if it is a specialized one.

The measured performance of applications developed using FDPS is quite good. Both for gravity-only calculation and SPH calculation, weak-scaling performance is practically perfect, up to the full-node configuration of K computer. Moreover, the measured efficiency, in terms of the fraction of the peak floating-point performance, is also very high. It is around 50% for gravity-only calculation. For SPH calculations, at the time of writing the performance is around 10%.

In FY 2015, we have extended FDPS in several important directions. The first one is the improvement of the strong scaling. The algorithm used for the domain decomposition contains one serial bottleneck. The "sampling" algorithm used in FDPS 1.0 works well only when the average number of particles per MPI process is significantly larger than the total number of MPI processes. We developed a new parallel algorithm, in which $O(p^{1/3}$ MPI processes are used to decompose the computational domain. Here p is the total number of MPI processes. Thus now the requirement for the number of particle is relaxed from larger than p to larger than $p^{2/3}$. Now we can achieve pretty good performance for around 1 billion particles, on the full nodes of K computer. Previously we need near 100 billion particle to achieve good efficiency.

The second one is the addition of new interface method to interaction calculation function, which allows efficient use of accelerator hardware such as GPGPU or Intel MIC. In order to achieve high performance on accelerators, it is important to pass a large chunk of work at one time. In order to achieve this goal, in the current version of FDPS the CPU creates the list of multiple interaction lists, and send all of them at once so that the overhead of the initialization of the accelerator would not become a bottleneck. This interface has been tested on NVIDIA GPGPUs as well as the PEZY-SC processor.

In FY 2016, we have released FDPS 3.0. The most important new feature of this release is the interface to application programs written in Fortran. FDPS itself is implemented using C++. The reason why we adopted

C++ is to use its "template" functions. Using templates, we can write library functions which accept user-defined data types as template arguments. This means we can effectively generate "specialized" libraries for user-specified particle data types, without knowing the data types beforehand.

In FY 2017, we have released several new versions of FDPS, up to 4.0a. There are a number of improvements, mostly for improved performance, For example, we have implemented the reuse of the interaction list. In the case of the calculation of short-range interactions, the neighbor-list method or so-called bookkeeping method has been used in many applications. On the other hand, to our knowledge, such a method has not been applied to Barnes-Hut treecode or FMM. There is no fundamental difficulty in combining the two methods, and the reason why such a combination has not tried before is probably it was not really necessary. The calculation cost of constructing the tree structure and traversing the tree to construct the interaction lists is, int the case of Barnes-Hut algorithm, a small fraction of the total calculation cost. Thus, it is usually unnecessary to try to reduce the cost of the tree construction and tree traversal.

However, some of recent high-performance computers have rather extreme ratios in various aspects, and thus require the performance improvements which were not necessary. One example is the Sunway SW26010. It's architecture is rather extreme in two aspects. First, its "core group" consists of one MPE (management processing element) and 64 CPEs (computing processing elements). MPE has data cache and runs the primary thread, and CPEs do not have cache. Thus, it is difficult and very time-consuming to develop the program which runs on CPEs, in particular for complex operations like tree construction. On the other hand, MPE is very slow compared to CPE, and thus we need to minimize the computational work of MPE.

Another aspect is the rather low memory bandwidth. The B/F number of SW26010 is around 0.03, which is around 1/15 of that of K computer. Thus, in order to achieve reasonable performance on SW26010, we need to minimized the main memory access per timestep.

The reuse of the interaction list turned out to be very effective on SW26010 and other machines with relatively low memory bandwidth, such as NVIDIA P100/V100 and PEZY-SC2.

In FY2018, we have improved the API of FDPS and also worked on further performance improvement. Concerning the improvement of API, we added the API in the C language in FDPS 5.0. Before 5.0, user programs should be written either C++ or Fortran. Although these two languages cover a fair fraction the needs of of HPC users, it is clearly desirable to have API in C language, since that would allow users to write programs not only in C languages but also in any other languages with FFI (foreign function interface), since FFI is usually defined in C. The C language API works much in the same way as Fortran API.

Concerning the improvment of performance, we worked mainly to remove performance bottlenecks on platforms on which the interaction calculation is relatively fast. One example of such systems is systems with GPGPUs. In order to allow easy use of GPGPUs, it is desirable that we use GPGPUs only for the calculation of interactions and let the host CPU do the rest of calculations. In fact, this is the calculation model for our GRAPE hardware. With FDPS 5.0, we perform detailed analysis of the algorithms used in FDPS and removed all unnecessary access to the host main memory. As a result, we have achieved quite high efficiency on modern GPGPUs.

11.3.3 Improvements on Particle-based CFD

SPH (Smoothed Particle Hydrodynamics) has been used in many field, including astrophysics, mechanical engineering and civil engineering. Recently, however, it was pointed out that the standard formulation of SPH has numerical difficulty at the contact discontinuity. The reason is that the formulation of the standard SPH requires that the density is differentiable, which is by definition no the case at the contact discontinuity.

We have been working on the solution of this problem, in which we replace the SPH formulation to evaluate the gradient to other schemes. SPH has a known problem that its kernel estimate contains O(1) error, since the summation of contributions from neighbor particles is not guaranteed to be unity. The reason why SPH uses this mathematically inconsistent formulation is to achieve symmetry and conservation. In SPH discretization, interaction between two particles is symmetric, which guarantees the conservation of linear and angular momenta. However, the use of SPH approximation resulted in rather low accuracy, which limits the reliability of the results obtained using SPH. We have developed a completely different scheme, which can achieve much higher accuracy, while losing some of the nice features of SPH such as the symmetry of interaction.

Our new approach, which we call CPHSF (Consistent Particle Hydrodynamics in Strong Form), is based on high-order MLS (moving least square fit). In SPH, particles have mass and energy (or entropy). Particle mass is automatically conserved, and SPH differentiation is constructed so that the total energy is conserved. Thus, SPH is quite robust, since conserved quantities are always conserved. However, this formulation makes it practically impossible to construct high-order schemes, express boundary condition explicitly or handle contact

discontinuity. Therefore, in CPHSF, we gave up the exact conservation of mass and energy, but instead achieved the conservation by the scheme which is of higher order in both space and time.

One unique feature of CPHSF is that with CPHSF we can obtain high-order space derivatives with very small additional cost, since we do construct high-order MLS fitting. Thus, instead of using usual Runge-Kutta method to achieve high-order accuracy in time, we can use high-order space derivatives to construct high-order time integration scheme. We adopted 4th-order Hermite scheme, which has been widely used in the field of stellar dynamics. The Hermite scheme is the generalization of Adams-Bashforth-Moulton (ABM) linear-multistep method. In the ABM method, previous values of first time derivatives (the rhs values of the ordinary differential equations) are used to construct high-order polynomial fitting through Lagrange interpolation. In Hermite method, not only the rhs value itself but also its time derivatives are used to construct high order fitting polynomial through Hermite interpolation. The 4th-order Hermite scheme is the simplest Hermite scheme, in which the second time derivatives are calculated directly from the original differential equation and two-point interpolation is used to construct third-order fitting polynomial. The clear advantage of the Hermite scheme is that it requires only one evaluation of the derivatives per one timestep, if used in the PEC form. Runge-Kutta schemes with 4th-order accuracy require four evaluations per timestep and thus four times more expensive.

11.4 Schedule and Future Plan

We plan to improve the performance of FDPS further in FY 2019. The main issue will be the porting and performance tuing on Fugaku supercomputer. Other issues include the implementation of FMM and PMMM (particle-mesh multipole method).

11.5 Publications

11.5.1 Articles/Journal

[1] D. Namekata, M. Iwasawa, K. Nitadori, A. Tanikawa, T. Muranushi, L. Wang, N. Hosono, K. Nomura and J. Makino, “Fortran interface layer of the framework for developing particle simulator FDPS”, Publications of the Astronomical Society of Japan, 70, 4, p.70-87, 2018.
[2] S. Ayuba, D. Suh, K. Nomura, T. Ebisuzaki and K. Yasuoka, “Kinetic analysis of homogeneous droplet nucleation using large-scale molecular dynamics simulations” J. Comp. Chem. 149, 044504, 2018.
[3] S. Yamamoto and J. Makino, “Hermite integrator for high-order mesh-free schemes”, Publications of the Astronomical Society of Japan, 70, 18, 2018.
[4] S. Hozumi, M. Iwasawa and K. Nitadori, “A Mean-Field Approach to Simulating the Merging of Collisionless Stellar Systems Using a Particle-Based Method”, The Astrophysical Journal, 2019.
[5] T. Yamazaki, J. Igarashi, J. Makino and T. Ebisuzaki, “Real-time simulation of a cat-scale artificial cerebellum on PEZY-SC processors”, The International Journal of High Performance Computing Applications, 33, p.155-168, 2019.
[6] M. Iwasawa, S. Oshino, M. Fujii S. and Y. Hori, “PENTACLE: Large-scale particle simulations code for planet formation”, Astrophysics Source Code Library, 2018.

11.5.2 Conference Papers

[7] M. Iwasawa, L. Wang, K. Nitadori, D. Namekata, T. Muranushi, M. Tsubouchi, J. Makino, Z. Liu, H. Fu and G. Yang, “Global Simulation of Planetary Rings on Sunway TaihuLight”, ICCS 2018 p.483-495, June 2018.

11.5.3 Posters

[8] Y. Hirai, T. Saitoh, R., S. Wananjo and M. Fujii, S, “Enrichment of heavy elements in chemo-dynamical simulations of dwarf galaxies” XXXth General Assembly of the International Astronomical Union, Vienna, Austria, August 20-24, 2018.
[9] K. Nomura, T. Nozawa, M. Iwasawa, D. Namekata, K. Nitadori, S. Ayuba, K. Yasuoka and J. Makino, “Development of molecular dynamics simulation code using accelerators on FDPS”, The 32nd Annual Meeting of the Molecular Simulation Society of Japan, Tsukuba, Japan, November 28-30, 2018. (in Japanse)

[10] K. Nomura, Y. Maruyama, K. Nitadori and J. Makino "Pieceise polynomial approximation algorithm for short-range intermolecular interaction on wide SIMD architectures" The 1st R-CCS International Symposium, Kobe, Japan, February 18-19, 2019.

11.5.4 Invited Talks

[11] Y. Hirai, T. Saitoh R. and M. Fujii, S., "Enrichment of Heavy Elements in the Local Group Galaxies", Taiwanese Theoretical Astrophysics Workshop, Taipei, Taiwan, September 25-27, 2018.
[12] Y. Hirai, "Origin and Evolution of r-process Elements", First Stars and First Galaxies Workshop 2018, Mito, Japan, November 19-21, 2018. (in Japanese)

11.5.5 Oral Talks

[13] N. Hosono, M. Iwasawa, D. Namekata, A. Tanikawa, K. Nitadori, T. Muranushi and J. Makino, "Speed-up efficiencies of an SPH code with FDPS on GPUs or PEZY-SCs", JpGU2018, Chiba, Japan, May 20-24, 2018. (in Japanese)
[14] Y. Hirai, "Enrichment of r-process Elements in Chemo-Dynamical simulations of galaxies", r-Process and Unstable Nuclei in Multi-messenger Astronomy, Wako, Japan, June 20-22, 2018. (in Japanese)
[15] E. Strohmaier, W. Lioen, K. Hiraki and J. Makino, "Pros and Cons of HPCx benchmarks", SC18, Dallas, USA, November 13, 2018.
[16] H. Tanaka, Y. Ishihara, R. Sakamoto, T. Nakamura, Y. Kimura, K. Nitadori, M. Tsubouchi and J. Makino, "Automatic Generation of High-Order Finite-Difference Code with Temporal Blocking For Extreme-Scale Many-Core Systems", 2018 IEEE/ACM 4th International Workshop on Extreme Scale Programming Models and Middleware (ESPM2), Dallas, USA, November 12, 2018.
[17] Y. Hirai, "Understanding the Enrichment of Heavy Elements by Galactic Chemo-Dynamical Evolution Models", Chemical evolution and nucleosynthesis across the Galaxy, Heidelberg, Germany, November 26-29, 2018.
[18] Y. Hirai, T. Saitoh, R. and S. Wananjo, "Metal Mixing in Galaxies as a Probe of Understanding Signatures from First Stars" Stellar Archaeology as a Time Machine to the First Stars, Kashiwa, Japan, December 3-7, 2018.
[19] Y. Hirai, "Enrichment of Light Neutron-Capture Elements in Dwarf Galaxies", National Astronomical Observatory of Japan, Center for Computational Astrophysics User's Meeting 2018, Mitaka, Japan, January 15-16, 2019. (in Japanese)
[20] Y. Hirai, "Origin and Evolution of r-process elements in Simulations of Galactic Chemo-Dynamical Evolution", Workshop of Nuclear Astrophysics for Nuclear Data and Synthesis of Heavy Elements, Sapporo, Japan, March 6-8, 2019. (in Japanese)
[21] Y. Hirai, "Enrichment of Light Neutron Capture Elements in Galactic Chemo-Dynamical Evolution Models", 2019 Spring Annual Meeting of the Astronomical Society of Japan, Koganei, Japan, March 14-19, 2019. (in Japanese)

11.5.6 Software

[22] Formura github.com/Formura

11.5.7 Patents

[23] Computing device and Computing unit, 2018/05/11, PCT/JP2018/018400

Chapter 12

Computational Climate Science Research Team

12.1 Members

Hirofumi Tomita (Team Leader (Concurrent))*

Yoshiyuki Kajikawa (Senior Research Scientist(Concurrent))**

Seiya Nishizawa (Research Scientist (Concurrent))***

Hisashi Yashiro (Research Scientist (Concurrent))***

Sachiho A. Adachi (Research Scientist)

Tsuyoshi Yamaura (Special Postdoctoral Fellow)****

Kenta Sueki (Postdoctoral Fellow)

Toshiki Matsushima (Postdoctoral Fellow)

Yuta Kawai (Research staff (part timer))

Keiko Muraki (Assistant (Concurrent))***

Kyoko Onda (Assistant)****

* Chief Scientist in RIKEN CPR; Team leader in RIKEN RCCS FS2020 Application Development team
** Specially appointed professor in Kobe University
*** Research Scientist in RIKEN RCCS FS2020 Application Development team
** Specially appointed assistant professor in Kobe University

12.2 Research Activities

The primary aim of Computational Climate Science Research Team is to indicate a direction of future climate modeling with a reliable suggestion for the age of high-performance computers. For this purpose, we intend to construct a basic library, in which model components and their numerical method are inter-exchangeable among multiple models. This work contributes directly to climate modeling community for enhancement of fast output/outcome creation. Using the library, we also develop a more advanced climate model with new techniques that is necessary for efficient climate simulation. We promote to develop them, taking the following issues into consideration; the readability of code, its convenience for users, and traceability of computational results. The second aim is to pursue the high efficiency of climate model in massive parallel computers. Computational meteorology and climatology always require large-scale numerical experiments. However, it is recently pointed out that the conventional computer architecture with the straightforward extension of existing simulation codes would be a limitation in getting higher performance. From the viewpoint of hardware and climate modeling,

we consider the numerical method, algorithm and their implementation to large-scale computers, cooperating with research teams of computational and computer sciences in R-CCS. The third aim is to apply our model to address the meteorological / climatological problems, collaborating with outside research institutes. The climate studies are widely spread from the basic understanding of phenomena to assessment of environment. The former is more scientific and the latter is more practical for the requirement of the society. Several issues we currently focus on are as follows; feedback mechanism between cloud, aerosol and radiation, theory for the moist process linked to the turbulence process, comprehensive understanding of our earth's particularity by investigation other planets and so on. The assessment of future environmental change for disaster prevention at the regional scale level is also one of our targets.

12.2.1 Research and development of SCALE

SCALE (Scalable Computing for Advanced Library and Environment) is a basic library for atmospheric numerical calculation. For the next generation atmospheric simulation, we evaluate the existing schemes and develop new schemes for higher resolution simulation. In this fiscal year, we evaluated the reproducibility of Super-droplet method (SDM), which is a cutting-edge cloud microphysics scheme, and developed a new surface flux scheme to solve the underestimation bias in conventional schemes.

12.2.1.1 Reproducibility of SDM

Size distribution of cloud particles is significantly important in cloud microphysical processes. In the conventional Eulerian cloud microphysics schemes, it is difficult to accurately simulate the distribution due to numerical diffusion. On the other hand, Lagrangian method has no numerical diffusion and can simulation the size distribution more accurately. SDM is a cutting-edge Lagrangian scheme, but its physical performance is not well known. We tried to evaluate its reproducibility of cumulus clouds.

Large-eddy simulations of cumulus were carried out with various simulation resolutions and the numbers of super-droplets; the resolution and the number of droplets in the largest simulations are 25 m and 256 droplets per grid cell, respectively. The cumulus observed in Small Cumulus Microphysics Study observation campaign in east central Florida in summer 1995 was simulated.

We succeeded in obtaining realistic cumulus as shown Fig. 12.1. It was confirmed that the mean and variance of the number density of the cloud droplet, liquid water content, and the k-value, which is a quantity related to the variance of size distribution, agree well with the observation results. It is also found that the spectrum width of the size distribution has a realistic value.

12.2.1.2 Development of a new surface flux scheme

Most atmospheric simulation models adopt the finite volume method, in which volume average quantities are prognostic in simulation. However, the volume average is used as a point value at the center of the grid cell in calculation of the fluxes of momentum, heat, and vapor at the ground surface. We found that this results in an underestimation bias in simulations. The underestimation becomes larger for the smaller grid

Figure 12.1: The cumulus simulated the large-eddy simulation with SDM

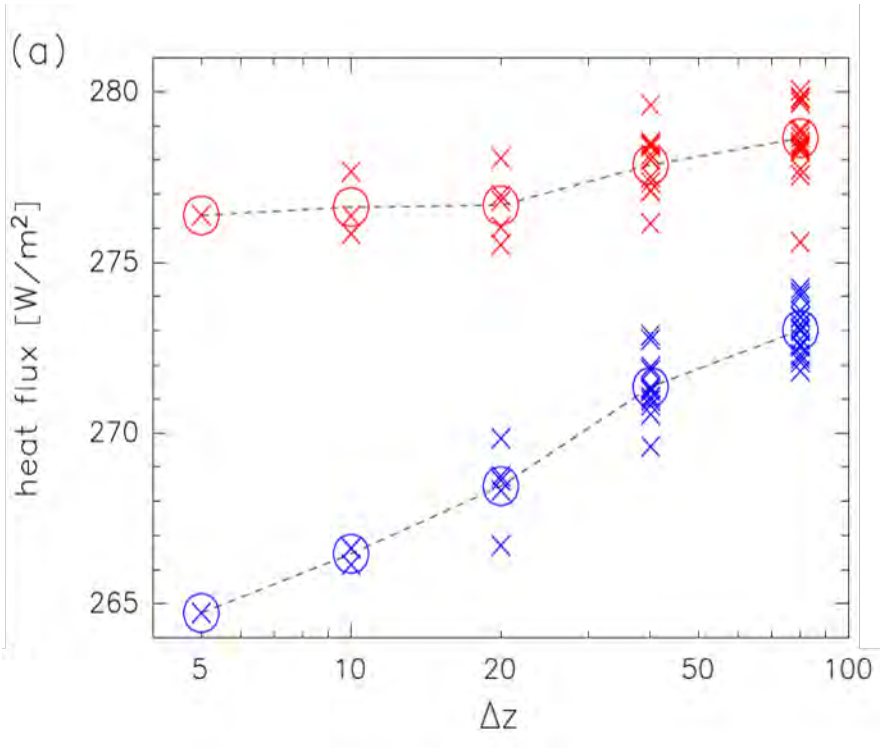

Figure 12.2: The surface heat flux in the large-eddy simulations with (blue) the conventional and (red) new schemes. The horizontal axis represents grid spacing.

spacing. Therefore, we developed a new surface flux scheme to solve the underestimation bias for high resolution simulations.

In order to evaluate the validity of the new scheme, large-eddy simulations were performed with a conventional and the new schemes. Figure 12.2 shows the surface heat flux obtained by the simulations. It was confirmed that the conventional scheme calculates smaller flux. We also found that the flux shows good convergence for the grid spacing in the simulations with the new scheme, while it does not with the conventional one.

12.2.2 Theory of numerical errors for mixed floating-point numbers

We carried out a theoretical investigation of the impact of the numerical errors caused by using floating-point numbers (FPNs) in simulations, such as rounding errors. Under the presupposition that model variables can be written as the linear sum of the true value and the numerical error, equations governing the time evolution of numerical errors due to FPNs (FPN errors) are obtained by considering the total errors of the results of simulations of shallow-water models and estimating the errors incurred by using FPNs with varying precision. We can use the time evolution equations to estimate the behavior of the FPN errors, then confirm these estimations by carrying out numerical simulations (Fig.12.3). The results are summarized as follows. In a geostrophic wind balance state, the FPN error oscillates and gradually increases in proportion to the square root of the number of time steps, like a random walk. We found that the error introduced by using FPNs can be considered as stochastic forcing. In a state of barotropic instability, the FPN error initially evolves as stochastic forcing, as in the case of the geostrophic wind balance state. However, it then begins to increase exponentially, like a barotropic instability wave. These numerical results are obtained by using a staggered-grid arrangement and stable time-integration method to retain near-neutral numerical stability in the simulations. The FPN error tends to behave as theoretically predicted if the numerical stability is close to neutral

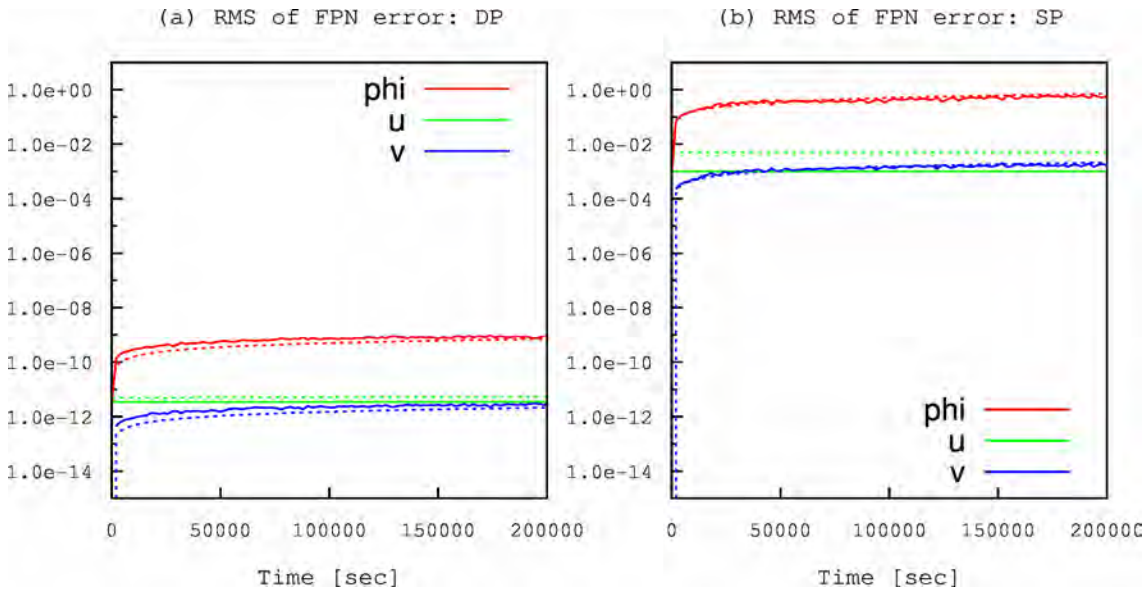

Figure 12.3: (a) The time evolution of the root-mean-square of the FPN errors from the geostrophic wind balance experiments using double-precision (DP) FPNs. The solid (dotted) lines are the experimental (ideal) values of the FPN errors. The ideal equation is described in detail in the text. (b) The same as (a), except for single-precision (SP) FPNs.

12.2.3 The Hyogo-Kobe COE establishment project

The Hyogo-Kobe COE establishment project started in FY2018. Our team participates the subject "Computational Research on Estimation to Complex Disaster Risk for Better Urban Planning" with being responsible for future regional climate projection by a model with high spatial resolution and the sophistication of the model. In the last fiscal year, we proposed a new downscaling method that uses four downscaling simulations and separates the regional climate change Δ into contributions of three large-scale atmospheric factors: changes in mean state ΔC, changes in perturbation ΔP, and the nonlinear effect Δcp, i.e., $\Delta = \Delta C + \Delta P + \Delta cp$ In this fiscal year, we propose applying this downscaling method to uncertainty problem in regional climate projections. The future climate change projected by general circulation models (GCM) has a large uncertainty due to systematic errors and imperfection of a GCM. The downscaled climate by a regional climate model (RCM) inevitably inherits the uncertainties. By applying the downscaling method to multiple future climate projections from GCMs, we can get not only range of regional climate changes (Δs) but also contributions of the three factors (ΔC, ΔP, and Δcp) to the range of the projection. We applied the procedure to regional projections of summertime climate in western Japan using four future climates simulated by MRI-AGCM. The results show that the primary factor that influences the spread of future climate projections is the climatology component (ΔC) for surface air temperature indices, whereas it is the perturbation component (ΔP) for the consecutive no-rain days. For the mean and maximum one-day precipitation indices, both the climatology and perturbation components are equally important factors. These results indicate usefulness of the proposed procedure to understand the spread of the regional climate projection(Fig.12.4).

12.3 Schedule and Future Plan

We continue to sophisticate the basic library SCALE. At the present, the main processes, both of dynamics and physics, have already been developed comprehensively. We will pursue higher usability for the outside users. We keep elaborating the advanced climate model based on schemes in principle and indicate a direction to future climate model. The sub-grid scale parameterization is a key of sophistication. For example, the RANS (Raynolds-Averaged Navier-Stokes) scheme should be sophisticated for high-resolution to solve the gray-zone problem. For this purpose, LES database will be useful with the aid of data science such as AI technique. To express the cloud physics much more accurately, the moist turbulence consideration may be needed. The combination of LES for turbulence and SDM (Super Droplet Method) for cloud microphysics will a useful tool

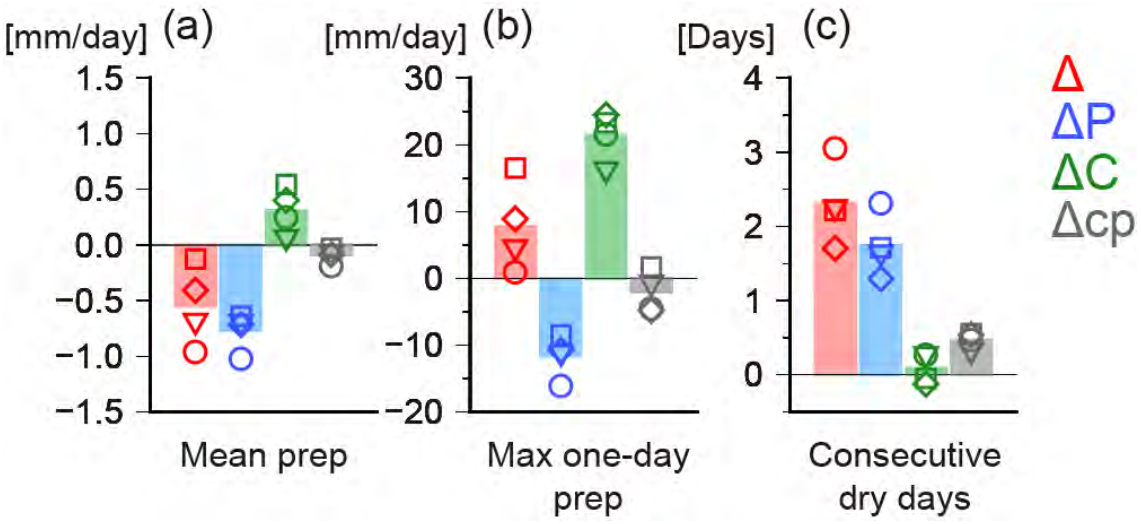

Figure 12.4: Variability among the future climate projections for (a) daily precipitation, (b) maximum one-day precipitation and (c) consecutive dry days. Each mark represents an individual future projection. Δ is the total change estimated from direct dynamical downscaling simulations for present climate and future climate. ΔP and ΔC indicate the perturbation and climatology change contributions, respectively. Δcp is the contribution of the nonlinear effect between the two component changes.

for this issue. Not only to make computational and physical performance of simulation code higher but also to provide useful analysis tool of simulation results is a main mission of team. This is of great importance for acceleration of scientific output and social outcome. Specifically, major analysis programs will be parallelized, suitable to massively parallel computer systems. Continuously, short-range/mid-range numerical weather prediction system is developed, collaborating with Data Assimilation Research Team. LETKF is a vital application for data assimilation. To coupling our models with LETKF in combination of high resolution, large ensembles, and observational big data enable us to transit a new stage for numerical weather prediction. The specific targets are NICAM-LETKF for global mid-range prediction and SCALE (RM)-LETKF for regional short-range prediction. Since the former system is a target application in the post-K prior subject 4, while the latter has already started in the CREST subject and will be a main application on the post-K. Our team bridges the above research and the post-K project.

12.4 Publications

12.4.1 Articles

[1] Yoshida, R., S. Nishizawa, H. Yashiro, S. A. Adachi, T. Yamaura, H. Tomita, and Y. Kajikawa (2018): Maintenance condition of back-building squall-line in a numerical simulation of a heavy rainfall event in July 2010 in Western Japan, Atmospheric Science Letters, Volume 20, Issue 1, Doi: 10.1002/asl.880

[2] Adachi, S. A., S. Nishizawa, K. Ando, T. Yamaura, R. Yoshida, H. Yashiro, Y. Kajikawa, and H. Tomita (2018): An evaluation method for uncertainties in regional climate projections, Atmospheric Science Letters, Volume20, Issue1, Doi: 10.1002/asl.877

[3] Nishizawa, S., and Y. Kitamura (2019): A surface flux scheme based on the Monin–Obukhov similarity for finite volume models, Journal of Advances in Modeling Earth Systems, Volume 10, Issue11, Doi: 10.1029/2018ms001534

[4] 加瀬紘熙, 筆保弘徳, 北本朝展, Danlan Chen, 吉田龍二, 竹見哲也 (2019): 深層学習を用いた台風強度推定に対する台風の特徴の影響, 日本気象学会機関誌 天気, Vol. 66, No. 1, Page 51-58

[5] Tochimoto, E., K. Sueki, and H. Niino (2019): Entraining CAPE for Better Assessment of Tornado Outbreak Potential in the Warm Sector of Extratropical Cyclones, Monthly Weather Review, Volume 147 No. 3, Doi: 10.1175/MWR-D-18-0137.1

[6] Zarzycki, C. M., C. Jablonowski, J. Kent, P. H. Lauritzen, R. Nair, K. A. Reed, P. A. Ullrich, D. M. Hall, M. A.Taylor, D. Dazlich, R. Heikes, C. Konor, D. Randall, X. Chen, L. Harris, M. Giorgetta, D. Reinert, C.

Kühnlein, R. Walko, V. Lee, A. Qaddouri, M. Tanguay, H. Miura, T. Ohno, R. Yoshida, S. Park, J. B. Klemp, and W. C. Skamarock (2019): DCMIP2016: the splitting supercell test case, Geoscientific Model Development, 12, 879-892, Doi: 10.5194/gmd-12-879-2019

12.4.2 Invited Talks

[7] 足立幸穂: 気候気象分野の紹介, 2018年度第1回計算科学フォーラム, 東京, 日本, Jul 31, 2018.
[8] 足立幸穂: 都市パラメータの影響, 第5回J-STREAMデータ検討会, 神戸, 日本, Aug 31, 2018.

12.4.3 Oral and Poster presentations

[9] Yamaura, T., S. Nishizawa, and H. Tomita.: Numerical weather/climate model for cost-performance using mixed precision floating point number, 8th JLESC Workshop, Barcelona, Spain, April 17, 2018. (Oral)
[10] Sueki, K., T. Yamaura, H. Yashiro, S. Nishizawa, R. Yoshida, Y. Kajikawa, and H. Tomita.: Numerical Convergence for Statistics of Deep Moist Convection in the Tropics, Japan Geoscience Union Meeting 2018, Chiba, Japan, May 22, 2018. (Oral)
[11] Nishizawa, S., and Y. Kitamura.: Improvement of the Surface Flux Scheme in Finite Volume Method Models, 15th Annual Meeting Asia Oceania Geosciences Society, Honolulu, Hawaii, USA, June 4, 2018. (Oral)
[12] Adachi, S. A., S. Nishizawa, R. Yoshida, T. Yamaura, K. Ando, H. Yashiro, Y. Kajikawa, and H. Tomita.: Evaluation procedure of uncertainty source due to GCM projections in downscaled regional climate, 15th Annual Meeting Asia Oceania Geosciences Society, Honolulu, Hawaii, USA, June 8, 2018. (Oral)
[13] 西澤誠也: 次世代気象・気候計算のための基盤ライブラリ環境 SCALE の開発と研究–次世代気象・気候シミュレーションへの取り組み– , 5th International Workshop on Nonhydrostatic Models, 東京, 日本, Nov 16, 2018. (Oral)
[14] Matsushima, T., S. Nishizawa, S. Shima, and H. Tomita.: Spectral broadening of cloud droplets in cumulus congestus cloud obtained by large eddy simulation with super droplet method, Workshop on particle-based modeling of cloud microphysics 2018, Kobe, Japan, Nov 19, 2018. (Oral)
[15] Nishizawa, S., S. A. Adachi, and H. Tomita.: Effect of sub-meso scale topography on precipitation, Workshop on particle-based modeling of cloud microphysics 2018, Kobe, Japan, Nov 20, 2018. (Oral)
[16] Tomita, H., S. Nishizawa, T. Yamaura, R. Yoshida, H. Yashiro , and K. Sueki.: Current status of SCALE and its future toward the accurate numerical weather prediction, 7th International Symposium on Data Assimilation, Kobe, Japan, Jan 24, 2018. (Oral)
[17] Yoshida, R., and H. Fudeyasu.: Environmental Flow Patterns of Tropical Cyclone Genesis over the Western North Pacific, AMS 33rd Conference on Hurricanes and Tropical Meteorology, Florida, USA, April 17, 2018.(Poster)
[18] Kashimura, H., H. Yashiro, S. Nishizawa, H. Tomita, K. Nakajima, M. Ishiwatari, Y. O. Takahashi, and Y. Hayashi.: Model development for a global, high-resolution, and non-hydrostatic simulation of the Martian atmospheric circulation, Japan Geoscience Union Meeting 2018, Chiba, Japan, May 23, 2018.(Poster)
[19] Sueki, K., T. Yamaura, H. Yashiro, S. Nishizawa, R. Yoshida, Y. Kajikawa, and H. Tomita.: Numerical Convergence for Statistics of Deep Moist Convection in the Tropics, 第5回メソ気象セミナー, Kashiwa, Japan, June 15, 2018.(Poster)
[20] Sueki, K.: Numerical Investigation on the Environment of Tornado Occurrences Associated with Typhoon 201318 (MAN-YI), 29th Conference on Severe Local Storms, Stowe, Vermont, USA, Oct 22, 2018.(Poster)
[21] Adachi, S. A., S. Nishizawa, K. Ando, T. Yamaura, R. Yoshida, H. Yashiro, Y. Kajikawa, and H. Tomita.: Evaluation procedure of uncertainty source due to GCM projections in downscaled regional climate, The 1st R-CCS International Symposium, Kobe, Japan, Feb 18, 2019.(Poster)
[22] Kajikawa, Y., K. Ando, S. A. Adachi, S. Nishizawa, and T. Yamaura.: Factor analysis in downscaled regional climate change, The 1st R-CCS International Symposium, Kobe, Japan, Feb 18, 2019.(Poster)
[23] 八代尚: 気象・気候のための基盤ライブラリSCALE への MATSIRO の導入, 次世代陸モデル開発・応用・社会実装に関する合同ワークショップ, 柏, 日本, April 19, 2018.(Oral)
[24] 末木健太, 山浦 剛, 八代尚, 西澤誠也, 吉田 龍二, 梶川 義幸, 富田浩文: 熱帯の深い湿潤対流の統計的性質の数値的収束性, 大気と海洋に関する研究集会, 東京, 日本, April 21, 2018.(Oral)
[25] 末木健太, 山浦 剛, 八代尚, 西澤誠也, 吉田 龍二, 梶川 義幸, 富田浩文: 深い湿潤対流の統計的性質の数値的収束性, 日本気象学会2018年度春季大会, つくば, 日本, May 16, 2018.(Oral)
[26] 足立幸穂, 西澤誠也, 安藤和人, 山浦剛, 吉田龍二, 梶川義幸, 八代尚, 富田浩文: 関西地域の夏季降水を対象としたSCALEによる将来変化予測,その３：将来領域気候予測における不確定性の要因評価手法の提案, 日本気象学会2018年度春季大会, つくば, 日本, May 17, 2018.(Oral)

[27] 山浦剛, 西澤誠也, 富田浩文: 混合精度浮動小数点演算を用いた数値気象モデルの構築, CREST「ビッグデータ応用」第4回若手研究者合宿, 三浦郡葉山, 日本, June 12, 2018.(Oral)
[28] 富田浩文, 末木健太, 山浦剛, 八代尚, 西澤誠也, 吉田龍二, 梶川義幸: 湿潤対流の統計的性質からみるRANSとLESの数値収束点実質的使用限界について, グレーゾーン研究会 2018, 柏, 日本, Jul 23, 2018.(Oral)
[29] 西澤誠也, 足立幸穂, 富田浩文: 降水に対する sub-km スケールの地形の影響, グレーゾーン研究会 2018, 柏, 日本, Jul 23, 2018.(Oral)
[30] 富田浩文, 梶川義幸, 山浦剛, 末木健太: 平成30年7月豪雨前の総観規模擾乱の役割, 平成30年7月豪雨に関する緊急対応研究会, 神戸, 日本, Aug 17, 2018.(Oral)
[31] 新田友子, 竹島滉、鳩野美佐子、八代尚、荒川隆、山崎大、芳村圭, 芳村圭: 統合陸域シミュレータ（ILS）の開発, 水文・水資源学会2018年研究発表会, 津, 日本, Sep 1, 2018.(Oral)
[32] 西澤誠也, 足立幸穂, 富田浩文: 強い降水に対するサブメソスケールの地形の影響, 気象学会2018年度秋季大会, 仙台, 日本, Oct 30, 2018.(Oral)
[33] 松嶋俊樹, 石岡圭一: 半無限領域のスペクトル法による竜巻を模した渦の数値実験に向けた研究開発, JHPCN：学際大規模情報基盤共同利用・共同研究拠点　第１０回 シンポジウム, 東京, 日本, Jul 12-13, 2018.(Poster)
[34] 山浦剛, 梶川義幸, 末木健太, 富田浩文: 平成30年7月豪雨におけるオホーツク海高気圧の役割, 平成30年7月豪雨に関する緊急対応研究会, 神戸, 日本, Aug 17, 2018.(Poster)
[35] 末木健太, 梶川義幸, 山浦剛, 富田浩文: 平成30年7月豪雨における降水特性の地域差～広島と兵庫の比較～, 平成30年7月豪雨に関する緊急対応研究会, 神戸, 日本, Aug 17, 2018.(Poster)
[36] 末木健太: 台風201318号に伴う竜巻の発生環境場に関する数値的研究, 気象学会2018年度秋季大会, 仙台, 日本, Oct 31, 2018.(Poster)
[37] 新田友子, 荒川隆，竹島滉，鳩野美佐子，八代尚，山崎大, 芳村圭: 統合陸域シミュレータの開発と気候モデルとの結合に向けた検討, 気象学会2018年度秋季大会, 仙台, 日本, Oct 31, 2018.(Poster)
[38] 末木健太, 山浦 剛, 八代尚,西澤誠也, 吉田 龍二, 梶川 義幸, 富田浩文: 原理的な物理過程に基づく対流雲の統計的性質についての数値収束性研究, 第5回「京」を中核とするHPCIシステム利用研究課題 成果報告会, 東京, 日本, Nov 2, 2018.(Poster)

12.4.4 Software

[39] Meteorlological and Climate model library SCALE,
`https://www.r-ccs.riken.jp/software_center/jp/software/scale/overview/` Current release version is SCALE 5.3.5.

Chapter 13

Complex Phenomena Unified Simulation Research Team

13.1 Members

Makoto Tsubokura (Team Leader)

Keiji Onishi (Researcher)

Rahul Bale (Researcher)

Koji Nishiguchi (Postdoctoral Researcher)

Wei-Hsiang Wang (Postdoctoral Researcher)

Chung-Gang Li (Visiting Researcher)

Ryoichi Kurose (Visiting Researcher)

Tetsuro Tamura (Visiting Researcher)

Duong Viet Dung (Visiting Researcher)

Huilai Zhang (Visiting Researcher)

Leif Niclas Jansson (Visiting Researcher)

13.2 Overview of Research Activities

The objective of our research team is to propose a unified simulation method of solving multiple partial differential equations by developing common fundamental techniques such as the effective algorithms of multi-scale phenomena or the simulation modeling for effective utilization of the massively parallel computer architecture. The target of the unified simulation is supposed to be complex and combined phenomena observed in manufacturing processes in industrial cycles and our final goal is to contribute to enhance Japanese technological capabilities and industrial process innovation through the high-performance computing simulation.

Most of the complex flow phenomena observed in manufacturing processes are relating to or coupled with other physical or chemical phenomenon such as turbulence diffusion, structure deformation, heat transfer, electromagnetic field or chemical reaction. While computer simulations are rapidly spreading in industry as useful engineering tools, their limitations to such coupled phenomena have come to realize recently. This is because of the fact that each simulation method has been optimized to a specific phenomenon and once two or more solvers of different phenomena are coupled for such a complicated target, its computational performance is seriously degraded. This is especially true when we utilize a high-performance computer such as K-computer. In such a situation, in addition to the fundamental difficulty of treating different time or spatial scales, interpolation of physical quantities like pressure or velocity at the interface of two different phenomena requires additional computer costs and communications among processor cores. Different mesh topology and hence data structures

among each simulation and treatment of different time or spatial scales also deteriorate single processor performance. We understand that one of the keys to solve these problems is to adopt unified structured mesh and data structure among multiple simulations for coupled phenomena. As a candidate of unified data structure for complicated and coupled phenomena, we focused on the building-cube method (BCM) proposed by Nakahashi [1].

In summary, the overview of Research Activities in FY2018 was as followings.

In the research and development of unified simulation framework 'CUBE', an empirical analysis was conducted based on the vehicle aerodynamic problem given the tire rotation conditions. We succeeded in predicting the difference of aerodynamic drag value of 6 specification differences that clears the certification condition of WLTP, and it was possible to clarify the influence of the difference of the flow field generated around the rotating wheel on the aerodynamics drag. However, there is still room for improvement in the prediction of the absolute value of the aerodynamic coefficient, and further demonstrations will be made in the future, and efforts will be made to make them approach closer to the true value. A narrow-band vehicle aeroacoustics noise analysis has been conducted. It could reproduce the generation of sound from around the engine-hood area successfully and could estimate the resolution for quantitative prediction in post-K computer. Since the peak frequencies obtained was about the half frequency of measurement, it is assumed that this calculation result does not have sufficient resolution yet. But this calculation succeeds in capturing the acoustic feedback sound in the vehicle for the first time. It can be said that the results implies that this method is promising for the future application. We will continue to work on speeding up the calculation method toward the 'post-K' computer and acquiring computational resources. A multi-objective shape optimization analysis on vehicle aerodynamics has been conducted. In multi-objective shape optimization design exploration, four objective functions about 5 generations for 18 individuals has been taken. It was possible to obtain a solution that shows the same tendency as the actual design knowledge. It can be said that the validity of this framework could be confirmed. To see the Pareto solution obtained in this study, it looks that the number of generations is still small and it can not be said that convergence has been sufficient. We will continue calculations while securing necessary calculation resources. In addition, we are also considering including more detailed design changes such as narrowing the shape change width and incorporating radius deformation to increase the freedom of deformation. The in-situ visualization has been enhanced to cope with large-scale visualization, which is a problem in demonstration vehicle aerodynamic analysis, and we succeeded in creating a 4K resolution animation for approximately 0.8 mm cells of 5.6 billion cells. This is probably the world's largest example of vehicle aerodynamics visualization using real vehicles. It was confirmed that current method is sufficiently efficient as a visualization method for practical use. In the future, we plan to deploy this method for empirical analysis, and improve calculation efficiency and support for users toward the 'post-K' computer. We tried to improve single and parallel performance of compressible solver in K computer and to evaluate it using post-K computer performance estimation tool. The effective parallelizm was 99.99954%, the parallelization efficiency was 89.142268%, and the parallelization efficiency when using all the nodes in the K-computer was 75.324899%. It has been confirmed that current framework can exhibit sufficient parallel performance on post-K computer. As for the tuning work, the problem of scheduling and the algorithm of loop division, SIMD conversion, compiler instruction were reviewed and further speeding up was achieved. The performance estimatied using the post-K performance evaluation tool was that have 12.8 times better performance per node than the K-computer, and it has approximately 25 times better performance in full nodes. However, in the RIKEN simulator, the performance improvement rate was slowing down. In the future, we plan to carry out further tuning and cause estimation using it. In the PIC method-based scheme of Euler structural analysis method, the algorithm was improved and a dynamic semi-implicit method was implemented. It succeeded in reducing the calculation time by up to 68.8% compared with the explicit method, and was able to make the prospect of applying this method to industrial application problems including vehicles. This method was applied to a thin plate structure targeting an automobile, and the solution was compared quantitatively with the solution by the commercial software (LS-Dyna) using the conventional method. As a result, it was confirmed that as the grid resolution was improved, the solution was asymptotically to the solution by the conventional method, and equivalent results were obtained when the grid was sufficiently fine. In the future, we will continue to conduct basic verifications and validation based on actual problems, and to improve basic functions by collaborating with industrial campanies, and will lead to the creation of results for 'post-K' computer project. On the dolphin kick analysis of sports CFD field as deployment of the framework to practical problems, basic verification of fluid force prediction acting on the swimmer in glide position, and direct and indirect 'free swimming simulation' have been conducted. The verification analysis showed that the framework developed in this research can predict phenomena in high accuracy. In the future, especially toward to the 2020 Tokyo Olympic Games, we will continue to work with related research institutes in order to create concrete results. On the DNS on RCEM, a validation for compression-expansion

process shows that the current method is conservative therefore it can be applied on engine simulation. Because fifth order accuracy is achieved by the current method, using DNS on RCEM becomes feasible. The result shows that the heat flux can be accurately captured and the heat transfer phenomena near the wall can be well described by using this framework. The future work is to apply this framework on more realistic engines to help the industries to use for the better product development. On the combustion simulation of RCEM, we have achieved accurate results by finer resolution and better piston motion profile comparing with last year. Due to the increasing of resolution, the total cell number is approaching 100M and can resolve more realistic flow and combustion field. For the improvement of physical prediction accuracy, we found the fact that a precise piston motion profile was vital on this problem. On the basic flow validation of gas turbine, it is shown that using the framework 'CUBE' to simulate the gas turbine is promising. The basic flow characteristics was compared with the well-established results of legacy code 'FFR', and confirmed that current framework showed reasonable results. We confirmed that the fine grid resolution is important to set accurate boundary condition and to capture clear turbulent structures which are important on combustion. We also have keep trying the study of different grid resolution, finer grid size, but due to the limitation of calculation resource in this year, it was difficult to get substantial statistical time for RMS evaluation. So, we are planning to proceed further investigation in next year, and toward the Post-K era, 10 billion gird, which can solved the whole turbulent scales without any model and much more accurate result are expected. The multi-scalar flamelet model for turbine combustor has been developed. The thermal properties and combustion source term are evaluated by the flamelet data and adopted in the flow calculation. In the future, we plan to continue the basic verification and validation of this method using the test with a simple burner and a simple spray test results and to deploy it to the application of the combustion problem of a realistic production turbine model. On the screw propeller simulation, we have conducted large-scale LES calculation around propeller using K-computer which is the highest-class performance computer in Japan for the purpose of investigating the feasibility of substitution of towing-tank test by large-scale numerical simulation. A detailed flow structure around blade was investigated and the knowledge about the influence of the grid resolution has been obtained.

[1]Nakahashi, K., "Building-cube Method for Flow Problems with Broadband Characteristic Length," In: Armfield S., Morgan R., and Srinivas K., editors. Computational Fluid Dynamics. (Springer, 2002, 2003), pp.77-81.

13.3 Research Results and Achievements

13.3.1 Empirical analysis using unified analysis framework CUBE

13.3.1.1 Verification analysis for WLTP in vehicle aerodynamics

In the field of automobile aerodynamics, establishment of evaluation method for the aerodynamic drag using comuputational fluid dynamics (CFD) on the fuel efficiency measurement is required in the new test method WLTP (Worldwide harmonized Light vehicles Test Procedure) [1] which has been enacted by Ministry of Land, Infrastructure, Transport and Tourism from 2018. It is recommended that the measurement conditions in WLTP be conditions involving tire-wheel rotation close to actual running conditions, and it is necessary to use an analysis method with moving boundaries also in CFD. Although commercial codes generally used in aerodynamic design are generally not easy to perform analysis of a real car model with tire rotation, they have problems in calculation time for unsteady flow and preparation time for grid generation work. The "CUBE" developed in this research is good at moving boundary problems, and can also be applied to tire rotation analysis on the real vehicle aerodynamics problems. In this research, the vehicle aerodynamics analysis has been performed repeatedly on the full-vehicle-model CAD data group of the aerodynamic base model and the improvement model provided by Suzuki Motor Corporation, Mazda Motor Corporation and Nissan Motor Motor Corporation, and then so far, efforts for the adjustment and improvement of the numerical method and calculation speed have been spent. In this fiscal year, further investigation has been conducted by obtaining measurement results of moving belt on wind tunnel provided by Honda R&D Co.,Ltd. A demonstration analysis by real vehicle CAD with tire rotation has been carried out, and it has been confirmed that the current framework have certain accuracy and workload to meet the requirement of WLTP [2]. Although CFD will be adopted for fuel consumption measurement for the first time in WLTP, it is expected that the aerodynamic drag value measured using CFD is not an absolute value but only a relative value due to a specification difference. In this subject, the aerodynamic drag difference ΔCdA m2 due to the specification difference is mainly evaluated.

Aerodynamic specification differences were calculated based on open grille and full model vehicle aerodynamic analysis for 6 different models. Fig. 13.1 shows the outline of the calculation model and the location of

the shape change due to the 6 specification differences. The grid resolution was about 6 mm, the number of calculation grid was about 100 million, and the calculation time was about 39 hours using the K-computer 617 node for unsteady-state calculation of 200,000 time steps (equivalent to about 2 seconds of physical time). This is about 2.8 times the calculation time of steady-state calculation, but at this time the geometry initialization process is applied every 0.8 degrees of tire rotation. If it can be reduced to about every 3 degrees, the calculation time could be reduced to about 28 hours. In addition, when the method of only the velocity boundary condition is applied, the calculation time was about 14 to 15 hours as in the steady condition. This is fast enough.

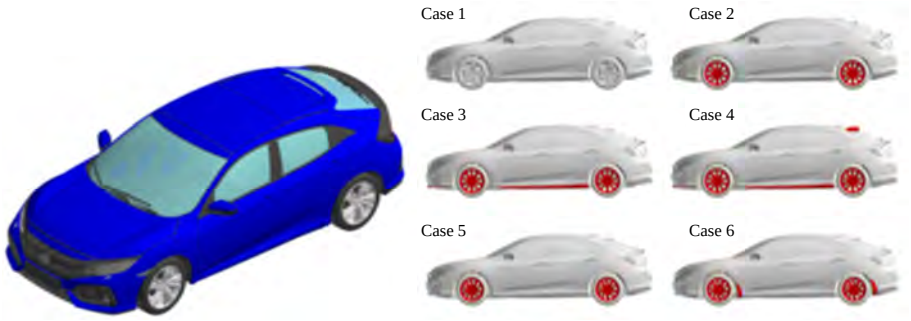

Figure 13.1: Full-vehicle geometry model for calculation (left) and six specifications of test cases (right).

The difference in the flow velocity distribution obtained is shown in Fig.13.2. In Case 4, a rear spoiler is added, and it can be seen that the wake shape is slightly expanded, but only a subtle difference in the flow field due to the specification difference was observed. The result of visualizing a typical time-averaged surface static pressure distribution and its difference from Case 1 is shown in Fig.13.3. However, the tire is shown as a 'blank' because the position changes from moment to moment. In Case 4, the distribution is largely different around the rear spoiler, but in Case 2, a small difference can be seen in the local area where the shape is different, and in the tire wake area and the vehicle's back surface induced by the change of the flow field. By measureing the difference of drag, it was comfirmed that all of these subtle changes have contributed to the difference in drag. In other words, it can be said that this framework could capture minute changes in flow due to the difference in shape of the details.

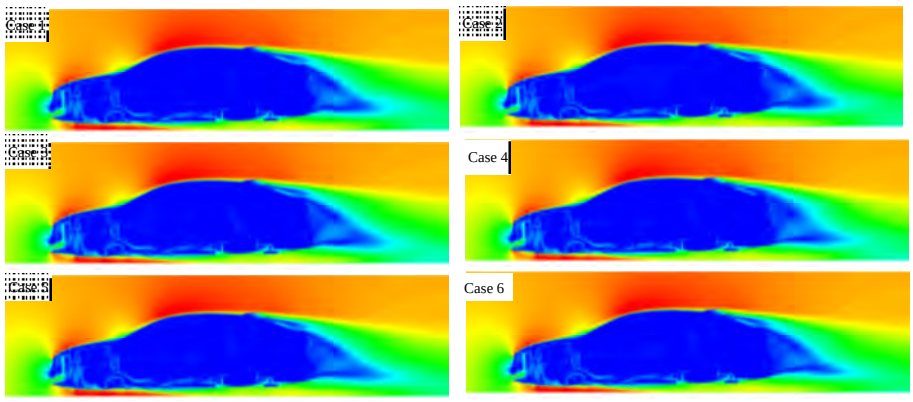

Figure 13.2: Profile of time-averaged dimensionless velocity magnitude in central section for all specifications, in stationary condition.

Fig.13.4 shows the drag coefficient (Cd value) and the delta drag (ΔCdA) by the difference of specification. The values are normalized by the experimental value. Under tire rotation conditions (Full Rotation), it was confirmed that the drag value can be predicted within the range of $DeltaCdA \pm 0.015$ which WLTP inspection requires. When only the flow velocity boundary condition is given (Velocity Boundary), the result shows a similar tendency but with a larger error. However, as shown in the flow velocity distribution of the tire center cross section in Fig. 13.5 and the wake structure of the total pressure iso-surface in Fig. 13.6, this two boundary conditions produced similar changes in flow from stationary conditions. Therefore, it has been found that the

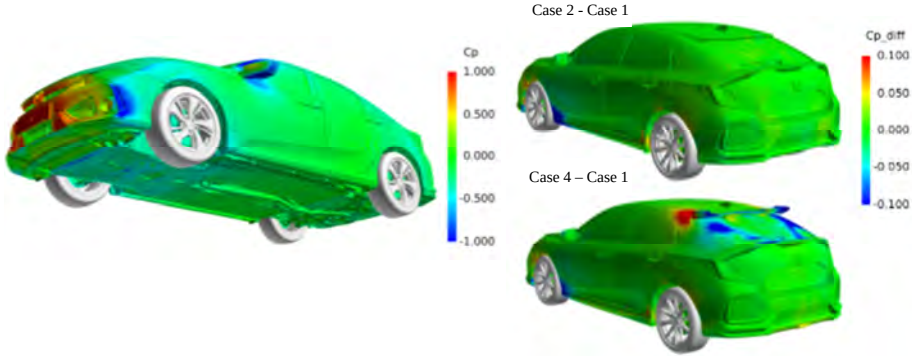

Figure 13.3: Surface pressure coefficient for case 1 in rotating boundary condition (left), difference of surface pressure coefficient from case 1 (right).

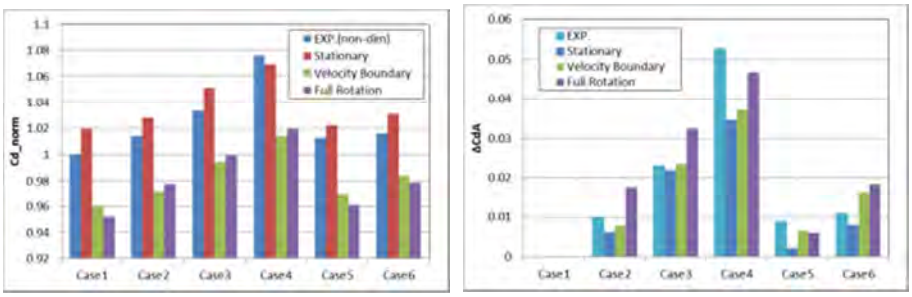

Figure 13.4: Predicted drag coefficients and drag delta for all specifications in three different boundary conditions.

flow velocity boundary condition can be a good alternative method considering that there is no calculation time penalty.

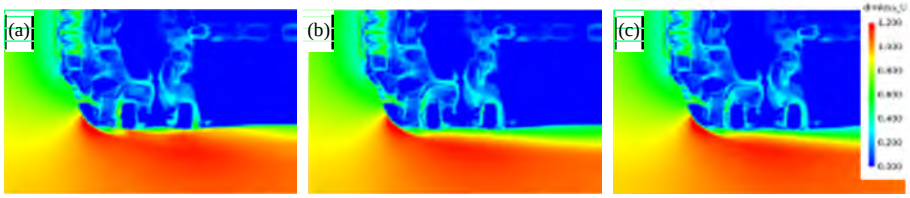

Figure 13.5: Profile of time-averaged dimensionless velocity magnitude in section parallel to ground passing through center of tire: (a) stationary condition, (b) velocity boundary condition, and (c) full rotation condition.

Thus, it has become clear that the difference in the application of the rotation conditions causes a significant difference in the flow field around the rotating wheel. In addition, it was found that the flow around the rotating tire interferes with the flow from the wake of the wheel arch, the flow from the engine room and the flow under the floor, and greatly affects the drag value. This is important fact in vehicle aerodynamics considering the actual driving conditions. Further, as shown in Fig. 13.7, it should be noted that the lift coefficient, which is generally difficult to predict, could reproduce the same tendency as the experimental value. However, there is still room for improvement in the prediction of the absolute value of the aerodynamic coefficients, and further demonstrations will be made in the future, and efforts will be made to make them approach closer to the true value.

13.3.1.2 Narrow-band aeroacoustics noise analysis around the engine hood of vehicle

Narrow band noise generated by automobiles is a quality problem, which requires a great deal of labor at a design process in automobile companies. The prediction accuracy is considered to be insufficient with the conventional

Figure 13.6: Total pressure field of front left wheel arch region: (a) stationary condition, (b) velocity boundary condition, and (c) full rotation condition.

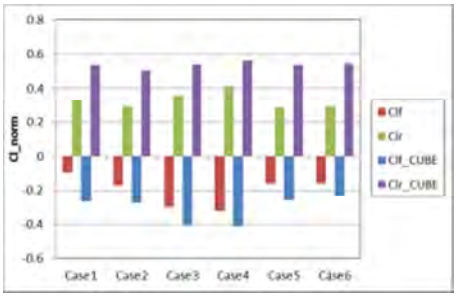

Figure 13.7: Predicted front and rear lift coefficients for all specifications in full rotation condition.

method including commercial softwares, and in this research, we have been developing a compressible unified solution framework of CUBE for the purpose of solving this issue to help automobile companies by reducing cost and shortening of development period. In the last year's efforts, the core technology was successfully developed, but in order to improve the calculation accuracy, it was in a state of waiting for allocation of resources for large scale simulation with high resolution. Therefore, in this fiscal year, we performed large-scale analysis as far as possible from given resources, and tried to predict narrow band nosise using a full vehicle model CAD data. This is a collaborative research with Suzuki Motor Corporation.

The calculation grid used has a minimum size of 0.2 mm which is concentrated in the tip gap (about 5 to 6 mm) as shown in Fig. 13.8 (left), so that it can supplement the acoustic feedback generated near the engine hood tip. The total number of calculation grids was about 2 billion. It has already been known that a hundred to several hundreds points are required to sufficiently resolve the feedback phenomenon, but due to the limitations of computing resources, this year's implementation was abandoned. The calculation was performed for about 50 hours using 13,086 nodes of K-computer. Fig. 13.8 (right) shows the pressure fluctuation component that occurs in the flow, and it can be seen that acoustic wave propagates in a circle shape from the tip of the hood is generated. It is understood that this is a completely different phenomenon compared to other noise components caused by fluid vortices around the vehicle body, but is a wave that does not appear without resonance due to acoustic feedback. The simulation results of sound pressure spectra at three measurement points near the hood are shown in Fig. 13.9. A characteristic peak is shown around about 2700 Hz, and some small peaks that are considered to be double wave components are also observed. Since the peak in the measurement was about the half frequency, it is assumed that this calculation result does not have sufficient resolution yet, but this calculation succeeds in capturing the acoustic feedback sound in the vehicle for the first time. It can be said that the results implies that this method is promising for the future application.

It is also essential to improve the computational grid resolution to improve the computational accuracy. Based on the resolution required for quantitative forecasting this fiscal year, we will continue to work on speeding up the calculation method toward the "post-K" computer and acquiring computational resources.

13.3.1.3 Multi-objective shape optimization analysis in vehicle aerodynamics

We developed a multi-objective optimization analysis framework in CUBE with the aim of efficiently optimizing aerodynamic performance in the early design stages of vehicle development process. In this framework, we used the multi-objective evolutionary optimization software CHEETAH [3] developed by and in cooperation with the Japan Aerospace Exploration Agency, and the shape morphing software MeshWorks [4] from Detroit Engineered

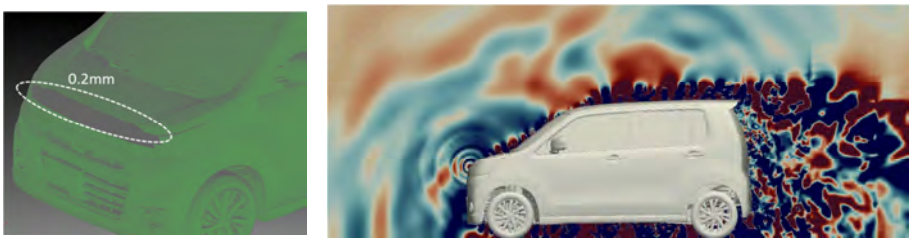

Figure 13.8: The computational grid overview (left) and the propagation of the pressure fluctuation (right).

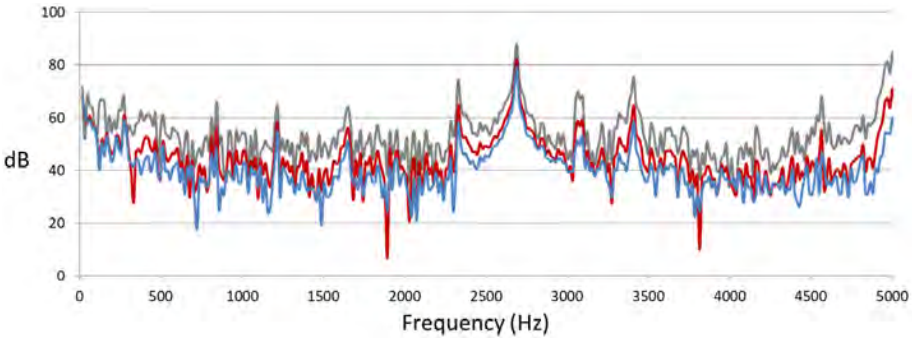

Figure 13.9: Sound pressure spectrum at each measurement point.

Products, Inc. of United States. This is a collaborative research with Mazda Motor Corporation.

Each software exchanges information by exchanging information via text-based file or parameter files. Although CUBE is based on hierarchical Cartesian grids, it can be shared with a single computational grid for multiple changing vehicle shapes, thus avoiding problems with computational grid generation and morphing. The target was a simplified sedan type vehicle model, and the objective function was the drag and lift when the vehicle was traveling straight and when the approaching flow had a yaw angle. The scale of optimization is about 5 generations for 18 individuals. This means that it is multi-objective optimization with 4 objective functions. Under these conditions, optimization calculations were performed using the developed framework and it was possible to obtain a solution that shows the same tendency as the actual design knowledge. It can be said that the validity of this framework could be confirmed.

Fig. 13.10 shows the Pareto solution obtained in this study. In this calculation, the number of generations is still small and it can not be said that convergence has been sufficient. We will continue calculations while securing necessary calculation resources. In addition, we are also considering including more detailed design changes such as narrowing the shape change width and incorporating radius deformation to increase the freedom of deformation.

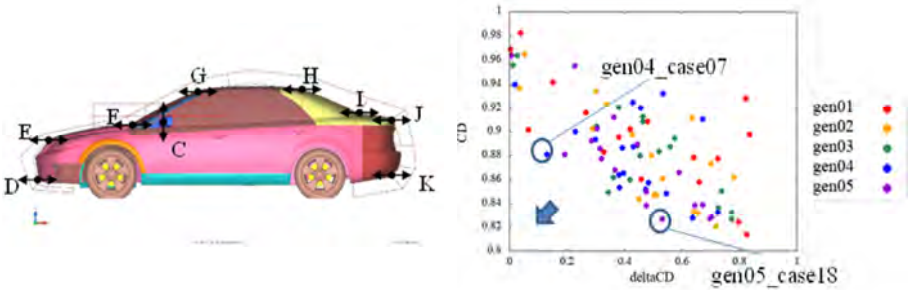

Figure 13.10: The geometry deformation parameters (left) and optimized results of Pareto solution on 5th generation (right).

13.3.1.4 References

[1] "About partial revision of notice etc. that defines the details of safety standards of road transport vehicles," Press Release of Ministry of Land, Infrastructure, Transport and Tourism and Minister of Economy, Trade and Industry, October 31, 2016.
[2] UNECE, Global Technical Regulations (GTRs), `http://www.unece.org/trans/main/wp29/wp29wgs/wp29gen/wp29glob_registry.html/`, [cited 1 May 2018].
[3] A. L. Jaimes, A. Oyama, and K. Fujii, "A ranking method based on two preference criteria: Chebyshev function and ϵ-indicator," Proceedings of 2015 IEEE Congress on Evolutionary Computation, 2015.
[4] MeshWorks web site, `https://www.depusa.com/meshworks/`, [cited 1 May 2018].

13.3.2 Speed-up and large-scale foundation application targeting post-K system

13.3.2.1 Large-scale in-situ visualization in demonstration vehicle aerodynamic analysis

In recent years, the data size obtained by the use of numerical analysis techniques in automobile development has dramatically increased, and as the scale of calculations has become large, visualization work has become difficult, and its speeding up has also become an issue. 'In-Situ Visualization' is a general term for technology that directly accesses and visualizes calculation data in memory in the HPC environment, and in this research we have implemented in-situ visualization technology [1] using Libsim (VisIt) [2], which is open source software. In this fiscal year, we carried out its computational scale up and tried to visualize the detailed flow structure with 4K resolution (3840×2160 pixels).

In vehicle aerodynamic design, not only evaluation of a two-dimensional cross section, but also visualization of a three-dimensional vortex structure around a vehicle body is often used to grasp flow characteristics. For example, visualization with a Q function, which is the second invariant of the velocity gradient tensor [3], and Lambda 2 [4], which is a vortex determination method with the sign of the eigenvalue obtained from the square sum of shear component and rotational component, are often used. At this time, since each vortex is represented as an isosurface, the number of polygons necessary for drawing increases, and it takes time and memory becomes large for rendering processing. Therefore, visualization may be difficult, especially in large-scale analysis using high-resolution computational grids. In in-situ visualization, distributed parallel processing is advantageous because it is not subject to memory usage constraints because the environment of flow calculation can be used as it is. Therefore, in this study, we tried to visualize and create 3D vortex structure by Q function against the flow around the vehicle body by 5.6 billion cells (minimum grid size about 0.76 mm). This is probably the world's largest example of vehicle aerodynamics visualization using real vehicles. Fig. 13.11 shows an example of the visualized image.

The 16,384 nodes (131,072 cores) of K computer were used for the calculation. The flow calculation is based on the result of the 'coarse' grid of 91 million cells as initial value, 10,000 time steps were executed until the flow field was well developed, and in-situ visualization was called once every 200 time steps of flow calculation. First, when visualization was performed using 840×840 pixels, the total calculation time was 14,397 seconds, and the in-situ 51 frame image generation time was 9,114 seconds. This corresponds to about 63% of the total calculation time. The amount of memory consumed at this time was about 5.6 GB at maximum per calculation node, including the amount of use by flow field calculation. Fig. 13.12 (a) shows an enlarged view of the vicinity of the door mirror of the obtained image. Since the resolution of the image is lower than that of the grid, some information is lost. Then, next, the result of performing visualization at 4K resolution is shown in Fig. 13.12 (b). Fine vortex structures corresponding to the grid resolution can be seen, and the appearance of interference between the flow separating from the A-pillar and the jet flow between the mirror and the side window is clearly captured. The image generation time was about 300 seconds for each frame, and the maximum memory consumption was up to about 5.9 GB per node. Although the total number of pixels was about 12 times, the image generation time was about 1.7 times and the memory usage was almost the same. From this result, it was confirmed that current method is sufficiently efficient as a visualization method for practical use.

In the future, we plan to deploy this method for empirical analysis, and improve calculation efficiency and support for users toward the 'post-K' computer.

13.3.2.2 Profile and tuning of compressible unified solution framework

Continuing from last fiscal year, we tried to improve single and parallel performance of compressible solver in K computer and to evaluate it using post-K computer performance estimation tool. The target problem was a simple cavity flow, using a scheme that assumed acoustic analysis. The MUSCL scheme and the Roe scheme

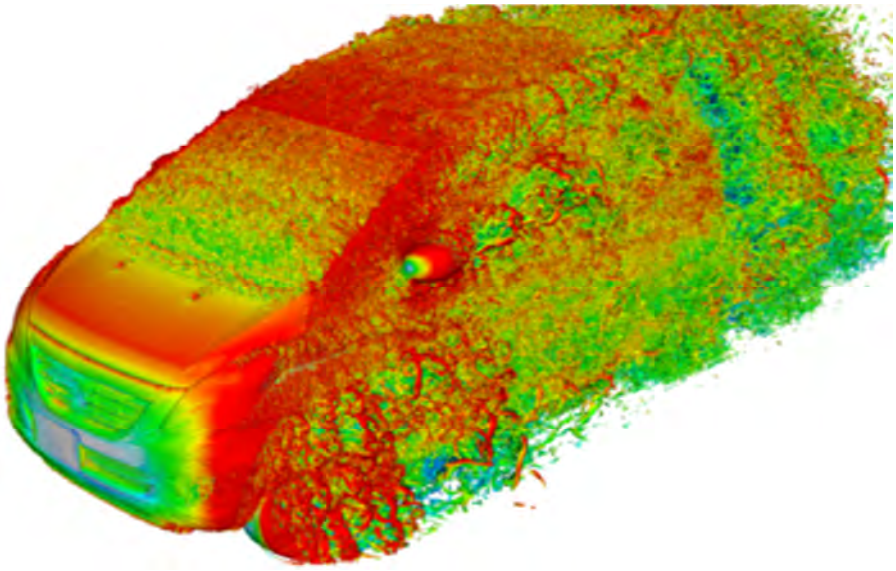

Figure 13.11: Visualization image of vortex structure around full vehicle body.

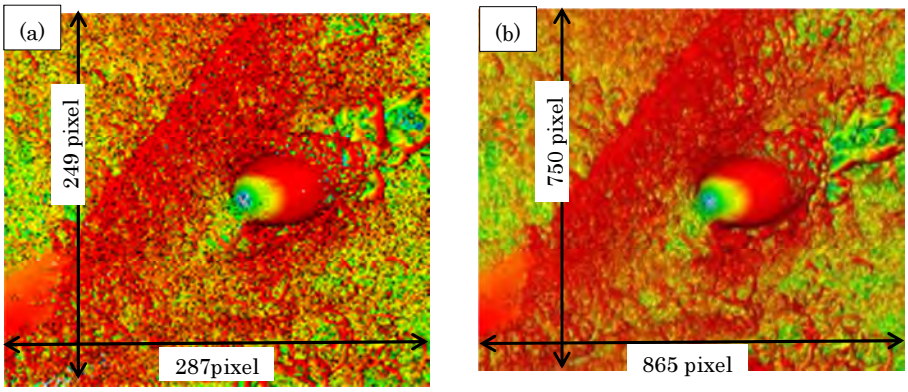

Figure 13.12: Comparison with pixel resolution, (a) low resolution (840x840 pixel), (b) high resolution (4K pixel).

were used to evaluate the flux at the cell face, and the third order Runge-Kutta method was used for the time integration, and the second order central difference scheme was used for the viscous term. First, the number of Cubes per node was fixed at 64, the cell was divided into 16 in each direction, and the parallel performance was measured by weak scaling up to the 32,768 nodes of K-computer. As a result, the effective parallelizm was 99.99954%, the parallelization efficiency was 89.142268%, and the parallelization efficiency when using all the nodes in the K-computer was 75.324899%. Parallel performance has been sufficiently secured even for large-scale computations with tens of thousands of nodes and hundreds of thousands of cores, and it has been confirmed that current framework can exhibit sufficient parallel performance on post-K computer.

In addition, based on the tuning work up to the previous fiscal year, the problem of scheduling such as waiting for floating point computation, and the algorithm such as loop division were reviewed, and further speeding up was achieved. As a result of software pipelining conversion by loop division in the convection term loop, about 8% performance improvement was obtained. Also, by clearly specifying the outermost loop of the structure array copy at the time of thread parallelization, the loop is speeded up from 8.61 seconds to 0.86 seconds. In addition, we have tried to separate loops (operations including the minmax function) that would inhibit SIMD conversion, to change memory access order of convection flux calculation routine, to promote SIMD conversion by specifying compiler instruction lines (!OCL NOALIAS etc.), etc. As a result of performance estimation using the post-K performance evaluation tool, it is expected to have 12.8 times better performance per node in the

post-K than the K-computer, and it was confirmed that it has approximately 25 times better performance if parallel performance is combined. The results are shown in Table 13.1. However, in the performance estimation using the RIKEN simulator, the performance improvement rate is slowing down. In the future, we plan to carry out further tuning and cause estimation using the RIKEN simulator.

Table 13.1: Results of performance evaluation and tuning of compressible solver.

Source ver. & Env.	Performance [GFLOPS]	Peak effic. on dble	Mem. through put [GB/s]	SIMD inst. ratio	Num. of instr. [GFLOP]	Wall time [sec]
ASIS + K-computer ver.180820	18.29	14.29%	7.32	1.89%	1405.05	76.81
+ eval. tool	234.59	8.49%	199	45.08%	5616.39	23.94

13.3.2.3 References

[1] Keiji Onishi, Niclas Jansson, Rahul Bale, Wei-Hsiang Wang, Chung-Gang Li, Makoto Tsubokura, "A Deployment of HPC Algorithm into Pre/Post-Processing for Industrial CFD on K-computer," SC17 - International Conference for High Performance Computing, Networking, Storage and Analysis, Denver(CO), 2017.
[2] VisIt web site, `https://wci.llnl.gov/simulation/computer-codes/visit/`, [cited 1 Oct. 2018].
[3] Tanaka, M., Kida, S., "Characterization of vortex tubes and sheets," Phys. Fluids A, Vol.5, pp.2079-2082, 1993.
[4] Jeong, J., Hussain, F., "On the Identification of a Vortex," J. Fluid Mechanics, Vol.285, pp.69-94, 1995.

13.3.3 Verification analysis of thin plate structure using Euler structure analysis framework

13.3.3.1 Development of dynamic semi-implicit method in structure-fluid unified PIC scheme

In this study, in order to cope with large-scale structural analysis problems that reproduce detailed shapes that are difficult to calculate using conventional methods, a unique the Euler-type structural analysis method with PIC (Particle in Cell) scheme, which is a type of particle method, coupled with fluid analysis have been developed in a unified solution framework. In this fiscal year, improvement of the algorithm and implementation of a dynamic semi-implicit method has been conducted.

Following last year, we adopted the Crank-Nicholson method for time integration in the PIC scheme and developed an enhanced scheme as a semi-implicit method. This is an essential technology in practical problems in order to avoid severe time increment constraints due to pressure oscillation. As a result, we confirmed the numerical validity of the solution in the fluid-structure interaction (FSI) benchmark problem, and succeeded in reducing the calculation time by up to 68.8% compared to the explicit method (Fig. 13.13). This made it possible to apply the method to industrial application problems such as vehicle-structure analysis.

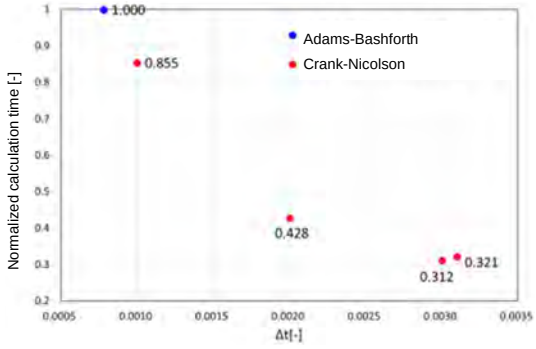

Figure 13.13: Comparison of calculation time (explicit vs. implicit scheme).

In addition, the final target of this subject is a thin plate structure such as a vehicle body, and it is necessary to confirm that it functions as an alternative to conventional shell elements. Therefore, this method was applied

to a benchmark problem for basic structural analysis, such as cantilever deformation (Figs. 13.14 and 13.16), flat plate deformation (Figs. 13.15 and 13.17), and benchmarks for complex plate structures of Ko [1] et al. (Fig. 13.18), then it has been confirmed its validity. In the analysis of these three benchmark problems, the time history of the displacement of the evaluation point was compared quantitatively with the solution by the commercial software (LS-Dyna) using the conventional method. As a result, it was confirmed that as the grid resolution was improved, the solution was asymptotically to the solution by the conventional method, and equivalent results were obtained when the grid was sufficiently fine. In the future, we will continue to conduct basic verifications and validation based on actual problems, and to improve basic functions by collaborating with industrial campanies, and will lead to the creation of results for 'post-K' computer project.

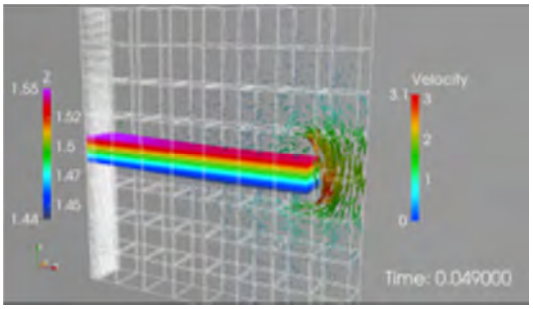

Figure 13.14: Gravity-driven deformation and velocity field of cantilever problem.

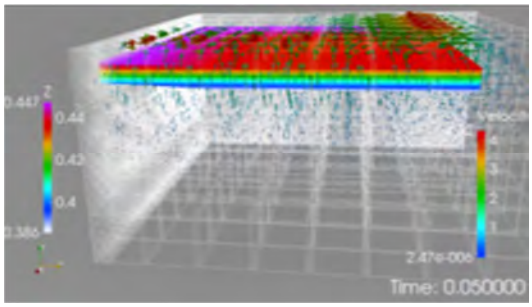

Figure 13.15: Gravity-driven deformation and velocity field of plate problem.

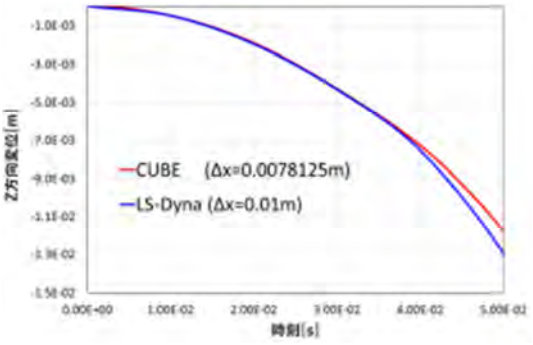

Figure 13.16: Comparison of displacement history of tip of cantilever.

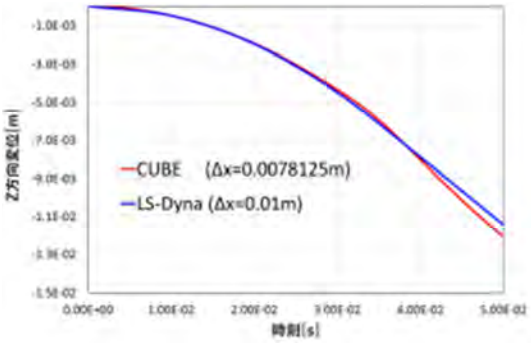

Figure 13.17: Comparison of displacement history of tip of plate.

13.3.3.2 Development of geometric boundary condition for complexed shape and validation of automobile white body stiffness analysis

This is a collaborative research with Suzuki Motor Corporation. In Euler-type solution, it is difficult to give boundary conditions because the nodes of the calculation grid and the object boundaries do not coincide. Therefore, it is necessary to devise a practical method of applying geometric boundary conditions in order to analyze a detailed complex shape such as a vehicle body using FSI analysis method based on PIC developed in this research. So, we developed the method of giving geometrical boundary condition based on the immersed boundary method and made it applicable to detailed complex shape. This is a method of reproducing a rigid body jig by providing displacement fixing or velocity boundary conditions.

Stiffness analysis of the vehicle white body based on the real vehicle CAD data provided by Suzuki Motor Corporation was performed using this method, and its validity was examined. In this example, the structure has the Young's modulus and mass density of the steel, and the fluid region is set as the viscosity and mass density

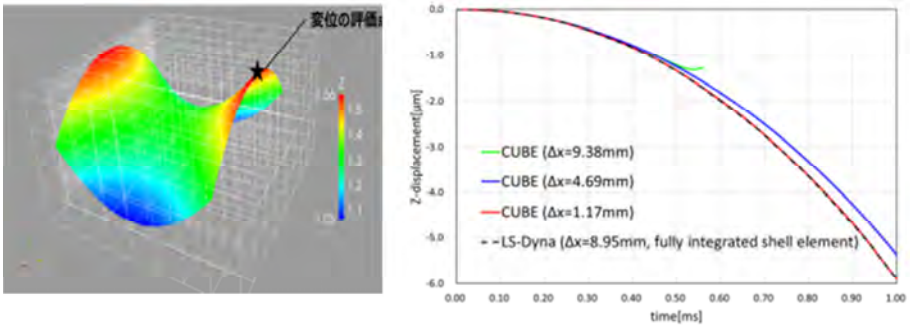

Figure 13.18: Displacement time history (right) of the evaluation point (left) of thin plate structure.

of air at 20°C. The grid resolution was about 1.86 mm, and the total number of cells was about 460 million, and 14,000 nodes of K-computer were used for the calculation. Fig. 13.19 shows a comparison of the Mises stress distribution between CUBE and LS-Dyna, one of the commercial structural analysis codes widely used in the automotive industry, and it can be confirmed that the qualitatively good Mises stress distribution has been obtained. In addition, as shown in Fig. 13.20, it has been proved that this method can significantly reduce the time required for vehicle structural simulation. This is probably the world's first successful example of stiffness analysis using Euler structural analysis method based on Cartesian grids in a three-dimensional model based on sheet steel of a vehicle.

Currently, we are preparing a grid resolution of 0.93 mm (total number of cells is about 2 billion), and are waiting for allocation of computational resources. In the future, in addition to accuracy confirmation by large-scale analysis, we will continue to work on development and improvement to improve analysis accuracy and modeling of 'spot welding' to improve quantitativeness.

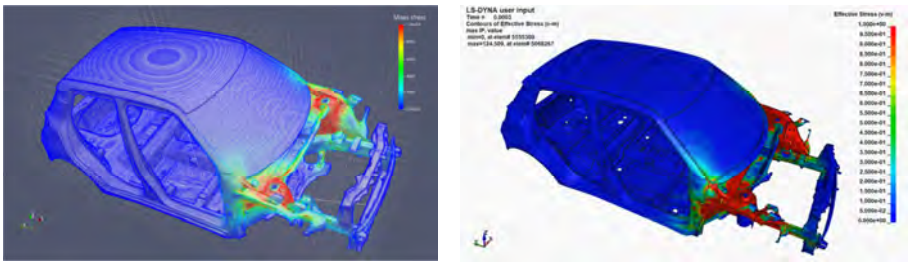

a) CUBE b) LS-Dyna

Figure 13.19: Comparison of Mises stress distribution: a) CUBE and b) LS-Dyna.

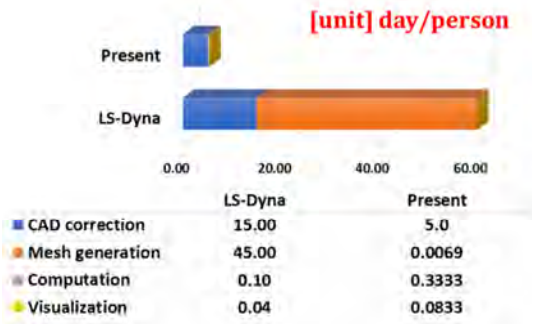

	LS-Dyna	Present
CAD correction	15.00	5.0
Mesh generation	45.00	0.0069
Computation	0.10	0.3333
Visualization	0.04	0.0833

Figure 13.20: Comparison of turnaround time of stiffness analysis of white body.

13.3.3.3 References

[1] Yeongbin Ko, Youngyu Lee, Phill-Seung Lee, Klaus-Jurgen Bathe, "Performance of the MITC3+ and MITC4+ shell elements in widely-used benchmark problems," Computers & Structures, Volume 193, pp. 187-206, 2017.

13.3.4 Deployment of simulation framework CUBE to complex unified multi-physics coupling practical problems

13.3.4.1 Sports CFD – underwater undulatory swimming hydrodynamics

The underwater undulatory swimming (UUS) is a swimming mode used by swimmers in competitive swimming. This mode of swimming is sometimes referred to as dolphin kick style of swimming. As the name suggests the dolphin kick style is similar to the subcarangiform swimming kinematics observed in dolphins and cetaceans. The particular form of the swimming kinematics involves body undulations, normal to the swimming direction, that progressively increase in amplitude from anterior to posterior. Typically, the amplitude at the anterior end, i.e in the stretched out hand region of the swimmer, is negligible which increases to a finite value at the posterior end, i.e. near the ankle and feet. While the undulations are symmetric in dolphins, due to asymmetric flexure of human limbs, the undulations are as symmetric in humans.

In order to understand the mechanics of human swimming, it is essential to accurately model the flow mechanisms of the coupled phenomena that is undulatory swimming. Locomotion by swimming is a coupled problem wherein the undulations of the swimmer affect the motion of the fluid, and the interaction of this moving fluid with the undulating swimmers gives rise to the swimming motion. Consequently, the accuracy of modeling this dynamic two way interaction between the fluid and the swimmer is important to capture the correct swimming motion. Furthermore, accurate representation of the undulatory kinematics of the swimmer is key to extract accurate results of the flow solver. In this work we present preliminary results of free swimming simulations of underwater undulatory swimming. Here, the term 'free swimming simulation' implies a simulation in which, given the kinematics of undulations of swimmer, the swimming motion along with the swimming velocity of the swimmer are computed as a solution of the simulation. Prior to presenting the free-swimming simulation results, we validate our solver by carrying out simulations of flow around a swimmer in a glide position. After validating the solver for stationary glide simulations, we further validate the solver for free swimming simulation by comparing the swimming speed of our results with experiments. We used the data gathered on swimmers from the laboratory of biomechanics of Chukyo University. We obtained the position of the joints of motion (tip of the fingers, wrists, elbows, shoulders, trunk, waist, thighs, knees, ankles and tip of the toes) of the swimmers during front-side UUS at maximum speed. The motion being almost exclusively 2D, only the vertical and the horizontal coordinates were needed. The stl files of the geometry of swimmer body were also obtained using a 3D scanner.

First, on the validation of swimmer in glide position, the experimental results of Vennell et al. [1] which showed that drag forces on a mannequin at different inflow velocities (from 0.1 m/s to 2.5 m/s) and at different depths (from 0.0 m to 1.0 m) was refered to cpmpare with our numerical results. In this study, we are not considering the wave drag on the surface. Thus, we will only compare to the measurements made at the biggest depth. Indeed, Vennel's study showed that the wave drag is negligible at a depth of 0.8m. So, we compared results corresponding to measurements at depth of 1m. In order to compare the simulation results to the experimental results, a swimmer geometry that had a size close to the one of the mannequin and that stood still in gliding position was chosen. The 5 cases of different inflow velocities (0.2, 0.6, 1.0, 1.2, 2.0) m/s has been conducted and the drag force was evaluated. We kept the same mesh for every simulation. The minimum cell size for those simulations was 3 mm, the number of calculation grid was 103 million. The 512 nodes of K-computer were used, and typically took 48 hours for calculation. The fact that they do not have precisely the same size body geometry was not an issue since the swimmer would not have had the exact same glide position as the mannequin. We simply looked at the evolution and the order of magnitude of the curve of drag force in function of inflow velocity. We have compared our results not only with Vennell, simulation results of Sato et al. who use a body fitted grid (BFC) approach [2], and the results of Mittal et al. who used Cartesian grid approach [3].

The results of our simulations along with data from Literature are shown in Fig. 13.21. It can be seen that the overall trend observed in the results of Vennell. is captured reasonably well, but the magnitude of the value of the drag forces differs from the experimental data. But, it appears that the overall general trend of simulation results of literature is that the simulation drag values are consistantly higher than Vennell's experimental data.

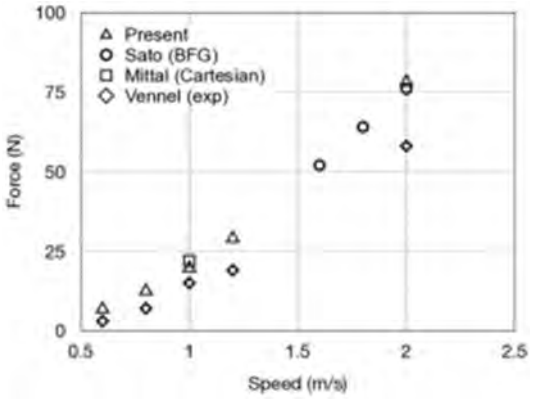

Figure 13.21: Drag forces on swimmer in glide position plotted as a function of flow speed. The results of the present work are compared with the date from literature [1,2,3].

Our results show very good agreement with the drag values of Mittal's results at flow speed of 1 m/s, and with the result of Sato for flow speed of 2 m/s.

Next, the validation of swimming speed has been conducted by comparing with the experimental data. Swimming speed can be evaluated directly or indirectly using the present framework. For the direct method the self-propulsion algorithm is used to carry out simulations in which the swimming kinematics are input to the flow solver and the solver dynamically evaluates the swimming speed through strong two-way coupled FSI formulation. Therefore, the swimming speed of swimmer in UUS motion was directly evaluated by our framework comparing with experimentally measured swimming speed of swimmer in the video capture data. The obtained flow field results is plotted in Fig. 13.22, and swimming speed is plotted in Fig. 13.23 (left) where we find that our result show satisfactory agreement with experimental result.

While an indirect method, the non-self propulsion algorithm is used to carry out simulation in which the swimming kinematics are input to flow solver with swimmers held at fixed location and the force generated by the swimmer is evaluated as output. If the ambient flow is stationary then the generated force will be proportional to the swimming velocity. If the swimmer is placed in a flow (opposite to the intended swimming direction) then the force generated by the swimmer will decrease. As the flow speed is increased the force will correspondingly decrease until the flow velocity is equal to the swimming velocity. At which point the mean force generated by swimmer will be 0, i.e. during steady self-propulsion the mean force on the swimmer is 0. Therefore, the flow at which the thrust generated by the swimmer is 0 would be the swimming speed. If the speed is increased even further then the swimmer no longer generates any force, but experiences net drag induced the flow. To this end, we carried out a set of 3 simulations with the flow speeds 0m/s, 1m/s and 2m/s in a direction opposite to the intended swimming direction. The force acting on the swimmer is presented in Fig. 13.23 (right). When the flow speed is 0 and 1m/s, the net force of interaction between the swimmer and the fluid is positive, which indicates the force exerted by the swimmer on the fluid. At flow speed on 2m/s, net force is negative implying the nature of the force has changed. The magnitude of the force indicated the force of the fluid acting on the swimmer. The sign change of the force in highlighted in the figure and it occurs at flow speed of 1.56m/s, which is equivalent to the swimming speed. This shows good agreement with the experimentally measured swimming speed of 1.63m/s.

In the future, especially toward to the 2020 Tokyo Olympic Games, there is a need for an effort to put the framework developed in this research into actual competition training. We will continue to work with related research institutes and the national training team of Japan in order to create concrete results.

13.3.4.2 References

[1] Vennell, R., Pease, D. and Wilson, B., "Wave drag on human swimmers," Journal of biomechanics, Vol.39 no.4, pp.664-671, 2006.

[2] Sato, Y., and Hino, T., "CFD simulation of flows around a swimmer in a prone glide position," Japanese Journal of Sciences in Swimming and Water Exercise," Vol.13, no. 1, pp.1-9, 2013.

[3] Von Loebbecke, A., Mittal, R., Mark, R. and Hahn, J., "A computational method for analysis of underwater dolphin kick hydrodynamics in human swimming," Sports Biomechanics, Vol. 8, no. 1, pp.60-77, 2009.

Figure 13.22: Instantaneous vortex structure visualization of flow field around the swimmer under the UUS motion.

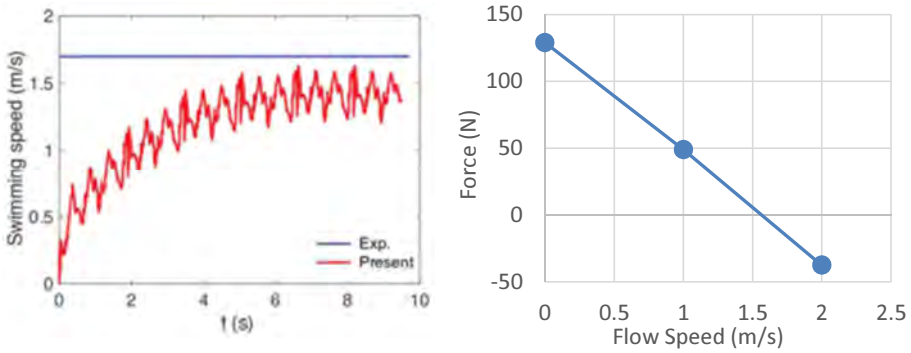

Figure 13.23: (left) A comparison of the swimming speed evaluated from the our simulation, of a swimmer in UUS, with experimental data. (right) Evaluation of swimming speed through three separate non-self propulsion simulations with uniform flow.

13.3.5 Strategic development and deployment of industrial software for the construction of digital engineering test beds

The objective of this research project is to realize large scale simulation in combustion simulation of automobile engines, gas turbines and in flow simulation of turbo-machinery by dramatically increasing the resolution of computational grid to be independent of empirical physical model or physical testing on the analysis. R-CCS promoted the activity named 'Forming the next-generation digital engineering base center on the manufacturing test bed' from last year, the research and development are being conducted. This issue is based on the knowledge obtained from the development and deployment for automobile engines carried out last year, it aims to expand the findings into the gas turbine combustion field and make a new entry into the turbo machine field, where R-CCS software is currently lacking. This is a developmental continuance activity to expand into the new field of combustion and strengthen the industry-academia collaboration.

The simulation framework has been developed through past 3 years coupling multi-physics problems such as thermal / fluid / chemical reaction / spraying on the same computational grid. In this fiscal year, in cooperation with automotive companies successively, a high-accuracy and large-scale empirical simulation using the K- computer is conducted as the final phase for commercialization. In addition, based on the reactive fluid simulation technology obtained here, it will be newly expand into the WG activity which is launched within the next-generation CAE consortium for combustion systems launched in 2018, and is promoted in cooperation with industry members.

13.3.5.1 Direct numerical simulation on piston-driven flow inside a cylinder

The Rapid Compression Expansion Machine (RCEM) is a large visualization experimental facility for engine combustion analysis based on the concept which has of an observation window, a high injection pressure, and

a high in-cylinder pressure. Spraying and combustion can be observed from the side from the rectangular combustion chamber. For the RCEM simulation, the numerical scheme which can treat the compressible flows at low Mach numbers and complex geometry is necessary. The purpose of this study is to develop a framework for solving this kind of simulation. In order to achieve high accuracy, LMRoe [1] with a higher order reconstruction (5th order) is adopted. A robust interpolation with the feature of easy implement is proposed to well-conditionedly assign the appropriate boundary condition for the compressible flow. The result shows that the current IBM is conservative so it can be used on the compression and expansion processes such as engines. Besides, because of using the high order reconstruction scheme, the direct numerical simulation becomes feasible. This is a collaborative research with Mazda Motor Corporation and Kyoto University.

In order to develop a framework for RCEM simulation, following the previous work in [2] and extending to the moving geometry, an IBM shown in Fig. 13.24 is developed.

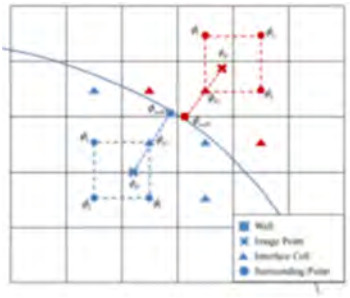

$$\phi_{IC} = \frac{\sum w_{ss}\phi_{ss} + \phi_{fix}}{2\sum w_{ss}\phi_{ss} - w_{IC}} \quad \text{Dirichlet condition} \quad (1)$$

$$\phi_{IC} = \frac{\sum w_{ss}\phi_{ss}}{\sum w_{ss} - w_{IC} + \varepsilon} \quad \text{Neumann condition} \quad (2)$$

Figure 13.24: The configuration of the IBM.

Where ss is the surrounding point which is located on the same side with IP. The current IBM can tr at the zero-thickness wall and moving geometry with high accuracy.

An adiabatic compression-decompression process inside a cylinder is conducted to estimate the conservation of the current IBM. The schematic of the physical model is shown in Fig. 13.25 (a) and the cell size is 0.8mm. When the piston reaches to the top dead center (TDC), the gap between the piston and upper wall is just 6.33mm and it can be only accumulated less than 8 grids. Under this situation, how to maintain the accuracy to keep the conservation becomes more severe for IBM due to the drastically decreasing of the resolution. Fig. 13.25 (b) shows the time history of the density and pressure at the point (0,0,0). The result is in excellent agreement with the distribution of the theoretical result which is an isentropic compression-decompression process for an ideal gas. Based on the results, it can be known that the IBM developed in this study is conservative and also available for the moving geometry.

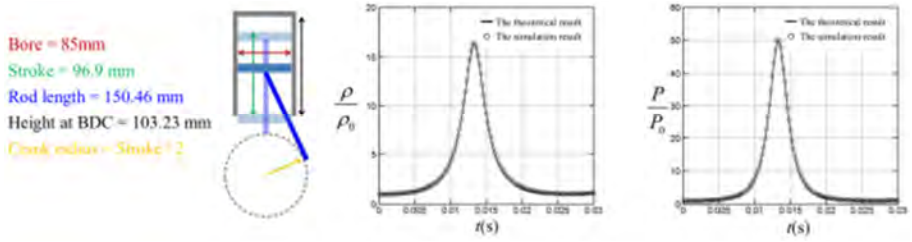

Figure 13.25: The adiabatic compression-decompression process of the engine.

The calculation condition of direct numerical simulation of RCEM is shown in Fig. 13.26. The Reynolds number was 14 thousand based on diameter of cylinder, and the CFL number for time step was over 138 for initial stabilization and 4 for main calculation. The finest grid size was 0.0125 mm and coarsest grid around cylinder was 0.4 mm, which has a Hierarchical grid system. In order to achieve the DNS accuracy, the extremely fine resolution (0.0125mm) is located on the left wall at the head part. Initial grid had a number of cubes of 174,918 with 716 million cells which is world largest level engine simulation with motion. But, it cost over 180 hours using 5 thousand nodes on K-computer. Then, we have developed the grid reduction functions which can suppress the region of unphysical space volume which is outside of the measurement region. This wasted a calculation time but it commonly happens on Cartesian grid system. Then, the number of cube became 99,994

and total number of cells was 409 million. The time increment was 5.0×10^{-6} which is extremely large by the benefit of using Solution Limited Time Scheme (SLTS) developed in this study. With the SLTS, the CFL number of the time step can be larger than 100 to drastically save the computational time. In the final case, total calculation time was 100 hours with 3,123 nodes on K-computer.

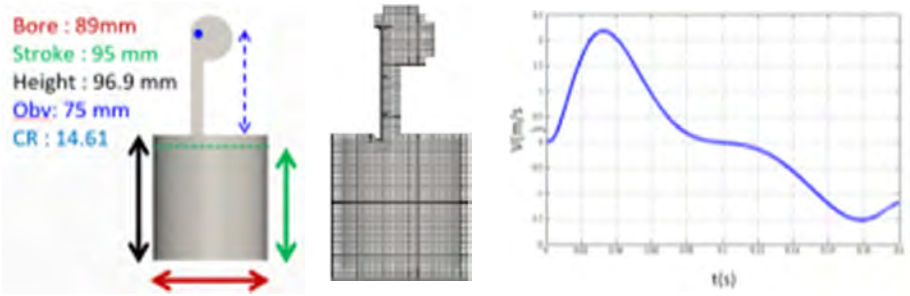

Figure 13.26: RCEM simulation conditions.

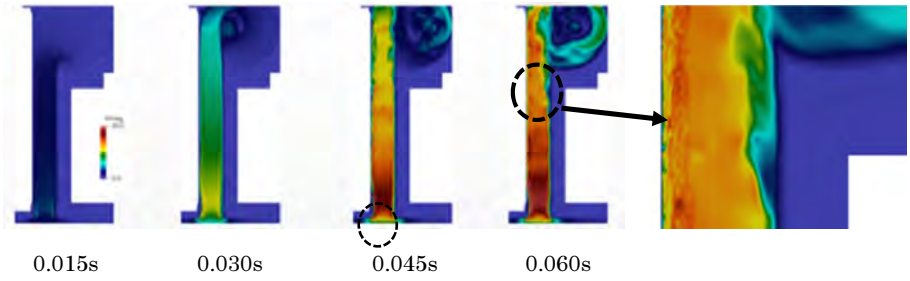

Figure 13.27: The temporal variation of the velocity magnitude.

Fig. 13.27 shows the velocity variation from 0.015s to 0.06s. It can be seen that the velocity transition happens around 0.045s. The flow is compressed by the motion of the position and the sharp corner at the bottom of the head causes the flow reattach on the wall. When the speed become higher and higher, the transition starts to appear. At 0.06s, after the transition, the flow field near the wall becomes turbulence and the turbulent boundary layer captured by the current numerical scheme is obviously shown. Fig. 13.28 shows the density variation from 0.015s to 0.06s.

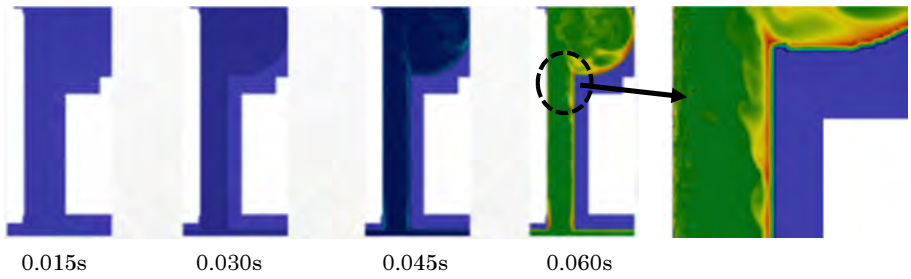

Figure 13.28: The temporal variation of the density.

From the density field, the transition is also happens around 0.045s. However, compared with the velocity turbulent boundary layer, the thickness is smaller. It also means that the resolution for capturing the temperature layer should be finer than that of the velocity boundary layer. The temperature, heat flux and pressure variation with time are shown in Fig. 13.29.

The total duration of time is around 0.015s and the calculation stops because of running out of CPU hours of this project. For the temperature, before 0.07s, the result is in good agreement with the experimental result. After 0.07s, the distribution is larger than the experimental data around 20%. A possible reason is that the

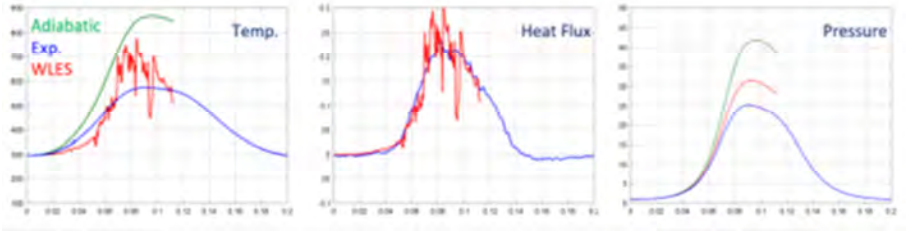

Figure 13.29: The temperature, heat flux and pressure variation with time.

current simulation adopts the isothermal condition, however, in real experimental setting; it's very difficult to reach completely identical condition as the simulation. For the heat flux, note here, the estimation of the heat flux ($q_w = -k\partial T/\partial x$) here is using DNS without any wall and turbulence model. As authors known, this is also the first time using DNS to estimate the heat flux all over the world. The result is in acceptable agreement with experimental result. The pressure variation also shows the same trend as temperature and heat flux. According the result, using DNS for RCEM simulation to estimate the heat flux becomes feasible.

Because of fine resolution, the phenomena caused by the transition can also be captured. Fig. 13.30 shows the velocity magnitude contour for several different time steps. At t=0.03s, there is a fluctuation

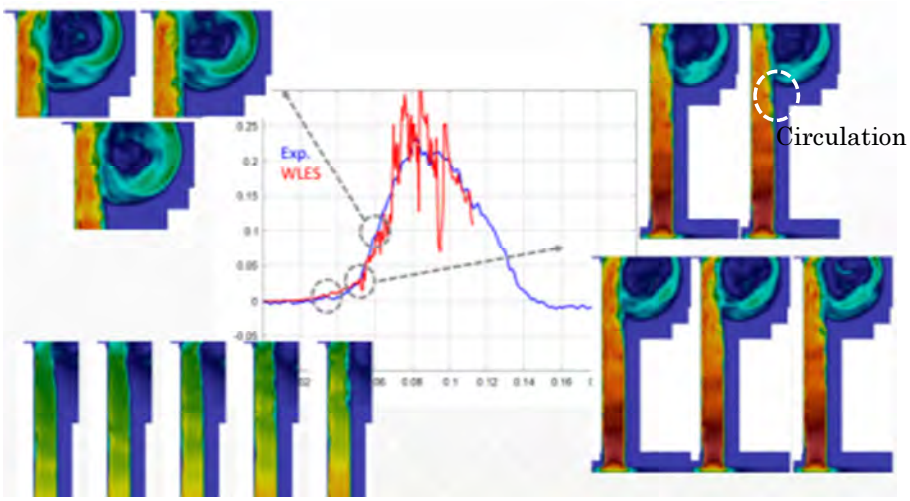

Figure 13.30: The series of temporal velocity magnitude field in different locations.

of heat flux. This fluctuation can be attributed to the starting point of the transition shown in the velocity magnitude contour. After the transition, the heat flux starts to obviously increase. At t = 0.05s, because the circulation front will bring the cold air to hit the heated temperature boundary layer, the heat flux will suddenly increase after t = 0.05s. At t = 0.06s, because the high temperature boundary layer is formed again, the fluctuation of the heat flux appears. The above important phenomena, which can help people to understand the heat transfer inside RCEM, can only be captured and described by using current framework.

In the current project, an IBM for using DNS on RCEM is developed. A validation for compression-expansion process shows that the current method is conservative therefore it can be applied on engine simulation. Because fifth order accuracy is achieved by the current method, using DNS on RCEM becomes feasible. The result shows that the heat flux can be accurately captured and the heat transfer phenomena near the wall can be well described by using this framework. The future work is to apply this framework on more realistic engines to help the industries to use for the better product development.

13.3.5.2 Engine combustion detailed analysis on RCEM

The combustion physical phenomena under the piston motion have been evaluated using this frame work 'CUBE'. The geometrical model is indicated in Fig. 13.31 (a). The piston is at the bottom of the chamber, and

moves up for the compression process. Fig. 13.31 (b) shows the detail spark plug, which is at the right part of the chamber. At the top of the chamber, an injector for fuel spraying is located. The calculation conditions is listed in Table 13.2. The initial pressure of 101.3 kPa is set and piston moves from Bottom Dead Centre (BDC) to Top Dead Centre (TDC). The fuel species is premix iso-octane/air and the equivalence ratio is equal to 1.0.

In order to simplify the chemical reaction calculation, only the main products of combustion are taken into consideration. The total species used are C8H18 (iso-octane), O2, H, O, OH, H2O, H2, CO, CO2 , NO and N2. The thermodynamics properties and transport coefficients are obtained from 'Cantera' of an open-source chemical dynamics solver which is part of this framework.

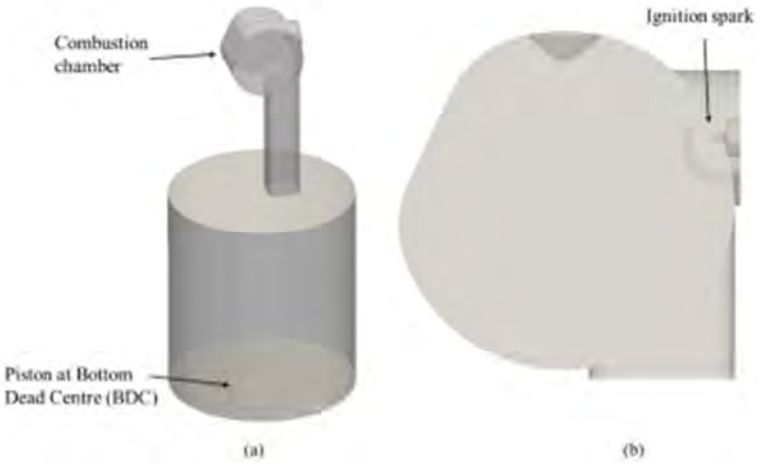

Figure 13.31: RCEM geometry with combustion chamber and moving piston.

Table 13.2: Calculation conditions.

Fuel	Initial temperature(K)	Initial pressure(kPa)	Equivalence ratio	Ignition time(ms)	Compression ratio
Iso-octane	300	101.3	1.0	80	13

The flow field of whole chamber is calculated, the total grid number is around 96M with 0.2mm, twice finer than last year, for finest grid. Since the fully compressible flow solver is adopted, according to the CFL number we can decide the time step size that $\Delta t \leq CFL \times \Delta x/c$. To make the simulation stable, usually the $CFL = 0.3$ is chosen, and c is the speed of sound. However, in combustion simulation, the speed of sound is not constant and varied with temperature by the expression of $c = \sqrt{\gamma RT}$, where is the specific heat ratio and R is the gas constant. For the combustion of iso-octane/air with equivalence ratio equals to 1.0, the temperature will be increased to about 3000K and makes the speed of sound also be increased to three times compared with ambient temperature($\simeq 300K$). Finally, the time step size of 6.25×10^{-8} s is used for the combustion part.

For the motion part of RCEM, the piston is moving from BDC to TDC, and then the ignition and combustion are started. In this situation, for the computation before combustion, there are only 3 species (N2, O2 and C8H18) solved by the transport equations without G equation because there is no flame, The time step size before combustion is 1.25×10^{7} s since the final temperature after piston compression process is about 700K. On the other hand, 11 species and one more G equation are solved after combustion, and the time step size is 6.25×10^{-8} s.

The total physical time is 0.1s, and the total time steps is 640 thousands (without combustion) plus 320 thousands (with combustion) steps. All the thermodynamic properties and transport coefficients are dependent of temperature and species, which are calculated from Cantera module. First, the premixed combustion phenomenon with piston motion is investigated. From t=0 to t=80ms, the piston moves from BDC to TDC as shown in Fig.13.32 which is obtained from an experimental data. The piston profile is important in simulation because in compressible flow, the density is changed due to the volume change between each timestep. At first, the preliminary test with low order curve fitting is used to simulate the piston motion profile, but the density and compression ratio results are smaller than experimental data, which lead to an inaccurate combustion results. In Fig. 13.33, although the piston profile has only small difference between experimental and curve fitting results, the density difference becomes larger and larger.

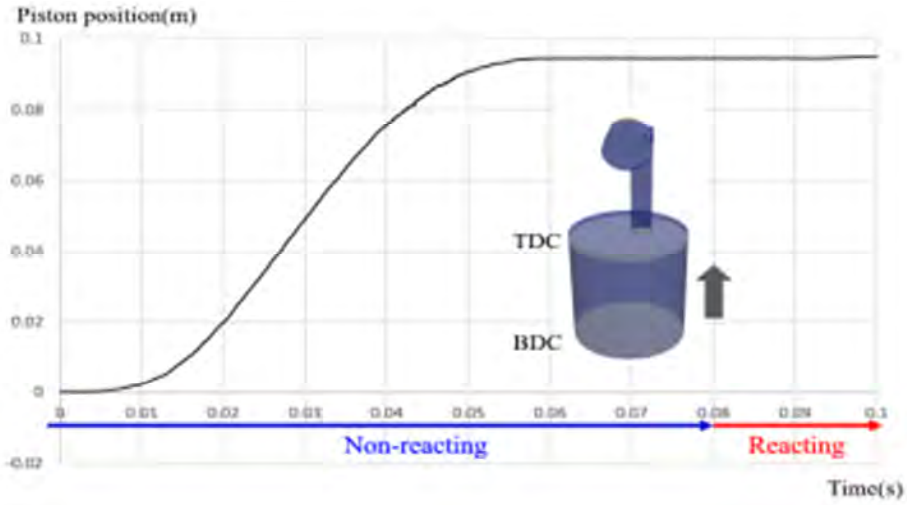

Figure 13.32: Piston motion of experimental data of RCEM.

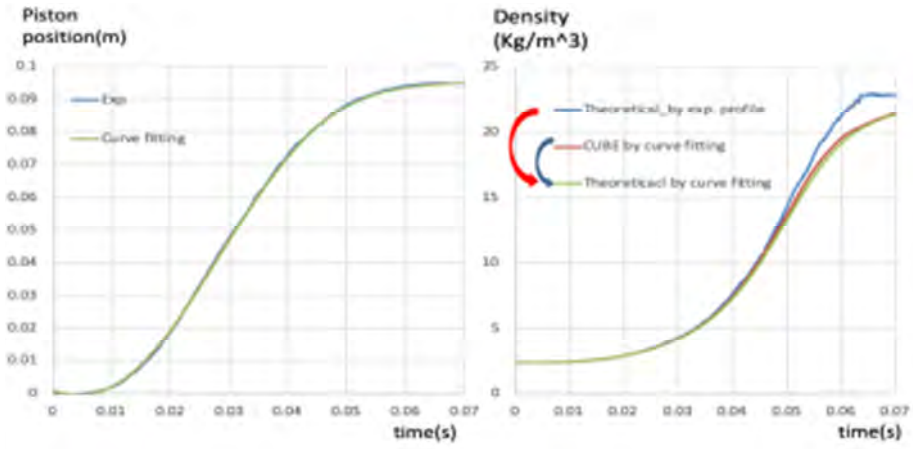

Figure 13.33: Piston motion profile and density of experimental and numerical results.

In order to solve this issue, a higher order curve fitting was used, and the comparison of piston motion profile is shown in Fig. 13.34. The density difference of new curve fitting results is shown in Fig. 13.35. The accuracy of piston motion is highly improved and the accuracy of density results compared with experimental results was also improved, which is an important insight to get accurate result in engine simulation.

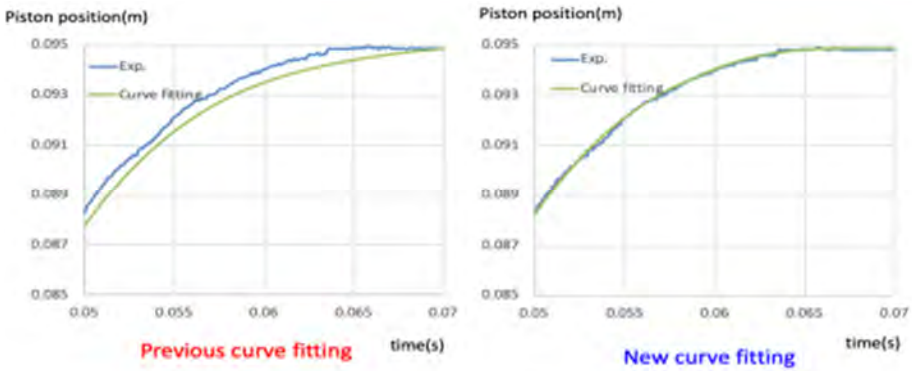

Figure 13.34: Comparison of piston motion profile.

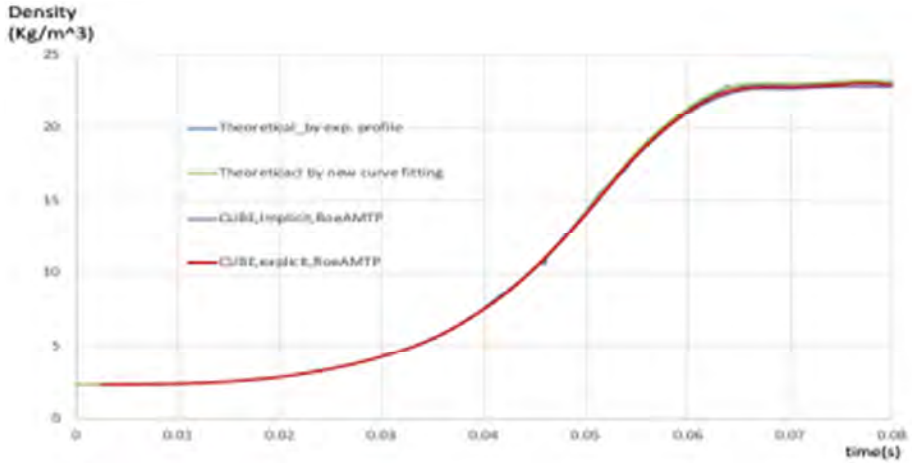

Figure 13.35: Comparison of density by high order curve fitting of piston motion.

For the flow visualization, the density is increased due to the compression process and is shown in Fig. 13.36 (a). In Fig. 13.36 (b), as the piston moves, the momentum magnitude inside the chamber is increased and even higher than the piston speed due to the geometry of the neck of the chamber. From t=80ms, energy source terms are added at the spark plug region to ignite the fuels, and then combustion is started. Fig. 13.37 shows the comparison of pressure between experimental and simulation results. Both results showed that the pressure is increased as the piston going to the TDC, and dramatically raised after 80ms due to the ignition. Before 40ms, the simulation results are well consistent with the experimental results, but higher after combustion. The main reason is that for simulation the adiabatic wall condition is adopted, where in real engine situation the heat is slightly conducted through the chamber wall.

In this year, we have achieved accurate results by finer resolution and better piston motion profile comparing with last year. Due to the increasing of resolution, the total cell number is approaching 100M and can resolve more realistic flow and combustion field. For the improvement of physical prediction accuracy, we found the fact that a precise piston motion profile was vital on this problem.

13.3.5.3 Basic flow validation for gas turbine simulation

For the gas turbine simulation, the numerical scheme which can treat the compressible flows and complex geometry is necessary. The purpose of this study is to validate the framework of the compressible flow in CUBE

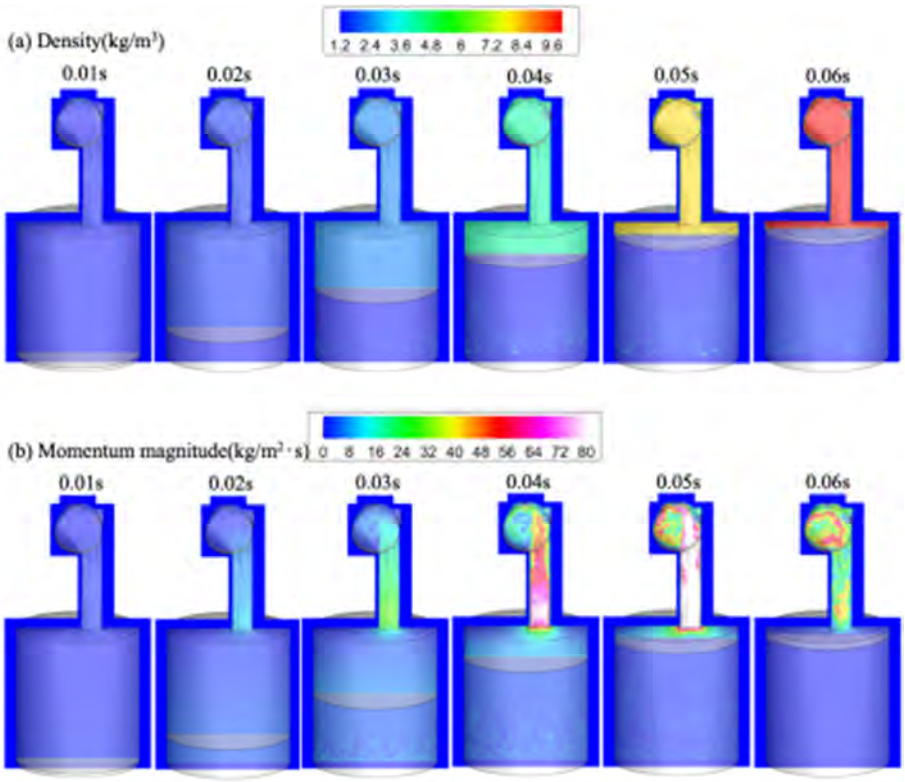

Figure 13.36: (a) Density and (b) Momentum magnitude contours of central slice of case B.

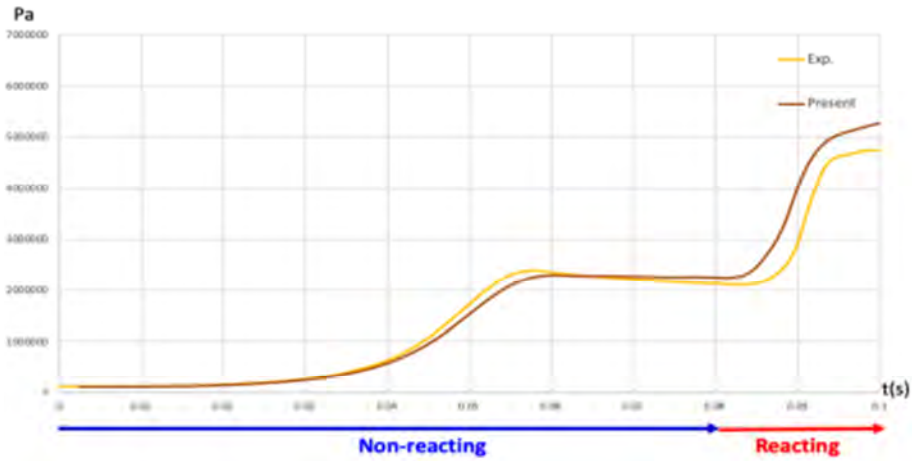

Figure 13.37: Pressure variations of experimental and CFD results of case B.

for gas turbine simulation and to make sure that the complex geometry with complex inflow-setup, usually it has several openings that supplies different kind of gas flow, can be executed successfully using current framework in highly parallel calculation. The result is also validated using well-established results which is calculated by legacy code, Frontflow/red (FFR) based on the unstructured grid. The results show that using CUBE can obtain comparable result with using FFR. This is a collaborative research with Mitsubishi Heavy Industries, Ltd. and Kyoto University.

The flow velocity boundary condition was imposed in various positions of openings on gas turbine geometry from 20 m/s to 60 m/s. It is not aligned to the Cartesian grid, so the arbitrary boundary condition using IBM is developed in the framework. The finest grid resolution was 0.25 mm that is put close to the inlet and the others had a coarser resolution of 1 mm in the all other calculation region. Near the inlet, the size for the hole or gap is fine of few mm widths, and then a local refinement technique was applied. Generally speaking, if finer resolution is adopted, in order to keep the numerical stable, very small step is necessary, which means the total calculation time will be extremely increased. However, current frame work has SLTS, which is mentioned above, and it is adopted while current time step can reach 5 of CFL condition for 1 mm grid and input fluid velocities. The number of cubes was 25,310, the number of cells was 102 million, and total calculation time was 50 hours with 1,055 nodes on K-computer.

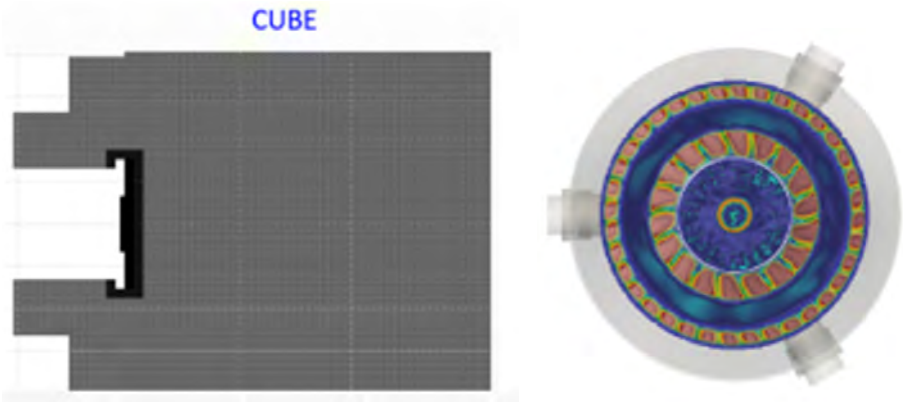

Figure 13.38: The computational grid overview around inlet region and typical inlet profile.

By comparing the instantaneous and time averaged velocity field, we confirmed that the present results were in good agreement with FFR. There was a small deviation in RMS value, but it might come from the difference of outlet condition, here the absorbing boundary condition is adopted, which allows the outlet velocity to be fully turbulent. The clear turbulent structures can be seen because the finer resolution is adopted here, that kind of structures have important effect for the combustion. Fig. 40 shows the result of the instantons velocity, time averaged velocity, RMS value and vortex structure of Q-criterion.

Using this framework 'CUBE' to simulate the gas turbine, it is shown that this framework is promising for the usage of gas turbine problems. The basic flow characteristics was compared with the well-established results of legacy code 'FFR', and confirmed that current framework showed reasonable results. We also have keep trying the study of different grid resolution, finer grid size, but due to the limitation of calculation resource in this year, it was difficult to get substantial statistical time for RMS evaluation. So, we are planning to proceed further investigation in next year, and toward the Post-K era, 10 billion gird, which can solved the whole turbulent scales without any model and much more accurate result are expected.

13.3.5.4 Development of multi-scalar flamelet model for turbine combustor

This is a collaborative research with Kawasaki Heavy Industries, Ltd. and Hokkaido University. The multi-scalar flamelet model is developed to solve the combustion in the combustion simulation frame work CUBE. The advantages of multi-scalar flamelet model are fixed number of equations, pre-made flamelet data with low computation load and high capabilities for premixed and non-premixed combustion.

In this study, a new theoretical model [3] is applied to put the unsteady analysis of a turbulent combustion field into practical use. The model is constructed with the application of a general mathematical model of a non-equilibrium interface to a non-premixed flame [4,5], a chemical equilibrium model with multiple conservation

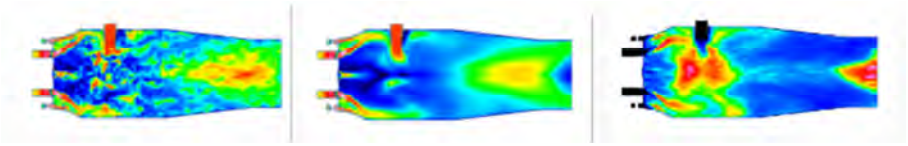

(a) Instaneous Velocity (b) Averaged Velocity (c) RMS Value

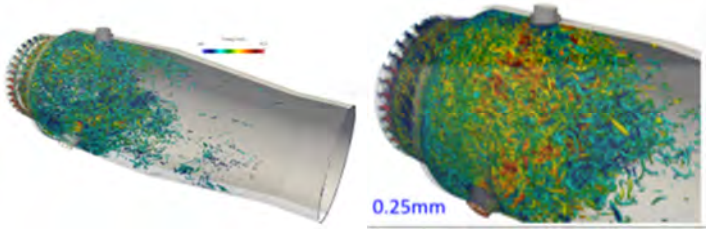

(d) Q-criterion

Figure 13.39: The calculation results of the gas turbine on cold flow condition.

scalars, and a non-adiabatic combustion models. It is designed to diverse to general-purpose turbulent combustion simulation methods formulated based on the scale separation principle of unsteady turbulence model, and aim to apply them to the next generation gas turbine combustor. As a result, instantaneous turbulent combustion field data with high prediction accuracy can realize the analysis of the combustion stabilization mechanism and quantitative prediction of emissions such as NO. With these theoretical models and implementation techniques, we aim to realize a practical forecasting simulation method that solves the problem of the complexity of the turbulent combustion field and the increase in computational load, which were conventionally difficult to achieve simultaneously.

The developed framework is shown in Fig. 41. The pre-made flamelet data is separated from the main solver of CUBE. The 5 scalar variables are calculated in main solver, and the flamelet data is read based on the values of scalar variables. The thermal properties and combustion source term are evaluated by the flamelet data and adopted in the flow calculation. In the future, we plan to continue the basic verification and validation of this method using the test with a simple burner and a simple spray test results and to deploy it to the application of the combustion problem of a realistic production turbine model.

13.3.5.5 LES Simulation of propeller performance by large scale calculation

In order to estimate the fuel consumption performance of a ship quantitatively, the performance confirmation by the towing-tank test is essential now. If the estimation value obtained by CFD can substitute for the test, the development cost can be reduced and the performance can be evaluated quickly. Furthermore, technology enhancement in design & development field is expected by using detailed flow field information that is difficult to obtain in the test. The purpose of this study is to obtain knowledge about the details of the flow field around the propeller as one of the studies to obtain knowledge on whether large-scale calculation can replace the tank test in the future. This stands for the activity that in order to promote new entry into turbo-machinery field, where R-CCS software is currently lacking, in cooperation with the shipbuilding company Japan Marine United. We have conducted empirical analysis targeting screw propeller using the Frontflow/red HPC version (FFR-HPC), which has a certain track record for turbo-machinery. We believe this activity will accelerate the construction of turbo-machine test beds, along with automobile engine test bed, gas turbine combustion test bed with CUBE.

Fig. 42 shows the shape of the model propeller and the calculation domain. The diameter of the propeller is 240 mm, which is generally used in towing-tank tests. The target propeller is arranged alone in the cylindrical area. The propeller-only test, a target of this study, is a test to measure the performance of the single propeller when the propeller rotates at a constant rotation speed in a uniform flow alone. The performance of the single propeller is an important factor that directly affects the performance of the entire ship.

The calculation grid is created, first with 100 million elements, and repeatedly divided in each element into two elements in each direction. It results to be divided into eight elements from original. It is repeated and then became 800 million elements and 6.4 billion elements. This technique is called as 'mesh refinement'. The calculation is performed using 3,840 nodes (30,720 cores) on K-computer with hybrid-parallel computation, on

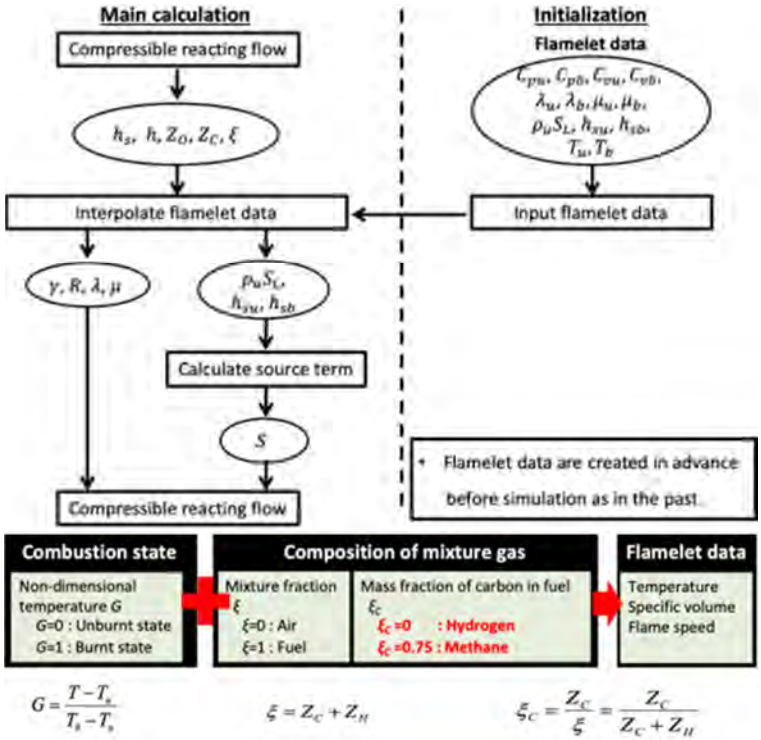

Figure 13.40: The framework of multi-scalar flamelet model in CUBE.

the 6.4 billion elements. The number of domain decomposition used in parallel computation is same as this number of CPU. The parallelization efficiency in weak-scaling test was about 60%.

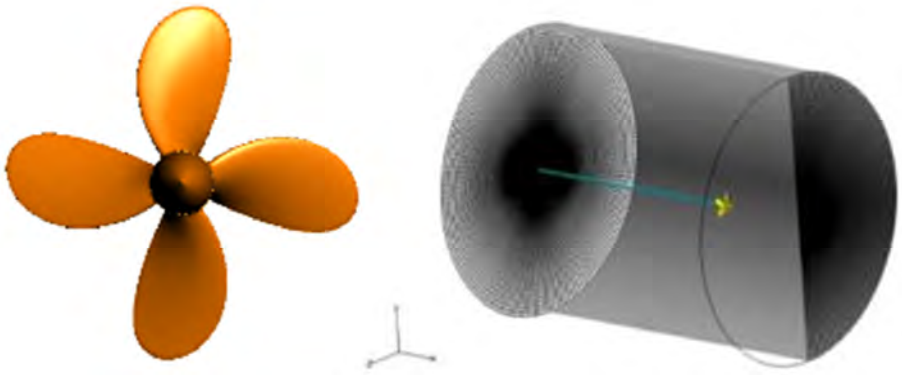

(a) Propeller geometry (b) Calculation domain

Figure 13.41: Overview of the geometry and calculation grid.

Fig. 43 shows the vortex structure in the vicinity of the propeller blade and it is compared with each result which is obtained from 100 million, 800 million and 6.4 billion elements. All of the cases has been done under the Large Eddy Simulation (LES) condition. On the propeller blade surface, a layered structure is formed on the leading edge (left side in the figure), and it becomes an elongated structure near the blade center, and in the downstream side (right end side of each figure), it turns out that it is in the turbulent state where fine vortex structure is intertwined complicatedly.

In large-scale LES calculations, it is known that the estimation accuracy of the flow field is improved by increasing the grid resolution. Comparing the flow with each result, the vortices became finer when the resolution is increased, especially in the region from the upstream side to near the center before it becomes turbulence.

However, there was no change in 800 million case and 6.4 billion case. From this fact, it is considered that about 800 million elements have reached sufficient resolution in the non-turbulent region. However, the fine structure of the vortices has been seen in the downstream which already became turbulence, it is indicated that fine grained refined resolution by increasing the scale of calculation is essential, to accurately capture the flow on the propeller blade surface. It turns out that the supercomputer K-computer is necessary in this kind of analysis.

In this study, we could not carry out further fine resolution calculations due to the limit of given resources, but it is thought that the calculation results of 6.4 billion grid are very close to the realistic flow. Then it is expected that we can obtain a useful knowledge by analyzing this flow field around the propeller in further detail.

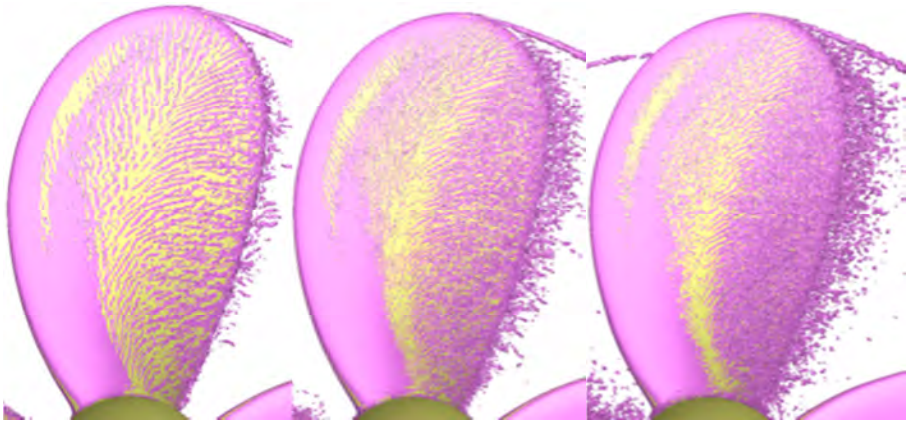

(a) 100 million (b) 800 million (c) 6.4 billion

Figure 13.42: Vortex structure on blade surface (iso-surface of 2nd invariant of velocity gradient).

In summary, we have conducted large-scale LES calculation around propeller using K-computer which is the highest-class performance computer in Japan for the purpose of investigating the feasibility of substitution of towing-tank test by large-scale numerical simulation. A detailed flow structure around blade was investigated and the knowledge about the influence of the grid resolution has been obtained.

13.3.5.6 References

[1] F. Rieper, "A low-Mach number fix for Roe's approximate Riemann solver," J. Comput. Phys. 230 (2011) 52635287. doi:10.1016/j.jcp.2011.03.025.
[2] C.-G. Li, M. Tsubokura, R. Bale, "Framework for simulation of natural convection in practical applications," Int. Commun. Heat Mass Transf. 75, pp.5258, 2016.
[3] R. Kishine, Tenshi Sasaki, Nobuyuki Oshima , et.al., "Application of Large-Eddy Simulation and the Multi-Scalar Flamelet Approach to a Methane-Hydrogen Mixed-Combustion-Type Industrial Gas-Turbine Combustor," Proc. ASME 2017 Power and Energy Conference, June 26-30, Charlotte, USA, 2017.
[4] N. Oshima, "An extensional formulation for a diffusive solution of the level-set equation by considering a relation to the scalar conservation equation," Mechanical Engineering Letters, Vol.2, 2016.
[5] N. Oshima, "A fluid interface model by phase field approach applied to the diffusive solution of level-set equation," Mechanical Engineering Letters, Vol.3 2017.

13.4 Schedule and Future Plan

In the research and development of unified simulation framework 'CUBE' from 2012, the following goals has been achieved:

[1] Construction and development of the simulation technology for bringing out the performance of K-computer

[2] Validation and practical usage of industrial applications such as vehicle aerodynamics, aeroacoustics, unsteady motion aerodynamics, engine combustion, city area wind environment analysys, sport CFD, and structure analysis

[3] Preparation of the simulation technologies of HPC toward EXA-scale

In the long-term objectives, the following target is considered:

[1] Establishment of the research and development center for industrial simulation technology

[2] Contribution to computer science by expanding the developed simulation technology to different fields

In terms of using Cartesian grids, the problems that the analysis accuracy in the vicinity of the wall surface decreases due to the limitation of immersed boundary method is becoming clear. In the future, through the deployment of CUBE to the industrial applications, the introduction of higher order schemes, wall modeling and advance sophisticated research of immersed boundary method are planning.

In terms of using Hierarchical grid system, the problems that the interface communication in each halo of cubes will spoil the performance on future supercomputers is becoming clear. In the future, the enhancement to the current communication / calculation overwrapping technique, or tuning for the interface communication, introduction of adaptive refinement scheme are planning.

From collaboratetive companies, including companies through the activities of the "Consortium for Next Generation Automotive CAE using HPC" and "Consortium for Next Generation Combustion CAE using HPC" organized by RIKEN, voices of surprises and expectation for software development have been received. We are planning to continue development for practical application in near future.

13.5 Publications

13.5.1 Articles/Journal

[1] Keiji Onishi, Rahul Bale, Makoto Tsubokura, "Assessment of Rotating Wheel Vehicle Aerodynamics Simulation Using Cartesian Grid Method and Open-Grill Full Vehicle Models", SAE Technical Paper 2019-01-0660, 2019.
[2] Niclas Jansson, Rahul Bale, Keiji Onishi, Makoto Tsubokura, "CUBE: A scalable framework for large-scale industrial simulations," The International Journal of High Performance Computing Application, 2018.
[3] Koji Nishiguchi, Rahul Bale, Shigenobu Okazawa, Makoto Tsubokura, "Full Eulerian deformable solid-fluid interaction scheme based on building-cube method for large-scale parallel computing," International Journal for Numerical Methods in Engineering, Vol.117 (2), pp.221-248, 2018.
[4] Koji NISHIGUCHI, Rahul BALE, Shigenobu OKAZAWA, Makoto TSUBOKURA, "IMPLICIT PARTICLE-IN-CELL FORMULATION FOR INCOMPRESSIBLE SOLID-FLUID INTERACTION PROBLEM," Journal of Japan Society of Civil Engineers, Ser. A2 (Applied Mechanics (AM)), 74(2), p. I_253-I_263, 2018.
[5] Wu-Shung Fu, Wei-Hsiang Wang, Chung-Gang Li, Makoto Tsubokura, "An investigation of the unstable phenomena of natural convection in parallel square plates by multi-GPU implementation," Numerical Heat Transfer, Part B: Fundamentals, An International Journal of Computation and Methodology, Vol.71(1), pp.66-83, 2017.

13.5.2 Conference Papers

[6] Keiji Onishi, Rahul Bale, Makoto Tsubokura. "An immersed boundary method based vehicle aerodynamics simulation with tire rotation," In: Proceedings of the Conference on Computational Engineering and Science, B-06-1, 2018.6.
[7] K. Onishi, N. Jansson, M. Tsubokura. "In-situ visualization using open source on K-computer," In: Proceedings of the 32th Computational Fluid Dynamics Symposium, B01-1, 2018.12.
[8] Rahul Bale, Amneet Pal Singh Bhalla, Niclas Jansson, Keiji Onishi, Makoto Tsubokura, "Moving least squares based constraint immersed boundary method," In: Proceedings of the Conference on Computational Engineering and Science, B-05-05, 2018.6.
[9] Rahul Bale, Amneet Pal Singh Bhalla, Niclas Jansson, Keiji Onishi, Makoto Tsubokura, "Moving least squares based constraint immersed boundary method," In: Proceedings of the 32th Computational Fluid Dynamics Symposium, F04-4, 2018.12.

[10] Jun Ikeda, Chung-Gang Li, Makoto Tsubokura, Kazuo Minami, Kiyoshi Kumahata, "Performance evaluation of BCM compressible flow solver and the validation by natural convection," In: Proceedings of the Conference on Computational Engineering and Science, C-03-05, 2018.6.
[11] Koji Nishiguchi, Rahul Bale, Shigenobu Okazawa, Makoto Tsubokura, "Fixed Cartesian mesh approach for large-scale parallel simulation of vehicular structures," The 8th Japan-Korea Workshop on Computational Mechanics, Nagoya, Japan, 2018.6.
[12] Koji Nishiguchi, Rahul Bale, Shigenobu Okazawa, Makoto Tsubokura, "Unified analysis of thin plate structure-fluid using particle-in-cell method," In: Proceedings of the Conference on Computational Engineering and Science, B-06-05, 2018.6.
[13] Wang Wei-Hsiang, Chung-Gang Li, Rahul Bale, Keiji Onishi, Makoto Tsubokura, "The four-stroke IC engine simulation using hierarchical Cartesian mesh framework by CUBE," In: Proceedings of the Conference on Computational Engineering and Science, B-05-01, 2018.6.
[14] Wang Wei-Hsiang, Chung-Gang Li, Makoto Tsubokura, "The Numerical Work of IC Engine Simulation by Fully Compressible Flow Solver in Hierarchical Cartesian Mesh System," 15th International conference on Flow Dynamics, Sendai, Japan, 2018.11.
[15] Wang Wei-Hsiang, Rahul Bale, Keiji Onishi, Chung-Gung Li, Makoto Tsubokura, "The numerical simulation of RCM combustion by CUBE," In: Proceedings of the 32th Computational Fluid Dynamics Symposium, A06-1, 2018.12.

13.5.3 Invited Talks

[16] Makoto Tsubokura, "HPC-CFD Frameworks for Industrial Problems Based on Fully Unstructured and Hierarchically Structured Mesh Systems, Automotive CFD as an example ," 27th Workshop on Sustained Simulation Performance, Sendai, Japan, 2018.3.
[17] Makoto Tsubokura, "Unified simulation framework for continuum mechanics based on HPC technique and its application to industrial problems," The 12th Asian Computational Fluid Dynamics Conference (ACFD 2018), Yilan, Taiwan, 2018.10.

13.5.4 Oral Talks

[18] Keiji Onishi, Niclas Jansson, Rahul Bale, Makoto Tsubokura, "A parallel algorithm of pre- and post-processing for industrial CFD applications," SIAM Conference on Parallel Processing for Scientific Computing, 2018.3.
[19] Keiji Onishi, Yasunori Ando, Kosuke Nakasato, Makoto Tsubokura, "Evaluation of an Open-grill Vehicle Aerodynamics Simulation Method Considering Dirty CAD Geometries," WCX18: SAE World Congress Experience, Detroit (MI), 2018.4.
[20] Keiji Onishi, Niclas Jansson, Makoto Tsubokura, "HIGH PERFORMANCE PARALLEL COMPUTING OF FULL VEHICLE AERODYNAMICS SIMULATION INCLUDING PRE- AND POST-PROCESSING," 7th European Conference on Computational Fluid Dynamics (ECFD 7), Glasgow, UK, 2018.6.
[21] Bale Rahul, Amneet PS Bhalla, Niclas Jansson, Keiji Onishi, Makoto Tsubokura, "Moving least squares based constraint immersed boundary method," 13th World Congress of Computational Mechanics, New York, NY, 2018.7.
[22] Makoto Tsubokura, "Unified simulation framework for continuum mechanics based on HPC technique and its application to industrial problems," The 12th Asian Computational Fluid Dynamics Conference (ACFD 2018), Yilan, Taiwan, 2018.10.
[23] Rahul Bale, Niclas Jansson, Keiji Onishi, Makoto Tsubokura, Amneet Pal Singh Bhalla, "Moving-least-squres immersed boundary method for thin rigid structures," The 12th Asian Computational Fluid Dynamics Conference (ACFD 2018), Yilan, Taiwan, 2018.10.
[24] Jun Ikeda, Makoto Tsubokura , "Numerical study of the unsteady aerodynamics on running stability and drivability of road vehicles," The 12th Asian Computational Fluid Dynamics Conference (ACFD 2018), Yilan, Taiwan, 2018.10.
[25] Koji Nishiguchi, "A novel method of automotive structural analysis for the post-K computer," Automotive Engineering Association Structural Strength Division Committee, 2018.4.
[26] Koji NISHIGUCHI, Rahul BALE, Shigenobu OKAZAWA, Makoto TSUBOKURA "IMPLICIT PARTICLE-IN-CELL FORMULATION FOR INCOMPRESSIBLE SOLID-FLUID INTERACTION PROBLEM," The 21st Applied Mechanics Symposium, 2018.5.

[27] Koji Nishiguchi, Rahul Bale, Shigenobu Okazawa, Makoto Tsubokura, "Strong coupling scheme for thin-shell structure and fluid with implicit particle-in-cell method," 7th European Conference on Computational Fluid Dynamics (ECFD 7), Glasgow, UK, 2018.6.
[28] Koji Nishiguchi, Rahul Bale, Shigenobu Okazawa, Makoto Tsubokura, "Particle-in-cell Formulation for Fluid-Structure Interaction Simulations with Hard Solid," 13th World Congress of Computational Mechanics, New York, NY, 2018.7.
[29] Chung-Gang Li, Makoto Tsubokura, "An Investigation of Implicit Turbulence Modeling for Laminar-Turbulent Transition in Natural Convection," XI-th International Conference on Computational Heat, Mass and Momentum Transfer (ICCHMT 2018), Cracow, Porland, 2018.5.
[30] Wei-Hsiang Wang, Chung-Gang Li, Wu-Shung Fu and Makoto Tsubokura, "Investigation of open boundary problem in pure thermal plume by hybrid boundary condition with multi-GPU implementation," The 3rd Thermal and Fluids Engineering Conference, Fort Lauderdale, FL, USA, March 4-7, 2018.
[31] Wang Wei-Hsiang, Chung-Gang Li, Rahul Bale, Keiji Onishi, Makoto Tsubokura, "The IC engine combustion simulation using hierarchical Cartesian mesh framework," 7th European Conference on Computational Fluid Dynamics (ECFD 7), Glasgow, UK, 2018.6.
[32] Wang Wei-Hsiang, Chung-Gang Li, Rahul Bale, Keiji Onishi, Makoto Tsubokura, "CFD Simulation of RCM Combustion by Building Cube Method," The 12th Asian Computational Fluid Dynamics Conference (ACFD2018), Yilan, Taiwan, 2018.10.
[33] Chung-Gang Li, Makoto Tsubokura, "A unified time stepping scheme for flow and aeroacoustic computations," The 12th Asian Computational Fluid Dynamics Conference (ACFD 2018) , Yilan, Taiwan, 2018.10.
[34] Tsukasa Hori, Makoto Tsubokura, Kazunari Kuwahara, Eriko Matsumura, Jiro Senda, "The development and application of detailed chemistry for multidimensional diesel engine simulation," The 12th Asian Computational Fluid Dynamics Conference (ACFD 2018), Yilan, Taiwan, 2018.10.
[35] Tamura T., H., Dung, D.V., Cao, Y., Onishi, K., Bale, R., Tsubokura, M, "Application of LES Based on BCM to Wind Engineering," 7th European Conference on Computational Fluid Dynamics (ECFD 7), Glasgow, UK, 2018.6.
[36] Ito, Y., Kawai, H., Sakai, Y., Tamura, T., Bale, R., Onishi,K., Tsubokura, M., "Validation of Cladding Wind Load Evaluation of a Precisely Modelled High-Rise Building Using Large Eddy Simulation," International Symposium on Computational Wind Engineering, Seoul, Korea, 2018.6.
[37] Yong Cao, Kawai, H., Tamura, T., Bale, R., Onishi,K., Tsubokura, M., "Flow Topology and Surface Pressure on a Wall-Mounted Square Cylinder," International Symposium on Computational Wind Engineering, Seoul, Korea, 2018.6.

Chapter 14

Next Generation High Performance Architecture Research Team

14.1 Members (as of FY2018)

Masaaki Kondo (Team Leader)

14.2 Overview of Research Activities

The next generation high performance architecture research team is conducting research and development of a next-generation high-performance computer architecture. Currently, we are mainly focusing on non-von Neumann architectures such as systolic arrays and neuromorphic computers based on the latest advances in device technologies, architectures that can integrate next generation non-volatile memories and/or various types of accelerators into a general-purpose processor, the advancement of scientific simulations by accelerating machine learning computations, and hybrid computing architectures that combine the benefits of quantum computing and classical computing. We are also performing detailed co-design evaluations of the computer architectures noted above as well as the co-design evaluations of algorithms that take advantage of them on the supercomputers K and Fugaku.

Another important aspect of designing future high-performance systems is power consumption. Power consumption is a prerequisite design constraint for developing exascale or next-generation computer systems. In order to maximize effective performance within a given power constraint, we need a new system-design concept in which the system's peak power is allowed to exceed maximum power provisioning using adaptively controlling power knobs incorporated in hardware components so that effective power consumption is maintained below the power constraint. This concept is recently known as hardware overprovisioning. In such systems, it is indispensable to allocate the power budget adaptively among various hardware component such as processors, memories, and interconnects, or among co-scheduled jobs, instead of fully utilizing all available hardware resources. We are researching strategies to improve the power efficiency and total system throughput for future hardware overprovisioned supercomputer systems.

14.3 Research Results and Achievements

14.3.1 Research and development of power-aware resource manager

In overprovisioned systems, power budget allocated for each node should be controlled by power-knobs such as dynamic voltage and frequency scaling (DVFS) or a power capping mechanisms. One of the key challenges is to develop a runtime system for optimizing and controlling power budget of executing jobs based on the available power budget of the entire system to maximize the total system throughput. To this end, a power-aware resource manager and several power allocation or job scheduling algorithms are necessary.

Though there have been several studies of hardware overprovisioned HPC systems, the impact of hardware overprovisioning in production environments at large scale has not yet been examined intensively. In order to provide a software stack which makes such systems accessible to users or administrators, we have been

developing an extensible power-aware resource management and job scheduling framework based on the widely tilized SLURM resource manager.

Figure 14.1 shows the design of our proposed power-aware resource manager, which is implemented as a SLURM extension. It enables the implementation of a wide spectrum of power management algorithms by flexible plugin interfaces that can be used by different HPC centers to enforce site-specific power management policies. We add a *power scheduler*, a *node power manager* and a *low-level power plugin interface* to the original SLURM code. The power scheduler schedules all of the system power by monitoring and distributing the compute nodes power. It consists of three components: Power monitor, Power analyzer, and Power allocator. The power allocator and power analyzer have extensible plugin interfaces. This allows other plugin developers to implement and test their own power management algorithms.

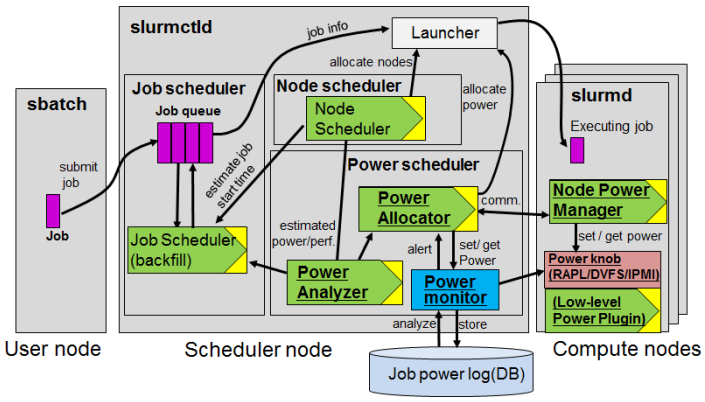

Figure 14.1: Power-aware Resource Management Framework

We validated the power management functionality of the extended SLURM using all the nodes in the HA8000 system. The system contains 965 compute nodes and each node has two Xeon processors with 128-GB DDR3 memory. We evaluated the power consumption of the system varying the total power budget. We evaluate three power budgets, 100kW, 110kW, and 120kW. Figure 14.2 shows the aggregate power consumption measured by RAPL for all the compute nodes. As shown in the figure, the actual power is almost the same as the allocated power budget when the system is fully loaded (middle section of each curve) This indicates that our power-aware SLURM successfully controls power usage of executing jobs.

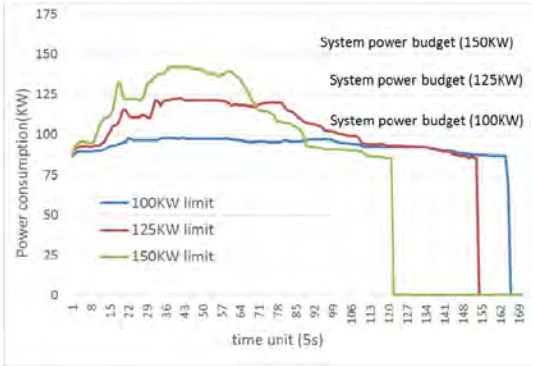

Figure 14.2: Validation Under Different System Power Budget

With the extension of SLURM, we investigated the impact of varying the number of extra compute nodes, or the degree of overprovisioning. We assume that the base system is a non-overprovisioned HPC system with 400 compute nodes whose system power budget is the peak power consumption of 400 nodes of the HA8000 system. Then, we evaluate several cases of overprovisioned systems: 540, 680, 820, and 960 compute nodes with the same system power budget.

Figure 14.3 (a) and (b) present average power resource utilization and system throughput, respectively, under several overprovisioned system configurations. We evaluated five job mixes varying average power demand of

jobs. From Figure 14.3 (a), it can be observed that power resource utilization increases if we increase the number of overprovisioned nodes to 680-nodes. However, utilization decreases when the node count increases any further. The node resource is exhausted in cases of small numbers of overprovisioned nodes and power resource is not fully consumed. On the other hand, the power resource is exhausted in cases of large numbers of overprovisioned nodes and the scheduler must leave some of the nodes being idle to maintain the power budget.

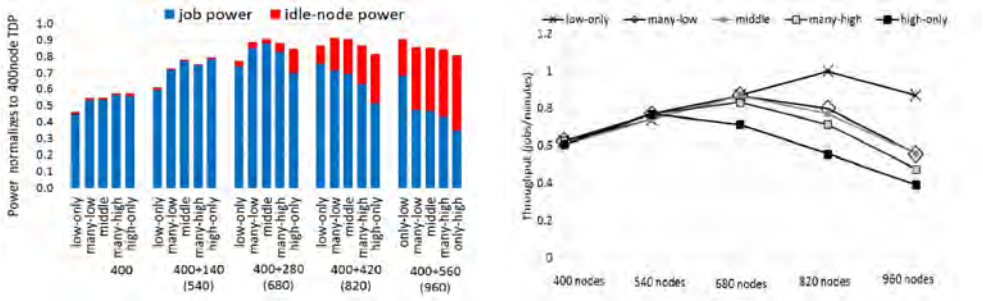

(a) Power usage (b) Total system throughput

Figure 14.3: Evaluation of Overprovisioned System with a Real 960-node System

In Figure 14.3 (b), system throughput tends to improve if we increase the number of nodes since overprovisioning provides more computational resources. However, the performance trends are more complex because utilization decreases in the case of 960-node and depends on job mixes. Power-hungry job mixes with many CPU intensive jobs prefer a relatively small number of overprovisioned nodes because the average node power consumption is high and power resource is easily exhausted by small number of nodes. On the other hand, low-power job mixes with more memory intensive jobs prefer relatively large numbers of overprovisioned nodes as the power resource does not tend to be exhausted and a larger number of nodes helps increase the number of jobs executing concurrently.

Through experimentation on a large scale production system, we have shown that our power management framework is safe for deployment on production systems. The experiment for overprovisioning presented above could not be possible without the production level power-aware resource management framework. Our developed SLURM extension is very useful in this point. The source code of the SLURM extension is available on a GitHub repository at https://github.com/pompp.

14.3.2 Scalable accelerator core design for deep neural networks

Recent advancnes in Deep Neural Network (DNN) technologies brings the opportunity to execute recognition and inference applications on wide variety of computer systems. For example, automobiles and smart phones offer advanced functionality with the image recognition using Convolutional Neural Network (CNN). One of the challenges for executing CNNs is developing a high-performance inference engine with high power efficiency. Therefore, several DNN accelerator architectures or LSI chips are proposed for high-performance and low-power CNN executions.

Though existing CNN accelerator architectures can successfully achieve high energy efficiency, they typically focus on optimized execution for either of convolutional or fully connected layers. They also sometimes need to change the network structure which may limit the applicability to the variety of network structures. Since DNN algorithm and organization is now continuing to evolve, it is desirable for CNN accelerators to have flexibility to handle various types of network structure.

To this end, we have been conducting research and development of the architecture and LSI design of a flexible and scalable DNN accelerator. This is a joint work with several universities in Japan. Our accelerator is a multi-core accelerator with several cores each of which consists of a micro-controller and a SIMD multiply and accumulate (MAC) unit. Figure 14.4 (a) presents the schematic view of the overall accelerator architecture with four cores. Each core has five scratch-pad memories, an instruction memory (inst), a stream buffer (sbuf), a temporal data memory (dmem), a lookup table (lut), and an output memory (omem). Each core has its own memory address space to read and write these memories and all of the memories except for omem are manages as distributed memory manner. All the cores share an omem to communicate each other for sharing output data when executing forward propagation calculation in parallel.

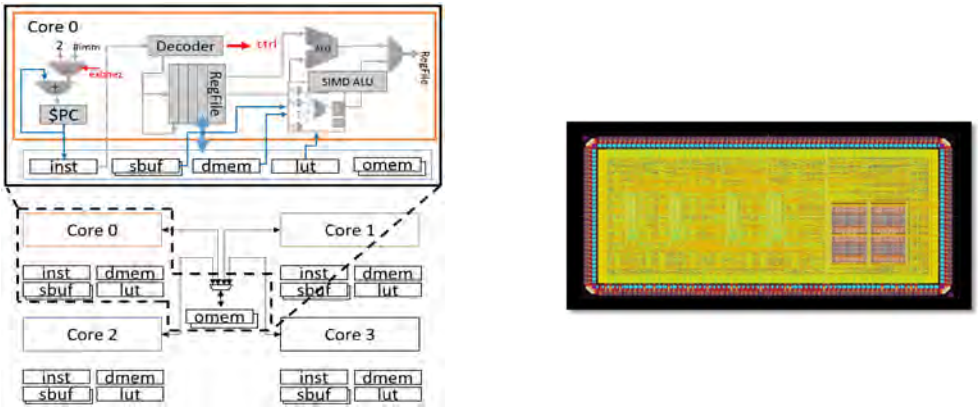

(a) Core architecture

(b) Chip layout

Figure 14.4: Core Microarchitecture and Chip Layout of Designed DNN Accelerator

A tiny micro-controller, a SIMD MAC unit, and some registers are major component of the core. The micro-controller controls the data path of the core with 4 x 16-bit fixed length instructions. We also support 8 x 8-bit SIMD execution for neural networks which do not require higher bit-width. We define an original instruction set architecture customized for DNN executions. It supports simple arithmetic/logical operations, memory access instructions, and special instructions dedicated for optimized loop executions. Since the number of instruction is small, the instruction decoder and control logic are very small, and hence power efficient. One of the important abilities for DNN accelerators is efficiently executing huge number of MAC operations. If every MAC operation and associated memory accesses in a large nested loop appeared in CNNs are initiated by instructions, energy overhead for instruction accesses and instruction handling is non-negligible. Therefore, a typical loop calculation is executed by only one special instruction in the core.

Based on the above architecture, we designed and implemented an accelerator core in real chip. we laid out the chip and taped out it with Renesas Electronics 65nm SOTB process technologies. Figure 14.4 (b) shows the layout of the chip. The chip size is 3mm times 6mm with four cores. Due to the chip size limitation, only four cores were implemented on the chip. The chip contains 68-KB of distributed on-chip SRAMs. One core has 2KB instruction and 2KB lookup table memories. The size of dmem and sbuf is 4KB each. The four cores share the 4KB of omem. Each core has 18,8864 logic gates.

The prototype chip was successfully operated at 60MHz clock frequency with about 0.65V. We evaluate power-efficiency of the prototype core varying the core clock frequency (from 10MHz to 60MHz) and the number of core used (from 1-core to 4-core). Figure 14.5 (a) shows the evaluation environment. The evaluation results in terms of performance per watt are presented in Figure 14.5 (b). We observe that the power-efficiency improves when we use more number of cores. If 8-bit SIMD mode (8 x 8-bit SIMD) is applied, power efficiency greatly improves. In total, the prototype chip achieves up to 250 Gops/W power efficiency. We will enhance the core microarchitecture of our accelerator to achieve higher performance with lower power consumption.

(a) Evaluation environment

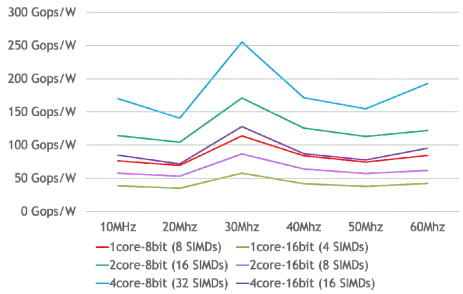

(b) Power-performance

Figure 14.5: Evaluation Environment and Power-Performance Results of Prototype Chip

14.4 Schedule and Future Plan

In order to achieve further performance improvement for next generation HPC systems in post-Moore era, it is necessary to explore various types of devices, hardware architectures, system software/programming models, and algorithms that may contribute to the future system designs. We need to evaluate and analyze huge amount of possible scenarios varying the architectural parameters on wide variety of underlying system architecture. To this end, we will select several benchmark applications which are expected to become important in future high-performance computing including big-data and AI as well as traditional simulation applications. We will also analyze their performance feature by constructing a mechanism to expose their execution characteristics using current supercomputer systems such as Supercomputer K/Fugaku, TSUBAME and Oakforest-PACS. We will also establish a performance model or performance simulation environment that enables to evaluate wide variety of future HPC architectures. Specially, we will focus on vector processing architectures, types of memory devices, optical connections among computing devices, and massively parallel system architectures.

Beside exploring traditional CMOS-based computer systems, we need to consider post-CMOS high-performance and low-power computing devices for post-Moore era. We also plan to study an ultra-high-performance accelerator system with an emerging device called SFQ (single-flux-quantum). Our approach stands on circuit/architecture/algorithm level co-designs with SFQ devices specially targeting on neural-network accelerator computations.

14.5 Publications

14.5.1 Conference Papers

[1] Ryuichi Sakamoto, Tapasya Patki, Thang Cao, Masaaki Kondo, Koji Inoue, Masatsugu Ueda, Daniel Ellsworth, Barry Rountree, and Martin Schulz, "Analyzing Resource Trade-offs in Hardware Overprovisioned Supercomputers", 32nd IEEE International Parallel & Distributed Processing Symposium (IPDPS2018), 10pages, May 2018.
[2] Mineto Tsukada, Masaaki Kondo, Hiroki Matsutani, "OS-ELM-FPGA: An FPGA-Based Online Sequential Unsupervised Anomaly Detector", The 16th International Workshop on Algorithms, Models and Tools for Parallel Computing on Heterogeneous Platforms (HeteroPar'18), Aug 2018.

14.5.2 Invited Talks

[3] Masaaki Kondo, "Reinforcement Learning-Based Adaptive Power Management for Energy Harvesting IoT Devices", International Forum on MPSoC for Software-de
ned Hardware (MPSoC '18), July 2018.

Chapter 15

High Performance Big Data Research Team

15.1 Members (as of FY2018)

Kento Sato (Team Leader)

15.2 Overview of Research Activities

The High Performance Big Data Research Team leads research and software development for accelerating "machine learning, deep learning and large-scale big data processing (AI techniques)" on the K and the post-K supercomputers (HPC for AI) in accordance with the RIKEN R-CCS mission. We also study for accelerating HPC applications and HPC systems by using these AI techniques. Over the next years, To tackle these research challenges, our team also study following research topics over the next seven years: (1) Fast and scalable parallel I/O by taking advantage of next-generation memory (e.g., Non-volatile memory) in big data processing and machine learning; (2) Scalable checkpointing for fault tolerance by taking advantage of next-generation memory (e.g., Non-volatile memory); (3) Scalable algorithms for deeply hierarchical memory and storage architecture; (4) Fast data transfer technique for multi-petabyte of big data on high-speed network; (5) Integration of software stacks of bigdata, machine learning and HPC, and their optimization; (6) Visualization and UI techniques of big data; (7) Other research and software development related to big data, machine learning and I/O.

15.3 Research Results and Achievements

15.3.1 HuronFS: Hierarchical, User-level and On-demand Filesystem and B2Sim: Burst Buffer Simulator

Computational performance in high performance computing (HPC) systems has been dramatically increased, driven by continuously advancing multi- and many-core architectures and fast memory technologies such as high bandwidth memory (HBM) and hybrid memory cube (HMC). The fastest supercomputer in the world first reached beyond a hundred PFLOPS in 2016. The advance is a factor of 400 compared to the fastest supercomputer in 2006. Although these recent HPC systems have been keeping pace with the requirements of compute- and memory-intensive applications, the current systems remain inadequate for I/O-intensive applications since the performance of the I/O subsystem, such as a parallel file systems (PFS), is much lower than that of processors and memory systems. For example, the latest top 1 supercomputer summit provides 200 Peta-Flops computational performance while having as low as 2.5 Tera Byte/s GPFS filesystem, a factor 80,000 in favor for compute. As we move towards higher performance and large-scale data-intensive applications on HPC systems, I/O performance has become more critical.

To alleviate the gap between computational and I/O performance, production supercomputers have been adopting burst buffer systems. Burst buffers are an additional storage tier, residing on top of the PFS in the storage hierarchy and provide non-volatile storage space with high bandwidth and lower latency than the PFS. Burst buffers are used as either local storage that has been installed on each compute node, node-local burst

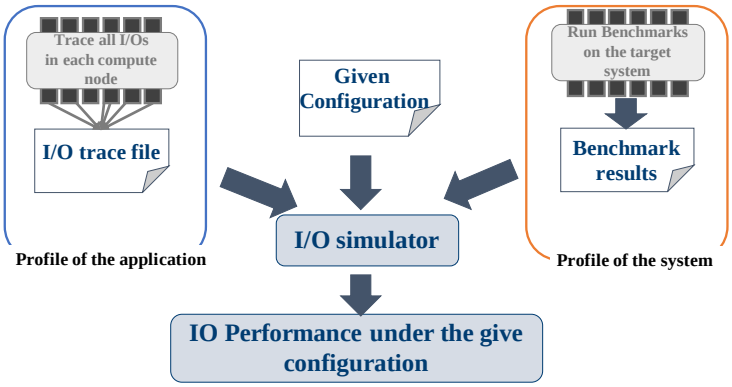

Figure 15.1: Overview of B2Sim

buffer (NLBB) or remote storage that is shared by compute nodes and serve as cache space for PFSs, remote shared burst buffer (RSBB).

In RSBB, the burst buffers are shared by all compute nodes. Users specify the total size of RSBB via APIs. However, while RSBB provides its users with flexibility in specifying the size of burst buffers, the RSBB size must be carefully determined, otherwise applications may crash due to I/O errors if applications attempt to use more RSBB capacity than requested size, i.e., overflow.

The current solution is to allocate a surplus in capacity that exceeds the usage estimate in order to avoid job failure. However, such solution causes significantly under-utilization of burst buffer, reduction in the system's job throughput, and increase in the job queuing time. Another solution is to stage-out data that the application does not use anymore and then stage-in data which the application accesses next, similar to the cache swapping. Recent RSBB systems provide APIs for dynamic stage-in/out, i.e., swapping, functionalities so that the application can process more data than the specified amount. However, due to the lack of system support and coarse swapping granularity, data swapping is not widely performed on RSBBs, and the effectiveness of the data swapping on RSBBs are unclear.

In this work, we explored the performance impact on I/O- intensive applications when RSBB systems support finer-grained granularity for dynamic swapping: chunk-level. Here, we define the performance impact as the performance reduction of applications when using a limited capacity buffer compare to when using unlimited capacity buffer, i.e., the theoretical maximum. This finer-grained granularity raises several interesting questions. Specifically, we explored the following three critical questions: (i) how do different RSBB swapping configurations, i.e., buffer size and data replacement algorithms impact performance? (ii) how can we efficiently utilize the chunk-level swap-in/out1 approach in RSBB? (iii) how do different chunk-level data replacement algorithms, i.e., FIFO, LRU and others, impact performance? We investigated these questions with a data swapping simulator for burst buffer, B2Sim. B2Sim is a trace-driven simulator and the simulation starts with tracing all I/O operations of an application, then B2Sim simulates the data swapping on RSBB based on the I/O trace from different applications under different configurations, i.e., buffer sizes, and data replacement algorithms. B2Sim provides a methodology for user to quickly search for the optimal configuration of RSBB for their applications.

In the evaluations, we conducted three sets of experiments to answer the three burst buffer configuration questions targeting HuronFS. Especially, we made the following contributions:

- A generic model of RSBB under a chunk-level and file- level swap-in/out scheme;
- A simulator, B2Sim, that simulates I/O behaviors of applications based on the RSBB model;
- Comprehensive explorations on three configurations of RSBB;
- Empirical simulations with five real-world applications.

Our key findings are that all three configurations, buffer size, granularity, and data replacement algorithms have impacts on the application performance, and should be carefully chosen to fully utilize the burst buffer system. With B2Sim, we can extrapolate more efficient use and better design space for burst buffer architectures. To the best our knowledge, our work is the first exploration in data swapping on burst buffer.

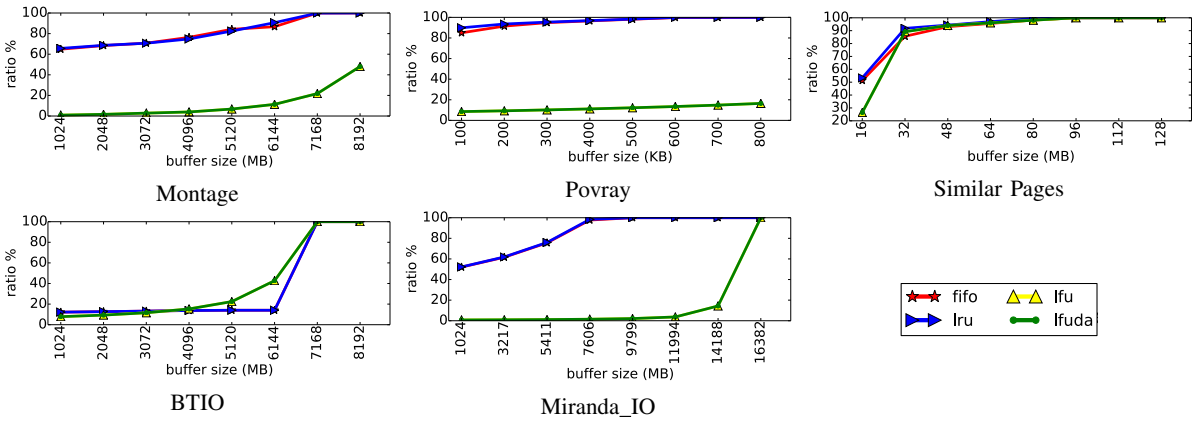

Figure 15.2: Simulation result with different data replacement algorithms

15.4 Schedule and Future Plan

The post-K computer (Supercomputer Fugaku) development plan under the FLAGSHIP 2020 Project, initiated by the Ministry of Education, Culture, Sports, Science and Technology in 2014, has set the target of developing (I) the next generation flagship supercomputer of Japan (the successor of the K computer) along with (II) a wide range of applications that will address top priority social and scientific issues. To alight with this R-CCS mission, our research team will study promising computer architectures and system software towards the upcoming post-K computer and beyond it, what we call "the Post-Moor Era". We explore new programming techniques, new algorithms and new applications of these techniques to AI techniques (Machine learning, deep learning and others) for the next generation HPC systems under the context of high performance big data. The year of 2028 is projected as a beginning of Post-Moore Era. It is expected that a wide range of applications will be boosted by a factor of 100 with respect to computational performance. However, to find the best architecture for reaching the 100x computational performance, co-designing from hardware devices, system software, programming models to algorithms is necessary. We will tackle this research challenge and explore the design space of the hardware architectures and system software under various system architectures, various system parameters and others. Especially, future research directions include: (1) New modeling/simulation/benchmarking techniques for design space exploration of new hardware, architectures and systems; (2) New APIs, interface and filesystem for scalable parallel I/O making use of new hardware, Non-volatile main memory (NVDIMM) and non-volatile storage class memory (NVRAM); (3) New fault tolerant architecture combining general-purpose processors and special purpose reconfigurable processors (FPGA); (4) Scalable algorithms for deeply-hieratical memory and storage architecture; (5) New communication algorithm making use of the Post-K Tofu 6D mesh/torus network for fast data transfer of for multi-petabyte of big data; (6) Scalable shared library loading for Python-based applications such as machine learning and deep learning (7) Usability enhancement of HPC systems with container techniques and multi-platform package manager; (8) Other research and software development related to big data, machine learning and I/O. We will proactively collaborate with domestic and international researchers from private companies, academia and national laboratories. With the momentum gained through these collaborations, we will strengthen our international presence in extreme-scale big data processing

15.5 Publications

15.5.1 Conference Papers

[1] Tianqi Xu, Kento Sato and Satoshi Matsuoka, "Explorations of Data Swapping on Burst Buffer", The 24th IEEE International Conference on Parallel and Distributed Systems (ICPADS 2018), Sentosa, Singapore, Dec, 2018.

[2] Yue Zhu, Fahim Chowdhury, Huansong Fu, Adam Moody, Kathryn Mohror, Kento Sato and Weikuan Yu, "Entropy-Aware I/O Pipelining for Large-Scale Deep Learning on HPC Systems", IEEE International Symposium on the Modeling, Analysis, and Simulation of Computer and Telecommunication Systems (MASCOTS 2018), Milwaukee, USA, Sep, 2018.

[3] Yue Zhu, Teng Wang, Kathryn Mohror, Adam Moody, Kento Sato, Muhib Khan and Weikuan Yu, "Direct-FUSE: Removing the Middleman for High-Performance FUSE File System Support", The 8th International Workshop on Runtime and Operating Systems for Supercomputers (ROSS 2018) in conjunction with the 27th International Symposium on High-Performance Parallel and Distributed Computing (HPDC 2018), Tempe, Arizona, USA, June 2018.

15.5.2 Posters

[4] Yue Zhu, Fahim Chowdhury, Huansong Fu, Adam Moody, Kathryn Mohror, Kento Sato and Weikuan Yu, "Multi-Client DeepIO for Large-Scale Deep Learning on HPC Systems", In Proceedings of the International Conference on High Performance Computing, Networking, Storage and Analysis 2018 (SC18), Regular Poster, Dallas, USA, Nov, 2018.
[5] Tianqi Xu, Kento Sato and Satoshi Matsuoka, "HuronFS: Hierarchical, User-level and On-demand Burst Buffer File System", In Proceedings of the International Supercomputing Conference (ISC 2018), Frankfurt, Germany, USA, June, 2018.

15.5.3 Software

[6] HuronFS: Hierarchical, user-level and on-demand file system, 2017

Chapter 16

Data Assimilation Research Team

16.1 Members

Takemasa Miyoshi (Team Leader)

Koji Terasaki (Research Scientist)

Shigenori Otsuka (Research Scientist)

Shunji Kotsuki (Research Scientist)

Guo-Yuan Lien (Postdoctoral Researcher/Visiting Scientist)

Takumi Honda (Postdoctoral Researcher)

Atsushi Okazaki (Postdoctoral Researcher)

Kohei Tatakama (Postdoctoral Researcher)

James Taylor (Postdoctoral Researcher)

Arata Amemiya (Postdoctoral Researcher)

Yasumitsu Maejima (Research Associate)

Hazuki Arakida (Technical Staff)

Taeka Awazu (Technical Staff)

Hideyuki Sakamoto (Technical Staff)

Marimo Ohhigashi (Technical Staff)

Kenta Kurosawa (Technical Staff)

Shinichiro Shima (Visiting Scientist)

Juan J. Ruiz (Visiting Scientist)

Shu-Chih Yang (Visiting Scientist)

Stephen G. Penny (Visiting Scientist)

Kozo Okamoto (Visiting Scientist)

Michiko Otsuka (Visiting Scientist)

Yohei Sawada (Visiting Scientist)

Shohei Takino (Visiting Scientist)

John C. Wells (Visiting Scientist)

Pierre Tandeo (Visiting Scientist)

Hironori Arai (Visiting Scientist)

Keiichi Kondo (Visiting Scientist)

Cheng Da (Student Trainee)

Stefan Geiss (Student Trainee)

Paula Maldonado (Student Trainee)

Aulia Febianda Anwar Tinumbang (Intern)

Viet Phi Huynh (Intern)

Andrew Pensoneault (Intern)

Tobias Necker (Intern/Student Trainee)

Yukie Komori (Assistant)

Rie Deguchi (Assistant)

Kuki Kuniya (Assistant)

Saeko Imano (Assistant)

16.2 Research Activities

Data Assimilation Research Team (DA Team) was launched in October 2012 and is composed of 28 research and technical staff including 12 visiting members as of March 2019. Data assimilation is a cross-disciplinary science to synergize computer simulations and real-world data, using statistical methods and applied mathematics. As computers become more powerful and enable more precise simulations, it will become more important to compare the simulations with actual observations. DA Team performs cutting-edge research and development on advanced data assimilation methods and their wide applications, aiming to integrate computer simulations and real-world data in the wisest way. Particularly, DA Team tackles challenging problems of developing efficient and accurate data assimilation systems for "big simulations" with real-world "big data" from various sources including advanced sensors. The specific foci include 1) theoretical and algorithmic developments for efficient and accurate data assimilation, 2) data assimilation methods and applications by taking advantage of the world-leading K computer and "big data" from new advanced sensors, and 3) exploratory new applications of data assimilation in wider simulation fields. These advanced data assimilation studies will enhance simulation capabilities and lead to a better use of the K computer.

In FY2018, we continued on the ongoing data assimilation research in the following aspects: 1) theoretical research on challenging problems, 2) leading research on meteorological applications, 3) optimization of computational algorithms, and 4) exploratory research on wider applications. We also explored close collaborations with several research teams within the R-CCS Research Division. We have made substantial progress on the following research items:

Theoretical research

- Non-Gaussian PDF in DA was investigated using the Lorenz-63 3 variable model.
- Non-Gaussian PDF in DA was investigated with the 10240-member ensemble produced previously in 2014 using a simplified atmospheric general circulation model SPEEDY (1 paper submitted).
- A particle filter was applied to the cellular automata of 3 state sheep model.
- Estimation of model and observation uncertainties in DA was investigated (1 review paper submitted).
- A local particle filter was developed and tested with SPEEDY.
- Weight structure of the Local Ensemble Transform Kalman Filter (LETKF) was investigated with SPEEDY.
- Bias correction methods including nonlinear and nonparametric approaches were explored and some preliminary experiments using the Lorenz96 model were performed.
- Non-Gaussian PDF in DA at convection-allowing resolutions was investigated using the Scalable Computing for Advanced Library and Environment (SCALE)-LETKF system.

Leading research on meteorological applications

- A 30-second update, 100-m-resolution, 100-member ensemble DA system for the Phased-Array Weather Radar (PAWR) assimilation was developed with SCALE-LETKF. SCALE and LETKF were combined to a single executable to accelerate the computation.
- Analyses on the SCALE-LETKF ensemble predictions during the July 2018 heavy rain event were conducted.
- Impact of assimilating all-sky Himawari-8 observations on Typhoon-induced precipitation was investigated (1 paper published).
- The SCALE-LETKF realtime system toward a very short-term localized rainfall forecast was developed on Oakforest-PACS.
- The observational operator for PAWR in SCALE-LETKF was improved, and its impact on forecasts was investigated.
- Impact of 30-second-update PAWR DA was investigated using the 100-m-mesh SCALE-LETKF for the west Japan heavy rainfall event in July 2018.
- An observation operator for high frequency lightning DA was investigated.
- A series of observing system simulation experiments for surface DA was conducted (1 paper published).
- 30-second-cycle LETKF assimilation of dual PAWR observations to short-range convective forecasts was investigated.
- Impact of three-body scatter spikes from PAWR to short-range convective forecasts was investigated.
- Radar data assimilation experiments with SCALE-LETKF were performed using RELAMPAGO-CACTI field campaing data in Argentina.
- Ensemble-based sensitivity analyses at convection-allowing resolution were performed using SCALE-LETKF (1 paper submitted).
- Impact of assimilating radar-based precipitation observations as fractions was investigated.
- We kept running the three-dimensional precipitation nowcasting system with the PAWR at NICT Kobe, and the prediction was disseminated on our website and a smart phone application by MTI Ltd.
- Experiments with NHM-LETKF were conducted to investigate an impact of assimilating Himawari-8 observations on detecting a local severe storm at an early stage of its development (1 paper published).
- The Nonhydrostatic Icosahedral Atmospheric Model (NICAM)'s precipitation forecasts were improved by model parameter estimation with DA (1 paper published).
- Predictability of the Heavy Rainfall in July 2018 was investigated with the NICAM-LETKF Japan Aerospace Exploration Agency (JAXA) Research Analysis (NEXRA) (1 paper published).
- Reproducibility of heavy rainfall in western Japan in July 2018 was investigated with the 28-km-resolution NICAM-LETKF system.
- An ensemble-based observation impact estimation algorithm was incorporated into the NICAM-LETKF.
- Heavy ice precipitation observed by the Global precipitation measurement (GPM) dual frequency precipitation radar (DPR) was compared with a 3.5-km NICAM simulation.
- Precipitation forecasts were improved by merging NICAM and spatio-temporal extrapolation forecasts GSMaP RNC (1 paper published in FY2019).
- Long-term stability of NICAM-LETKF was investigated (1 paper published).
- Including the observation error correlation in DA was investigated with the NICAM-LETKF system. We found that reconditioning the observation error covariance matrix stabilizes the data assimilation and improves the analyses.
- The NICAM-LETKF system was upgraded to assimilate the satellite radiance data of the advanced technology microwave sounder (ATMS).
- We kept running the global precipitation nowcasting system with the Global Satellite Mapping of Precipitation (GSMaP) by JAXA, and the prediction was disseminated on our website and JAXA's website (1 paper submitted).
- Impact of precipitation radar onboard next-generation satellite on NWP was investigated (1 paper submitted).
- An object-based verification method of precipitation pattern was investigated using pattern recognition techniques (1 paper submitted).
- An LETKF system to assimilate pattern features of precipitation areas was implemented with an intermediate AGCM. A feature based on the fractions skill score was tested.
- Regional atmospheric DA coupled with an ocean mixed layer model was developed and tested with a case of typhoon Soudelor in 2015.

- A coastal ocean DA system was developed and tested with a case of Tokyo Bay.
- A lake DA system was developed and tested with a case of Lake Biwa.
- The local weather around Lake Biwa was simulated with SCALE, including notably winds.
- A prototype system of machine-learning-based dam operation optimization was developed in collaboration with Tokyo Electric Power Company Holdings, Incorporated.
- Land-atmosphere-coupled DA system was developed based on the NICAM-LETKF.
- Deep learning for the prediction of rainfall was investigated in collaboration with IMT Atlantique.

Computational optimization

- A new NICAM-LETKF system was developed for the next-generation flagship supercomputer "Fugaku" in collaboration with the Computational Climate Science Research Team and FS2020.
- The computational performance of the "Big Data Assimilation" problem with the SCALE-LETKF was improved. We achieved the goal of updating the analyses every 30 seconds at 250-m resolution.
- We implemented the SCALE-LETKF with the Data Transfer Framework (DTF) developed by the System Software Research Team to enable the real-time "Big Data Assimilation" experiments.

Wider applications

- DA experiments were performed with the Moderate resolution Imaging Spectroradiometer (MODIS) leaf area index (LAI) observations and the Spatially-Explicit, Individual-Based Dynamic Global Vegetation Model (SEIB-DGVM) over Siberia.
- SEIB-DGVM DA experiments were performed with the MODIS LAI observations at Takayama Flux site in Japan.
- A feasibility study was conducted for the application of the SEIB-DGVM DA system to vegetation management toward the sustainable development goals (SDGs).
- A particle filter was applied to a press-forming manufacturing simulation.

Several achievements are selected and highlighted in the next section.

16.3 Research Results and Achievements

16.3.1 Predictability of the heavy rainfall in July 2018 by NICAM-LETKF

The record-breaking rainfall in Japan in July 2018 (hereafter RJJ18) was successive torrential rains occurred in Hokkaido and western Japan from late June to mid July 2018. RJJ18 caused a number of floods and debris flows throughout western Japan, making it the severest flood-related disaster in Japan since the Nagasaki flood in 1982. As shown above, the DA-team has been developing regional and global NWP systems. The Japan Meteorological Agency (JMA) issued "special heavy rainfall warnings" to 11 prefectures on July 6 and 7, 2018. We focus on intense rain on July 6 and 7. Therefore, this study investigates predictabilities and characteristics of RJJ18 on July 6, with SCALE-LETKF and NICAM-LETKF.

With a coarser-resolution version of NICAM-LETKF (112 km for horizontal), we found that the intense rains in July 6 was tied to the generation of a low-pressure system in the middle of the frontal system over the Sea of Japan. With the near-real-time NICAM-LETKF system (NEXRA), intense precipitation in western Japan on July 6 was well predicted 3 days in advance (Fig. 16.1). Observation impact estimates showed that radiosondes in Kyusyu and off the east coast of China significantly reduced the forecast errors. Since the forecast errors grew more rapidly during RJJ18, data assimilation played a crucial role in improving the predictability (Kotsuki et al. 2019).

We also performed data assimilation and forecast experiments using NICAM-LETKF at horizontal resolution of 112 and 28 km. A cold air inflow from Okhotsk high is one of the important factors to intensify the heavy rainfall in western Japan. The results show that the 28-km resolution forecast experiment outperforms the 112-km resolution forecast experiment in terms of the location and intensity of the heavy rainfall (Fig. 16.2). The 112-km forecast experiment also successfully reproduces the heavy rain by the Baiu front; however, the location of the heavy rain is shifted northward compared with the observation and 28-km experiment.

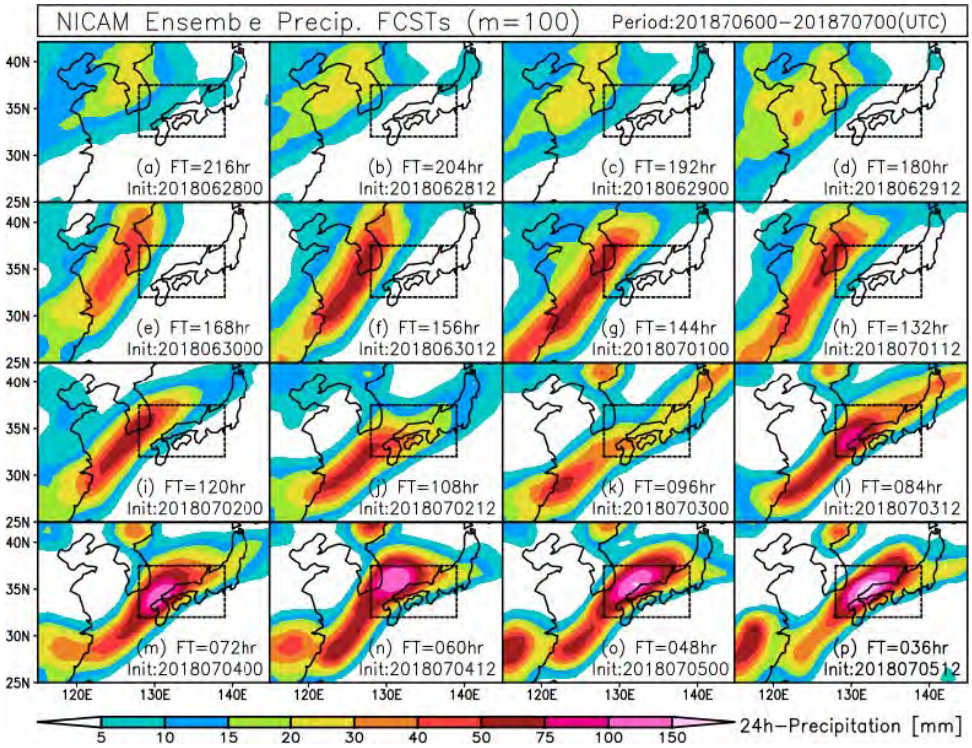

Figure 16.1: Ensemble-mean precipitation (mm), accumulated over 0000–2400 UTC 6 July 2018 for 16 forecasts initialized every 12 h from (a) 0000 UTC 28 June to (p) 1200 UTC 5 July 2018. (Adopted from Kotsuki et al., 2019).

16.3.2 SCALE-LETKF experiments during the July 2018 heavy rain event

16.3.2.1 Analyses on the predictability using the ensemble predictions

The near-real-time (NRT) SCALE-LETKF system was developed by Lien et al. (2017) and has been running since May 2015. The system assimilates conventional observations every 6 hours with a 50-member ensemble. In July 2018, stationary precipitation band associated with the Baiu front induced a record-breaking rainfall and caused catastrophic destruction in Japan. This study aims to investigate the predictability of this torrential rainfall event and important factors that contributed to the heavy precipitation by conducting ensemble forecasts.

Figure 16.3 shows the 24-hour accumulated precipitation amount in the NRT SCALE-LETKF ensemble forecasts and Japan Meteorological Agency (JMA) radar data on July 5. In the ensemble forecasts initiated at 00 UTC July 1 (hereafter 00Z/01), a heavy precipitation band is predicted, but the predicted precipitation area is too large compared to the JMA radar data. In the 00Z/02 ensemble forecasts, the precipitation region becomes narrow, and the precipitation amount is close to the JMA radar data compared to that in the 00Z/01 ensemble forecasts. Therefore, the July 2018 heavy precipitation is well predicted by the NRT SCALE-LETKF system about 3 days in advance.

To clarify important factors for predicting the heavy precipitation, we compare the 00Z/01 and 00Z/02 ensemble forecasts. Figure 16.4 shows the meridional wind at the 1.6 km height and mean sea level pressure valid at 00 UTC July 5. In the 00Z/02 ensemble forecasts, the intensity of Typhoon Prapiroon (2018) over the Sea of Japan is strong and close to the Best track estimate compared to the 00Z/01 forecasts. Strong northerly wind over the Sea of Japan may play an important role in predicting the heavy precipitation band at the correct location.

16.3.2.2 30-second-update, 100-m-mesh PAWR DA

We performed 30-second-update, 100-m-mesh DA experiments with and without PAWR observations for a severe rainfall event that occurred on July 6, 2018 around Kobe city. By assimilating the PAWR data (TEST), radar reflectivity at 2-km level shows better matching with the PAWR observation compared to NO-DA analysis

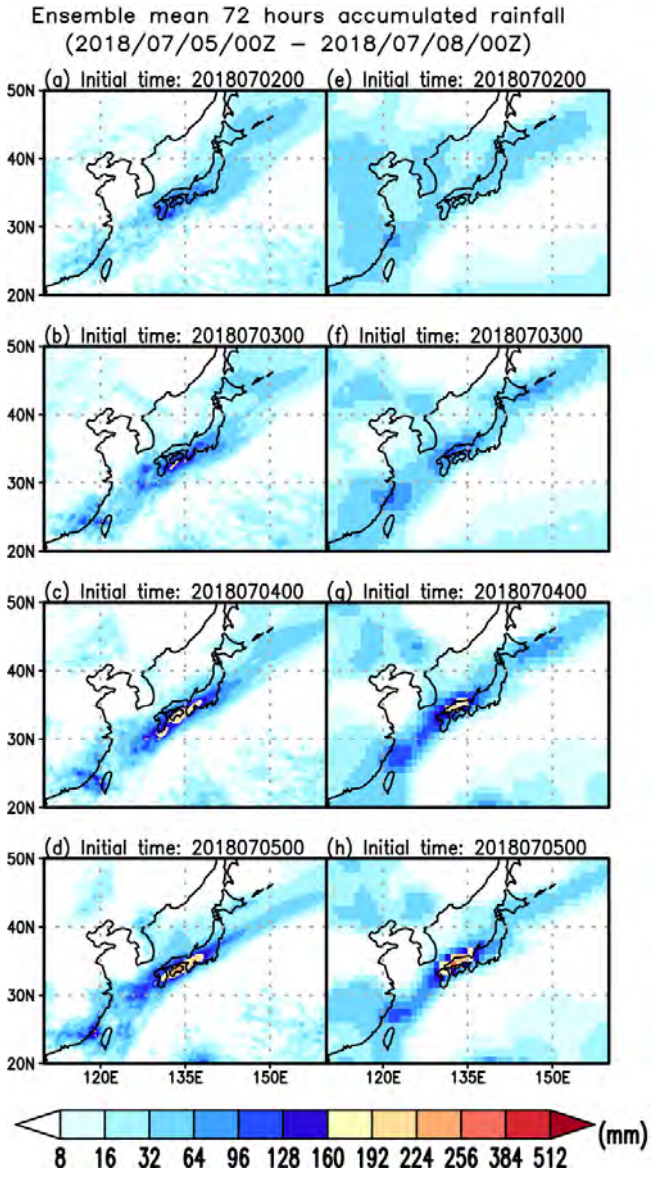

Figure 16.2: 72 hours accumulated rainfall from 0000 UTC 5 July 2018 to 0000 UTC 8 July 2018 with (a–d) glevel-8 and (e–h) glevel-6 experiments (Adopted from Terasaki and Miyoshi, 2019, in prep.).

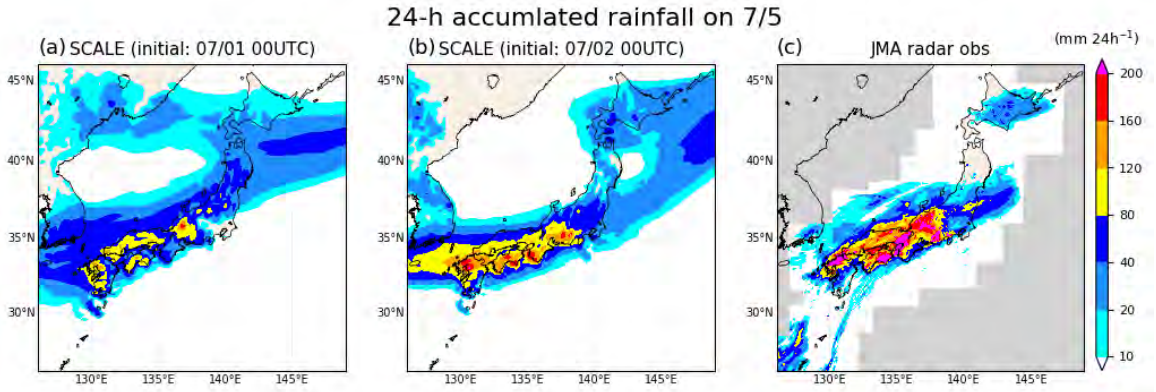

Figure 16.3: (a), (b) Ensemble-mean 24-hour accumulated precipitation amount on July 5 in the SCALE ensemble forecasts initiated at (a) 00 UTC July 1 and (b) 00 UTC July 2. (c) 24-hour accumulated precipitation amount in the JMA radar data on July 5. (Adopted from Honda et al., 2019, in prep.)

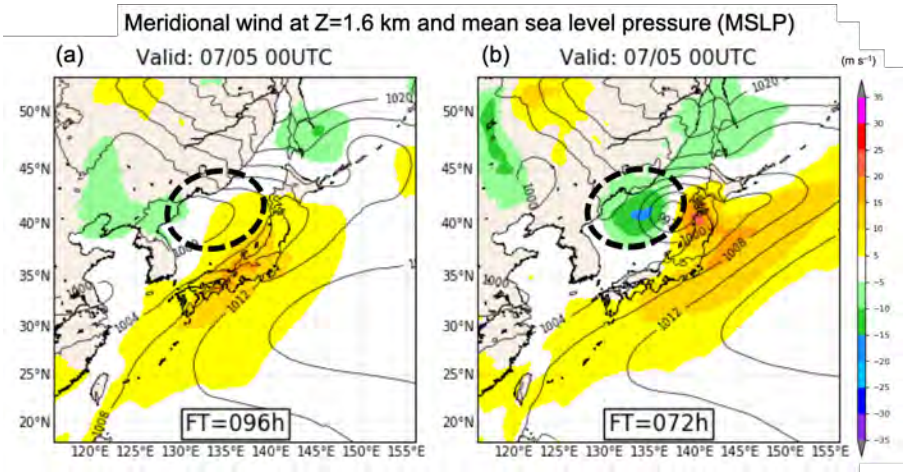

Figure 16.4: Horizontal maps of ensemble-mean meridional wind at the 1.6 km height (color shading, m s^{-1}) and mean sea level pressure (contours, hPa) in the ensemble forecasts initiated at (a) 00 UTC July 1 and (b) July 2 valid at 00 UTC July 5. The dashed circles denote the northerly wind region over the Sea of Japan in the 00Z/02 forecasts. (Adopted from Honda et al., 2019, in prep.)

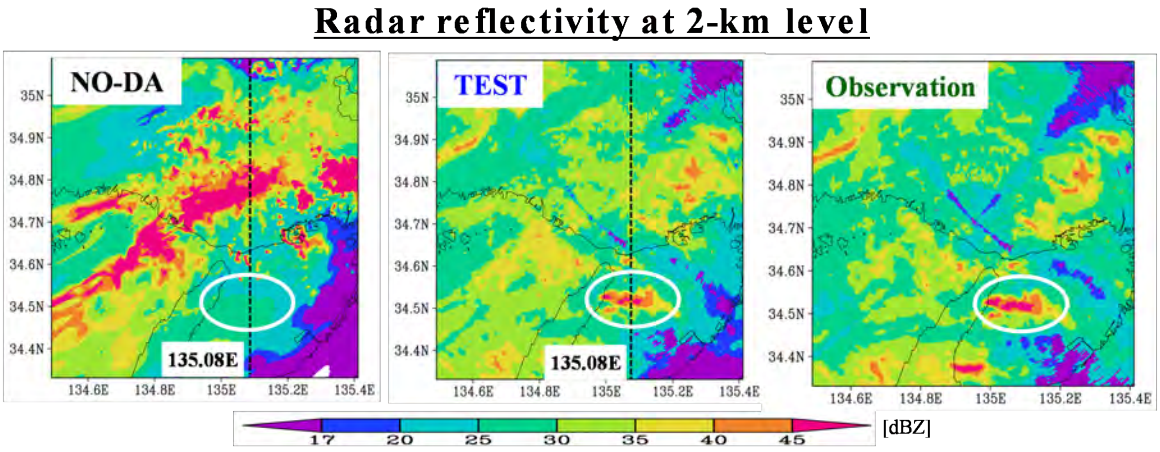

Figure 16.5: Radar reflectivity at the 2-km elevation at 1040 JST on July 6, 2018 after 50 LETKF cycles for (a) NO-DA analysis, (b) TEST analysis, and (c) PAWR observation. (Adopted from Maejima et al., 2019, in prep.)

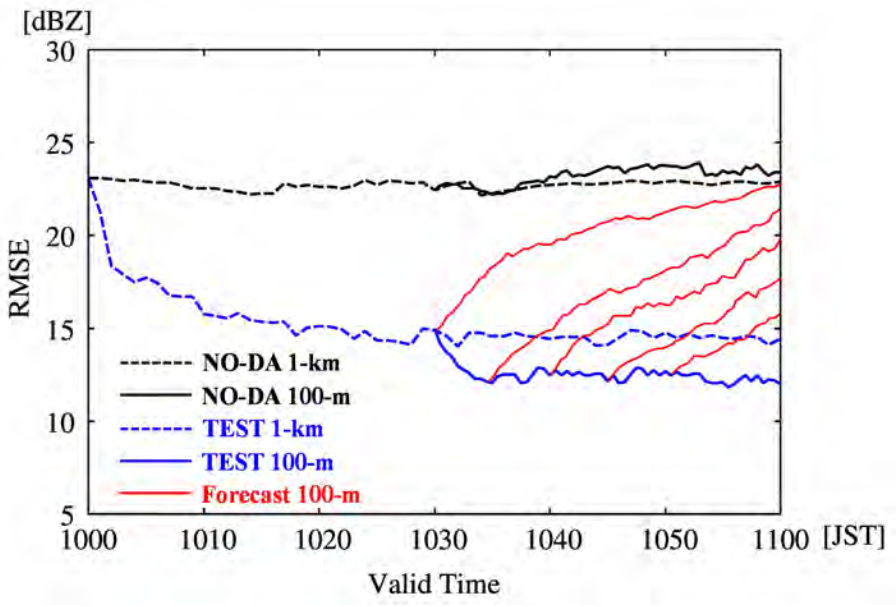

Figure 16.6: Time series of RMSE for radar reflectivity [dBZ] at the 2-km elevation on July 6, 2018. (Adopted from Maejima et al., 2019, in prep.)

(Fig. 16.5). The forecasts initialized by the analyses of TEST were also skillful compared with NO-DA, although the skill decreased rapidly (Fig. 16.6). The results suggest that the PAWR DA has a potential to improve the numerical simulation for this torrential rainfall event.

16.3.3 Optimizing hydroelectric dam operations with machine learning techniques

This study aims to achieve more efficient dam operations using state-of-the-art machine learning techniques in collaboration with Tokyo Electric Power Company. For that purpose, we are developing successive three machines as follows. The first machine improves precipitation forecasts by numerical weather prediction, extending the traditional model output statistics (MOS) methods. The second machine emulates a river runoff model and predicts the river inflow using the precipitation forecasts from the first machine. In the first and second machines, we apply supervised learning using observed radar and river inflow data as the references, respectively. The third machine aims to maximize the total power generation following operational restrictions for safety by using the reinforcement learning technique. Figure 16.7 shows the predicted precipitations by the first machine, showing successful precipitation movements associated with the typhoon. Our preliminary experiments demonstrated that the machine-learning-based dam operations potentially increased hydroelectric power generations compared to heuristic dam operations.

16.3.4 Accounting for observation error correlations in an ensemble Kalman filter

It is known that observations measured with the same instrument such as atmospheric motion vectors and satellite radiances have correlated errors. Satellite radiances have error correlations not only between channels but also in the horizontal. Previous studies successfully assimilated the satellite radiances with explicit consideration of inter-channel error correlations. For better use of dense observations, it would be essential to account for the horizontal observation error correlations, but no study has investigated the impact so far. In this study, we extended the NICAM-LETKF system to include the horizontal error correlation in observation error covariance $\mathbf{R}$. Figure 16.8 shows the time-series of the analysis RMSEs for temperature examined with the idealized OSSE case. Accounting for the horizontal observation error correlations improves the analyses by drawing more information from observations. We also tested to account for the observation error correlations with real observations and showed beneficial impacts on the analyses.

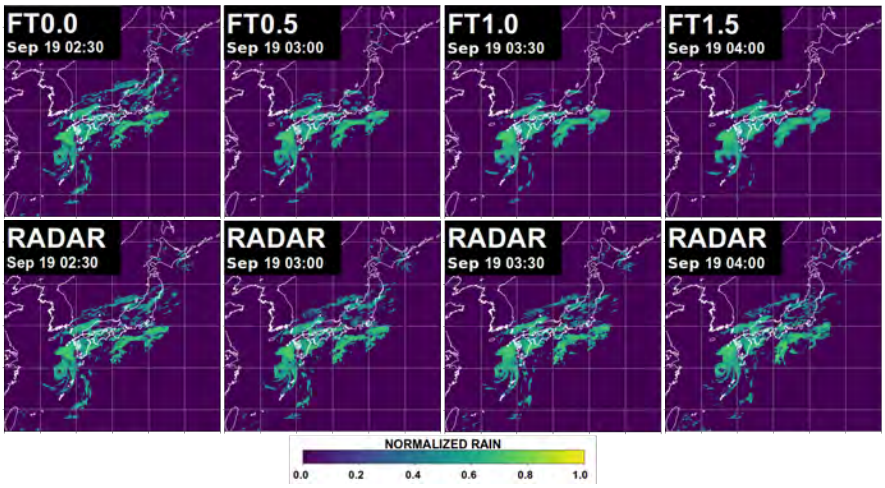

Figure 16.7: Predicted precipitations with machine learning (top panels) versus the actual rainfall (bottom panels) for forecast lead times 0, 0.5, 1.0 and 1.5 hours.

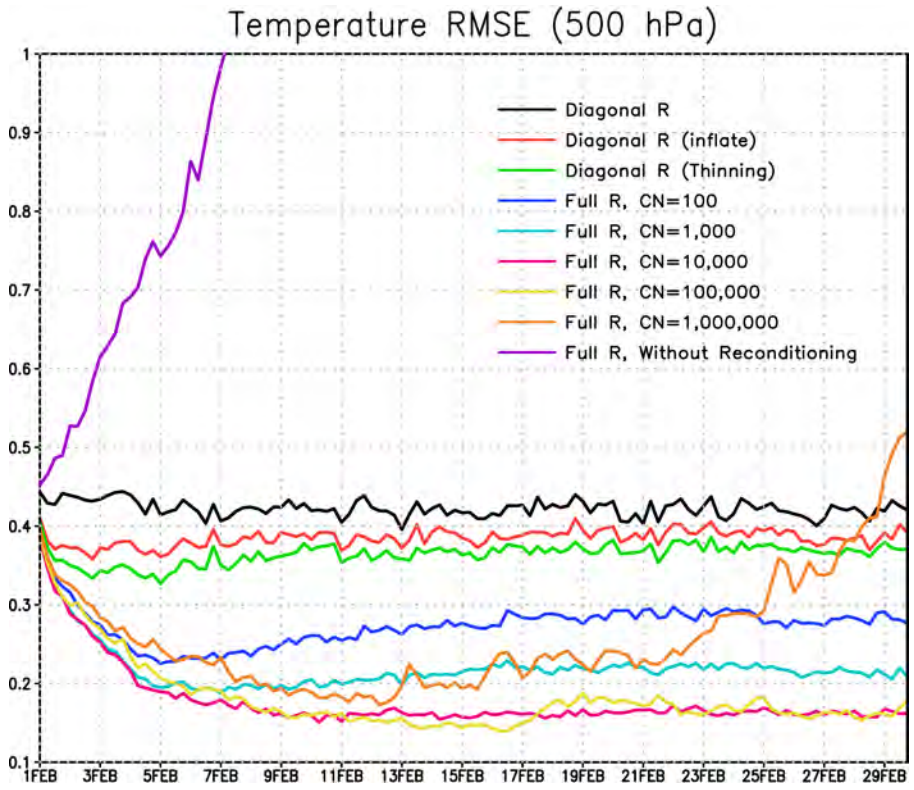

Figure 16.8: Time-series of the analysis root mean square errors (RMSEs) for temperature (K) at 500 hPa. Black, red, and green lines are the diagonal **R** matrix. Purple line is the full **R** matrix without reconditioning. Blue, light blue, magenta, yellow, and orange lines are the full **R** matrix with reconditioning.

16.4 Schedule and Future Plan

DA Team aims to explore the frontier of large-scale DA problems, and to be a world's leader in DA research. With the goals in mind, we plan to continue working on the three fundamental foci: 1) theoretical and algorithmic developments for efficient and accurate DA (core focus), 2) DA methods and applications by taking advantage of the Japan's flagship supercomputer and "Big Data" from new advanced sensors (lead focus), and 3) exploratory new applications of DA in wider simulation fields (pioneer focus). We have very strong projects in weather forecast applications, and we will enhance the leading research to the world's top level. Also, we will pioneer new application fields that have direct connection with societal benefits. For direct benefit to society, "real-time" application is essential with efficient computational algorithms, which are also an important aspect of our research.

"Big Data Assimilation" (BDA) is one of the major activities that we have developed in the past years. The prototype system showed promising results, but the physical performance for the 30-minute forecast of precipitation patterns can be improved. We will continue to work on the development of the BDA system to further improve the computational and physical performances toward the upcoming "Fugaku" era.

Beyond the direct future of the BDA effort, we can extend the idea of BDA to a broader perspective: integration of "Big Data" and "Big Simulation." New sensors provide orders of magnitude more data, and simulations become more precise. Collaborative work with computer scientists will be essential to utilize the complex high-performance computer systems effectively. In addition, dense sensor data tend to have complicated error structures such as correlated errors, and the proper treatment is necessary to fully utilize the "Big Data." The current DA methods usually assume no observation error correlation. Based on our previous theoretical research on the observation-error correlations, we plan to develop methods to consider the observation error correlations in realistic NWP applications.

Treating the model errors and non-Gaussian probability distribution has been grand challenges in DA. "Big Ensemble Data Assimilation" with the largest-ever 10240 samples was a milestone providing fundamental data to investigate the non-Gaussian probability distribution. We have developed expertise and exclusive dataset to tackle these challenges.

DA is a cross-disciplinary science based on statistical mathematics and dynamical systems theory. In addition, DA connects simulations and real-world data. Therefore, it is naturally beneficial to enhance close collaborations with experts in mathematics, sensor technology, and various application fields. The current weather-forecast projects involve active collaborations with observation experts. In addition, we have been teaching semester-long courses on DA at the Department of Mathematics, Kyoto University, and this will lead to more collaborations with mathematicians. Moreover, TL Miyoshi has joint appointments at RIKEN iTHEMS (Interdisciplinary Theoretical and Mathematical Sciences Program) and RIKEN CPR (Cluster for Pioneering Research), and these will enhance broader collaborations. Collaborations with other R-CCS Research Teams will also be beneficial. The challenges for future DA systems require cross-disciplinary collaborations to most effectively use the massive supercomputers with more heterogeneous architecture design. Further, RIKEN's Engineering Network already gave us opportunities to collaborate among different disciplines among RIKEN centers. RIKEN President's Initiative for "DA innovation hub" also helped expand collaboration. We also started collaborations with industry partners for more direct benefit to society. Enhancing the broader collaborations is a key to success, i.e., to make a new scientific movement across the borders through DA as an innovation hub, to establish DA as a new scientific paradigm, and to change the world through innovation and education of DA.

16.5 Publications

16.5.1 Awards

[1] Takemasa Miyoshi, Gold Medal Prize, Yomiuri Techno Forum, ビッグデータ同化によるゲリラ豪雨予測の研究, 4/25/2018

[2] Takemasa Miyoshi, RIKEN BAIHO Award (RIKEN Excellent Achievement Award), For FY2017 excellent achievement on Research and Development for Research to Fuse Data Analysis with Simulations, 6/5/2018

[3] Takumi Honda, the Yamamoto Award, Meteorological Society of Japan, A study on data assimilation of new-generation geostationary satellite observations, 10/30/2018

[4] Takemasa Miyoshi, Excellent Achievement Award, HPCI (High Performance Computing Infrastructure) Project Report Meeting Program Committee, 11/2/2018

[5] Shunji Kotsuki, RIKEN Oubu Research Incentive Award, Advancing Ensemble Data Assimilation-based Global Weather Forecast System, 3/12/2019

16.5.2 Articles

[1] Kotsuki, S., Terasaki, K., Yashiro, H., Tomita, H., Satoh, M., and Miyoshi, T. (2018). Online model parameter estimation with ensemble data assimilation in the real global atmosphere: A case with the Nonhydrostatic Icosahedral Atmospheric Model (NICAM) and the Global Satellite Mapping of Precipitation data. *J. Geophys. Res. Atmos.*, **123**, 7375–7392, doi:10.1029/2017JD028092.

[2] Otsuka, M., H. Seko, K. Shimoji, and K. Yamashita, 2018: Characteristics of Himawari-8 rapid scan atmospheric motion vectors utilized in mesoscale data assimilation. *J. Meteorol. Soc. Japan*, **96B**, 111–131, doi:10.2151/jmsj.2018-034.

[3] Kotsuki, S., K. Terasaki, K. Kanemaru, M. Satoh, T. Kubota, and T. Miyoshi, 2019: Predictability of Record-Breaking Rainfall in Japan in July 2018: Ensemble Forecast Experiments with the Near-Real-Time Global Atmospheric Data Assimilation System NEXRA. *SOLA*, **15A**, 1–7, doi:10.2151/sola.15A-001.

[4] 荒木田葉月, 三橋 弘宗, 鎌田 磨人, アンケート調査に基づくシギ・チドリ類への影響要因の関連性分析, 保全生態学研究, 2018, **23 (2)**, 199–221, doi:10.18960/hozen.23.2_199.

[5] Furue, R., K. Takatama, H. Sasaki, N. Schneider, M. Nonaka, and B. Taguchi, 2018: Impacts of sea-surface salinity in an eddy-resolving semi-global OGCM. *Ocean Modelling*, **122**, 36–56, doi:10.1016/j.ocemod.2017.11.004.

[6] 筒井浩行, 澤田洋平, 小池俊雄, 植生動態－陸面データ同化システムアウトプットを用いたオーストラリア大陸の渇水解析, 土木学会論文集*B1*（水工学）, 2017, **73 (4)**, I_1237–I_1242, doi:10.2208/jscejhe.73.I_1237.

[7] 田中智大, 渡部哲史, 小槻峻司, 林義晃, 丸谷靖幸, 峠嘉哉, 山崎大, 木村匡臣, 田上雅浩, 江草智弘, 橋本雅和, 仲吉信人, 最前線の水文・水資源学, 水文・水資源学会誌, 2018, **31 (6)**, 509–540, doi:10.3178/jjshwr.31.509.

[8] Honda, T., S. Takino, and T. Miyoshi, 2019: Improving a precipitation forecast by assimilating all-sky Himawari-8 satellite radiances: a case of typhoon Malakas (2016). *SOLA*, **15**, 7–1, doi:10.2151/sola.2019-002.

[9] Komori, N., T. Enomoto, T. Miyoshi, A. Yamazaki, A. Kuwano-Yoshida, and B. Taguchi, 2018: Ensemble-based atmospheric reanalysis using a global coupled atmosphere-ocean GCM. *Mon. Wea. Rev.*, **146**, 3311–3323, doi:10.1175/MWR-D-17-0361.1.

[10] Hatfield, S. E., Düben, P. D., Chantry, M., Kondo, K., Miyoshi, T., and Palmer, T. N. (2018). Choosing the optimal numerical precision for data assimilation in the presence of model error. *Journal of Advances in Modeling Earth Systems*, **10**, 2177–2191, doi:10.1029/2018MS001341.

[11] Okamoto, K, Sawada, Y, Kunii, M. Comparison of assimilating all-sky and clear-sky infrared radiances from Himawari-8 in a mesoscale system. *Quart. J. Roy. Meteorol. Soc.*, 2019, **145**, 745–766, doi:10.1002/qj.3463.

[12] Sawada, Y., Okamoto, K., Kunii, M., and Miyoshi, T. (2019). Assimilating every-10-minute Himawari-8 infrared radiances to improve convective predictability. *J. Geophys. Res. Atmos.*, **124**, 2546–2561, doi:10.1029/2018JD029643.

[13] Maejima, Y., T. Miyoshi, M. Kunii, H. Seko, and K. Sato, 2019: Impact of dense and frequent surface observations on 1-minute-update severe rainstorm prediction: a simulation study, *J. Meteorol. Soc. Japan*, **97 (1)**, 253–273, doi:10.2151/jmsj.2019-014.

[14] Terasaki, K., S. Kotsuki, and T. Miyoshi, 2019: Multi-year analysis using the NICAM-LETKF data assimilation system. *SOLA*, **15**, 41–46, doi:10.2151/sola.2019-009.

16.5.3 Invited Talks

[1] T. Miyoshi, 天気予報の数理：データ同化と予測可能性, 第26回JST数学キャラバン, Osaka, Japan, 5/13/2018

[2] T. Miyoshi, データ同化：シミュレーションと実測データを融合するデータサイエンス, 九大–理研–福岡市・ISIT 三者連携シンポジウム「数理・ＡＩが解く未来！～計算科学の展開と期待～」, Fukuoka, Japan, 5/15/2018

[3] T. Miyoshi, 次世代スーパーコンピュータとビッグデータが拓く未来の気象予測,「日本気象学会2018年度春季大会」シンポジウム, Tsukuba, Japan, 5/18/2018

[4] T. Miyoshi, ゲリラ豪雨を予測する, 2018年ゴールド・メダル賞受賞記念講演会, Tokyo, Japan, 5/19/2018

[5] Terasaki, K., T. Miyoshi, Accounting for the observation error correlation in data assimilation, JpGU2018, Chiba, Japan, 5/20/2018

[6] Okazaki, A., Miyoshi, T., Yoshimura, K., Zhang, F., Toward online data assimilation for the millennium reanalysis, JpGU 2018, Chiba, Japan, 5/22/2018

[7] Guo-Yuan Lien, Takemasa Miyoshi, Issues regarding maintaining ensemble spreads, balance, and high-resolution information in rapid-update-cycle radar data assimilation with the LETKF, JpGU2018, Chiba, Japan, 5/20/2018

[8] Guo-Yuan Lien, Seiya Nishizawa, Ryuji Yoshida, Hisashi Yashiro, Tatiana Martsinkevich, Takumi Honda, Shigenori Otsuka, Takemasa Miyoshi, Hirofumi Tomita, and Yutaka Ishikawa, The computational aspect of the SCLAE-LETKF data assimilation system for rapid-update-cycle, high-resolution radar data assimilation, JpGU2018, Chiba, Japan, 5/20/2018

[9] Takemasa MIYOSHI, Shunji KOTSUKI, Koji TERASAKI, Keiichi KONDO, Guo-Yuan LIEN, Kenta KUROSAWA, Masaki SATOH, Hirofumi TOMITA, and Eugenia KALNAY, Enhancing Data Assimilation of GPM Observations, AOGS, Honolulu, Hawaii, 6/4/2018

[10] T. Miyoshi, 気象予測研究の最先端！～ゲリラ豪雨を予測せよ！, 2018年度葦クラブ研究会, Nagoya, Japan, 8/6/2018

[11] T. Miyoshi, Advancing Data Assimilation as a Science Hub: From Weather Forecasting and Beyond, MADA2018, Le Bourget-du Lac, France, 8/29/2018

[12] T. Miyoshi, データ同化：シミュレーションと実測データを融合するデータサイエンス, 10回放射光学会若手研究会, Tokyo, Japan, 9/3/2018

[13] T. Miyoshi, ポスト京時代のデータ同化応用拡大への展望, 日本機械学会2018年度年次大会, Osaka, Japan, 9/10/2018

[14] Guo-Yuan Lien, Takemasa Miyoshi, Takumi Honda, Shigenori Otsuka, Rapid-update-cycle high-resolution assimilation of radar data: Results from exploratory experiments and potential for operational prediction, 2018 Conference on Weather Analysis and Forecasting, Taipei, Taiwan, 9/11/2018

[15] Hironori Arai, Wataru Takeuchi,Kei Oyoshi, Lam Dao Nguyen,Towa Tachibana, Ryuta Uozumi,Koji Terasaki, Takemasa Miyoshi, Hisashi Yashiro, Kazuyuki Inubushi. GHG observation of rice field, Joint JECAM/Asia-RiCE Meeting, Taichung City, Taiwan, 9/17/2018

[16] T. Miyoshi, Innovating “Big Data Assimilation” technology for revolutionizing very-short-range severe weather prediction, CREST Symposium on Big Data Application, Tokyo, Japan, 9/30/2018

[17] T. Miyoshi, Satellite data assimilation and parameter estimation with NICAM-LETKF, CEN/CliSAP WORKSHOP “Climate Data Assimilation,” Hamburg, Germany, 10/5/2018

[18] Sawada, Y., T. Nakaegawa, T. Miyoshi, and T. Ushiyama, Hydrometeorology as an inversion problem: Can river discharge observations improve the atmosphere by ensemble data assimilation?, 9th Japanese Data Assimilation Workshop, Tokyo, Japan, 10/10/2018

[19] T. Miyoshi, Data assimilation for nonlinear ensemble forecasts, Fourth meeting of the WWRP PDEF Working Group, Tokyo, Japan, 10/11/2018

[20] T. Miyoshi, Pushing the limits: Big Data Assimilation research at RIKEN, Open session with JMA: Sharing plans for international research, JMA HQ Auditorium, Tokyo, Japan, 10/12/2018

[21] T. Miyoshi, データ同化による最先端予報研究：予報士と切り拓く、これからの天気予報, 日本気象予報士会東京支部第63回会合, Tokyo, Japan, 10/20/2018

[22] Hironori Arai, Wataru Takeuchi,Kei Oyoshi, Lam Dao Nguyen,Towa Tachibana, Ryuta Uozumi,Koji Terasaki, Takemasa Miyoshi, Hisashi Yashiro, Kazuyuki Inubushi. Satellite data based transparent MRV system of GHGs emission from Asian agricultural ecosystems. 11th GEOPSS Asia Pacific Sympodium, Group on Earth Observations, Kyoto, Japan, 10/24/2018

[23] Hironori Arai, Wataru Takeuchi,Kei Oyoshi, Lam Dao Nguyen,Towa Tachibana, Ryuta Uozumi,Koji Terasaki, Takemasa Miyoshi, Hisashi Yashiro, Kazuyuki Inubushi. Monitoring GHG emission from rice cropping and the dissemination status of mitigation activities. 11th GEOPSS Asia Pacific Sympodium, Group on Earth Observations, Kyoto, Japan, 10/25/2018

[24] T. Miyoshi, Big Data Assimilation: achievements and future directions, Meteorological Society of Japan 2018 Fall Meeting, Ogura Special Lecture Joint Session, Sendai, Japan, 10/29/2018

[25] T. Honda, 新世代静止気象衛星観測のデータ同化に関する研究, 日本気象学会2018年山本賞受賞記念講演, 日本気象学会秋季大会, Sendai, Japan, 10/30/2018

[26] T. Miyoshi, 気象学におけるAI活用を考える, 日本気象学会2018年度秋季大会専門分科会「人口知能（AI）は気象学にブレイクする—をもたらすか？」, Sendai, Japan, 10/31/201

[27] T. Miyoshi, ゲリラ豪雨予測を目指した「ビッグデータ同化」の研究, 第5回「京」を中核とするHPCIシステム利用研究課題成果報告会, Tokyo, Japan, 11/2/2018

[28] T. Miyoshi, データ同化研究～ゲリラ豪雨予測からその先へ～, 理化学研究所科学講演会, Tokyo, Japan, 11/3/2018

[29] T. Miyoshi, NICAMとSCALEを使ったデータ同化研究－観測ビッグデータとスパコン「京」のコラボレーション、ビッグデータで見える世界－, 5th International Workshop on Nonhydrostatic Models(NHM2018) オープンセミナー「非静力学モデリングの進展と数値気象予測の今後の展望」, Tokyo, Japan, 11/16/2018

[30] T. Miyoshi, Prediction Science: The 5th Paradigm Fusing the Computational Science and Data Science, BDEC2, Indiana, USA, 11/29/2018

[31] T. Miyoshi, 「ポスト京」による高度天気予報活用社会、基礎科学力の強化に関する勉強会（自民）, Tokyo, Japan, 12/4/2018

[32] T. Miyoshi, Big Data, Supercomputing, and Data Assimilation: Weather Prediction and Beyond “RIKEN BAIHO Awards,” The All-RIKEN Workshop 2018, Wako, Japan, 12/14/2018

[33] T. Miyoshi, データ同化研究：ゲリラ豪雨予測からその先へ, 第5回CFD技術部門委員会, Tokyo, Japan, 1/11/2019

[34] Takemasa Miyoshi, Hirofumi Tomita, Shinsuke Satoh, Tomoo Ushio,Yutaka Ishikawa, Project Report, CREST International Symposium on Big Data Application, Tokyo, Japan, 1/14/2019

[35] T. Miyoshi, Enhancing Data Assimilation of GPM Observations, The Joint PI Meeting of JAXA Earth Observation Missions FY2018, Tokyo, Japan, 1/25/2019

[36] Hironori Arai, Wataru Takeuchi,Kei Oyoshi, Lam Dao Nguyen,Towa Tachibana, Ryuta Uozumi,Koji Terasaki, Takemasa Miyoshi, Hisashi Yashiro, Kazuyuki Inubushi, Satellite data based MRV system of GHGs emission from tropical rice paddies, ALOS Kyoto & Carbon Initiative 25th Science Team meeting, Tokyo, Japan, 2/5/2019

[37] T. Miyoshi, Big Data, Supercomputing, and Data Assimilation: Weather Prediction and Beyond, LMD-X seminar, Paris, France, 2/26/2019

[38] Takemasa Miyoshi, Shigenori Otsuka, Takumi Honda, Guo-Yuan Lien, Yasumitsu Maejima, Yoshito Yoshizaki, Hiromu Seko, Hirofumi Tomita, Shinsuke Satoh, Tomoo Ushio, Tatiana V. Martsinkevich, Balazs Gerofi, Yutaka Ishikawa, Big Data Assimilation: Past 5 Years and Perspectives for the Future, ICMCX-XIII, Okinawa, Japan, 3/6/2019

[39] Hironori Arai, Wataru Takeuchi,Kei Oyoshi, Lam Dao Nguyen,Towa Tachibana, Ryuta Uozumi,Koji Terasaki, Takemasa Miyoshi, Hisashi Yashiro, Kazuyuki Inubushi, Low cost and transparent MRV system of GHG emissions based on satellite remote sensing data —case study on CH4 emission from the Mekong delta—, 27th IIS forum "Earth observation, disaster monitoring and risk assessment from space," Tokyo, Japan, 3/6/2019

[40] T. Miyoshi, ビッグデータ同化による新世代気象予測［CREST］, JST戦略的創造研究推進事業 新技術説明会～製造技術・情報・材料～, Tokyo, Japan, 3/8/2019

[41] T. Miyoshi, 「ビッグデータ同化」の技術革新の創出によるゲリラ豪雨予測の実証, ビッグデータ基盤/応用 合同領域会議, Kyoto, Japan, 3/13/2019

[42] T. Miyoshi, データ同化が拓く予測の科学, 第3回ものづくりワークショップ：バイオ車載材料の情報科学 シミュレーションとデータ同化が未来のものづくり設計を変える, Wako, Japan, 3/15/2019

[43] T. Miyoshi, Introductory Lecture for data assimilation, RIMS Gasshuku Seminar 2019 for Data assimilation, Kyoto, Japan, 3/18/2019

[44] T. Miyoshi, Big Data Assimilation: A New Science for Weather Prediction and Beyond, RIMS Gasshuku Seminar 2019 for Data assimilation, Kyoto, Japan, 3/20/2019

[45] T. Miyoshi, Big Data Assimilation: A New Science for Weather Prediction and Beyond, ADAPT Co-Sponsoresd Seminar, University Park, PA, USA, 3/25/2019

[46] T. Miyoshi, Big Data Assimilation: A New Science for Weather Prediction and Beyond, ESSIC seminar, College Park, MD, USA, 3/28/2019

16.5.4 Oral Presentations

[1] T. Miyoshi, Enhancing Data Assimilation of GPM Observations, NICAM-LETKF and Satellite DA Mtg, Kobe, Japan, 4/5/2018

[2] Takemasa Miyoshi, Shunji Kotsuki, Koji Terasaki, Keiichi Kondo, Guo-Yuan Lien, Kenta Kurosawa, Masaki Satoh, Hirofumi Tomita, and Eugenia Kalnay, Enhancing data assimilation of GPM observations, EGU, Vienna, Austria, 4/9/2018

[3] Takemasa Miyoshi, Juan Ruiz, Guo-Yuan Lien, Toshiki Teramura, Yasumitsu Maejima, Keiichi Kondo, and Hideyuki Sakamoto, How fast shall we go? Lessons learned from 30-second-update convection-resolving data assimilation experiments, EGU, Vienna, Austria, 4/10/2018

[4] Takatama, K., T. Honda, T. Miyoshi. Regional atmospheric data assimilation coupled with an ocean mixed layer model: a case of typhoon Soudelor (2015), Data Assimilation Seminar, Kobe, Japan, 4/17/2018

[5] 高玉孝平, T. Honda, 三好建正, 海洋混合層モデルを導入した大気データ同化: 台風 Soudelor (2015) の事例, 第2回 理研・気象庁データ同化研究会, Tokyo, Japan, 4/25/2018

[6] S. Kotsuki, K. Kurosawa, 三好建正: 全球大気データ同化システムNICAM-LETKFを使ったEFSO観測インパクト推定, 第2回 理研・気象庁データ同化研究会, Tokyo, Japan, 4/26/2018

[7] S. Otsuka, ナウキャストと予測可能性, 第2回理研・気象庁データ同化研究会, Tokyo, Japan, 4/26/2018

[8] Kotsuki S., Kurosawa K., and Miyoshi T.: Ensemble Forecast Sensitivity to Observations Verified with Multiple References. The 8th EnKF Data Assimilation Workshop, Montreal, Canada, 5/7/2018

[9] Takemasa Miyoshi, J. Ruiz, G.-Y. Lien, T. Teramura, Y. Maejima, K. Kondo and H. Sakamoto, "Is 30-second update fast enough for convection-resolving data assimilation?," EnKF workshop, Montreal, Canada, 5/7/2018

[10] Honda, T., T. Miyoshi, G.-Y. Lien, S. Nishizawa, R. Yoshida, S. A. Adachi, K. Terasaki, K. Okamoto, H. Tomita and K. Bessho, Assimilating All-Sky Himawari-8 Satellite Infrared Radiances: A Case of Typhoon Soudelor (2015), The 8th EnKF Data Assimilation Workshop, Montreal, Canada, 5/9/2018

[11] T. Honda, 三好建正, 降水予報改善へ向けた雲域赤外輝度温度観測同化の重要性, 日本気象学会春季大会, Tsukuba, Japan, 5/17/2018

[12] Y. Maejime, 高密度地上観測データ同化実験における観測要素別のインパクト, 日本気象学会春季大会, Tsukuba, Japan, 5/17/2018

[13] Honda, T., T. Miyoshi, On the importance of assimilating cloudy-sky infrared radiances from Himawari-8 for heavy rainfall prediction, JpGU2018, Chiba, Japan, 5/20/2018

[14] Sawada, Y., K. Okamoto, M. Kunii, and T. Miyoshi, Assimilating Himawari-8 infrared radiances to improve convective predictability, JpGU2018, Chiba, Japan, 5/20/2018

[15] Yasumitsu Maejima, Impacts of dense surface observations on predicting a torrential rainfall event on September 9 and 10, 2015 in the east Japan area, JpGU2018, Chiba, Japan, 5/20/2018

[16] 庄司悟, 岡崎淳史, 芳村圭, 気候プロキシを用いたデータ同化による千年紀気候復元, JpGU2018, Chiba, Japan, 5/22/2018

[17] Yasumitsu Maejima, Guo-Yuan Lien and Takemasa Miyoshi, Impacts of Dense Surface Observations on Predicting a Torrential Rainfall Event on September 9 and 10, 2015 in the East Japan Area, AOGS2018, Honolulu, Hawaii, 6/5/2018

[18] Otsuka, S. and T. Miyoshi, Applying data assimilation to precipitation nowcasting, AOGS2018, Honolulu, Hawaii, 6/5/2018

[19] Takemasa MIYOSHI, Juan RUIZ, Guo-Yuan LIEN, Toshiki TERAMURA, Yasumitsu MAEJIMA, Keiichi KONDO,and Hideyuki SAKAMOTO, How Fast Shall We Go? Lessons Learned from 30-second-update Convection-resolving Data Assimilation Experiments, AOGS2018, Honolulu, Hawaii, 6/5/2018

[20] S. Otsuka, Applying data assimilation to precipitation nowcasting, CREST「ビッグデータ応用」第4回若手研究者合宿, Kanagawa, Japan, 6/12/2018

[21] T. Miyoshi, 高玉孝平, 湖沼流動場へのデータ同化の適用, 戦略的国際共同研究プログラム（SICORP）, Shiga, Japan, 6/20/2018

[22] T. Miyoshi, HPC Challenges in Weather Forecast research: data-assimilation science, International HPC Summer School 2018, Ostrava, Czech Republic, 7/10/2018

[23] T. Miyoshi, Innovating “Big Data Assimilation” technology for revolutionizing very-short-range severe weather prediction, DATAIA-JST International Symposium, Paris, France, 7/11/2018

[24] S. Kotsuki, K. Terasaki, T. Miyoshi, NICAM-LETKFを用いたGPM/DPRデータ同化実験, 衛星シミュレータ—研究会, Tokyo, Japan, 7/12/2018

[25] S. Kotsuki, T. Miyoshi, EFSO観測インパクト推定を用いた予報を改悪する観測を同化しない「観測選択手法」の探索, 第9回 理研・京大データ同化研究会, Kyoto, Japan, 7/17/2018

[26] 高玉孝平, T. Honda, T. Miyoshi, SCALE-LETKF への海洋混合層モデルの導入:台風 Soudelor (2015) の事例, 旧OREDAミーティング, Yokohama, Japan, 7/25/2018

[27] T. Miyoshi,「データ同化研究」－ゲリラ豪雨予測からその先へ－, 第50回理研イブニングセミナー, Kobe, Japan, 8/1/2018

[28] T. Miyoshi, 7月豪雨の理研システムでの検討状況について, 平成30年度第1回高解像度豪雨予測とアンサンブル同化摂動手法に関する研究会, 帯広, 8/4/2018

[29] T. Miyoshi, Enhancing Data Assimilation of GPM Observations, NICAM-LETKF and Satellite DA Mtg, Kobe, Japan, 8/9/2018

[30] T. Miyoshi, 理研での予測結果：全球NICAM、領域SCALE、ナウキャスト, 平成30年7月豪雨に関する緊急対応研究会, Kobe, Japan, 8/17/2018

[31] T. Miyoshi, GPM観測のデータ同化の高度化, 2018年度降水観測ミッションサイエンスチーム国内会合, Tokyo, Japan, 9/5/2018

[32] S. Kotsuki, K. Kurosawa, T. Miyoshi, 全球大気・水文結合データ同化システムの開発; 水文ビッグデータ同化による大気・水文予測の改善に向けて, 水文・水資源学会2018年研究発表会, Mie, Japan, 9/12/2018

[33] H. Arakida, S. Kotsuki, S. Otsuka, Y. Sawada, T. Miyoshi, SDGsを目指した生態系の現地観測とシミュレーションの融合, 第 2 回生態系データ同化に関する研究会, Kobe, Japan, 9/18/2018

[34] K. Terasaki, 八代尚, 富田浩文, T. Miyoshi, 全球3.5km・1000メンバー実験に向けた新NICAM-LETKFの開発, ポスト京重点課題4サブ課題A研究連絡会, Tokyo, Japan, 9/20/2018

[35] 高玉孝平, T. Honda, T. Miyoshi, SCALE-LETKF への海洋混合層モデルの導入: 台風 Soudelor (2015) の事例, ポスト京平成30年度第2回研究連絡会, Tokyo, Japan, 9/20/2018

[36] Arakida H, Kotsuki S, Otsuka S, Sawada Y, and Miyoshi T: Data assimilation experiments with MODIS LAI observations and the dynamic global vegetation model SEIB-DGVM over Siberia, iLEAPS-Japan研究集会2018「大気－陸面プロセスの研究の進展：観測とモデルによる統合的理解」, Nagoya, Japan, 9/22/2018

[37] T. Miyoshi, 理研研究紹介, 理研－水産機構 スジアラ養殖技術高度化検討ワークショップ, Okinawa, Japan, 9/26/2018

[38] K. Terasaki, T. Miyoshi, NICAM-LETKFシステムの更新 全球28km解像度での平成30年7月豪雨事例実験, NICAM開発者会議, Gunma, Japan, 10/9/2018

[39] Kotsuki S., Pensoneault A., Okazaki A., and Miyoshi T.: Weight structure of Local Ensemble Transform Kalman Filter: A case with an intermediate AGCM, 9th Japanese Data Assimilation Workshop, Tokyo, Japan, 10/10/2018

[40] K. Terasaki, S. Kotsuki, T. Miyoshi, GSMaP降水データの観測誤差相関を考慮したデータ同化実験, 秋季日本気象学会, Sendai, Japan, 10/29/2018

[41] T. Awazu, S. Otsuka, T. Miyoshi, Fraction Skill Score を用いた降水データ同化, 日本気象学会秋季大会, Sendai, Japan, 10/30/2018

[42] T. Honda, S. Takino, T. Miyoshi, ひまわり 8 号の輝度温度同化研究:台風に伴う降水予報の改善; 日本気象学会秋季大会, Sendai, Japan, 11/1/2018

[43] Y. Maejime, T. Ushio, T. Miyoshi, 高頻度・高分解能雷観測データと100mメッシュSCALE-LETKFによるシミュレーションとの比較, 日本気象学会秋季大会, Sendai, Japan, 11/1/2018

[44] K. Kurosawa, S. Kotsuki, S. Otsuka, K. Terasaki, T. Miyoshi, 数値天気予報とナウキャストを組み合わせた全球降水予測, 日本気象学会秋季大会, Sendai, Japan, 11/1/2018

[45] K. Kurosawa, S. Kotsuki, K. Terasaki, T. Miyoshi, GPM/DPR の固体降水フラク゛の初期検証:3.5km NICAM との比較, 日本気象学会秋季大会, Sendai, Japan, 11/1/2018

[46] Honda, T., G.-Y. Lien, T. Miyoshi, Near-real-time SCALE-LETKF forecasts of the record breaking rainfall in Japan in July 2018, NHM2018, Tokyo, Japan, 11/14/2018

[47] Kotsuki S., Sato Y., Terasaki K., Yashiro H., Tomita H., Satoh M. and Miyoshi T., Model Parameter Estimation with Data Assimilation using NICAM-LETKF, NHM2018, Tokyo, Japan, 11/15/2018

[48] T. Miyoshi, シミュレーションと実測データを融合するデータサイエンス, 古気候復元研究に資する古文書データの共有化・構造化に関する研究集会, Tokyo, Japan, 11/19/2018

[49] T. Miyoshi, Enhancing Data Assimilation of GPM Observations, NICAM-LETKF and Satellite DA Mtg, Kobe, Japan, 12/17/2018

[50] T. Miyoshi, Local Particle Filter(penny&Miyoshi)手法の紹介, 第2回高解像度豪雨予測とアンサンブル同化摂動手法に関する研究会, Fukuoka, Japan, 12/22/2018

[51] Takemasa Miyoshi, RIKEN, Kobe, Japan; and S. Otsuka, T. Honda, G. Y. Lien, Y. Maejima, Y. Yoshizaki, H. Seko, H. Tomita, S. Satoh, T. Ushio, T. V. Martsinkevich, B. Gerofi, and Y. Ishikawa, Big Data Assimilation:Past 5 Years and Perspectives for the Future, AMS 99th Annual Meeting, Phoenix, USA, 1/7/2019

[52] Sawada, Y., K. Okamoto, M. Kunii, and T. Miyoshi, Assimilating every-10-minute Himawari-8 infrared radiances to improve convective predictability, AMS 99th Annual Meeting, Pheonix, USA, 1/8/2019

[53] Sawada, Y., T. Nakaegawa, and T. Miyoshi, Hydrometeorology as an inversion problem: Can river discharge observations improve the atmosphere by ensemble data assimilation?, AMS 99th Annual Meeting, Pheonix, USA, 1/9/2019

[54] Shigenori Otsuka and Takemasa Miyoshi, Three-dimensional precipitation nowcasting with the Phased-Array Weather radar, CREST Big Data App. Camp WS, Kanagawa, Japan, 1/16/2019

[55] Taylor, J., G-Y Lien, S. Satoh, T. Miyoshi and Y. Maejima, 30-second cycle LETKF assimilation of dual phased array weather radar observations to short-range convective forecasts, ISDA2019, Kobe, Japan, 1/21/2019

[56] Kotsuki S., Sato Y., Terasaki K., Yashiro H., Tomita H., Satoh M. and Miyoshi T., Model Parameter Estimation with Data Assimilation using NICAM-LETKF, ISDA2019, Kobe, Japan, 1/22/2019

[57] Okazaki, A., Honda, T., Kotsuki, S., Miyoshi, T., Precipitation radar data assimilation with an ensemble Kalman filter: an observing system simulation experiment for a typhoon case, ISDA2019, Kobe, Japan, 1/22/2019

[58] T. Miyoshi, Big Data Assimilation: Past 5 Years and Perspectives for the Future, ISDA2019, Kobe, Japan, 1/24/2019

[59] S. Kotsuki, 天気予報研究の最前線－平成30年7月豪雨の予測可能性を探る－, ポスト「京」重点課題４シンポジウム, Tokyo, Japan, 1/29/2019

[60] T. Miyoshi, データ同化から予測科学へ：水産分野の予測に向けて, 理化学研究所－水産研究・教育機構　水産資源・海洋研究連携検討ワークショップ, Yokohama, Japan, 2/6/2019

[61] Taylor, J., G-Y Lien, S. Satoh, T. Miyoshi and Y. Maejima, 30-second cycle LETKF assimilation of dual phased array weather radar observations to short-range convective forecasts, The 1st R-CCS International Symposium, Kobe, Japan, 2/18/2019

[62] T. Miyoshi, Activities at RIKEN Data Assimilation Research Team, Workshop IMT Atlantique & RIKEN, Brest, France, 2/22/2019

[63] Honda, T. and T. Miyoshi, Assimilating all-sky satellite radiances with SCALE-LETKF, Workshop IMT Atlantique & RIKEN, Brest, France, 2019/2/22

[64] Shigenori Otsuka, Marimo Ohhigashi, and Takemasa Miyoshi, A machine-learning approach for three-dimensional precipitation nowcasting. Workshop IMT Atlantique & RIKEN, Brest, France, 2019/2/22.

[65] Arata Amemiya and Takemasa Miyoshi, Parametric and non-parametric approaches to model bias estimation. Workshop IMT Atlantique & RIKEN, Brest, France, 2019/2/22.

[66] Y. Maejime, T. Ushio, T. Miyoshi, ゲリラ豪雨予報高度化に向けた 高頻度・高解像度データ同化実験, 第20回地球流体力学研究集会, Fukuoka, Japan, 3/8/2019

[67] K. Terasaki, S. Kotsuki, T. Miyoshi, NICAM-LETKFを用いた平成30年7月豪雨の予測可能性及び解像度依存性, ポスト「京」重点課題４第３回成果報告会, Yokohama, Japan, 3/14/2019

[68] H. Sakamoto, T. Miyoshi, データ同化による加工シミュレーションの高精度化, 第三回ものづくりワークショップ: バイオ車載材料の情報科学 シミュレーションとデータ同化が未来のものづくり設計を変える, Wako, Japan, 3/15/2019

[69] S. Kotsuki, K. Terasaki, K. Kurosawa, K. Kanemaru, T. Miyoshi, NICAM-LETKFを用いたGPM/DPRデータ同化実験, 平成30年度GPMおよび衛星シミュレータ合同研究集会, Nagoya, Japan, 3/18/2019

[70] K. Kurosawa, S. Kotsuki, S. Otsuka, K. Terasaki, T. Miyoshi, 数値天気予報とナウキャストを組み合わせた全球降水予測, 平成30年度GPMおよび衛星シミュレータ合同研究集会, Nagoya, Japan, 3/18/2019

16.5.5 Poster Presentations

[1] Kotsuki S., Greybush S. J., and Miyoshi T.: On the assimilation order of the serial ensemble Kalman filter: A study with the Lorenz-96 model, The 8th EnKF Data Assimilation Workshop, Montreal, Canada, 2018/5/7

[2] Kotsuki S., Terasaki K., and Miyoshi T.: Ensemble-Based Data Assimilation of GPM/DPR Reflectivity into the Nonhydrostatic Icosahedral Atmospheric Model NICAM, The 8th EnKF Data Assimilation Workshop, Montreal, Canada, 2018/5/9

[3] Y. Sawada, K. Okamoto, M. Kunii, T. Miyoshi, 積乱雲スケールの予測可能性改善に向けたひまわり8号雲域輝度温度同化, 日本気象学会春季大会, Tsukuba, Japan, 5/19/2018

[4] Okazaki, A., Honda, T., Kotsuki, S., Miyoshi, T., Dense precipitation radar data assimilation: an observing system simulation, JpGU 2018, Chiba, Japan, 5/20/2018

[5] Otsuka, S. and T. Miyoshi, Applying data assimilation to precipitation nowcasting, JpGU2018, Chiba, Japan, 5/20/2018

[6] S. Otsuka, 神戸PAWRおよびGPM/DPRで観測された平成30年7月豪雨の降水システム, 平成30年7月豪雨に関する緊急対応研究会, Kobe, Japan, 8/17/2018

[7] Y. Maejime, フェーズドアレイ気象レーダーを同化した平成30年7月豪雨の高解像度シミュレーション, 平成30年7月豪雨に関する緊急対応研究会, Kobe, Japan, 8/17/2018

[8] S. Kotsuki, K. Terasaki, T. Miyoshi, 平成30年7月豪雨の予測可能性: NICAM-LETKFを用いた100アンサンブル予測実験, 平成30年7月豪雨に関する緊急対応研究会, Kobe, Japan, 8/17/2018

[9] K. Terasaki, T. Miyoshi, NICAM-LETKFを用いた水平解像度による豪雨の再現性について, 平成30年7月豪雨に関する緊急対応研究会, Kobe, Japan, 8/17/2018

[10] T. Honda, G.-Y. Lien, T. Miyoshi, 準リアルタイムSCALE-LETKFシステムによる平成30年7月豪雨の予測, 平成30年7月豪雨に関する緊急対応研究会, Kobe, Japan, 8/17/2018

[11] M. Ohhigashi, S. Kotsuki, T. Miyoshi, S. Takino, 機械学習を用いたダム操作最適化システムの開発への取り組み, 水文・水資源学会2018年研究発表会, Mie, Japan, 9/12/2018

[12] S. Otsuka, M. Ohhigashi, T. Miyoshi, Y. Ishikawa, S. Satoh, T. Ushio, K. Koike, フェーズドアレイ気象レーダを用いた三次元降水ナウキャストの精度評価, 日本気象学会2018年度秋季大会, Sendai, Japan, 10/31/2018

[13] M. Otsuka, H. Seko, M. Hayashi, K. Koizumi, ひまわり8号最適雲解析プロダクトの同化実験（その２）, 日本気象学会2018年度秋季大会, Sendai, Japan, 10/31/2018

[14] Okazaki, A., Miyoshi, T., and Yoshimura, K., Millennium reanalysis using proxy and data assimilation, The 11th International Atmospheric Circulation Reconstructions over the Earth (ACRE) Meeting, Tokyo, Japan, 11/12/2018

[15] Koji Terasaki, Takemasa Miyoshi. Data assimilation and forecast experiments for the record-breaking rainfall event in Japan in July 2018 with NICAM-LETKF at 112-km and 28-km resolution, NHM2018, Tokyo, Japan, 11/14/2018

[16] Shigenori Otsuka, Marimo Ohhigashi, Yutaka Ishikawa, Shinsuke Satoh, and Takemasa Miyoshi, Precipitation nowcasting with Phased-Array Weather Radar: a case of July 2018 record-breaking rainfall in Western Japan, NHM2018, Tokyo, Japan, 11/14/2018

[17] Sawada, Y., K. Okamoto, M. Kunii, and T. Miyoshi, Assimilating every-10-minute Himawari-8 infrared radiances to improve convective predictability, NHM2018, Tokyo, Japan, 11/15/2018

[18] Taylor, J., G-Y Lien, S. Satoh, T. Miyoshi and Y. Maejima, 30-second cycle LETKF assimilation of dual phased array weather radar observations to short-range convective forecasts, NHM2018, Tokyo, Japan, 11/15/2018

[19] Okazaki, A., Honda, T., Kotsuki, S., and Miyoshi, T., Dense precipitation radar data assimilation with an ensemble Kalman filter: an observing system simulation experiment for a typhoon case, NHM2018, Tokyo, Japan, 11/15/2018

[20] Otsuka, M., H. Seko, M. Hayashi, K. Koizumi, Data assimilation experiments with Himawari-8 optimal cloud analysis (OCA) products, NHM2018, Tokyo, Japan, 11/15/2018

[21] Okazaki, A., Miyoshi, T., Yoshimura, K., and Zhang, F., An online data assimilation method to assimilate time-averaged observations, AGU2018, Washington DC, USA, 12/13/2018

[22] Sakamoto H, Teramura T, Miyoshi T, Non-Gaussian Measure in Gaussian Filtering Problem, ISDA2019, Kobe, Japan, 1/21/2019

[23] Koji Terasaki, Shunji Kotsuki, Takemasa Miyoshi. Accounting for the horizontal observation error correlation of precipitation observation, ISDA2019, Kobe, Japan, 1/21/2019

[24] Maejima, Y., S. Otsuka and T. Miyoshi, Assimilating every 30-second phased array weather radar data in a torrential rainfall event on July 6, 2018 around Kobe city, ISDA2019, Kobe, Japan, 1/21/2019

[25] Kurosawa, K., Kotsuki, S., Otsuka, S., Terasaki, K., Miyoshi, T., Locally Optimal Weighting of Global Precipitation Forecasts from Precipitation Nowcasting and Numerical Weather Prediction, ISDA2019, Kobe, Japan, 1/21/2019

[26] Okazaki, A., Miyoshi, T., Yoshimura, K., Zhang, F., Paleoclimate Reconstruction with Iterative Data Assimilation: An Observing System Simulation Experiment with an Intermediate AGCM, ISDA2019, Kobe, Japan, 1/21/2019

[27] Kotsuki S., Ota Y., and Miyoshi T., Adaptive covariance relaxation methods for ensemble data assimilation based on innovation statistics. ISDA2019, Kobe, Japan, 1/22/2019

[28] Kotsuki S., Terasaki K., and Miyoshi T., Ensemble-Based Data Assimilation of GPM/DPR Reflectivity into the Nonhydrostatic Icosahedral Atmospheric Model NICAM, ISDA2019, Kobe, Japan, 1/22/2019

[29] Kotsuki S., Kurosawa K., and Miyoshi T., Properties on Ensemble Forecast Sensitivity to Observations, ISDA2019, Kobe, Japan, 1/22/2019

[30] Kotsuki S., Pensoneault A., Okazaki A., and Miyoshi T., Spatial structure of weights in the Local Ensemble Transform Kalman Filter: A case with an intermediate AGCM, ISDA2019, Kobe, Japan, 1/22/2019

[31] Marimo Ohhigashi (RIKEN), Shunji Kotsuki (RIKEN), Shohei Takino (TEPCO), Takemasa Miyoshi (RIKEN), Optimizing Hydroelectric Dam Operations with Machine Learning, ISDA2019, Kobe, Japan, 1/22/2019

[32] Takatama, K., T. Honda, and T. Miyoshi, Regional atmospheric data assimilation coupled with an ocean mixed layer model: a case of typhoon Soudelor (2015), ISDA2019, Kobe, Japan, 1/22/2019

[33] Arakida, H., S. Kotsuki, S. Otsuka, Y. Sawada, T. Miyoshi, Data assimilation experiments with MODIS LAI observations and the dynamic global vegetation model SEIB-DGVM over Siberia, ISDA2019, Kobe, Japan, 1/23/2019

[34] Honda, T., G.-Y. Lien, T. Miyoshi, Near-real-time SCALE-LETKF forecasts of the record breaking rainfall in Japan in July 2018, ISDA2019, Kobe, Japan, 1/23/2019

[35] Taeka Awazu, Shigenori Otsuka, and Takemasa Miyoshi, Assimilating fractions of precipitation area: an idealized study with an intermediate AGCM, ISDA2019, Kobe, Japan, 2019/1/23

[36] Kurosawa, K., Kotsuki, S., Takemasa, M., Can hydrological observations improve global NWP in land-atmosphere-coupled data assimilation?, ISDA2019, Kobe, Japan, 1/23/2019

[37] Takatama, K., K. Kurosawa, Y. Uchiyama, and T. Miyoshi, A preliminary analysis of a newly-developed regional ocean data assimilation system: a case of Tokyo Bay in summer, ISDA2019, Kobe, Japan, 1/23/2019

[38] Taylor, J., G-Y Lien, S. Satoh, T. Miyoshi and Y. Maejima, 30-second cycle LETKF assimilation of dual phased array weather radar observations to short-range convective forecasts, AMS 99th Annual Meeting, Phoenix, USA, 2019/1/24

[39] Kotsuki S., Sato Y., Terasaki K., Yashiro H., Tomita H., Satoh M. and Miyoshi T., Model Parameter Estimation with Data Assimilation using NICAM-LETKF, 1st R-CCS International Symposium, Kobe, Japan, 2/18/2018

[40] Arakida, H., S. Kotsuki, S. Otsuka, Y. Sawada, T. Miyoshi, Data assimilation experiments with MODIS LAI observations and the dynamic global vegetation model SEIB-DGVM over Siberia, 1st R-CCS International Symposium, Kobe, Japan, 2/18/2018

[41] Marimo Ohhigashi (RIKEN), Shunji Kotsuki (RIKEN), Shohei Takino (TEPCO), Takemasa Miyoshi (RIKEN), Optimizing Hydroelectric Dam Operations with Machine Learning, 1st R-CCS International Symposium, Kobe, Japan, 2/18/2018

[42] Koji Terasaki, Takemasa Miyoshi. Data assimilation and forecast experiments for the record-breaking rainfall event in Japan in July 2018 with NICAM-LETKF at 112-km and 28-km resolution, 1st R-CCS International Symposium, Kobe, Japan, 2/18/2018

[43] Honda, T., G.-Y. Lien, T. Miyoshi, Near-real-time SCALE-LETKF forecasts of the record breaking rainfall in Japan in July 2018, 1st R-CCS International Symposium, Kobe, Japan, 2/18/2018

[44] Maejima, Y., S. Otsuka and T. Miyoshi: Assimilating every 30-second phased array weather radar data in a torrential rainfall event on July 6, 2018 around Kobe city, 1st R-CCS International Symposium, Kobe, Japan, 2/18/2018

[45] Kurosawa, K., Kotsuki, S., Takemasa, M., Can hydrological observations improve global NWP in land-atmosphere-coupled data assimilation?, 1st R-CCS International Symposium, Kobe, Japan, 2/18/2018

[46] Takatama, K., K. Kurosawa, Y. Uchiyama, and T. Miyoshi, A preliminary analysis of a newly-developed regional ocean data assimilation system: a case of Tokyo Bay in summer, 1st R-CCS International Symposium, Kobe, Japan, 2/19/2018

[47] Arakida, H., S. Kotsuki, S. Otsuka, and T. Miyoshi, Data assimilation experiments with MODIS LAI observation and the dynamic global vegetation model SEIB-DGVM at a deciduous broad-leaved forest in Japan, ESJ66, Kobe, Japan, 3/18/2019

Chapter 17

Computational Disaster Mitigation and Reduction Research Team

17.1 Members

Satoru Oishi (Team Leader)

Muneo Hori (Senior Visiting Scientist)

Hideyuki O-tani (Research Scientist)

Jian Chen (Research Scientist)

Kazuki Yamanoi (Postdosctoral Researcher)

Yasuyuki Nagano (Senior Visiting Scientist)

Masaaki Yabe (Senior Visiting Scientist)

Tsuyoshi Ichimura (Visiting Scientist)

Lalith Maddegedara (Visiting Scientist)

Kohei Fujita (Visiting Scientist)

Hiroki Motoyama (Visiting Scientist)

Tomohide Takeyama (Visiting Scientist)

17.2 Research Activities

Computational Disaster Mitigation and Reduction Research Team is aimed at developing advanced large-scale numerical simulation of natural disasters such as earthquake, tsunami, flood and inundation, for Kobe City and other urban areas in Hyogo Prefecture. Besides for the construction of a sophisticated urban area model and the development of new numerical codes, the team seeks to be a bridge between Science and Local Government for the disaster mitigation and reduction.

Computational Disaster Mitigation and Reduction Research Team is also conducting to integrate all kinds of geo hazards, water hazards and related hazards. Demand for natural disaster simulations increased related to growing number of disasters in recent years. Therefore, we are developing appropriate sets of programs which meet the demand of calculations. Computational Disaster Mitigation and Reduction Research Team is dealing with the following three kinds of research topics.

Urban model development: Research for urban hazards requires urban models which represent structure and shape of cities in numerical form. However, it takes very long time to create urban models consisting of buildings, foundations and infrastructures like bridges, ports and roads with ordinary way. Therefore, it is indispensable to invent methods which automatically construct urban models from exiting data that is basically

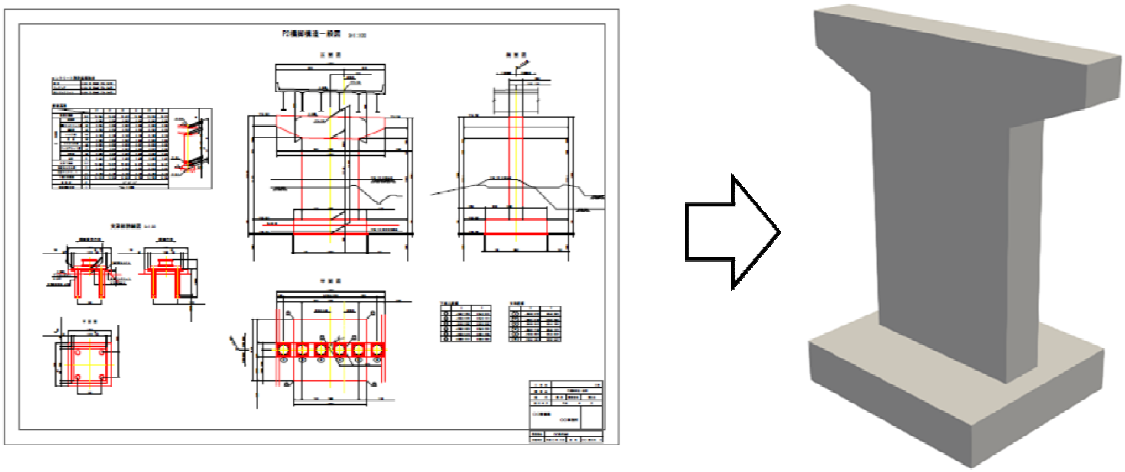

Figure 17.1: Automatically created three dimensional model of bridge pier.

ill-structured. Computational Disaster Mitigation and Reduction Research Team developed Data Processing Platform (DPP) for such purpose. By using DPP, construction of a national-wide urban model and 3D model construction from engineering drawings are achieved.

Development and improvement of simulation-based assessment for geohazards: For liquefaction hazard assessment, we extended our current framework for Monte-Carlo (MC) simulations considering multiple soil parameters which follow certain statistical distributions. The feasibility of such a prediction for an urban area of target site of the order of 10^4 has been tested. For assessing slope failures, we started to develop large scale simulations based on particle methods. Using a framework of developing parallel particle simulation code (FDPS)[1], we focused on the numerical schemes and the mechanisms of landslides in this fiscal year. A new numerical method for particle-based simulations was proposed.

Water related disaster: Frequency of water disaster has increased. Not only water itself, but sometimes also sediment cause damage to residents and their assets cooperatively. Understanding possible hazards is necessary for a measure of precaution and making less damage. Therefore, Computational Disaster Mitigation and Reduction Research Team started to deal with water and sediment related disasters by making numerical simulation model for river basins in Kobe city and Hyogo prefecture. In this year, the simulation model was also applied to the actual disaster happened in Fukuoka prefecture to evaluate its validity.

17.3 Research Results and Achievements

17.3.1 Urban model development

In this year, we developed sets of programs for creating three dimensional urban model automatically. Those programs consists of several programs developed by our original system, namely Data Processing Platform (DPP). One program extracts information from ill-constructed information sources like blue-prints and/or point group position data. Other program gives thematics of elements on blue-prints according to their levels of recognition, contexts of blue-prints which come from arrangement of lines, figures and types of blue-prints. Fig. 17.1 shows the result of three dimensional model of bridge pier from vector type design drawing. Their programming design also allows to apply it to blue-prints and point group position data by replacing elements of recognition. The programs utilize rule-base processes for recognizing elements on the drawings in order to adopting the contexts and levels of recognition. However, the programs also utilize other kinds of process for recognizing elements, then it is possible to develop each software for many kinds of drawings using division of programming the software.

[1] M. Iwasawa, et al., Publ. Astron. Soc. Japan (2016) 68 (4), 54 (1–22)

17.3.2 Improvement for liquefaction hazard assessment

In last fiscal year (FY), we incorporated Monte-Carlo (MC) simulations to take into account the uncertainties in permeability parameter. In this FY, we have enhanced it with a functionality to consider multiple soil parameters with uncertainties. Those soil parameters can be considered alone or in pairs. We also enhanced the visualization of liquefaction assessment results. In borehole logs, sometimes only the types of soil are known not the exact densities. As a demonstration, we constructed 100 soil models automatically for every individual site with an uncertainty in the specific weight of soils. From the statistical features of the simulation results, we can make predictions. The worst scenario can be determined by picking up the maximum of excessive pore water pressure (EPWP) ratio of each site and the most optimistic case using the minimum of EPWP ratio of each site. Also the median value can be used. The median value is more appropriate than the arithmetic mean value since it is a pressure ratio that is used for assessing liquefaction hazard. In Fig. 17.2 (a), we show the median values of EPWP for the total 11151 sites in the target urban area. We also worked to enhance the visualization of simulation results, e.g., using a heat map as shown in Fig. 17.2 (b). This study has been presented as a keynote in a mini-symposium of an international conference, ICCM2018 Rome, Italy. We also succeeded to publish this high performance computing based liquefaction assessment as a journal paper in Engineering Geology, see Article 4 in the list below.

17.3.3 Development for landslide hazard assessment

For assessing landslide hazards, we started to develop a simulation code for landslides based on FDPS. Since FDPS provides those common routines needed for parallelizing a general particle method, we focused on the numerical schemes and the mechanisms of landslides. We firstly developed a new scheme for particle simulation, which is an improvement of a mathematical reformulation of MPS, improved MRMPS (iMRMPS) for short. To test the applicability and robustness of iMRMPS and its simplification, different types of target functions have been used. For each target function, we create 20 different configurations of neighboring particles, see Fig. 17.3 (a) as an example, to obtain the relative errors for the gradient and for the Laplacian. Numerical experiments showed that using 20 samples is sufficient to obtain statistically meaningful results from the iMRMPS. In Fig. 17.3 (b), we show the performance of iMRMPS, together with the conventional MPS and MRMPS, for a third-order polynomial function. As can be seen, the results from iMRMPS demonstrate the highest accuracy. The relative error of the simplification of iMRMPS is about 4 orders smaller than the original MPS and MRMPS. The details of this research was published as a journal paper, see Article 5 in the list below. We also presented this study as an invited talk in ISSPDS Shanghai 2018.

17.3.4 Application of Distributed Rainfall-Sediment Runoff/Inundation Simulator

From last fiscal year, Computational Disaster Mitigation and Reduction Research Team have been developing the DRSRIS (Distributed Rainfall-Sediment Runoff/Inundation Simulator) which deal with underground flow, overland flow, river flow, bed load transport, and suspended load transport employing the finite volume method on Cartesian staggered grid. In order to make a validation of the simulator, we conduct the simulation on the Akatani river catchment, Asakura city, Fukuoka prefecture which is damaged by the heavy rainfall event in July 2017. In this calculation, radar-based precipitation observation data (XRAIN) and 10m resolution DEM data by Geospatial Information Authority of Japan (GSI) and satellite-based land use data opened by JAXA are used for the input conditions. Fig. 17.4 (left) shows the topographic deformation expressed by the difference of the ground level before and after the disaster event. Fig. 17.4 (right) shows the snapshot of the water level at the peak of the rainfall event [7]. These results are agreed with the actual inundated area which surrounded by the white lines, however, the width of the inundated area is thinner compared with the actual one at some lower sections. The reason for this underestimation seems that the current simulation method doesn't consider the sediment movement as debris flow. Currently, we are trying to integrate the debris flow movement process on the simulator. By this integration, it is expected that not only improvement of reproducibility but also the direct input method of landslides as the upper boundary conditions will be established.

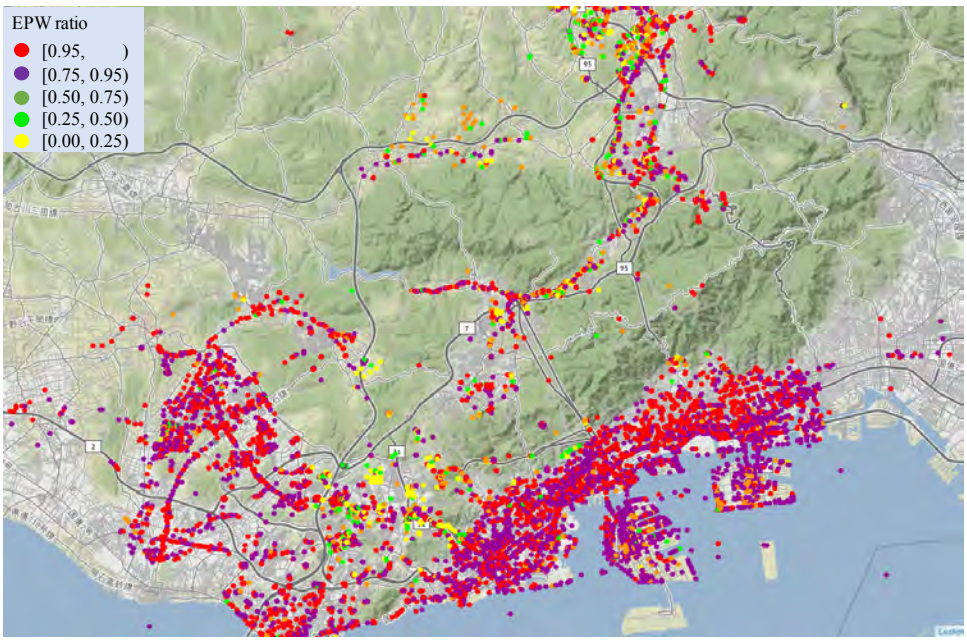

(a)

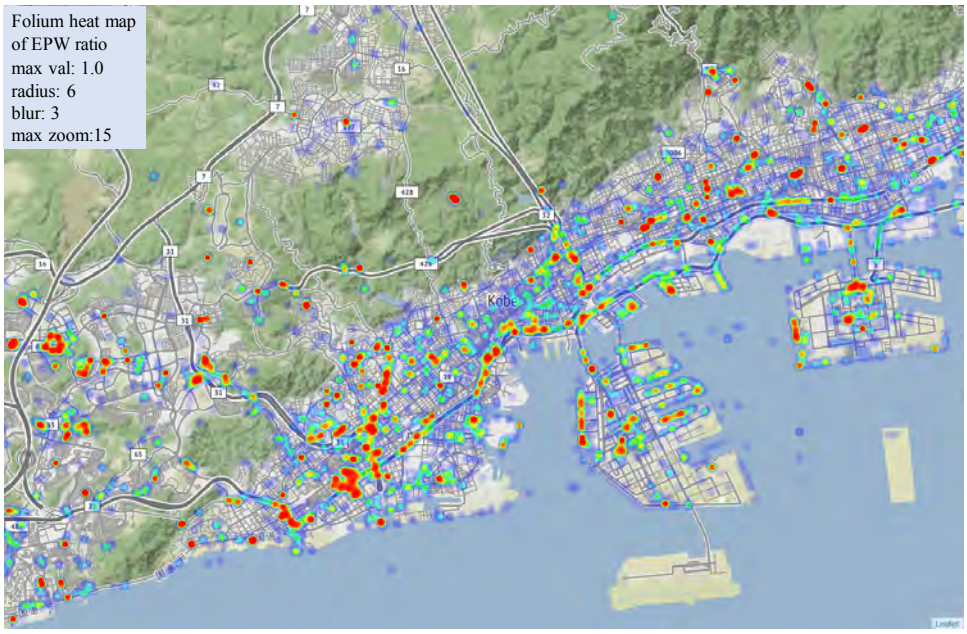

(b)

Figure 17.2: Monte-Carlo simulations considering soil uncertainties: (a) The median value of the excessive pore water pressure (EPWP) ratio of each site from the simulations of 100 statistical soil models with uncertainties in soil specific weight. (b) A heat map visualization of the same EPWP ratio results using python and folium.

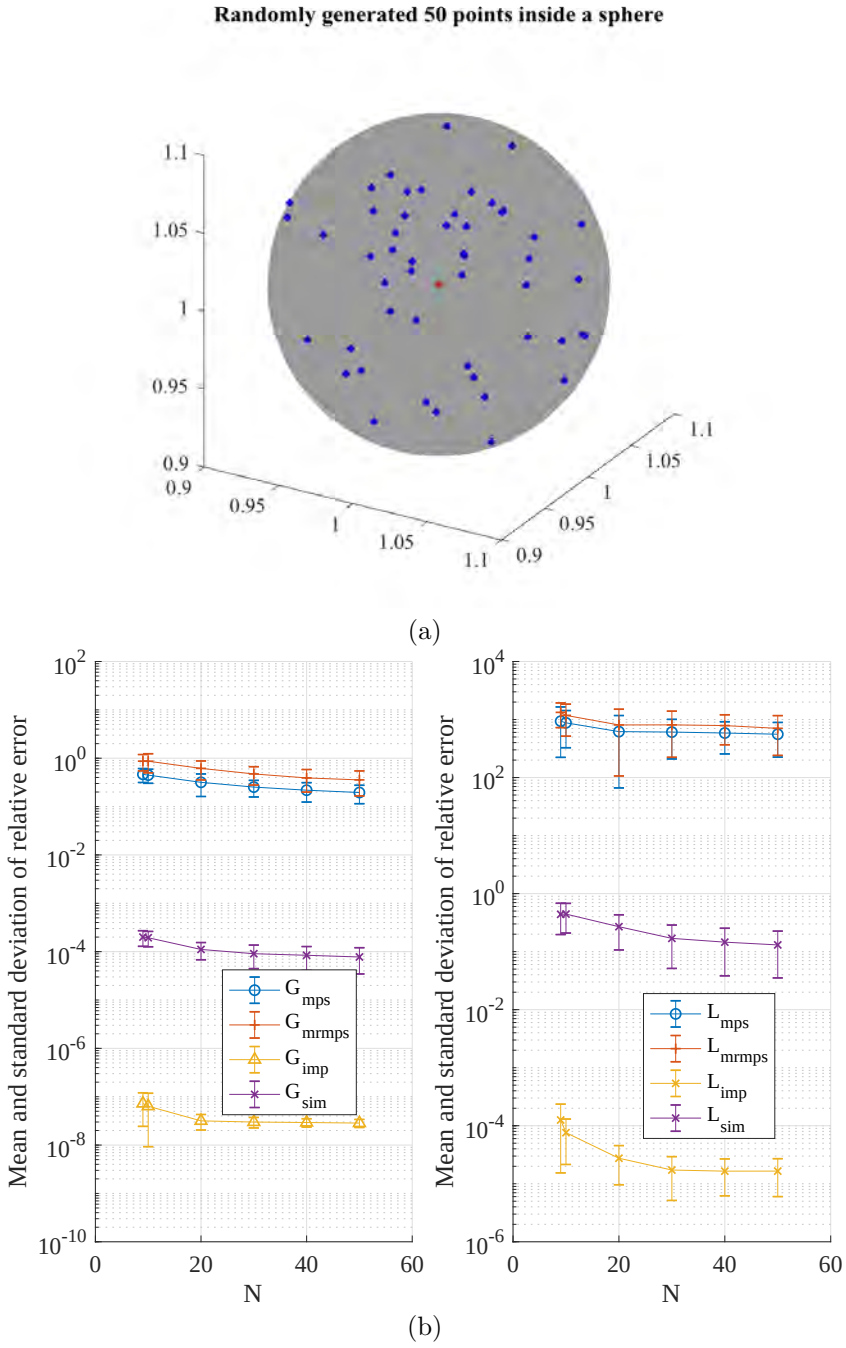

Figure 17.3: Configuration of test settings and comparison with conventional methods: (a) A target point in red and randomly distributed neighboring particles in a sphere; (b) The mean and standard deviation of the relative errors in computing the gradient (G) and the Laplacian (L) of the third order polynomial function. Four methods, i.e., MPS, MRMPS, iMRMPS (imp) and its simplification (sim) are compared.

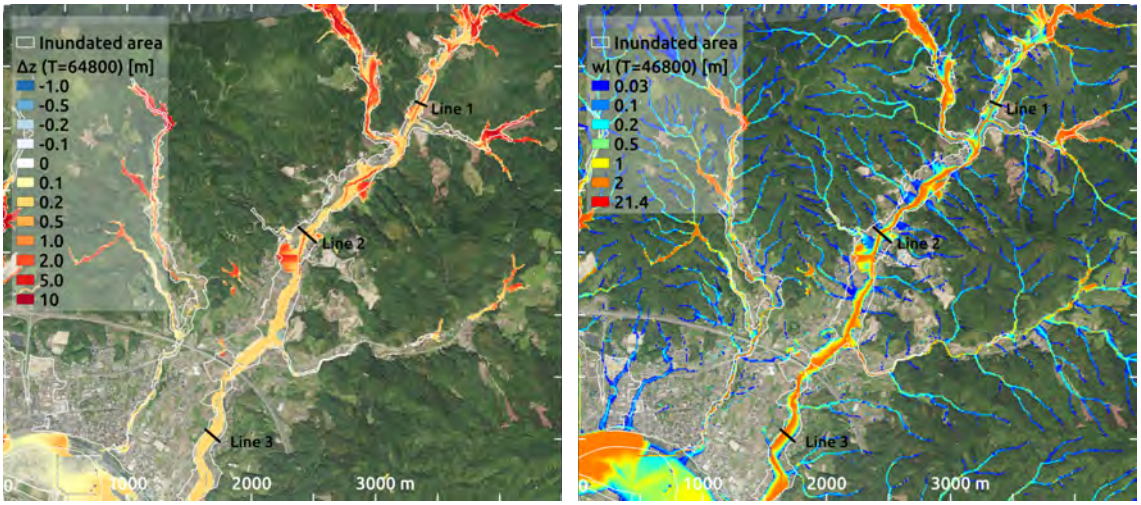

Figure 17.4: The results on the topographical deformation (left) and snapshot of the water level which is defined as the water surface height from the original ground level[1].

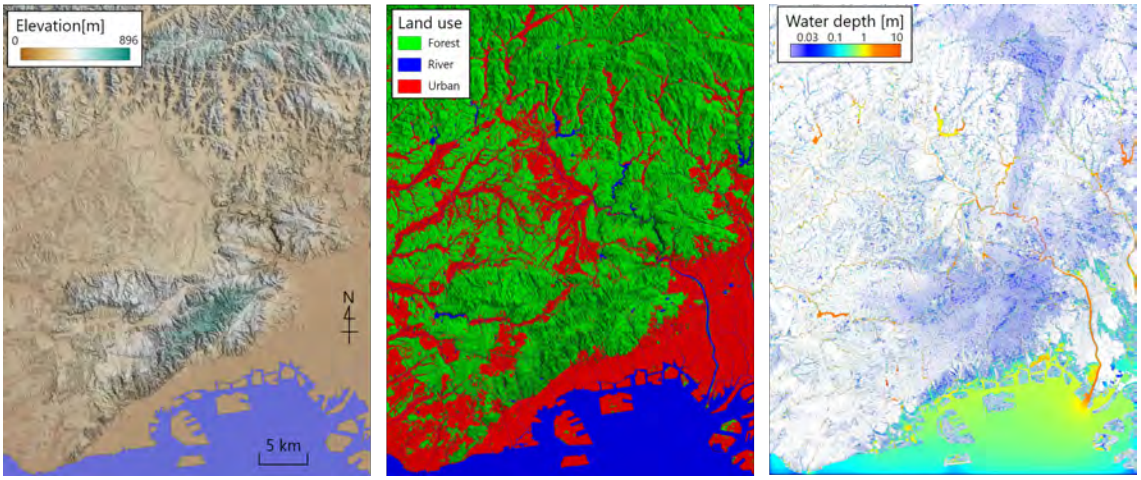

Figure 17.5: Input condition of the elevation (left) and landuse (center) in the simulation, and shapshot of the simulated water depth at 12:00, Augst 10, 2014 in the target region.

17.3.5 Application of DRSRIS to the Mukogawa River Basin and Rokko Mountain Area

The area including Mukogawa river watershed and Rokko mountain in Hyogo Prefecture has a high potential of the sediment and water-related disasters, because of its dense population and frequent slope failures. Additionary, landslides and/or weakening of the strength of the ground due to large-scale earthquakes can increase its potential. To estimate the risk of such a multi-hazard oriented disaster, we are now trying to apply DRSRIS to this area by using a large number of nodes of the K computer. As a first application, flood by Typhoon Halong in 2014 (T1411), which is one of the recent large rainfall events, is selected to verify the reproducibility. Fig. 17.5 (left) and Fig. 17.5 (center) shows the input condition on the topographic elevation and land use respectively. One example of the simulated water depth at noon, Augst 10, 2014 are shown in Fig. 17.5 (right). In the results, inundation took place in some areas where inundation did not actually occur. One of the reasons is the error of the ground survey data around embankments and bridges. Manual modifications may solve the problem, however, it requires large effort. For this reason, we have been started to develop an algorism for automatic resolution of the topographic error.

17.4 Schedule and Future Plan

[1] Developing a national-wide real-time disaster simulation: We will enhance the automation of DPP to collect real-time seismic information and to perform an automated disaster simulation in a certain target area. This will reveal the extent to which speeding up is required for real-time characteristics.

[2] Construction of templates for high fidelity models of highway network: In the template-based methodology, we need to ready the templates in beforehand, and the quality and quantity of templates will be critical to the output model.

[3] Developing an algorism for resolving the topographic error to improve the quality of the simulation and establish efficient data preparation on the large-scale simulation.

[4] Testing the rapid extraction from SAR observation employing AI based method using the multiple simulation results as learning data.

[5] Damage estimation of the sediment and water-related disasters in urban area considering the ground condition change due to an earthquake.

17.5 Publications

17.5.1 Articles

[1] H. O-tani, M. Hori, L. Wijerathne: Automated Model Construction for Seismic Disaster Assessment of Pipeline Network in Wide Urban Area, Earthquakes, Intech (2018), doi: 10.5772/intechopen.78725
[2] M. Hori, T. Ichimura, L. Wijerathne, H. Ohtani, J. Chen, K. Fujita and H. Motoyama: Application of High Performance Computing to Earthquake Hazard and Disaster Estimation in Urban Area, Front. Built Environ. (2018) , doi: 10.3389/fbuil.2018.00001
[3]Hiroyuki Fujiwara, Hiromitsu Nakamura, Shigeki Senna, Hideyuki Otani, Naoya Tomii, Kiyonori Ohtake, Toshiya Mori, Shojiro Kataoka, Development of a Real-Time Damage Estimation System, Journal of Disaster Research, Vol.14, No.2, 315-332, 2019.
[4] Chen, J., O-tani, H., Takeyama, T., Oishi, S. and Hori, M. (2019). "Toward a numerical-simulation-based liquefaction hazard assessment for urban regions using high-performance computing." Engineering Geology, 258, 105153.
[5] Chen, J., Hori, M., O-tani, H. and Oishi, S. (2018). "An Improvement of a Mathematical Interpretation of Moving Particle Semi-Implicit Method." Journal of Japan Society of Civil Engineers, Ser. A2, 74 (2), p. I_167-I_178.
[6] Bi, C.K., Fu, B.R., Chen, J., Zhao, Y.D., Yang L., Duan Y.L. and Shi, Y. (2018). "Machine Learning Based Fast Multi-Layer Liquefaction Disaster Assessment." World Wide Web: Internet and Web Information Systems, Online.
[7] Yamanoi, K., O-TANI, H., Chen, J., Oishi, S., and Hori, M. (2018). "Development of a Distributed Water-Sediment Runoff-Inundation Model and Its Application to Haki Area, Asakura City.",Journal of Japan Society of Civil Engineers, Ser. B1 (Hydraulic Engineering), Vol. 74, No. 5, pp. I_889- I_894.

17.5.2 Oral Talks

[8] Chen, J., Nonaka, S., O-tani, H., Yamanoi, K., Takeyama, T., Oishi, S. and Hori, M. (2018). "Developing large scale simulations for slope stability analysis based on FDPS." The 1st International Symposium on Seismic Performance and Design of Slopes (ISSPD), Shanghai, August 2018, Invited talk.
[9] Chen, J., Takeyama, T., O-tani, H., Oishi, S. and Hori, M. (2018). "Stochastic Liquefaction Hazard Assessment for Urban Regions Based on Soil Dynamics." The 9th International Conference on Computational Methods (ICCM2018), Rome, August 2018, Keynote.

Chapter 18

Computational Structural Biology Research Team

18.1 Members

Florence Tama (Team Leader)

Miki Nakano (Research Scientist)

Sandhya Tiwari (Special Postdoctoral Researcher)

Sahil Chhabra (Intern - 3months from University of Michigan)

Yumeno Kusahara (Assistant)

18.2 Overview of Research Activities

Biological molecular complexes of such as proteins and RNAs are of great interest in the area of molecular biology, as they are involved in cell replication, gene transcription, protein synthesis, regulation of cellular transport and other core biological functions. Those systems undergo large conformational transitions to achieve functional processes. Therefore, characterization of dynamical structures of these macromolecular complexes is crucial to understand their functional mechanisms and play an important role in the development of new drugs to treat human disease.

Experimentally, X-ray crystallography has been the primary tool to study protein conformations, providing high-resolution structures. Even though cryo electron microscopy (EM) had provided limited resolution data, it revealed critical information on structure and dynamics of large biological molecules. More recently, efforts like in RIKEN/SPring 8 have focused on developing intense X-ray free-electron laser (XFEL) light sources, which offer a new possibility to image single biological macromolecules. Since crystallization is not necessary for such a protein structure analysis, it would be possible to investigate the structure of biomolecules under various physiological conditions or to observe elementary steps of a biochemical function. However, at the current experimental condition, it cannot achieve atomic level resolution such as obtained by X-ray crystallography.

Computationally, methods have been developed to predict structures from low-resolution data such as cryo-EM either using rigid body fitting or flexible deformations of known atomic structures. In addition, even when structures of the molecules are unknown, atomic models can be predicted using homology modeling and ab initio predictions. While ab initio prediction still remains difficult for large proteins, success in predicting small proteins have been observed. Finally, algorithms to analyze protein/proteins interactions also have shown success in predicting proteins complexes.

The ultimate line of our interdisciplinary research is to bring experimental data as obtained from X-ray, cryo-EM and XFEL with development and applications of computational tools through high performance computer to acquire knowledge on the structure of a physiologically important protein complexes that are unattainable with existing experimental techniques.

18.3 Research Results and Achievements

18.3.1 Developments of computational tools for XFEL experimental data

Recent development of intense X-ray free-electron laser (XFEL) light sources offers a new possibility to image single biological macromolecules. Since crystallization is not necessary for such structure analysis, it would be possible to investigate the structure of macromolecular complexes under various physiological conditions or to observe elementary steps of a biochemical function. Currently five facilities including SPring-8/SACLA in Japan are operational in the world.

However, with current experimental conditions, atomic level resolution such as obtained by X-ray crystallography cannot yet be achieved. As XFEL experiments are very recent and still undergoing further development for routine study of biological molecules, computational algorithms and tools to understand and analyze experimental data need to be developed simultaneously. One focus of our research is the development of such computational tools. We have started to tackle these issues from multiple angles described below.

18.3.2 Denoising images

In collaboration with Dr. Jonic (CNRS, France) we presented a new method for reducing Poisson noise from images and compared it with several state-of-the-art methods. We showed that the proposed method, referred to as Piecewise Principal Component Analysis (PWPCA), has the best overall performance with respect to other methods when denoising images with Peak = 0.5, 1, 2 and 4. The overall performance of a method for a particular Peak value was evaluated by averaging the Peak Signal-to-Noise Ratio (PSNR) values that the given method achieved on different images with the same, given value of Peak. The visual quality of recovered images was consistent with the obtained PSNR values. Additionally, we showed that PWPCA can be used to preprocess single-particle XFEL diffraction data of biological macromolecules in order to improve the resolution of 3D reconstruction of the macromolecular structure from such data. These experiments were performed using simulated data. For our future works, we plan to extend the method to applications with experimental XFEL data, which should allow gaining new biological insights.

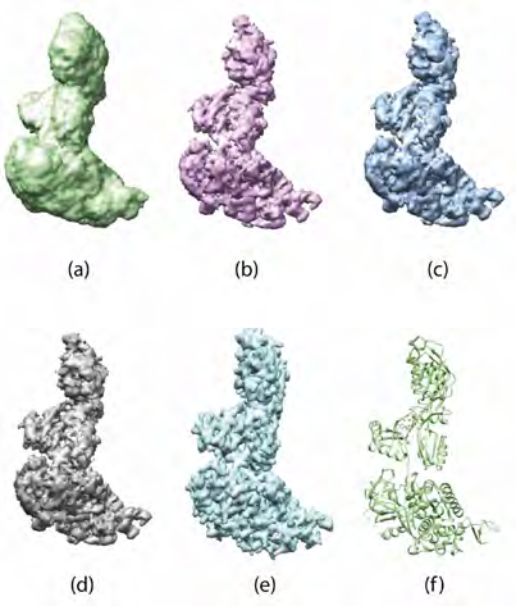

Figure 18.1: 3D reconstructions in the case of beam intensity of 10^{14} photons/pulse/μm^2. (a-d) 3D reconstructions from the following four data sets: the original data set (a), the set processed by our PWPCA (b), the set processed by the established Block-matching and 3D filtering method (c), and the ground-truth data set (d) (ground-truth phases and orientations were used in each set). As a reference, the ground-truth atomic structure (f) and the corresponding density map (e) are also shown.

18.3.3 Parameter Optimization for 3D-Reconstruction from XFEL Diffraction Patterns

In single particle XFEL experiments, the incident beam orientation of each diffraction pattern is unknown, therefore angles between 2D-diffraction patterns have to be estimated to assemble them into 3D-diffraction intensity distribution. Several algorithms have been developed for such purpose. In these approaches, 2D-diffraction patterns are assembled into a 3D-diffraction intensity distribution through iterative procedures. In the "maximum correlation coefficient" approach, a single orientation is assigned to each diffraction pattern based on its consistency against the tentative 3D-diffraction intensity at each iteration. This algorithm is simple and it has better scalability when it is applied to a large number of diffraction patterns. Usually, experimental diffraction patterns are binned before analysis to increase signal and noise ratio, SNR, and to reduce image size to make data handling easier. Even using the bright pulse of XFEL, diffraction intensities from single particle are quite low especially on the high wavenumber area, which are located on the outer region of the diffraction pattern. Binning improves the quality of experimental diffraction pattern by reducing the number of zero and low-count pixels by averaging multiple pixels. However, by binning, there is possible loss of detailed information within the binned pixels. Therefore, we need to investigate the optimal binning size to keep the quality of restored structures. We found that the resolution of a restored molecular structure is sensitive to the interpolation parameters. For the diffraction patterns with larger oversampling ratio, the more distant pixels need to be interpolated with sufficient strength. By using the optimal parameter set, resolutions of restored structures are almost the same regardless of the oversampling ratio values. Our results suggest that for single particle analysis by XFEL, linear oversampling ratio of four is sufficient and the corresponding binning procedure is beneficial for reducing both the Poisson noise and the computational time for the analysis.

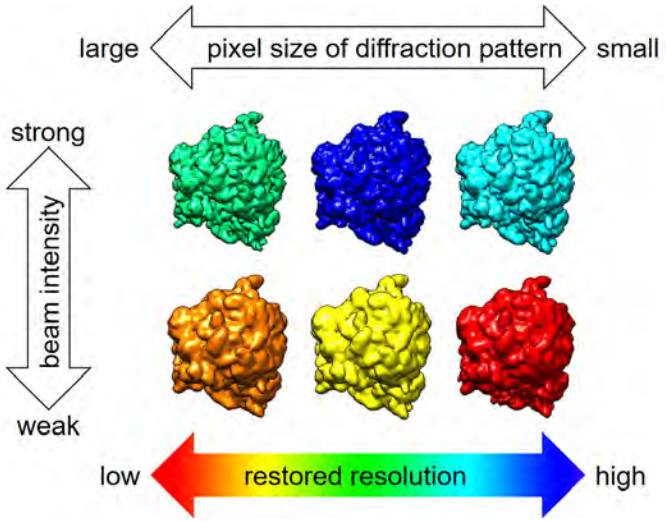

Figure 18.2: Resolution of the 3D-molecular structures retrieved using our algorithm as a function of beam intensity and oversampling ration.

18.3.4 "Idea generator" from 2D XFEL data of biological systems

Data analysis for XFEL data remains challenging. XFEL diffraction pattern is an unintuitive representation of the projection image of the sample in reciprocal space. For biological systems, the current standard approach to reconstruct a real-space image of the sample, phase recovery, often fails due to the low diffraction power of biological samples. Therefore, we are developing a new hybrid approach to interpret diffraction patterns that utilizes image analysis with database search. We have previously shown the feasibility with images from electron microscopy. In the XFEL adaptation, we have had to overcome the challenge of aligning 2D images that are in Fourier space, considering they do not contain phase information. Diffraction intensities from biomolecules are weak at high and strong at low wavenumber pixels, requiring careful selection of the matching region when aligning the diffraction images in Fourier space. We selected specific parameters for a generalized method to identify the appropriate matching regions between the images. Using spherical form factors, we estimated the diameter of the shape in the diffraction pattern. In general, as we have observed for real space 2D projection

image matching, we find that the success of the strategy relies on the complexity of the shape and its availability in the database. Nevertheless, the features of the shape in the input images are still captured within in the top ten matching hits.

18.3.5 Effect of temperature on protein conformation

Another important aspect of our research is the study of specific biological molecules to address important biological questions to complement experimental data. Cryo-cooling is routinely performed before x-ray diffraction image collection to reduce the damage to crystals due to ionizing radiation. It has been suggested that although backbone structures are usually very similar between room temperature and cryo-temperature, cryo-cooling may hamper biologically relevant dynamics. We have studied the crystal of Escherichia coli dihydrofolate reductase with replica-exchange molecular dynamics simulation and compared the results with the crystal structure determined at cryo-temperature and room temperature with the time-averaged ensemble method. Although temperature dependence of unit cell compaction and root mean-square fluctuation of Cα is found in accord with experiment, it is found that the protein structure at low temperature can be more heterogeneous than the ensemble of structures reported by using the time-averaged ensemble method, encouraging further development of structure refinement methods considering large conformational ensemble and indicating that data should be examined carefully to avoid overinterpretation of one average structure.

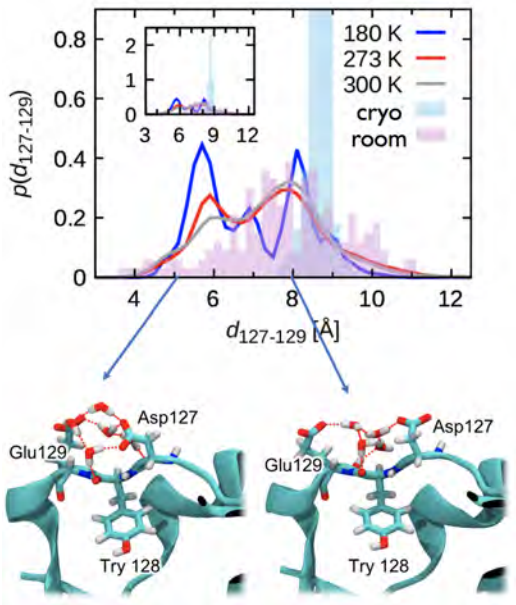

Figure 18.3: Conformational states observed during cryo crystal MD simulations and comparison to experimental data. Distribution of distance between carboxyl carbons in residues 127 and 129 at three temperatures (blue, red, and gray lines) and experimental counterparts (light blue and pink bars for PDB: 4P3R and 4P3Q, respectively). The inset is the same plot with different range of abscissa.

18.3.6 Conformational dynamics in Tom20-mitochondrial presequence tethered complexes

The translocase of the outer membrane (TOM) mediates the membrane permeation of mitochondrial matrix proteins. Tom20 is a subunit of the TOM complex and binds to the N-terminal region (ie, presequence) in mitochondrial matrix precursor proteins. Previous experimental studies indicated that the presequence recognition by Tom20 was achieved in a dynamic-equilibrium among multiple bound states of the α-helical presequence. Presumably due to such dynamics, the co-crystallization of Tom20 and a presequence peptide required a disulfide-bond cross-linking, for which A 3-residue spacer sequence (XAG) was inserted between the presequence and the anchoring Cys residue at the C-terminus to not hinder the dynamics of the presequence peptide in the binding site of Tom20. Two crystalline forms were obtained according to Ala or Tyr at the X

position of the spacer sequence, which may reflect the dynamic-equilibrium of the presequence. Interpretations of these crystal structures and actual effect of cross-linking on protein dynamics have remained unclear. Therefore, we performed replica-exchange molecular dynamics (REMD) simulations to study the effect of disulfide-bond linker and single amino acid difference in the spacer region of the linker on the conformational dynamics of Tom20-presequence complex. We showed that the disulfide-bond tethering, neither the choice of Ala or Tyr at the X position did not strongly affect the main conformational ensemble of the presequence peptide in the complex. Our study provides a rational basis for the disulfide-bond tethering to study the dynamics of weakly binding complexes.

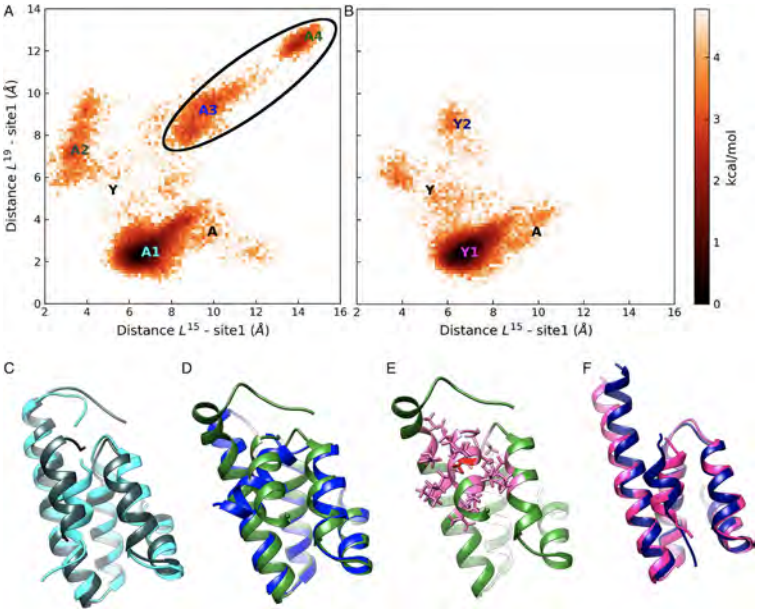

Figure 18.4: Free energy profile for distances between the hydrophobic residues of Tom20 and the presequence from simulations (A) Ala sequence and (B) Tyr sequence. A1, A2, A3, and A4 denote the representative structures from Ala sequence simulations. Y1 and Y2 denote the representative structures from Tyr simulations. (C) Superimposed structures of A1 (cyan) and A2 (darkslategray) (colored in (A)). (D) Superimposed structures of A3 (blue) and A4 (green) (colored in (A)). (E) A4 from the encircled distribution of REMD data from A showing that the Ala residue at the X position of the spacer (red) is fully packed with nearby residues (pink). (F) Superimposed structures of Y1 (magenta) and Y2 (navy) (colored in (B)).

18.4 Schedule and Future Plan

Cryo-EM experiments are quickly becoming an essential tool for studying biomolecular complexes. New XFEL facilities are getting into operation every year in the world, providing opportunities for new experiments. The amount of data from such experiments will continue to grow in numbers and analysis of such big datasets will increase the necessity of high-performance computing. We aim to utilize high performance computer such as Fugaku to break the limitation of current processing power and to obtain a new level of structural information of biological complexes from EM and XFEL data. For this goal, we plan to develop algorithms and software to analyze large dataset to obtain not only structural models but also dynamical information that can utilize computers in different sizes such as cluster and supercomputer. By sharing the software and results from structural modeling with other research institutes, we aim to contribute to the structural biology community.

18.5 Publications

18.5.1 Articles/Journal

[1] A. Srivastava, T. Nagai, A. Srivastava, O. Miyashita & F. Tama. Role of computational methods in going beyond X-ray crystallography to explore protein structure and dynamics. Int. J. Mol. Sci. 19(11) (2018)

[2] T. Nagai, Y. Mochizuki, Y. Joti, F. Tama & O. Miyashita. Gaussian mixture model for coarse-grained modeling from XFEL. Optics Express 26:26734-26749 (2018)
[3] S. P. Tiwari, F. Tama & O. Miyashita. Searching for 3D structural models from a library of biological shapes using a few 2D experimental images. BMC Bioinformatics 19(320) (2018)
[4] Q. Jin, O. Miyashita, F. Tama, J. Yang & S. Jonic. Poisson image denoising by piecewise principal component analysis and its application in single-particle X-ray diffraction imaging, IET Image Processing 12:2264-2274 (2018)
[5] M. Nakano, O. Miyashita, S. Jonic, A. Tokuhisa, F. Tama. Single-particle XFEL 3D Reconstruction of Ribosome-size Particles based on Fourier Slice Matching: Requirements to Reach Subnanometer Resolution. J. Synchrotron Rad. 25:1010-1021 (2018)
[6] A. Srivastava, T. Hirota, S. Irle and F. Tama. Conformational dynamics of human Protein Kinase CK2α and its effect on function and inhibition. Proteins. 86:344-353 (2018)

18.5.2 Book

[7] O. Miyashita & F. Tama. Hybrid Methods for Macromolecular Modeling by Molecular Mechanics Simulations with Experimental Data. In: Nakamura H., Kleywegt G., Burley S., Markley J. (eds) Integrative Structural Biology with Hybrid Methods. Advances in Experimental Medicine and Biology 2018

18.5.3 Invited Talks

[8] Computational tools to characterize structure and dynamics of biomolecular systems from single molecule experiments. Seminar, Institute Laue Langevin, Grenoble, France, Feb 2nd, 2018
[9] Hybrid modeling approaches to study structures and dynamics of biological systems. Coarse-Grained Modeling of Structure and Dynamics of Biomacromolecules Workshop. Telluride US, July 23-27, 2018
[10] Computational tools to characterize structure and dynamics of biomolecular systems from single molecule experiments. American Chemical Society National Meeting, Boston, US, Aug. 19-23, 2018
[11] Modeling structure and dynamics from low to high resolution data via normal mode analysis. Normal modes of biological macromolecules: methods and applications, CECAM workshop, Paris France, Oct. 12-14, 2018
[12] Hybrid modeling approaches to study structures and dynamics of biological. Annual Meeting of Biophysical Society of Japan, systems. Okayama, Sept 15-17, 2018
[13] Hybrid modeling approaches to study structures and dynamics of biological systems. Second workshop on Advances in Theory and Computation of Complex Systems - Biological Systems. Nanjing, China, Dec. 2-5, 2018
[14] Development of computational tools to characterize structure and dynamics of biomolecular systems from single molecule experiments. Physics Department Colloquium, Freie University. Berlin, Dec. 13th, 2018

Part II

Operations and Computer Technologies Division

Chapter 19

Facility Operations and Development Unit

19.1 Members

Toshiyuki Tsukamoto (Unit Leader)

Satoshi Matsushita (Technical Staff)

Katsuyuki Tanaka (Technical Staff)

Fumio Tsuda (Technical Staff)

Hajime Naemura (Technical Staff)

Makoto Igasaki (Technical Staff)

Hiroshi Shibata (Technical Staff)

19.2 Overview of Research Activities

The K computer facilities possess multiple features not found at other supercomputer sites. These features include an expansive and pillar-free computer room, a power supply system that consists of a co-generation system (CGS) and a high-speed current-limiting circuit breaker without uninterruptible power supply (UPS), distribution boards installed not on the computer-room walls but under a raised floor, extremely quiet and high-efficiency air conditioners, and a water-cooling system for the CPUs featuring precise temperature control.

To ensure stable operation of the K computer and its peripherals, the facility operations and development unit (FODU) of the operations and computer technologies division, RIKEN R-CCS, is responsible for the operation and enhancement of the facilities. Furthermore, FODU conducts research on the advanced management and operations of the R-CCS facilities.

One of the most serious problems is the rapid and substantial increase in the electricity prices since 2011. Therefore, we are investigating the most suitable driving conditions to allow the R-CCS facilities to achieve effective cost reductions.

Another problem is the increased power consumption by R-CCS. The use of electricity by R-CCS is strictly limited by a contract between R-CCS and the local electric supply company. However, in the early stage of operation, the facility's power consumption exceeded the contract limit. This is important because the company requires us to accept an increase in the upper/lower power limit, which amounts to an increase in the electricity cost. To prevent this, we have investigated methods to control the power consumption of the K computer using emergency job stopping together with the system operations and development unit and the application tuning development team of the operations and computer technologies division, RIKEN R-CCS.

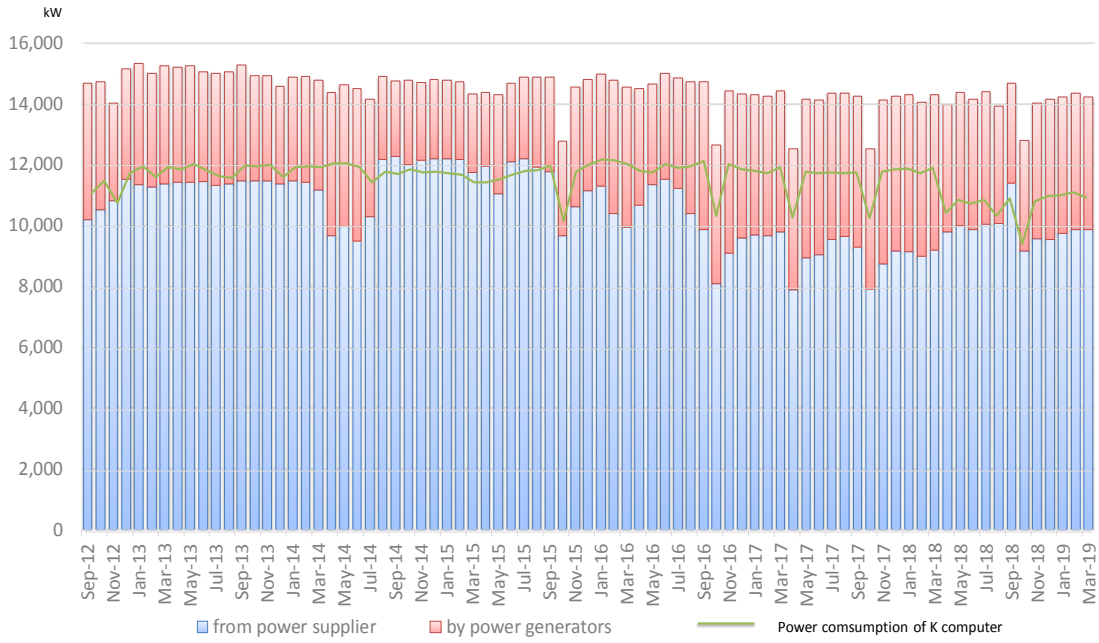

Figure 19.1: Monthly power supply and K computer power consumption.

19.3 Research Results and Achievements

19.3.1 Optimum operation of electric power

Figure 19.1 shows the monthly total power supply and power consumption of the K computer from September 2012 to March 2019. The power supply consists of commercial power purchased from a supply company and power generated by CGS.

The R-CCS power consumption is nearly synchronized with that of the K computer. The power consumption of R-CCS is nearly 14,000 kW on average, and the power consumption of the K computer accounts for approximately 80% (11,000 kW) of the total consumption of R-CCS.

As shown in Figure 19.1, the electric power supply of R-CCS consists of commercial and CGS power. There are two CGS systems at R-CCS, and they are used in turn for two weeks at a time. Therefore, at least one CGS is always in use. Commercial electric power is contractually set at approximately 12,500 kW, and the power consumption was approximately 11,000 kW (annual average), which corresponds to approximately a 90% load factor.

To minimize the cost, we try to optimize the ratio of the commercial and CGS electricity. To investigate the optimized conditions that minimize the sum of the electricity and gas cost, we determined the costs of several ratios of commercial electricity to CGS electricity. We also constructed a model to describe the energy flow of the electric power supply and the cooling system. Then, we performed computer simulations using the model and the actual operating data. In the near future, we intend to identify the cost-optimized conditions that contribute to reducing costs.

19.3.2 Improvements to the power usage effectiveness (PUE)

We have continued to work on improvements for the effective use of electricity. PUE is a well-known indicator of the effectiveness of electricity use.

To improve the PUE, we have attempted to optimize the operation of the cooling equipment (e.g., chillers and air-handlers) since FY2013.

Figure 19.2 indicates the change in the annual average power consumption of the K computer (including the peripheral devices) and the cooling equipment. Since FY2013, the power consumption of the K computer has been nearly flat at approximately 11,800 kW; however, the power consumption of the equipment decreased gradually from FY2013 to FY2017. Accordingly, the PUE of R-CCS improved to 1.322 in FY2018 from 1.447

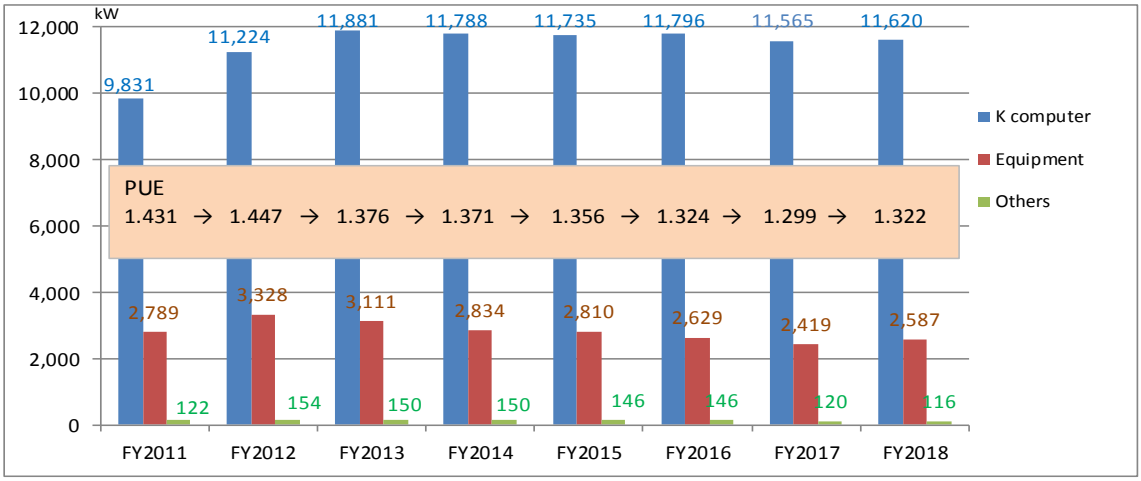

Figure 19.2: Trend in the annual average electric power consumption.

in FY2012, contributing to the reduction in the electricity cost.

In FY2013, we reduced the electricity cost of the air conditioners by reducing the number of working air conditioners. The total cooling performance was maintained by lowering the air temperature. We achieved a reduction in the power consumption of 217 kW.

In FY2014, we focused on the fault-tolerance feature of the air-conditioning equipment. Each air conditioner has two motors for fault tolerance. We found that if one of the two motors could be stopped, the airflow could be maintained at approximately 60%. Therefore, we reduced the power consumption by a further 277 kW in FY2014 and by 24 kW in FY2015.

In FY2016, we worked on improving the efficiency of the cooling tower. As a result, we achieved a reduction of 181 kW in the power consumption.

In FY2017, we focused on optimizing the operation control of the refrigerator using a heat storage tank. This reduced the power consumption by 210 kW.

In FY2018, we carried out the overhaul of a cooling tower and a large number of pumps. However, we were not able to operate CGS by the effective output because the electric equipment disorder caused by the typhoon occurred. Therefore we were not able to improve PUE of FY2018 from last year.

19.4 Schedule and Future Plan

We will continue to improve the advanced management and operation of the R-CCS facilities and contribute to the user service of the K computer. We will work on reducing costs by investigating and applying the most suitable driving conditions to all the electric power supply and cooling equipment. Further, we will improve the electric power control of the entire R-CCS facility with the system operations and development unit to prevent overshooting of the contracted power demand.

19.5 Publications

19.5.1 Papers (refereed)

[1] M. Matsuda, H. Matsuba, J. Nonaka, K. Yamamoto, H. Shibata and T. Tsukamoto: "Modeling the Existing Cooling System to Learn its Behavior for Post-K Supercomputer at RIKEN R-CCS". Energy Effcient HPC State of the Practice Workshop (EE HPC SOP) 2019.

19.5.2 Oral Talks

[2] Jorji Nonaka, Fumiyoshi Shoji, Motohiko Matsuda, Hiroya Matsuba, Toshiyuki Tsukamoto, "Analysis of the CPU Cooling Temperature Effect on the Performance and Power Consumption for the HPC Operational Decision Support", Supercomputing Frontiers Asia 2019 (SCFA19), Singapore, 2019. (Abstract Presentation)

19.5.3 Software

19.5.4 Patents

Chapter 20

System Operations and Development Unit

20.1 Members

Atsuya Uno (Unit Leader)

Yuichi Tsujita (Senior Technical Scientist)

Keiji Yamamoto (Technical Scientist)

Fumio Inoue (Research & Development Scientist)

Hitoshi Murai (Research & Development Scientist)

Mitsuo Iwamoto (Technical Staff)

Katsufumi Sugeta (Expert Technician)

20.2 Research Activities

K computer, a distributed-memory parallel computer comprising 82,944 computing nodes, has played a central role in the High Performance Computing Infrastructure (HPCI) initiative funded by the Ministry of Education, Culture, Sports, Science and Technology. The HPCI has achieved an integrated operation of the K computer with other supercomputer centers in Japan. Furthermore, it has enabled seamless access from user machines to a cluster of supercomputers that includes the K computer. Moreover, the HPCI has provided large-scale storage systems that are accessible from all over Japan.

The system operations and development unit (SODU) has conducted research and development for the advanced management and operations of the K computer. While analyzing operational statistics collected during its shared use, the SODU has improved the system configuration, including aspects involving job scheduling, the file system, and user environments.

In the fiscal year 2018 (FY2018), we primarily implemented improvements to the following operational issues:

- Active termination of I/O racing jobs towards high compute node utilization
- Information exchanges among HPC centers
- File system operation excluding hard disk drives with high error rate
- Prevention of high load on MDS
- Improvement of information provision to users
- Energy-aware system operation

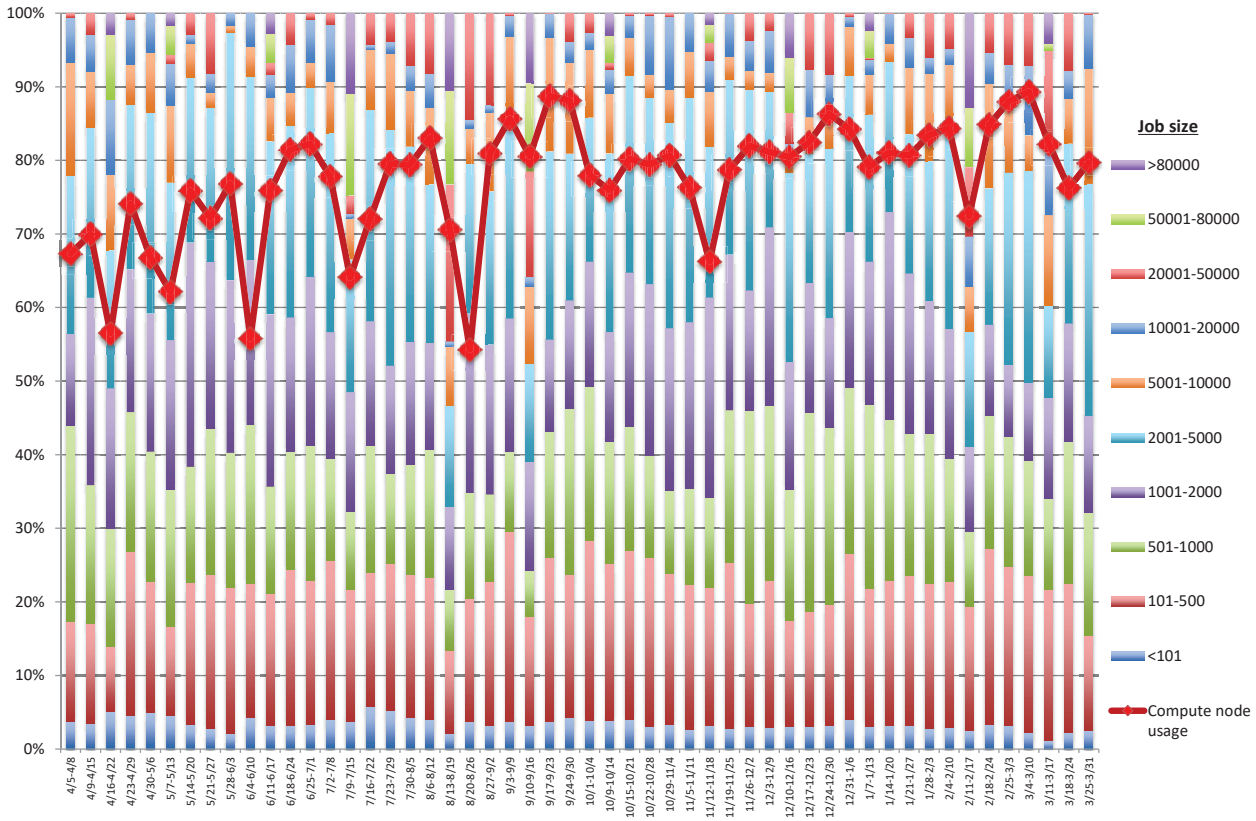

Figure 20.1: Resource usage in FY2018

20.3 Research Results and Achievements

Figure 20.1 shows the resource usage details, and table 20.1 indicates the major failures of the system down for FY2018. Most of the failures in FY2018 are related to the hardware trouble and the local file sytem (LFS).

As usual, the resource usage is low at the beginning of the fiscal year, and there was relatively low usage in April. In June, usage was low due to an instantaneous voltage drop caused by a stroke of lightning. We took time to ensure the safety of the whole system and to restart the K computer. The resource usage was low in August because of the electrical facility trouble. The typhoon caused a blackout and the K computer was down for approximately 2 days. Apart from those incidents, we maintained a high utilization rate, approximately 77%, which is nearly equal to that achieved in FY2017 (78%).

Table 20.1: Major failures in FY2018

Date	Details	Maintenance period (H)
2018/4/17	Network switch failures (HW trouble)	3.8
2018/6/8	Instantaneous voltage drop	43
2018/7/9	LFS (HW trouble)	11.7
2018/7/17	Job management server down	3.3
2018/8/24	Electrical facility trouble	46.4
2018/9/10	LFS (HW trouble)	2.8
2018/9/27	LFS (HW trouble)	3.4
2018/11/14	LFS (HW trouble)	8.2
2019/3/22	LFS (HW trouble)	2.8

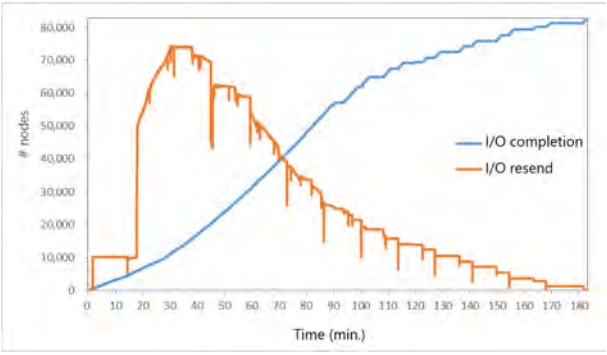

Figure 20.2: Long I/O contention due to a high number of concurrent I/O at the same directory

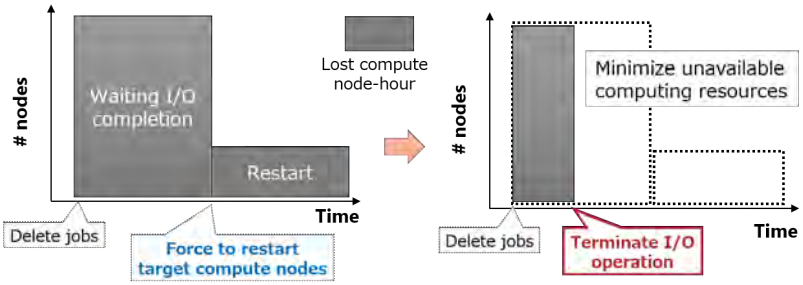

Figure 20.3: Improvement in compute node-hour minimization using active I/O job termination (Left: previous scheme, Right: proposed scheme)

20.3.1 Active Termination of I/O Racing Jobs Towards High Compute Node Utilization

A large number of concurrent I/O accesses at the same directory leads to poor performance, and sometimes such situation continues until its I/O operation finishes even if job termination is initiated as shown in Fig. 20.2. If such I/O contention exceeds pre-defined timeout of the job scheduler, such job is terminated by re-starting the assigned compute nodes. Although the compute nodes are available after the restart, it takes a sort of time until the compute nodes are ready. Thus, we may lose a sort of expected resources in compute node-hours until the start-up of the compute nodes. Especially, such negative impact is very big if the number of affected compute nodes is very large.

In order to minimize such inefficiency in compute node-hour utilization, we have proposed active I/O job termination by using client eviction provided by a file system. Figure 20.3 depicts minimization effect in lost compute node-hours by introducing the active I/O job termination. After a pre-defined interval from the initiating time for the normal job deletion, the system operation issues eviction for the target compute nodes. Then I/O racing jobs on the evicted compute nodes are terminated, and it can avoid to restart target compute nodes as we did in the previous scheme. The proposed scheme can eliminate a large amount of lost in compute node-hour resources relative to the previous scheme, and thus we can increase compute node utilization.

20.3.2 Information Exchanges among HPC Centers

Recent growth in HPC systems has bring us complexity in HPC system operation. On the other hand, system operation is required to manage a high demand from a variety of HPC users. Each HPC center has been struggling to build own sophisticated operation environment and user support service system. However, there has not been any inter-relationship among HPC centers in Japan to make some information exchanges about HPC system operation and user support.

As the first step of such inter-relationship, our unit started inter-relationship with the HPC center at JAMSTEC. The HPC center at JAMSTEC is operating Earth Simulator (hereinafter, ES) developed by NEC, while R-CCS is operating the K computer developed by FUJITSU. Although both HPC systems are different in system architecture and system software, there is not enough information about differences in system configuration and behavior of applications. In order to make clear what different each other to foster effective HPC system

selection, we have addressed to exchange each technical issues including some benchmark results.

In the primary stage, we have carried out file system performance evaluation in order to show characteristics of each HPC system. We believe such performance comparison is useful for HPC users to select appropriate system for their applications, for instance. Our MPI-IO evaluation using IOR showed distinct differences among the two HPC systems due to different architecture and system configuration of each parallel file system (ScaTeFS for the ES and FEFS for the K computer). During the activity, the HPC center at TITECH, which is operating TSUBAME 3.0, has joined the activity, and the center has started the similar MPI-IO performance measurement at their machine.

As a future work, we will expand the similar information exchanges to cover all of HPC system operation. It is expected to improve each HPC operation skill through the activity. Besides, more wider inter-relationship in HPC centers in Japan is also considered in the next fiscal year.

20.3.3 File System Operation Excluding Hard Disk Drives with High Error Rate

More than seven years have passed since the beginning of operation of the K computer. Since various devices are aged, they have affected operations. In particular, the number of failures of HDDs in the Global File System (GFS), which stores user's data, tends to be increasing. GFS has a redundant configuration (RAID 6) to cope with HDD failures. Nevertheless, if the number of HDD failures increases, it is difficult to cover those failures by the redundancy and data may be lost. In order to prevent this problem, we considered the operation to detach the Object Storage Target (OST) when there are multiple HDDs with high failure rate in the same OST.

We studied a method to determine the possibility of HDD failure by analyzing an error log when reading data and failure status for each HDD. In the future, we plan to operate the file system excluding HDDs with high error rate based on this method.

20.3.4 Prevention of High Load on MDS

In order to prevent high load of the Meta Data Server (MDS) of LFS, we implemented the following process.

- Automatic alleviation of MDS load

  When the MDS becomes highly loaded, the system response decreases and all running jobs are affected. In order to prevent this situation, we have implemented a mechanism to detect the jobs causing MDS to become a high load and to stop them automatically.

- MDS load reduction when using OSS

  In the K computer, various types of Open Source Software (OSS) are provided. If these OSSs are used in highly parallel jobs, the MDS may be heavily loaded. Therefore, we prepared the environment that these OSS can be used in the rank number directory. As a result, no load is applied to MDS even in high parallel.

20.3.5 Improvement of Information Provision to Users

The users can get the information of the submitted jobs by the pjstat command, and also can see the usage status of the node in two dimensions in the user portal. In FY2018, we made a tool that can see the scheduling situation of jobs in the three-dimensional view as the actual scheduling of the K computer. At the moment, it can only display the scheduling situation of all jobs. In the future, it will be possible to see the scheduling situation of the user's own jobs.

20.3.6 Energy-aware System Operation

We have studied the job scheduling considering power consumption of each job to prevent power excess. In this method, we estimate the application from the submitted job script in order to estimate the power consumption for each job when the job submission, In JFY2018, we have studied the estimation method of the time-series power consumption for each job from that information. To estimate the time-series power consumption, we associate the executed job's information and its power consumption, and estimate the power consumption using the job's information obtained when the job submission. In the future, we plan to improve the prediction method and implement job scheduling algorithm considering the time-series power consumption based on the prediction result.

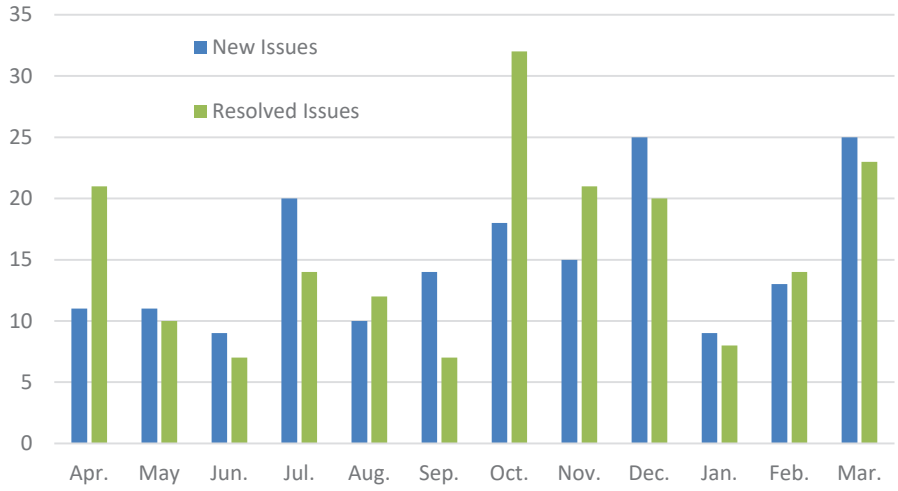

Figure 20.4: Number of issues addressed in FY2018

20.4 User Support

The K computer executed approximately 200 projects in FY2018. The number of active daily users was approximately 190. We supported users through the K support desk and provided them with technical information regarding the K computer, including information regarding its system environment, system tools, and software libraries. In addition, we performed user registrations, failures investigation, software installation, etc. We offered our consulting services together with the HPC Usability Development Unit and Application Tuning Development Unit. Figure 20.4 presents the number of issues addressed in FY2018, showing the number of new issues in FY2018 to be approximately 180. The number of resolved issues was approximately 190. The number of new issues in FY2017 was approximately 140.

20.5 Schedule and Future Plan

In this fiscal year, we analyzed the operation of the K computer and examined the operation improvement, and also examined the prediction method of the time series power consumption for each job about the power excess. In addition, we predicted HDD failure from the analysis results of the log output in the operation of the K computer. As stable operation of GFS, we examined the operation without using HDD with high failure rate. We will continue to study the detection and handling of operation's problems by analyzing the operation log. Moreover, we will continue to perform the stable operation of the K computer.

20.6 Publications

20.6.1 Articles

[1] Yuichi Tsujita, Yoshitaka Furutani, Hida Hajime, Keiji Yamamoto, Atsuya Uno, and Fumichika Sueyasu, "I/O Interference Alleviation on Parallel File Systems Using Server-Side QoS-Based Load-Balancing," HPC I/O in the Data Center Workshop (HPC-IODC 2018), Lecture Notes in Computer Science, Vol. 11203 , pp. 36-48, Springer, 2018
[2] Keiji Yamamoto, Yuichi Tsujita, and Atsuya Uno, "Classifying Jobs and Predicting Applications in HPC Systems," ISC High Performance 2018, Lecture Notes in Computer Science, Vol. 10876, pp.81–99, 2018

20.6.2 Oral Talks

[3] Yuichi Tsujita, "Improving Meta-Data Access Performance Towards High Availability of Large Scale Parallel File Systems," Japan Lustre User Group 2018, October 25, 2018, Chiyoda-ku, Tokyo, Japan
[4] Yuichi Tsujita, Atsushi Hori, Atsuya Uno, and Yutaka Ishikawa, "Enhancing MPI-IO with Topology-Awareness at the K computer," The first R-CCS Symposium, February 18-19, 2019, Kobe, Hyogo, Japan

[5] Atsuya Uno, and Toshiaki Mikamo, “Operations Management Software for the Post-K computer,” The first R-CCS Symposium, February 18-19, 2019, Kobe, Hyogo, Japan

Chapter 21

Application Tuning Development Unit

21.1 Members

Kazuo Minami (Unit Leader)

Akiyoshi Kuroda (Research & Development Scientist)

Kiyoshi Kumahata (Research & Development Scientist)

Kazuto Ando (Technical Staff I)

21.2 Overview of Research Activities

In the case of the K computer, the collaboration between the system and the applications in use is the key to create innovative results. In order to maximize the performance and usability of both the system and such applications, the Application Tuning Development Unit conducted the following activities:

(1) Activities related to the RIKEN Center for Computational Science (R-CCS) software center

(2) Activities to establish a deep learning (DL) environment on the Post-K computer

(3) Effort for the Post-K computer development

21.3 Research Results and Achievements

The application tuning development team has been conducting performance evaluation and enhancement aimed at popularizing the applications developed by the RIKEN Center of Computational Science (R-CCS) research team (i.e., R-CCS software) from applications on the K computer. By improving and enhancing the software, we expect industries and communities that have not used the R-CCS software to start using it. Furthermore, along with above activities, we are also trying to systemize performance optimization technology. Improving application performance will lead to a shortening of the elapsed time, which makes it possible to use more computational resources. This will help in the more effective utilization of resources. We kept these factors in mind while carrying out the following tasks.

21.3.1 Activities related to the R-CCS software center

The RIKEN R-CCS Software Center is developing and deploying high-quality software for numerous high-performance computers (HPCs), including the K computer. Up to now, we have paid attention to improving and utilizing the following four software products developed by R-CCS: (1) NTChem and (2) OACIS.

21.3.1.1 Enhancement of the R-CCS software (NTChem)

NTChem is the molecular chemistry software developed by RIKEN R-CCS. This application has been provided for the analysis of life science and material science, and it can be used for examining the electronic state of a material. The molecular orbital method and the density functional method are employed in this software. We implemented a number of functions such as the various basis functions and many algorithms for acceleration of calculation. This application is good for calculating the density functional theory including the relativistic effect.

In this year's work, the density functional theory calculation part in the KAIN method was a working target. In the beginning of the survey, the limitations of the number of parallel and I/O was raised as a problem limiting parallel performance. Therefore, we carried out parallel design carefully. Specifically, we improved the process dividing method with modification of distributed I/O and reduced the imbalance by thread parallelization. As a result, the parallel performance was improved to 28.5 times faster than the original of 191 seconds.

As the result of this year's work, the execution time on 1,024 parallel was compressed to the time that is almost equivalent to the time of the four-center integration calculation[Figure 21.1].

In order to further improvement of the performance in the future, we proposed the method to further reduce the load imbalance between atoms, and showed its effect.

The other regions of the KAIN method was investigated last year. As a result, we found the possibility of performance improvement by changing the algorithm for the region of the four-center integral. We will work on these performance improving of KAIN method in the future.

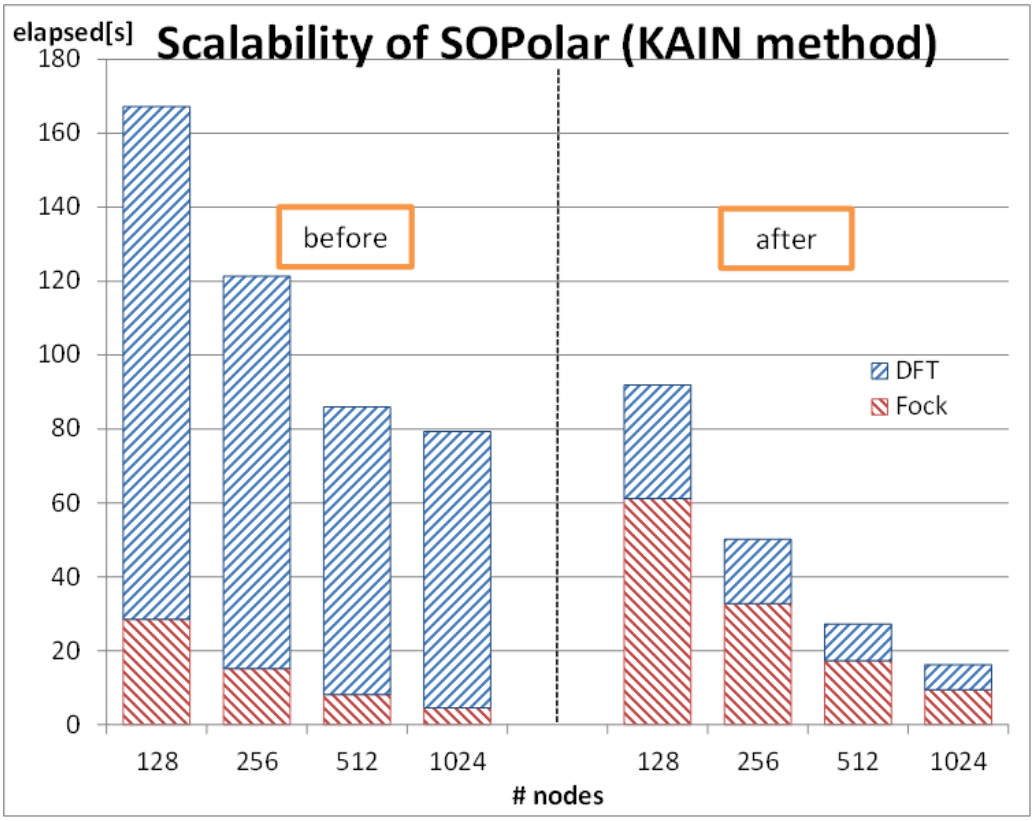

Figure 21.1: Scalability of SOPolar (KAIN method).

21.3.1.2 Enhancement of the R-CCSsoftware (OACIS)

The Organizing Assistant for Comprehensive and Interactive Simulations (OACIS) is a tool that assists users in exploring the parameter space that frequently occurs during computer simulations. More specifically, OACIS helps users to control parameter and input file generation corresponding to the given conditions. It also facilitates job submissions and helps manage numerous results via its easy-to-use web interface. OACIS itself is not an application; it is a tool for improving application convenience.

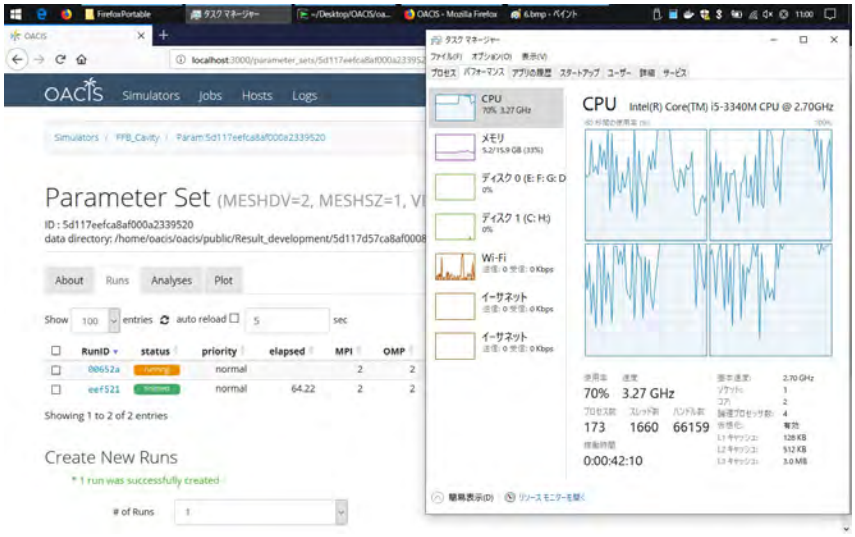

Figure 21.2: This image shows that OACIS system and simulation program run on a PC.

Therefore, it was necessary to make efforts in several application areas in order to enhance the convenience appeal that could result from using OACIS.

In FY2017, the Application Tuning Development Unit have supported upgrades to the web interface GUI that improved operational consistency, which allowed database modifications to treat more data and improved the responsiveness of the search function.

Currently, OACIS is a tool that is must be installed in the user machine environment. However, in FY2018, we constructed an OACIS system demo environment that will eliminate installing OACIS system. This demo environment will make it easy for users who want to try using OACIS before making a firm decision on whether to install the tool. The demo environment will be available in two styles. One is a server type environment that manages the jobs running on the K computer, whereas the other is a PC type demo environment that allows all OACIS operations on a user's PC.

These efforts were performed based on the budget about the R-CCS software center in cooperated with a software vendor.

21.3.2 Activities to establish a deep learning environment on the Post-K computer

Recently, machine learning by deep learning (DL) has become popular. And applications and research using graphics processing units (GPUs) are advancing in computational science fields. However, it is also possible to make numerous calculations by taking advantage of CPU characteristics, even with massively parallel computers.

21.3.2.1 Investigation on DL frameworks

To facilitate DL on the post-K computers, we tried to build DL environment on the K computer. In particular, we performed to investigate function, measure performance, and improve performance of TensorFlow and Chainer which are representative frameworks. TensorFlow is an internationally used machine learning framework developed by Google. Although it can be introduced easily in the widely used Intel environment, it was necessary for us to build for a special environment such as the K computer. Building such environments requires the use of special building tools such as Bazel and making adjustments to the versions of various other tools including the Linux libraries and compilers. Although it was difficult to build the required special environment in the K computer, the knowledge obtained from that effort can be used for the Post-K computer.

Chainer expresses the hierarchical structure of deep learning using Python, and all calculations can be realized using numPy without requiring the use of special libraries. Since most of the cost is convolution, it has become possible to perform calculations with a performance efficiency of 46.2% by calling threads parallelized gemm. The square root calculation of the array element in the Adam algorithm that is used when updating the filter is also very costly. In fact, it was found that this cost accounts for about 90% of the total. Applying software pipelining by approximating the inverse number expansion and controlling the floating point

calculation underflow in this part has resulted in a total reduction of elapsed time of about 1/16. Through these tuning and evaluation efforts, it was possible to calculate a DL framework with a total performance efficiency of about 14% [Figure 21.3].

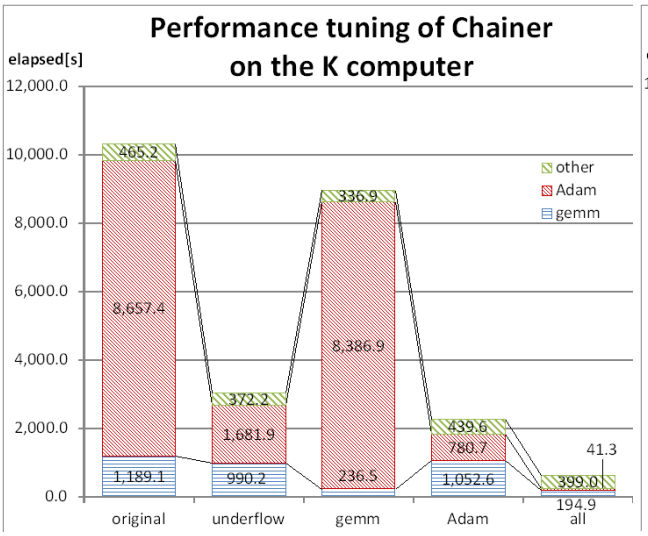

Figure 21.3: Elapsed time on the all tuning step.

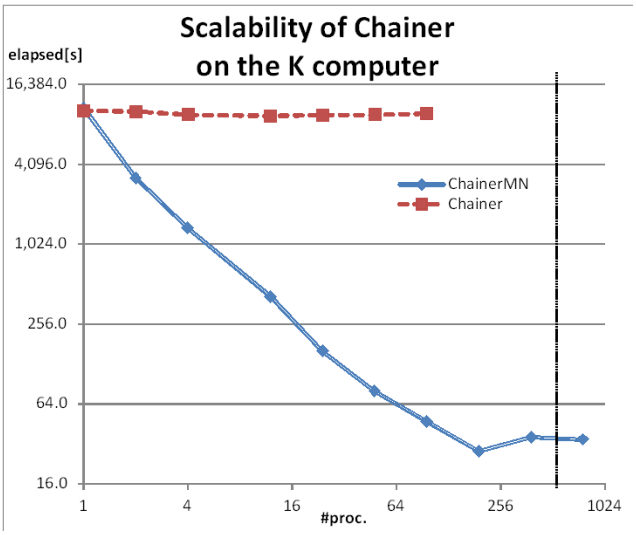

Figure 21.4: Elapsed time of the scaling result.

Therefore, it can be said that training and inference using DL are also possible using the K and Post-K computers. We also evaluated a parallel CPU version of Chainer that provided users with a machine learning environment on the K computer [Figure 21.4].

21.3.2.2 DNN Investigation

Since special deep neural network (DNN) libraries are normally provided for major convolution calculations in order to speed up DL calculations on GPUs and Intel CPUs, the development of such a library is also necessary for the K and Post-K computers. Accordingly, we investigated the function and performance of cuDNN provided by NVIDIA and MKL DNN provided by Intel and then summarized those results as guidelines for the development of the new DNN library that will be required in the future.

cuDNN is a library that contains functions to automatically select and use other high-speed functions from various methods such as gemm, FFT, and Winograd, etc., for convolution calculations. Various parameters are used for the actual convolution calculations and it turned out that gemm was suitable for many of these problems. Additionally, Winograd was suitable for problems requiring a large filter size, and FFT was suitable for some other cuDNN parameters. Numerous ideas were implemented such as using gemm inside these calculations, and the performance of convolution calculations (at about 30% on average) provides a sufficiently high level of efficiency.

In addition to gemm, the Math Kernel Library for Deep Neural Networks (MKL-DNN) provides a highly useful just-in-time (JIT) compiler method that is compatible with the AVX512 extensions for convolution calculations. A maximum high-performance of 62.4% and average performance levels of 43.6% were achieved for many actual problems using this JIT compiler method. It appears that these special libraries, such as cuDNN and MKL DNN, were developed to facilitate the effective use of small arithmetic units such as AVX512 and tensor core for convolution calculations. For this reason, the convolution process is divided into small units and calculates repeatedly.

The above survey results were fed back to framework and library developers for utilization in the Post-K computer[Table 21.1].

21.3.2.3 Evaluations for the K and Post-K computers

Since there are currently are no special DNN libraries that can be used to speed up evaluations on the K and Post-K computers, we prototyped a general DNN kernel that is designed to work on both computers. This kernel performs evaluations based on the information obtained via investigations using libraries such as cuDNN

Table 21.1: Performance efficency of DNN libraries.

library	cuDNN	MKL DNN	K	FX100
algorithm	PRECOMP_ GEMM	JIT	GEMM	GEMM
max.	92.67%	62.42%	86.03%	73.67%
ave.	62.42%	43.55%	54.93%	36.72%
min.	14.91%	2.16%	14.27%	8.18%

and MKL DNN. The prototyped kernel is a general convolution calculation similar to direct, gemm, DFT, FFT, Winograd, and the like.

On the K computer, a performance maximum of 77.59% and an average performance level of 42.05% were achieved via the Gemm kernel by using the survey results of dedicated DNN libraries such as cuDNN and MKL DNN to tune the general evaluation kernel. These performances were about the same as or higher than those achieved using Intel MKL and the JIT compiler. Unlike the special DNN library, this gemm convolution in the general kernel was immediately implemented as a large size gemm, but further performance improvements can be expected by adjusting it to a more optimal size.

After tuning several parameters that were automatically selected by cuDNN, it was confirmed that the FFT and DFT kernels could calculate faster than gemm on the general kernel. Thus, it can be said that these general kernels were able to provide the same functions and achieve the same performance as cuDNN.

Currently, we are evaluating the performance of the general kernel prototyped here on the Post-K computer.

21.3.3 Effort for the Post-K computer development

The FLAGSHIP 2020 (FS2020) Project is engaged in research and development the Japanese national flagship supercomputer, post K computer. As part of the FS2020 project, application tuning development unit are involved with co-designing the applications and Post-K system through performance optimization and sophistication of target applications. In particular, our unit is responsible for these three applications:

- ADVENTURE, a structural analysis application based on the finite-element method in Priority Issue No. 6

- RSDFT, a first-principles material simulation and optimization application based on density functional theory, Priority Issue No. 7

- FrontFlow/blue, a fluid analysis application based on the finite-element method in Priority Issue No. 8

For these applications, we have paid significant attention to the following efforts:

- Application performance tuning

- Establishing methods for estimating application performance on the Post-K computer

- Investigating demands for hardware and software arising from application development

- Supplying kernel codes for determining CPU specifications

- Investigating the effect of changing hardware specifications for calculations of each priority issues

The following subsections describe application performance tuning.

21.3.3.1 RSDFT

The main procedures in RSDFT are DGEMM and collective communications are based on message passing interfaces (MPIs) such as MPI_Allreduce and MPI_Bcast. By performance tuning conducted during K computer development, RSDFT achieved a performance efficiency of about 43.6% for the Si nano-wire problem and won the Gordon-Bell Award in 2011.

RSDFT is parallelized on two axes, grid space and energy band. In order to deal with 100,000-atom-scale target problems on the Post-K computer, it will be necessary to further improve parallel performance. Since the amount of memory per process will be reduced in the Post-K computer, it is particularly important to further improve memory distribution for the band direction, which is one of the parallel axes. Gram-Schmidt orthogonalization which is the main calculation of RSDFT needs calculating row elements sequentially because of data dependency. The original RSDFT implementation, which used cyclic parallelization for orthogonalization, encountered calculation imbalances and increased barrier waiting times. When the K computer was developed, we achieved imbalance reductions by improving the allocation of calculations to each node without changing the cyclic parallelization. However, there are data dependency only in the calculation of diagonal terms and subdiagonal terms. Imbalance and elapsed time were reduced by concealment of communication using asynchronous communication and dynamic load balancing for non-diagonal terms having no dependency.

The Post-K computer can communicate at high speed by using "representative process communication" such as MPI_Allreduce and MPI_Bcast for collective communications. This is a two level communication method. First, using high speed intra node communication, it gathers data into representative node. Second, inter node communication are performed between representative nodes. By optimizing communication algorithms and rank placement, the communication time for RSDFT is expected to be shortened by as much as one-sixth.

Molecular dynamics (MD) calculations using the first-principles electronic state theory also have a large scientific impact, but we can now only perform calculations involving fewer than 1,000 atoms. However, we are now developing a memory decomposition version for Car-Parrinello MD with the aim of creating an MD simulation involving more than 10,000 atoms.

21.3.3.2 ADVENTURE

ADVENTURE is composed of two major parts. One is a sub-domain solver and the other is coarse grid correction. Its major calculations are dense matrix and vector multiplication. Since this multiplication is performed by an MPI parallel, the matrix shape for an MPI process is rectangular and is decomposed by row orientation.

Each MPI process has such rectangular submatrix and an entire right-hand-side vector. An especially hot kernel called "CoarseMatVec" performs quadruple precision operations and we paid significant attention at improving this kernel. Since the essential calculation is a dot product of two vectors, it was meaningful to improve the summation calculation having data dependency. However, original source code implementation was unsatisfactory. And the initial peak performance ratio on the K computer was just 3.61%. Implementing the improvements below allowed us to achieve a 42.01% performance ratio.

1. Previously, there were numerous data streams in the loop of the kernel due to unrolled implementations. And none suitable unrolling numbers involved cache thrashing. Therefore, the use of unrolled implementations was discontinued.

2. The dot product operation was separated into two steps: (1) making an element-wise product vector from two vectors, and (2) summation of element-wise product vectors. Step (1) obviously employs SIMD. However, Step (2) can also employ SIMD by treating a single element-wise vector as two separate half-length vectors. From these two vectors, an element-wise summation vector can be easily obtained. By repeating this procedure until the final obtained vector size is one, summation operations can be performed with a high level of effectiveness.

3. The number of data streams was decreased in order to avoid cache thrashing due to prefetching.

4. Changing the element-wise product vector location from heap to stack shortened memory allocation times.

5. We decreased the number of temporary arrays used by the recursive-summation procedure mentioned in "2" above.

6. Blocking was performed, and the number of recursive-summation procedures was decreased to just one by use of a coding technique.

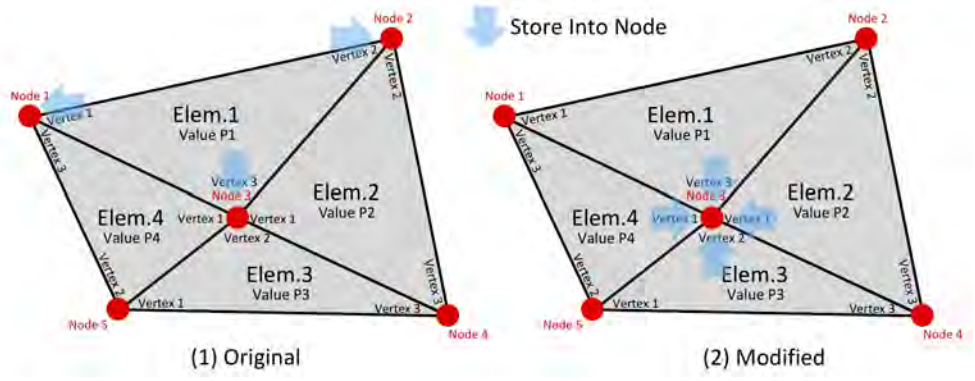

Figure 21.5: FFB tuning. Store order modification: (1) is original order. (2) is modified order.

21.3.3.3 FrontFlow/blue

The major kernels of FrontFlow/blue are the so-called "kernels depending on memory bandwidth". The performances of these kernels are strongly dependent on data transfer rather than CPU calculation performance. An unstructured grid involves indirect memory access via a list of relations between elements and nodes. For such type of memory access, in the Post-K computer, the effect of a broader SIMD width than possessed by the K computer prevents good indirect data store performance. Therefore, we formulated a strategy that avoids indirect stores in such kernels.

By modifying the loop structure so that loops iterate from element order to node order, the following memory access changes were derived. (1) Store memory access was changed from indirect to sequential access. (2) The number of data stores for a node was decreased from multiple to one. (3) Since there is no data dependency, SIMD and software pipelining were employed. As a result, execution time on the K computer was reduced by half from 91 to 44 s and the peak performance ratio increased from 5% to 12%, which is the theoretical maximum of this algorithm on the K computer. Additionally, memory throughput increased from 27 GB/s to 47 GB/s, which approaches the practical K computer maximum. When this technique was used for similar kernels, execution times were also successfully reduced by nearly half.

In addition, by employing other subsequent techniques on some kernels, we successfully improved the application performance on the K computer to a speed nearly twice that of its original performance. The current official speedup ratio of FrontFlow/blue between the K and Post-K computer is expected to nearly double. The knowledge obtained in efforts aimed at improving FrontFlow/blue was also used for other applications in Priority Issue No. 8.

21.4 Schedule and Future Plan

21.4.1 R-CCS software center activities

Activities related to the following two areas should be continued for use with the Post-K computer after the service of the K computer ends this summer. One is application improvements from the viewpoint of both performance and usability, whereas the other is activities to promote the advancement of a utilization environment for R-CCS software users via demonstrations, tutorials, documents, and other methods. Although we focused on four R-CCS software products in our activities up to this point, it is undisputable that the focus could be expanded to additional software applications.

21.4.2 Activities to establish DL environment on the Post-K computer

With regards to DL, we summarized the usage scenarios and performance levels of other computers. In the future, we will work to develop a high-performance DL library and scalable DL frameworks for use on the Post-K computer.

First, to improve the performance of the special DNN libraries developed by ARM Scalable Vector Extension (SVE), we will feed back knowledge gained during evaluations of the general DNN kernel prototyped here.

Furthermore, we will evaluate how much performance can be achieved for real training problems in order to build a general DNN kernel and special DNN library for use in a DL framework.

The elapsed time of single convolution calculation depends on the DNN library performance, but the total training time of scalable DL framework depends on the communication method. For this reason, the study of new communication algorithms also will needed to facilitate high-performance training.

In the past, we proposed a model in which software kernels were classified into six types corresponding to the calculation characteristics such as busy time of cache, memory, and calculation unit. This model is useful for estimation and for improving performance. This model is based on the information from the precision PA function of Fujitsu. To use this model not only the K computer and FX100 but also for other architecture, such as ARM, Intel, GPU, and the Vector machine, it is necessary to investigate ways to obtain busy time similar to FX100. Therefore, we will expand this model to other architectures in our future studies.

21.4.3 Post-K computer efforts

We continue to improve the applications that we are now in charge. And it is required to verify that the performance of the application would achieve estimated performance on the Post-K computer. For applications we are now in charge, these activities will be planned below.

For RSDFT, Memory distribution improvements are nearly complete. In the future, we will strictly verify the performance of those improvements using the Post-K CPU and confirm that there are no problems (such as performance degradation) resulting from the changes to the memory distributional algorithm. We will also conduct further tuning using the Post-K CPU to reduce communications by optimizing process mapping as part of overall efforts to achieve our target performance.

For ADVENTURE, performance improvements were performed kernel-by-kernel separately. Therefore, it will be necessary to integrate these improved kernels into the entire application. In addition, since application developers intend to make implementations based on the new algorithm, application performance re-estimations on the Post-K computer will be required. In the verification process, it will be necessary to confirm whether the application has achieved its expected performance. The abovementioned improvements have increased the estimated performance of the application by a significant value, but it will still be necessary to verify these performance improvements on real Post-K computer.

For FrontFlow/blue, room for improvement was found in some kernels. Originally, the running time ratios to the running time values of all these kernels were extremely low. However, due to the hot kernel improvements made thus far, significant running time reductions have been made and the running time ratio has improved. We intend to further improve these kernels using the methods mentioned above or by newly created methods. In the verification stage, it will be necessary to confirm whether the application has achieved its expected performance. In the original plan, application performance on the Post-K computer was expected to be a certain magnification than the K computer performance. However, as mentioned above, the application is now nearly twice as fast on the K computer, so it is expected that Post-K computer performance will be more than twice faster than current estimation.

It is also anticipated that other applications might be investigated to ensure good performance on the Post-K computer.

21.5 Publications

21.5.1 Articles/Journal

[1] T. Yamasaki, A. Kuroda, T. Kato, J. Nara, J. Koga, T. Uda, K. Minami and T. Ohno, “Multi-axis decomposition of density functional program for strong scaling up to 82,944 Nodes on the K Computer: Compactly folded 3D-FFT communicators in the 6D torus network”, Computer Physics Communications, North-Holland, 2019. (DOI:10.1016/j-cpc.2019.04.008).

21.5.2 Conference Papers

[2] K. Kumahata, K. Minami, Y. Yamade and C. Kato, “Performance improvement of the general-purpose CFD code FrontFlow/blue on the K computer”, Proceedings of the International Conference on High Performance Computing in Asia-Pacific Region (HPC Asia), Tokyo, Japan, pp.171-182, 2018. (DOI:10.1145/3149457.3149470).

[3] M. Hashimoto, M. Terai, T. Maeda, K. Minami,“An Empirical Study of Computation-Intensive Loops for Identifying and Classifying Loop Kernels”, Proceedings of the 8th ACM/SPEC on International Conference on Performance Engineering, L’Aquila, Italy, pp.361-372, 2017. (DOI:10.1145/3030207.3030217).
[4] K. Yamada, T. Katagiri, H. Takizawa, K. Minami, M. Yokokawa, T. Nagai and M. Ogino,“Preconditioner auto-tuning using deep learning for sparse iterative algorithms”, 2018 Sixth International Symposium on Computing and Networking Workshops (CANDARW), Takayama, Japan, pp.257-262, 2018. (DOI:10.1109/CANDARW.2018.00055).

21.5.3 Posters

[5] A. Kuroda, K. Kumahata and K. Minami: “Performance Tuning of Deep Learning Framework Chainer on the K computer.”, The 1st R-CCS International Symposium, Kobe, JAPAN, P-68 (2019.02.18-19).
[6] T. Imamura, Y. Hirota, D. Mukunoki, S. Kudo and A. Kuroda: “Development of Scientific Numerical Libraries on post-K computer”, The 1st R-CCS International Symposium, Kobe, JAPAN, P-64 (2019.02.18-19).
[7] A. Kuroda, K. Kumahata, S. Chiba, K. Takashina and K. Minami: “Performance Tuning of Deep Learning Framework Chainer on the K computer.”, Frontiers of Statistical Physics (FSP2019), Koshiba-Hall in Hongo Campus, The University of Tokyo, JAPAN, P-20 (2019/06/07-08).
[8] A. Kuroda, K. Kumahata, S. Chiba, K. Takashina and K. Minami: “Performance Tuning of Deep Learning Framework Chainer on the K computer.”, ISC High Performance 2019 (ISC2019) Research Poster, Frankfurt Messe, Germany, PR-28 (2019/06/16-19).
[9] A. Kuroda, K. Kumahata, S. Chiba, K. Takashina and K. Minami: “Performance Tuning of Deep Learning Framework Chainer on the K computer.”, ISC High Performance 2019 (ISC2019) HPC in Asia, Frankfurt Messe, Germany, PR-28 (2019/06/16-19).
[10] M. Hashimoto, M. Terai, T. Maeda, K. Minami,“CCA/EBT: Code Comprehension Assistance Tool for Evidence-Based Performance Tuning”, International Conference on High Performance Computing in Asia-Pacific Region (HPC Asia), Tokyo, Japan. 2018.

21.5.4 Invited Talks

[11] 南一生, ポスト「京」におけるADVENTUREのCPU単体性能チューニングについて, 第2回HPCものづくり統合ワークショップ, (September 26, 2018).
[12] 加藤千幸, 熊畑清, 山出吉伸, ポスト「京」重点課題プロジェクトにおけるFrontFlow/blue (FFB)の開発状況とコ・デザインによる高速化の状況, 第2回HPCものづくり統合ワークショップ, (September 26, 2018).

21.5.5 Oral Talks

[13] K. Minami, “Expectation to Supercomputer Benchmarks from the Viewpoint of Performance Optimization”, SIAM PP, pp.198 (Tokyo, March 7-10, 2018).

21.5.6 Software

[14] Chainer for K, https://k.r-ccs/riken.jp/

21.5.7 Patents

21.5.8 Book

[15] 下司雅章, 南一生, 高橋大介, 尾崎泰助, 安藤嘉倫, 小林正人, 成瀬彰, 黒澤一平, “計算科学のためのHPC技術2”, 大阪大学出版会, 2017.

Chapter 22

HPC Usability Development Unit

22.1 Members

Fumiyoshi Shoji (Unit Leader)

Hiroshi Harada (Technical Scientist)

Jorji Nonaka (Technical Scientist)

Masaaki Terai (Research & Development Scientist)

Shun Ito (Research & Development Scientist)

Tomohiro Kawanabe (Technical Staff I)

Hidetomo Kaneyama (Technical Staff I)

Megumi Takeuchi (Technical Staff I)

Kenji Ono (Senior Visiting Scientist)

Naohisa Sakamoto (Visiting Scientist)

Kengo Hayashi (Student Trainee)

Kazuki Koiso (Student Trainee)

Yoshiaki Yamaoka (Student Trainee)

22.2 Overview of Research Activities

The HPC Usability Development Unit has covered a wide range of topics including software, service, and infrastructure, aiming to improve the overall usability of the K computer environment. In addition, we also have some activities dedicated to one of the HPCI shared storage sites, located at the R-CCS, which is a commissioned project funded by the MEXT (Ministry of Education, Culture, Sports, Science and Technology). In the sixth year (in FY2018) since the beginning of the official operation of the K computer, R-CCS has conducted several projects related to the replacement of the K computer by its successor, which has recently named "Fugaku." We took into consideration these ongoing projects and focused on some considerable topics utilizing the current K computer environment.

The summary of our activities based on these topics is listed below.

- **Open-Source Software (OSS) Install and Maintenance:** In the K computer environment (K computer itself and its auxiliary subsystems, such as the "K Front-End Servers" and "K Pre/Post Processing Servers"), the vendors (Fujitsu and Intel) have provided their proprietary compilers and numerical libraries, which have been periodically updated to the latest version. On the other hand, most of the OSS installed on the K computer environment have not been maintained to provide the latest version because

of the costly installation and/or maintenance. Most of the OSS have been developed to the x86 architecture environment, while the K computer employs the SPARC architecture. Eventually, the maintenance process usually requires considerable time and effort, and it also needs to be continuous. In the FY 2018, we selected some OSS, taking into consideration the requests from the users, for the installation and/or update trials.

- **Large Data Visualization and Analysis (HIVE and ChOWDER):** We have worked on tools and applications for assisting the visualization and analysis of large data sets being generated at the K computer environment. In FY 2018, we have mainly worked on the HIVE (Heterogeneously Integrated Visual-analytics Environment) visualization framework, and the ChOWDER (COoperative Workspace DrivER) tiled display driver.

- **Workflow Management Software (WHEEL):** We have worked on a workflow management software named WHEEL, which was initially developed by the former Advanced Visualization Research Team, looking for more efficient use of the "Micro" class jobs on the K computer. In FY 2018, we added new functionality to WHEEL in order to efficiently perform capacity computing and have also integrated with some production-level applications for the initial trial and evaluation.

- **K Pre-Post Cloud (Data Analysis Server using Virtualization Technology):** Data analysis has become an important topic in the field of HPC/Data Centers. However, the existing data analysis servers in the K computer environment are disproportionately small compared to the K compute nodes. Nowadays, the virtualization technology has sufficiently matured and can provide an ideal software environment for the users. Therefore, to accelerate the data analysis without compromising the usability, we have considered the application of OpenStack-based virtualization technology for data analysis and worked on the design and deployment of an experimental cloud system.

- **Log Data Analysis (Evaluation of the Effectiveness of the File Staging-in Mechanism):** The Operations and Computer Technologies Division has operated a logging database system that collects several operational and facility related logs and event information from the K computer environment. We have worked on these collected data sets seeking valuable pieces of information, to serve as the feedback, in improving the operation. As a case study, we have worked on the evaluation of the overlapping effect in the file staging-in mechanism of the K computer.

- **HPCI Shared Storage:** In the commissioned project of the HPCI shared storage, we have collaboratively worked with the University of Tokyo who maintains the other shared storage. We have operated in the data-duplication mode to provide high availability, and avoiding the interruption of the service even if a serious failure occurs at one of the sites.

Furthermore, we have other activities that have been conducted in collaboration with universities and research institutes, in various fields of science and technology (e.g., Econophysics, Software Engineering, Materials Informatics, and Bioinformatics), and what they have in common is the investigation and exploration on how to enhance the usability, and to improve the productivity of the K computer environment. Although we have a wide variety of missions, we can say that our common objective is to improve the usability of the K computer environment as well as of the HPCI shared storage. Under this main goal, we have investigated and explored new usage for the K computer and the HPCI storage, trying to embrace not only the traditional HPC users but especially new users from various other fields. In the rest of this chapter, we will detail these aforementioned research and development projects carried out in FY 2018.

22.3 Research Results and Achievements

22.3.1 Open-Source Software (OSS) Install and Maintenance

In the software environment of the K computer, the Non-OSS (or proprietary) compilers and libraries (e.g., Fujitsu and Intel compilers) have been maintained by the vendors and been periodically updated, at least once a year. That is, the users are able to take advantage of the latest version of the compilers and the libraries on the K computer without additional efforts. On the other hand, common OSS developed for the x86 architecture are often not officially supported on the SPARC architecture. Due to this architecture difference, most of the OSS on the K computer have not been maintained at the same pace compared to the aforementioned examples of

the compilers and libraries provided by the vendors. Sometimes, the maintenance work to install an OSS on the K computer requires considerable time and effort, and the amount of necessary work, including the unavoidable engineering tasks, may nearly by equal to a pure porting case.

In FY 2018, by taking into consideration some of the requests from the users, we selected twenty-five OSS for the installation and maintenance (update). Most of the requests were for updating to newer versions, while some of them were for completely new installations. Finally, among these twenty-five OSS, we successfully installed/updated twenty OSS. The complete list of these OSS released for the users in FY 2018 is shown in the Table 22.1. It is worth noting that some of the installation/maintenance tasks have been conducted in collaboration with the RIST (Research Organization for Information Science and Technology). As a result, our work has also contributed to widening the user support service.

Table 22.1: List of the newly installed/updated OSS in the FY 2018.

Name	Version	Hardware Environment	Utilized Compiler Suite
boost	1.65.0	K compute node	Fujitsu
HDF5	1.10.1	K compute node	Fujitsu
Ruby	2.4.2	K compute node	GCC
z-Pares	0.9.6a	K compute node	Fujitsu
ParaView	5.4.1	K Pre/Post Server	GCC
pkg-config	0.29.2	K compute node	Fujitsu
ParMETIS	4.0.3	K Pre/Post Server	GCC
XZ Utils	5.2.3	K compute node	GCC
Python	3.5.5	K compute node	Fujitsu
OpenJDK	1.8.0 (jdk8u192-b03)	K compute node	GCC
OpenMPI	3.1.1	K Pre/Post Server	GCC/Intel
MPICH	3.2.1	K Pre/Post Server	GCC/Intel
Chainer	4.4.0	K compute node	Fujitsu
ChainerMN	1.3.0	K compute node	Fujitsu
Mesa3D	Mesa-17.2.3 LLVM-5.0.1	K compute node	GCC
gdb	8.1	K Front-End Server	GCC
Parallel NetCDF	1.8.1	K compute node	Fujitsu
NetCDF (C)	4.5.0	K compute node	Fujitsu
NetCDF (C++)	4.3.0	K compute node	Fujitsu
NetCDF (Fortran)	4.4.4	K compute node	Fujitsu

22.3.2 Large Data Visualization and Analysis (HIVE and ChOWDER)

Most of the research activities related to visualization and analysis have been done in close collaboration with research collaborators from Kyushu University and Kobe University, who have been working as visiting scientists and student trainees of this Unit. As a result, in addition to the SPARC64-based K computer and the x86-based pre- and post-processing oriented systems (K Pre/Post Server and K Pre-Post Cloud), we have also used the SPARC64-based π-computer and the x86-based π-VizStudio installed at the Kobe University in order to accelerate the developments. We have focused on both Post hoc and In situ approaches for the visualization and analysis of large-scale, time-varying numerical simulation results generated from the K computer.

We have continued working on the Particle-Based Volume Rendering (PBVR) method and developed a fully parallel PBVR by utilizing a parallel image compositing module [4, 5, 18]. This approach also brought a gain in memory efficiency [1, 3] compared to the traditional parallelization approach. In addition to the Post hoc visualization approach by using a distributed volume data stored in a disk, we have also developed an API for the simulation codes in order to enable In situ PBVR. We evaluated this API by integrating with the OpenFOAM CFD simulation code [8]. Although the final target was the K computer, this PBVR method has only been tested on x86-based K Pre-Post Cloud and π-VizStudio systems. Focusing on the ever-increasing demands for In Situ visualization, we have worked on two complementary approaches (tightly- and loosely-coupled approaches). The tightly-coupled approach was focused on using the KVS (Kyoto Visualization System) and Mesa 3D graphics library [7] for the 3D visualization. The loosely-coupled approach was focused on using the Pi2D [24] In Situ API [3] for the 2D visualization, and in addition, it also uses a so-called "Temporal Buffer" [6] in order to handle time-varying data sets. These approaches are still in the developmental stage.

We have also continued working on the HIVE (Heterogeneously Integrated Visual-analytics Environment) in order to provide more flexibility in adding functionalities provided by the third-party tools and libraries. We developed the "Render Plugin" functionality in order to facilitate the integration of external rendering engines and ported a part of the KVS via KVSHiveModule [1]. This redesigned cross-platform, modular visualization framework (Figure 22.1) [19, 20] is expected to serve as a basis for developing visualization tool and application on the future coming Post-K computer environment. Regarding the HIVE, we have also worked on enhancing auxiliary modules such as performance monitoring [13], and data management [14], and the usage via Docker [26]. We have also worked on a visual data analysis technique focusing on the operational improvements of the system and the facility. We have focused on a transfer entropy based visual causal analysis [9], and interactive visual exploration [11, 21]. We have investigated its applicability for the analysis of CPU failures on the K computer [10, 12], and it is still in the developmental stage. We have also worked on an analysis of the CPU cooling temperature effect on the performance and power consumption, trying to better understand the pros and cons of the warm water cooling approach [15].

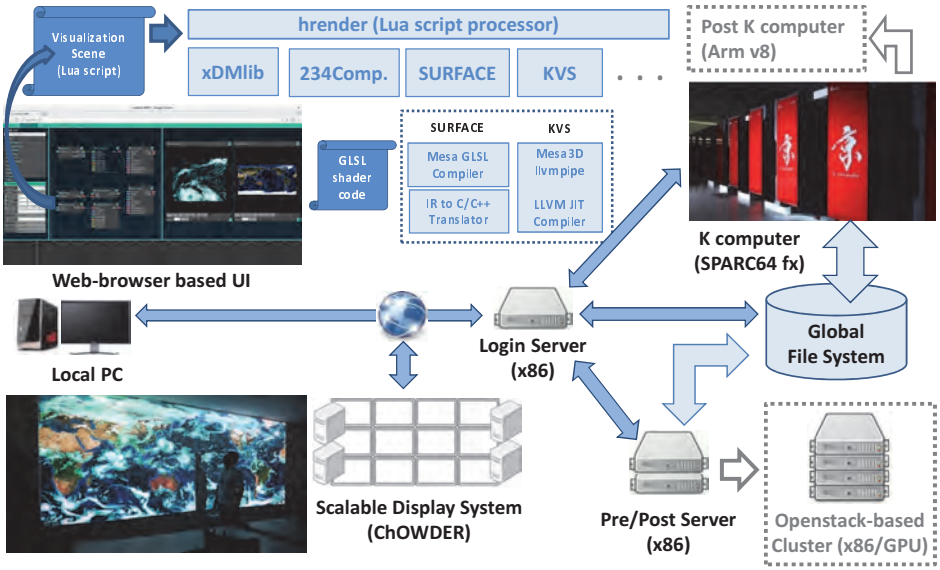

Figure 22.1: An overview of the HIVE (Heterogeneously Integrated Visual-analytics Environment) framework.

In addition, we have continued the research and development of the ChOWDER (COoperative Workspace DrivER) [29], a simple yet flexible tiled display driver. Tiled display is a method that tiles multiple physical display devices to form a single large pixel space. In recent years, it is possible to build the tiled display that connects multiple physical displays to a single PC by using a high-performance graphics card. However, ChOWDER is a software-based system and enables the building of a large pixel space by using multiple PCs and displays. Since ChOWDER is a Web-based software, it only requires ordinary Web browsers for the displaying thus it has high availability. In addition, the ChOWDER Server manages a logical pixel space called Virtual Display Area, [16, 22], and it enables to build a tiled display system composed of physical displays with different resolutions and aspect ratios. It is also possible to use this as a remote collaboration tool for displaying the same content on tiled displays situated at different sites due to the aforementioned high availability given by the Web-based technology. In FY 2018, we evaluated two different ChOWDER-based tiled display systems: One system was installed at the R-CCS, and was composed of twelve 4K displays (with a total resolution of 15360×6480 pixels), and has used to display super high-resolution images generated by the HIVE; The other system owned by Chiba University and composed of 36 Full-HD displays (with a total resolution of 17280×5120 pixels) was used in a collaborative research with NICT (National Institute of Information and Communications Technology), Chiba University, Kyushu University, and R-CCS. This system has been used to display ultra high-resolution meteorological satellite images.

22.3.3 Workflow Management Software (WHEEL)

To easily handle with many computational tasks on the HPC resources, we have developed a scientific workflow management system which was named WHEEL (Workflow in Hierarchical distributEd parallEL) [28] jointly developed with Kyusyu University. WHEEL can support typical HPC simulation with a workflow consisted of pre-processing, simulation, and post-processing and can work on various HPC computing resources including not only the K computer but also other computing resources. Also, this system is a web-based application written in JavaScript and is running on a common web browser for Windows, macOS, and Linux. WHEEL employs ordinary SSH and login shell to communicate with remote computers when it performs job submitting, monitoring, and file transfer. Therefore, the additional middleware is not required on the remote computers. In addition, WHEEL has the iteration/conditional branch functionality (e.g., For, Foreach, While, and If), and a parameter study functionality that allows multiple simulations simultaneously with the given parameter range specified by the user. By both features, the users can construct more complex workflows.

In FY 2018, WHEEL has been experimentally used in several research institutes and has been improved by their feedbacks. For example, in the development of innovative clean energy systems (Priority Issue 6 in the post-K computer project), using the K computer's micro-queue, we improved the usability of a parameter study with ABINIT-MP which is the Fragment Molecular Orbital method simulator, under the cooperation of Rikkyo University. In this case, we succeeded in automatically executing 6,000 simulation jobs in a single workflow project, and demonstrated that WHEEL is a suitable and practical workflow tool for capacity computing applications.

22.3.4 K Pre-Post Cloud (Data Analysis Servers using Virtualization Technology)

In the K computer environment, there exist auxiliary x86-based data-analysis servers, known as "Pre/Post Processing Servers," where the users are allowed to submit jobs using large memory, and with longer duration than compared to those allowed on the K computer. The primary target usage of these servers is data preparation, analysis, and visualization, which are some of the essential processes needed in the early and/or late phases of a regular end-to-end scientific workflow. In addition, these servers were built using the traditional x86 architecture, in order to provide a readily available environment for the users to exploit various OSS packages.

The Pre/Post Processing Servers can currently be considered as outdated since they were installed several years ago. In addition, although data analysis is one of the significant topics in HPC/Data Centers, their computational resources have gradually become insufficient for the data analysis. As a result, there was a strong demand from the academic/industrial users to enhance the pre/post processing capabilities in the K computer environment. In FY2018, to address the problem of the pre/post data processing by using OSS in the environment, we have launched a new experimental IaaS platform which was named "K Pre-Post Cloud," following the investigation and procurement processes completed in the previous fiscal year.

The K Pre-Post Cloud is a private cloud system/service, and an experimental platform in the K computer environment, build to enhance the pre/post data processing features including data analysis and visualization. This system consists of 11 compute nodes and some auxiliary servers. Each compute node has 48 x86-based physical cores, and 384 GiB of RAM, and connects to other nodes with a 25 GiB Ethernet network switch. In addition, the system has an external Ceph-based 150 TiB storage. To improve the usability regarding OSS environment, we applied the server virtualization technology using the OpenStack framework. By using this framework, the users are able to install and uninstall any software on their own virtualized environment, including not only the OSS but even the operating system they want to use. Furthermore, we also added GPUs on some of the compute nodes to enhance and accelerate the data processing capabilities.

In FY 2018, we started providing experimental service (https://www.r-ccs.riken.jp/ungi/prpstcloud/) to the users, and also conducted some local and remote (WebEx-based) explanatory and training sessions for the current K computer users, HPCI-ID holders, and potential future users. It is worth noting that, at almost the end of FY 2018, we have already issued 22 projects and 44 user accounts.

22.3.5 Log Data Analysis (Evaluation of the Effectiveness of the File Staging-in Mechanism)

To acquire better I/O performance in compute nodes, the K computer system employs two-tier, local/global file storage. While the global storage cannot be directly accessed from compute nodes, the local storage can only be accessed from connected compute node to improve locality. As one of the typical usage on the K computer, we expect that users utilize the file staging mechanism to transfer their programs/files among global and local file

storage. Furthermore, to reduce the duration of the file staging, under some conditions, the system is allowed to overlap with job execution and file staging needed by subsequent jobs at the same compute node. If the overlapping mechanism completely works, the users can ignore the duration of the file staging. Eventually, the turnaround time for each job can be reduced.

In FY 2018, we evaluated the overlapping effect in file staging-in mechanism based on actual log data throughout the past two years. As a result of the evaluation for target jobs used from 12289 to 36864 compute nodes, we confirmed 80 % of the jobs were overlapped with other jobs. Also, 55.1 % of the duration of the file staging-in were overlapped with other jobs. On the other hand, most of the jobs on the K computer tends to spend less execution time than staging-in duration. For such kind of jobs, we found that the overlapping mechanism was not effective. Finally, we have reported this study in [17].

22.3.6 HPCI Shared Storage

From the beginning of FY 2018, the HPCI shared storage has been operated by replicating the data files among the two HPCI shared storage sites (R-CCS and the University of Tokyo). This data duplication operation made possible to continue the service without stopping the operation even if a serious failure occurs at one of the sites. As a result, in FY 2018, there was no service interruption, except for the planned service outage due to the simultaneous system maintenance at both sites.

In preparation for the assignment in April 2019, the service was stopped in October 2018, due to the large-scale network configuration changes including the domain name change from “AICS” to “R-CCS.” After that, the R-CCS equipment was shut down on August 24, due to the impact of Typhoon No. 20, but the service was continued by the University of Tokyo via single site operation. At the time, the master metadata server in the University of Tokyo equipment correctly worked by the failover mechanism. On the other hand, on August 31, the University of Tokyo equipment was forced to shut down due to the lightning damage, but the service continued by the R-CCS via single site operation. At the beginning of FY 2018, the read-only service was provided to protect data during the single site operation.

In order to improve the usability to the users, data files are replicated to the R-CCS and the University of Tokyo, and since November 2018, the Read-Write service mode was started to be used during the single site operation. As a result of these measures, the annual operation rate in FY 2018 has improved to 99.26% [22].

Figure 22.2 shows the monthly operation rate of the HPCI shared storage system.

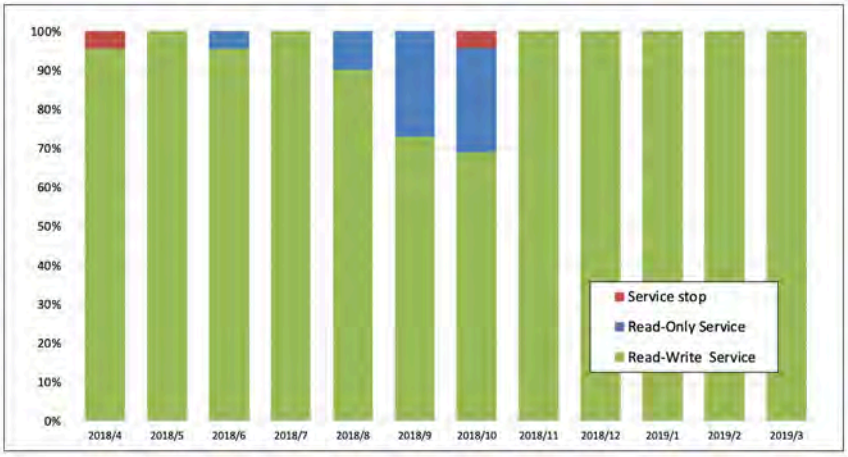

Figure 22.2: FY 2018 monthly operation rate of the HPCI shared storage.

22.3.7 Other Activities

In addition to those activities detailed in the previous section, we have also contributed to the following projects, which produced some publications:

- Graph-based Economic Simulation under the Exploratory Challenges on Post-K computer (Studies of Multi-level Spatiotemporal Simulation of Socioeconomic Phenomena, Macroeconomic Simulations) [2]
- Evidenced-based Performance Tuning in collaboration with the Software Technology and Artificial Intelligence Research Laboratory (STAIR), at the Chiba Institute of Technology [27]
- Materials Informatics using the "Micro" resource group in collaboration with the NIMS (National Institute for Materials Science)
- To share knowledge and actual usage regarding cutting-edge cloud resources in Bioinformatics and HPC, we started to collaborate with the Laboratory for Bioinformatics Research at the RIKEN Center for Biosystems Dynamics Research (BDR).

22.4 Schedule and Future Plan

During the FY 2018, we have worked on a variety of projects, mainly focusing on the improvements of the software environment of the K computer, and on maximizing the utilization of the K computing resources via "Micro" resource group. We have also dedicated to the commissioned project, funded by the MEXT, for operating one of the HPCI shared storage sites, located at the R-CCS. This was the second year of the activities with the new system, and we could continue further enhancing the works initiated in the last fiscal year. For the next fiscal year, we are planning to continue working on these ongoing projects by continuously striving to improve the usability of the K computer environment, as well as the HPCI shared storage system. In addition, we will continue trying our best to investigate and explore new usages for both facilities seeking not the traditional HPC users, but especially the potential new users from different fields.

22.5 Publications

22.5.1 Articles

[1] Yoshiaki Yamaoka, Kengo Hayashi, Naohisa Sakamoto, Jorji Nonaka, "A Memory Efficient Image Composition-based Parallel Particle Based Volume Rendering," Journal of Advanced Simulation in Science and Engineering, 2019, Volume 6, Issue 1, Pages 1–10, 2019.
[2] Hazem Krichene, Abhijit Chakraborty, Yoshi Fujiwara, Hiroyasu Inoue, Masaaki Terai, "Tie-formation process within the communities of the Japanese production network: Application of an exponential random graph model," Applied Network Science, 4:5, (2019).

22.5.2 Oral Talks

[3] Yoshiaki Yamaoka, Kengo Hayashi, Naohisa Sakamoto, Jorji Nonaka, "A Memory Efficient Parallel Particle-Based Volume Rendering for Large-Scale Distributed Unstructured Volume Datasets in HPC Environments," Asian Simulation Conference, pp. 552–562, Kyoto, Japan, 2018.
[4] Yoshiaki Yamaoka, Kengo Hayashi, Naohisa Sakamoto, Jorji Nonaka, "Particle Based Volume Rendering using 234 Image Composition," 37th JSST Annual International Conference on Simulation Technology (JSST 2018), Muroran, Japan, 2018.
[5] Yoshiaki Yamaoka, Kengo Hayashi, Naohisa Sakamoto, Jorji Nonaka, "Parallel Particle Based Rendering using 234 Image Composition," 46th VSJ Visualization Symposium, Tokyo, Japan, 2018. (in Japanese)
[6] Kenji Ono, Jorji Nonaka, Hiroyuki Yoshikawa, Takeshi Nanri, Yoshiyuki Morie, Tomohiro Kawanabe, Fumiyoshi Shoji, "Design of a Flexible In Situ Framework with a Temporal Buffer for Data Processing and Visualization of Time-Varying Datasets," Springer LNCS 11203 (ISC 2018 Revised Selected Papers (ISC Workshop on In Situ Visualization 2018)), pp. 243–257, Frankfurt, Germany, 2018.
[7] Kengo Hayashi, Naohisa Sakamoto, Jorji Nonaka, Motohiko Matsuda, Fumiyoshi Shoji, "An In-Situ Visualization Approach for the K Computer Using Mesa 3D and KVS," Springer LNCS 11203 (ISC 2018 Revised Selected Papers (ISC Workshop on In Situ Visualization 2018)), pp. 310–322, Frankfurt, Germany, 2018.

[8] Kengo Hayashi, Tsukasa Yoshinaga, Kazunori Nozaki, Jorji Nonaka, Naohisa Sakamoto, "In-situ Visualization of Air Flow and Sound Source for the Simulation of Sibilant Fricative Production," 32th CFD Symposium (CFD32), Tokyo, Japan, 2018. (in Japanese)

[9] Kengo Hayashi, Takashi Shimizu, Naohisa Sakamoto, Jorji Nonaka, Yasumitsu Maejima, Koji Koyamada, "A Visual Causality Exploration Technique for Large-Scale Numerical Simulations," 46th VSJ Visualization Symposium, Tokyo, Japan, 2018. (in Japanese)

[10] Kazuki Koiso, Naohisa Sakamoto, Jorji Nonaka, Fumiyoshi Shoji, "A Transfer Entropy Based Visual Analytics System for Identifying Causality of Critical Hardware Failures Case Study: CPU Failures in the K Computer," Asian Simulation Conference, pp. 563–574, Kyoto, Japan, 2018. (Honorable Mention Paper Award)

[11] Kazuki Koiso, Naohisa Sakamoto, Jorji Nonaka, Fumiyoshi Shoji, "Development of a Visual Analytic System of Exploring the Failure Causes using Big Log Data on HPC Systems," 37th JSST Annual International Conference on Simulation Technology (JSST 2018), Muroran, Japan, 2018.

[12] Kazuki Koiso, Naohisa Sakamoto, Jorji Nonaka, Fumiyoshi Shoji, "Development of a Visual Analytics System of Exploring the Failure Causes using Big Log Data on HPC Systems," 46th VSJ Visualization Symposium, Tokyo, Japan, 2018. (in Japanese)

[13] Kazunori Mikami, Kenji Ono, Jorji Nonaka, "Performance Evaluation and Visualization of Scientific Applications using PMlib," 2018 Sixth International Symposium on Computing and Networking Workshops (CANDAR 2018), pp. 243–249, Takayama, Japan, 2018.

[14] Eduardo Camilo Inacio, Jorji Nonaka, Kenji Ono, Mario Antonio Ribeiro Dantas, Fumiyoshi Shoji, "Characterizing I/O and Storage Activity on the K Computer for Post-Processing Purposes," 2018 IEEE Symposium on Computers and Communications (ISCC), pp. 730–735, Natal, Brazil, 2018.

[15] Jorji Nonaka, Fumiyoshi Shoji, Motohiko Matsuda, Hiroya Matsuba, Toshiyuki Tsukamoto, "Analysis of the CPU Cooling Temperature Effect on the Performance and Power Consumption for the HPC Operational Decision Support," Supercomputing Frontiers Asia 2019 (SCFA19), Singapore, 2019. (Abstract Presentation)

[16] Tomohiro Kawanabe, Jorji Nonaka, Kazuma Hatta, Kenji Ono. "ChOWDER: An Adaptive Tiled Display Wall Driver for Dynamic Remote Collaboration." In International Conference on Cooperative Design, Visualization and Engineering 2018 Oct 21 (pp. 11–15). Springer, Cham. Hangzhou, China, 2018. (Short paper)

[17] Shun Ito, Keiji Yamamoto, Motohiko Matsuda, Yuichi Tsujita, Shoji Fumiyoshi, "Analysis and Evaluation of the File-staging mechanism based on log data in the K computer," IPSJ-HPC-168, 23, pp. 1–6, 2019. (in Japanese)

22.5.3 Posters

[18] Kengo Hayashi, Yoshiaki Yamaoka, Naohisa Sakamoto, Jorji Nonaka, "A Fully Parallel Particle-based Volume Rendering for Large-Scale Unstructured Volume Datasets," IEEE Pacific Visualization Symposium (PacificVis 2018), Kyoto, Japan, 2018. (Poster) (Honorable Mention Poster Award)

[19] Jorji Nonaka, Kenji Ono, Naohisa Sakamoto, Kengo Hayashi, Tomohiro Kawanabe, Fumiyoshi Shoji, Masahiro Fujita, Kentaro Oku, Kazuma Hatta, "HIVE: A Cross-Platform, Modular Visualization Ecosystem for Heterogeneous Computational Environments," The International Conference for High Performance Computing, Networking, Storage, and Analysis (SC'18). Dallas, USA, 2018. (Poster)

[20] Jorji Nonaka, Kenji Ono, Naohisa Sakamoto, Kengo Hayashi, Motohiko Matsuda, Fumiyoshi Shoji, Kentaro Oku, Masahiro Fujita, Kazuma Hatta, "A Large Data Visualization Framework for SPARC64 fx HPC Systems - Case Study: K Computer Operational Environment," IEEE Symposium on Large Data Analysis and Visualization (LDAV 2018). Berlin, Germany, 2018. (Poster)

[21] Kazuki Koiso, Naohisa Sakamoto, Jorji Nonaka, Fumiyoshi Shoji, "Development of a visual analytics system which can search for the cause of failure interactively," The 1st R-CCS International Symposium, Kobe, Japan, 2018. (Poster)

[22] Tomohiro Kawanabe, Jorji Nonaka, Kenji Ono. "Chowder: Dynamic contents sharing through remote tiled display system." In 11th International Symposium on Visual Information Communication and Interaction, VINCI 2018 2018 Aug 13 (pp. 108-109). Association for Computing Machinery. Vaxjo, Sweden, 2018. (Poster)

[23] Hiroshi Harada, Osamu Tatebem Hidetomo Kaneyama, Seiichiro Naka, Toshihiro Hanawa, "An Improvement of availability by inter-site data redundancy in HPCI shared storage," The 1-st R-CCS International Symposium, Japan, 2019. (Poster)

22.5.4 Software

[24] Pi2D: 2D visualization library for In Situ processing (https://github.com/RIKEN-RCCS/In-situ2DLib).
[25] KVSHiveModule: Extension for enabling the use of KVS on HIVE (https://github.com/RIKEN-RCCS/HIVE/tree/KVSHiveModule).
[26] HIVE-docker: Docker module for HIVE (https://github.com/RIKEN-RCCS/HIVE-docker).
[27] CCA/EBT : Code Comprehension Assistance for Evidence-Based performance Tuning, R-CCS Software, (https://github.com/ebt-hpc).
[28] WHEEL : Scientific workflow Management System. (https://gitlab.com/aicshud/WHEEL)(Currently managing as a private repository).
[29] ChOWDER : Scalable Display System. (https://github.com/SIPupstreamDesign/ChOWDER).

Part III

Flagship 2020 Project

Chapter 23

Flagship 2020 Project

23.1 Members

Primary members are only listed.

23.1.1 System Software Development Team

Yutaka Ishikawa (Team Leader)

Masamichi Takagi (Senior Scientist)

Atsushi Hori (Research Scientist)

Balazs Gerofi (Research Scientist)

Masayuki Hatanaka (Research & Development Scientist)

Takahiro Ogura (Research & Development Scientist)

Tatiana Martsinkevich (Postdoctoral Researcher)

Fumiyoshi Shoji (Research & Development Scientist)

Atsuya Uno (Research & Development Scientist)

Toshiyuki Tsukamoto (Research & Development Scientist)

23.1.2 Architecture Development

Mitsuhisa Sato (Team Leader)

Yuetsu Kodama (Senior Scientist)

Miwako Tsuji (Research Scientist)

Jinpil Lee (Postdoctoral Researcher)

Hitoshi Murai (Research Scientist)

Masahiro Nakao (Research Scientist)

Toshiyuki Imamura (Research Scientist)

Kentaro Sano (Research Scientist)

Tetsuya Odajima (Postdoctoral Researcher)

23.1.3 Application Development

Hirofumi Tomita (Team Leader)

Yoshifumi Nakamura (Research Scientist)

Hisashi Yashiro (Research Scientist)

Soichiro Suzuki (Research & Development Scientist)

Kazunori Mikami (Research & Development Scientist)

Kiyoshi Kumahata (Research & Development Scientist)

Mamiko Hata (Technical Staff I)

Hiroshi Ueda (Research Scientist)

Naoki Yoshioka (Research Scientist)

Yiyu Tan (Research Scientist)

23.1.4 Co-Design

Junichiro Makino (Team Leader)

Keigo Nitadori (Research Scientist)

Yutaka Maruyama (Research Scientist)

Masaki Iwasawa (Research Scientist)

Daisuke Namekata (Postdoctoral Researcher)

Kentaro Nomura (Research Associate)

Miyuki Tsubouchi (Technical Staff)

23.2 Project Overview

The Japanese government launched the FLAGPSHIP 2020 project [1] in FY 2014 whose missions are defined as follows:

- Building the Japanese national flagship supercomputer, the successor to the K computer, which is tentatively named the post K computer, and
- developing wide range of HPC applications that will run on the post K computer in order to solve the pressing societal and scientific issues facing our country.

RIKEN is in charge of co-design of the post K computer and development of application codes in collaboration with the Priority Issue institutes selected by Japanese government, as well as research aimed at facilitating the efficient utilization of the post K computer by a broad community of users. Under the co-design concept, RIKEN and the selected institutions have been collaborated closely. The official name of the post K computer was decided in May 2019. It is now named Fugaku.

As shown in Table 23.1, four development teams are working on Fugaku system development with the FLAGSHIP 2020 Planning and Coordination Office that supports development activities. The primary members are listed in Section 23.1.

The Architecture Development team designs the architecture of Fugaku in cooperation with Fujitsu and designs and develops a productive programming language, called XcalableMP (XMP), and its tuning tools. The team provides a cycle-level Fugaku processor simulator for the performance tuning and verification. The team also specifies requirements of standard languages such as Fortran and C/C++ and mathematical libraries provided by Fujitsu.

[1] FLAGSHIP is an acronym for Future LAtency core-based General-purpose Supercomputer with HIgh Productivity.

Table 23.1: Development Teams

Team Name	Team Leader
Architecture Development	Mitsuhisa Sato
System Software Development	Yutaka Ishikawa
Co-Design	Junichiro Makino
Application Development	Hirofumi Tomita

The System Software Development team designs and specifies a system software stack such as Linux, MPI and File I/O middleware for the Fugaku in cooperation with Fujitsu and designs and develops multi-kernel for manycore architectures, Linux with light-weight kernel (McKernel), that provides a noise-less runtime environment, extensibility and adaptability for future application demands.

The Co-Design team leads to optimize architectural features and application codes together in cooperation with RIKEN teams and Fujitsu. It also designs and develops an application framework, FDPS (Framework for Developing Particle Simulator), to help HPC users implement advanced algorithms.

The Application Development team is a representative of nine institutions aimed at solving Priority Issues. The team figures out weakness of target application codes in terms of performance and utilization of hardware resources and discusses them with RIKEN teams and Fujitsu to find out best solutions of architectural features and improvement of application codes. Published papers, presentation and posters are summarized in the final subsection in this chapter.

23.3 Target of System Development and Achievements in FY2018

The Fugaku's design targets are as follows:

- A one hundred times speed improvement over the K computer is achieved in maximum case of some target applications. This will be accomplished through co-design of system development and target applications for the nine Priority Issues.
- The maximum electric power consumption should be between 30 and 40 MW.

23.3.1 Programming Environment and System Software

In FY2018, the fourth phase of the detailed design was completed. The major components of programming environment and system software are summarized as follows:

- Highly productive programming language, XcalableMP
  XcalableMP (XMP) is a directive-based PGAS language for large scale distributed memory systems that combines HPF-like concept and OpenMP-like description with directives. Two memory models are supported: global view and local view. The global view is supported by the PGAS feature, i.e., large array is distributed to partial ones in nodes. The local view is provided by one-sided data transfer with Coarray notation. In 2018FY, We have been working on XcalableMP 2.0 which newly supports task-parallelism and the integration of PGAS models for distributed memory environment. We are are still working on C++ Front-end based on LLVM clang.
- Domain specific library/language, FDPS
  FDPS is a framework for the development of massively parallel particle simulations. Users only need to program particle interactions and do not need to parallelize the code using the MPI library. The FDPS adopts highly optimized communication algorithms and its scalability has been confirmed using the K computer. In 2018FY, we implemented several new algorithms to remove potential bottlenecks which can appear in runs with extremely large number of MPI processes. We also worked on high-performance implementation of particle-particle interaction calculation on Fugaku.
- MPI + OpenMP programming environment
  The current de facto standard programming environment, i.e., MPI + OpenMP environment, is supported. Two MPI implementations are being developed. Fujitsu continues to support own MPI implementation based on the OpenMPI. RIKEN is collaborating with ANL (Argonne National Laboratory) to develop MPICH for Fugaku. Achievements of our MPI implementation have been described in Section **??**.

- New file I/O middleware
  Fugaku does not employ the file staging technology for the layered storage system. The users do not need to specify which files must be staging-in and staging-out in their job scripts in the Fugaku environment. The LLIO midleware, employing asynchronous I/O and caching technologies, has been being designed by Fujitsu in order to provide transparent file access with better performance. LLIO was implemented and its component-leve tests was completed in FY2018.

- Application-oriented file I/O middleware
  In scientific Big-Data applications, such as real-time weather prediction using observed meteorological data, a rapid data transfer mechanism between two jobs, ensemble simulations and data assimilation, is required to meet their deadlines. In FY2018, a framework called Data Transfer Framework (DTF), based on the PnetCDF file I/O library, that silently replaces file I/O with sending the data directly from one component to another over network was designed and its prototype system was improved and evaluated. The detailed achievement has been described in Section 1.3.2.

- Process-in-Process
  "Process-in-Process" or "PiP" in short is a user-level runtime system for sharing an address space among processes. Unlike the Linux process model, a group of processes shares the address space and thus the process context switch among those processes does not involve hardware TLB flushing. It was evaluated using SNAP, one of CORAL benchmarks in FY2018. The detailed achievement has been described in Section 1.3.3.

- Multi-Kernel for manycore architectures
  Multi-Kernel, Linux with light-weight Kernel (McKernel) is being designed and implemented. It provides: i) a noiseless execution environment for bulk-synchronous applications, ii) ability to easily adapt to new/future system architectures, e.g., manycore CPUs, a new process/thread management, a memory management, heterogeneous core architectures, deep memory hierarchy, etc., and iii) ability to adapt to new/future application demands, such as Big-Data and in-situ applications that require optimization of data movement. In FY2018, McKernel was ported to an Arm architecture.

It should be noted that these components are not only for Fugaku, but also for other manycore-based supercomputer, such as Intel Xeon Phi.

23.3.2 Tools

The architecture development team is also working on the researches on co-design tools as well as the design of Fugaku:

GEM5 processor simulator for the Fugaku processor
We have been developing a cycle-level processor simulator for the Fugaku processor based on GEM-5, which is a general-purpose processor simulator commonly used for the processor architecture research. We enhanced the Armv8 gem5 simulator with Scalable Vector Extension (SVE), upstreamed by Arm, with Fugaku processor's architecture parameters and more precious memory access mechanism such as prefetch. It enables the cycle-level performance evaluation of application kernels. We have been working on the adjustment of parameters and performance with Fujitsu-in-house processor simulator for more accurate performance evaluation. In 2018, we are providing the service to provide "Fugaku performance evaluation environment" including this simulator for performance evaluation and tuning by potential Fugaku users. And, for researches on more general architecture exploration based on Arm, we published the docker file containing our Armv8-SVE gem-5 simulator with "open" parameters and Arm-SVE gcc compiler on the Linaro docker site.

Performance estimation tools for co-design study
We have tools for co-design study for future huge-scale parallel systems. The MPI application replay tool is a system to investigate a performance and behavior of parallel applications on a single node using MPI traces. SCAMP (SCAlable Mpi Profiler) is other system to simulate a large scale network from a small number of profiling results. In 2018, we have implemented a pseudo MPI event trace file generator based on the analysis of LLVM intermediate representations. We compared the real and estimated execution times by our method on K-computer for a 2-D stencil code to indicate the simulation with pseudo trace files approximates the simulator with real traces.

Study on performance metrics
We have been developing a new metric, called Simplified Sustained System Performance (SSSP) metric, based on a suite of simple benchmarks, which enables performance projection that correlates with applications. In 2018, we applied the SSSP metric for Arm-based system, HPE Apollo 70.

In addition to co-design tools, we are working on the evaluation of compilers for ARM SVE. There are two kinds of compiler for ARM SVE: Fujitsu Compiler and ARM compiler. The Fujitsu compiler is a proprietary compiler supporting C/C++ and Fortran. The ARM compiler is developed by ARM based on LLVM. Initially, LLVM only supports C and C++, and supports Fortran recently by flang. We are evaluating the quality of code generated by both of the compilers with collaboration of Kyoto University. Since these compilers are still immature, we give several feedbacks by examining the generated code.

23.3.3 Target Applcations

The application development team discusses and improves the computational performance of applications on Fugaku, using the nine target applications.

Performance estimation of target applications
So far, we have improved efficiency of the nine target applications in cooperation with the priority issue project and Fujitsu. These applications cover the computational characteristics, because the system is a general-purpose machine. In this fiscal year, the system specifications were almost fixed. Through the application review meeting held once a month, we discussed how to write the program to pull out potential of Fugaku within limit of power consumption in cooperation with the compiler and system software development group. Using the kernels that was extracted from the each of target applications, the computational performance of theses kernels was evaluated on several computer nodes of actual machine. Based on such data, the performance estimation as full-applications on Fugaku was conducted using the magnification from K Computer as an index. As a result, the target performance is expected to be achieved in all of target applications (https://postk-web.r-ccs.riken.jp/perf.html).

23.4 International Collaborations

23.4.1 DOE/MEXT Collaboration

The following research topics were performed under the DOE/MEXT collaboration MOU.

- Efficient MPI for exascale
  In this research collaboration, the next version of MPICH MPI implementation, mainly developed by Argonne National Laboratory (ANL), has been cooperatively developed. The FY2018 achievements have been described in Section 1.3.1.

- Metadata and active storage
  This research collaboration, run by the University of Tsukuba as contract, studies metadata management and active storage.

- Storage as a Service
  This research collaboration explores APIs for delivering specific storage service models. This is also run by the University of Tsukuba.

- Parallel I/O Libraries
  This research collaboration is to improve parallel PnetCDF I/O software for extreme-scale computing facilities at both DOE and MEXT. To do that, the RIKEN side has designed DTF as described in Section 1.3.2.

- OpenMP/XMP Runtime
  This research collaboration explores interaction of Argobots/MPI with XcalableMP and PGAS models.

- LLVM for vectorization
  This research collaboration explores compiler techniques for vectorization on LLVM.

- Exascale co-design and performance modeling tools
  This collaborates on an application performance modeling tools for extreme-scale applications, and shared catalog of US/JP mini-apps.
- Power Monitoring and Control, and Power Steering
  This research collaboration explores APIs for monitoring, analyzing, and managing power from the node to the global machine, and power steering techniques for over-provisioned systems are evaluated. This collaboration was done mainly by Dr. Kondo's group.
- FPGA for future architecture
  This research collaboration explores the technology of FPGA as an accelerator for future high performance computing. This collaboration was done mainly by Dr. Sano's group.

23.4.2 CEA

RIKEN and CEA, Commissariat *à* l'*é*nergie atomique et aux *é*nergies alternatives, signed MOU in the fields of computational science and computer science concerning high performance computing and computational science in January 2017.

The collaboration on following topics are on-going:

- Programming Language Environment
- Runtime Environment
- Energy-aware batch job scheduler
- Large DFT calculations and QM/MM
- Application of High Performance Computing to Earthquake Related Issues of Nuclear Power Plant Facilities
- Key Performance Indicators (KPIs)
- Human Resource and Training

23.5 Schedule and Future Plan

A prototype implementation and its basic evaluation were completed in FY2018. The hardware will be installed from the end of 2019 and the development of the system software, conducted by Fujitsu, will be finished in September 2020. The service is expected to start public operation in 2021. In FY2019, we will also continue to improve the performance of applications on actual machine through co-design with compilers and system software development, including improvements of application algorithm.

23.6 Publications

23.6.1 presentation and poster

[1] Tetsuya Odajima, Yuetsu Kodama, Mitsuhisa Sato: Power performance analysis of ARM scalable vector extension. COOL CHIPS 2018: 1-3
[2] Tetsuya Odajima, Yuetsu Kodama, Miwako Tsuji, Mitsuhisa Sato: Performance and Power Consumption Analysis of ARM Scalable Vector Extension by using Gem5 Processor Simulator, ModSim 2018, Seattle, WA, USA, Aug. 2018.
[3] Tetsuya Odajima, Yuetsu Kodama, Mitsuhisa Sato: Performance and Power Consumption Analysis of ARM Scalable Vector Extension, Arm Research Summit 2018, Cambridge, UK, Sep. 2018.

[4] Kazunori Mikami, Kenji Ono, Jorji Nonaka: Performance evaluation and visualization of scientific applications using Pmlib, 2018 Sixth International Symposium on Computing and Networking Workshops (CANDARW), Takayama, Japan, Nov. 2018
[5] Hisashi Yashiro: Co-design of Post-K Priority Issue 4 Application, 3rd Research Result Meeting, Post-K Priority Issue 4, Yokohama, Japan, Mar. 2019

23.6.2 Articles and Technical Paper

[1] Yuetsu Kodama, Tetsuya Odajima, Akira Asato, Mitsuhisa Sato: Evaluation of the RIKEN Post-K Processor Simulator. CoRR abs/1904.06451 (2019)
[2] Kazunori Mikami, Kenji Ono, Jorji Nonaka: Performance evaluation and visualization of scientific applications using Pmlib, 2018 Sixth International Symposium on Computing and Networking Workshops (CANDARW), 243-249 (2018)